Programa de doctorado: Ciencias y Tecnologías del Medio Ambiente

EFFECT OF ULTRASOUND, LOW-TEMPERATURE THERMAL AND ALKALI TREATMENTS ON PHYSICOCHEMICAL AND BIOLOGICAL PROPERTIES OF WASTE ACTIVATED SLUDGE

Tesis Doctoral

Maria Ruiz Hernando

Directores de la tesis doctoral:

Dr. Jordi Labanda Angulo

Departamento de Ingeniería Química

Universitat de Barcelona

Dr. Joan Llorens Llacuna

Departamento de Ingeniería Química

Universitat de Barcelona

Acknowledgements

Mi más sincero agradecimiento a mis directores de tesis, el Dr. Jordi Labanda y el Dr. Joan Llorens. Gracias por guiarme a lo largo de este trabajo, por vuestra paciencia y apoyo, y por el aprendizaje recibido. Además, quiero agradecer a Jordi Labanda la confianza depositada en mí desde que aceptase ser mi tutor del proyecto de final de carera, por allá en 2008. ¡Siete años ya!

También quiero que estén entre estas líneas Natalia de la Cruz, Xavier Simón, Sergi Astals, Ricard Reynaldos y Bryshila Lupo. ¡Me ha encantado coincidir con vosotros estos años en el Departamento! Quiero hacer mención especial a la Dra. Elisabet Rudé, a quien aprecio y espero que se recupere muy pronto.

Al personal de Técnicas Separativas de los Centros Científicos y Tecnológicos de la *Universitat de Barcelona*. En especial, quiero agradecer al Dr. Isidre Casals y a Eva María del Álamo su valiosa ayuda para el análisis de la cromatografía de permeación en gel.

Al Dr. Francisco Lucena y a Julia Martín, del Departamento de Microbiología de la *Universitat de Barcelona*. Ha sido un verdadero placer colaborar con vosotros. La afinidad con Julia desde el primer momento ha facilitado mucho la tarea. ¡Gracias!

Gracias al personal de la depuradora Baix-Llobregat por facilitarme el muestreo. En particular, quiero dar gracias a Ignasi Batallé por su implicación directa y por resolverme numerosas dudas.

Gracias a Guille y Esther, que se animaron a trabajar conmigo en sus proyectos de final de carrera y máster, respectivamente. Esther, conseguir extraer y cuantificar las EPSs ha sido un logro 100% compartido. ¡Eres una crack!

En mis agradecimientos no pueden faltar mis amigos, cuyo apoyo ha sido vital en todo este proceso. Quiero citar a Laura Abad (autora de la fantástica portada de esta tesis), Alexandra, Berta, Noemi, Marta (Pitu), Elena (Vija), Patri, Estefanía y Xavi. Gracias por vuestro cariño, ¡soy muy afortunada de teneros!

A mi familia, a la que quiero y admiro. En especial, gracias a mi tía Conchi por el cariño puesto en sus menús y a mi primo Héctor por salir a correr conmigo y ayudarme a desconectar. Y ya para acabar, a mis padres, Julia y Santi. Aunque a ellos nunca les podré agradecer suficientemente todo lo que hacen por mí. Gracias por quererme y por soportar lo peor de mí. ¡Os quiero!

«*The beautiful thing about learning is that nobody can take it away from you*»

B. B. King (1925-2015)

Summary

The generation of sewage sludge is a remarkable issue on environmental management. Specifically, the annual sludge production within the European Union has been estimated to exceed 13 million tons (dry sludge) in 2020. In this context, the development of treatment processes to reduce or reuse sludge is crucial for a proper environmental management. Segregating primary from secondary sludge allows for better reuse of secondary sludge, since digested secondary sludge is better suited for agricultural application, containing about double concentration in nutrients but significantly less organic contaminants. However, secondary sludge (also called waste activated sludge (WAS)) is difficult to dewater compared with primary sludge due to the existence of colloidal materials and extracellular polymeric substances (EPSs), which strongly retain water. Moreover, WAS, which is primarily formed by microorganisms, is more difficult to digest under anaerobic conditions due to the presence of glycan strands in microbial cell walls. The low dewaterability and digestibility of WAS can be improved by applying treatments, such as ultrasound, thermal or alkali. These treatments can partially disintegrate the WAS by disrupting flocs and cells and solubilising the EPSs, thus releasing part of the interstitial water trapped in sludge flocs and the intracellular

organic matter. Accordingly, these treatments affect the viscosity of sludge because of the reorganisation of the sludge flocs with the EPSs and free water molecules.

The aim of this work is to study the influence of ultrasound, low-temperature thermal and alkali treatments on physicochemical and biological properties of WAS. Specifically, it has been analysed the effect of the aforementioned treatment on WAS rheology, dewatering, hygienisation and anaerobic digestion.

Rheology, which is the study of stress-strain relationships of viscoelastic materials, is a useful tool for the characterisation of sludge and to control sludge treatment processes. Rheological measurements performed within the linear viscoelastic region, far away from the normal flow conditions, can be used to describe the internal structure of WAS because the applied stress does not change the internal structure of materials. In this context, the treatments reduced the sludge initial elasticity and zero shear rate viscosity. Conversely, when the measurements are performed within the non-linear viscoelastic region, the stress changes the structure of the WAS and therefore its viscosity (non-Newtonian behaviour). All the sludges analysed (untreated and treated) behaved as non-Newtonian pseudo-plastic fluids, which indicates that the viscosity decreases with the applied shear rate. The sludges were also thixotropic (showing a hysteresis area in the plot of stress versus shear rate), which means that the viscosity is also time dependent. The three aforementioned treatments resulted in the reduction of the steady state viscosity and the hysteresis area of the sludge. In the case of the ultrasound and alkali treatments, these reductions were more significant as the treatment intensity was increased, whereas the thermal treatment caused similar reductions between the different tested temperatures.

A rheological structural model was proposed to examine the variations in the thixotropic behaviour of WAS after the application of the treatments. The model was based on the definition of the time dependence of a structural parameter, S, which quantifies the structural level of the internal structure at any time and shear rate, and the instantaneous variations in the alignment and deformation of flocs (m parameter). The time evolution of the structural parameter was defined as a function of the thixotropic kinetic coefficients for the breakdown and build-up processes.

Knowing how water is distributed within the WAS is essential to examine dewatering difficulties. Usually, two primary types of water are identified: the free (or bulk) water, which is not influenced by the solid particles and can be easily removed, and the bound water, whose properties are modified due to the presence of hydrophilic particles. Bound water is generally considered a gross estimate of several states of water including vicinal (or surface) water, water of hydration and some fraction of interstitial water. The distribution of each water type will depend on the nature and composition of the internal sludge structure, which is stabilised primarily by the EPSs. The vicinal water content increased when the treatment intensities increased because the organic matter released after sludge floc disruption created extra surfaces for water binding. Nevertheless, the centrifugation tests revealed that the three conditions of the thermal treatment (60, 80 and 90 ºC; 1 h of treatment, including the heating time to reach the temperature) and the higher intensities of ultrasound (27,000 kJ/kg TS; TS stands for total solids) and alkali (157 g NaOH/kg TS) treatments improved sludge dewatering by releasing the interstitial water.

To further evaluate the effect of treatments on the sludge dewatering, the EPSs contained in sludge were extracted and characterised. The EPS analyses were conducted on the untreated sludge and on a unique condition of each treatment (ultrasound: 27,000 kJ/kg TS; thermal: 80 ºC (1 h of treatment, including the heating ramp); alkali: 157 g NaOH/kg TS). EPSs were fractionated to generate two different EPS fractions: loosely bound EPSs (LB-EPSs) and tightly bound EPSs (TB-EPSs), where the latter is the innermost fraction and harder to release. An analysis of the untreated sludge revealed that the proteins, followed by the humic acids and polysaccharides, were the major constituents of the EPSs. Each of these components was primarily observed in the TB-EPS fraction. The treatments, particularly the alkali treatment, thoroughly solubilised (released) the EPS, as indicated by the increase in the TOC, protein, humic acid and polysaccharide contents in the LB-EPS fraction. The thermal treatment solubilised less EPSs than the alkali treatment but denatured the high-molecular-weight proteins, which act as flocculants. Nevertheless, more water was removed by centrifugation after the alkali treatment, suggesting that the solubilisation of EPSs is decisive for WAS dewatering.

Although untreated sewage sludge has beneficial plant nutrients and soil conditioning properties, it may also contain pathogenic microorganisms that can cause disease. Thereby, the hygienisation of the sludge is of uttermost importance if the sludge is intended for agriculture. The level of hygienisation was evaluated using three indicator organisms: *Escherichia coli*, somatic coliphages (SOMCPH) and spores of sulfite-reducing clostridia (SSRC). The thermal treatment at 80 ºC and the alkali treatment at 157 g NaOH/kg TS allowed the hygienisation of the sludge, thus satisfying normal levels accepted by the Environmental Protection Agency (EPA) and the 3rd official draft from the European Union. Conversely, the conditions tested for the ultrasound treatment barely reduced the levels of microbial indicators.

Mesophilic anaerobic digestion is a widely used method to stabilise the sludge. The biomethanisation studies were analysed on the untreated sludge and at one condition of each treatment (ultrasound: 27,000 kJ/kg TS; thermal: 80 ºC (15 min of treatment, including the heating ramp); alkali: 157 g NaOH/kg TS). The alkali pre-treatment exhibited the greatest methane production increase (34%) followed by the ultrasonication (13%), whereas the thermal pre-treatment presented a methane potential similar to the untreated sludge. However, the use of NaOH as a pre-treatment is rather limited because of the rising sodium concentration in the digester.

Table of contents

List of figures

List of tables

Chapter 1 Introduction

1.1. Sewage sludge - an inherent cause of wastewater treatment

The treatment of wastewater invariably produces a residual that must be disposed of into the environment. Most often this residual is a semisolid, odoriferous and difficult to manage material and is commonly termed *sludge* (Sanin et al., 2011).

Sludge quantity and quality is largely dependent on the wastewater treatment. Biological processes are an effective way of treating wastewater and ensuring minimum residual impact on the aquatic environment, but they have the drawback of producing huge amounts of waste activated sludge (WAS): the more effective the process is in removing contaminants from the wastewater, the more sludge is produced (Neyens et al., 2004). According to Weemaes and Verstraete (2001), the removal of 1 kg of chemical oxygen demand (COD[1]) from wastewater gives rise to the formation of approximately 0.4 kg of sludge.

[1] The chemical oxygen demand (COD) is an index to assess the organic pollution in aqueous systems. It is a quantitative measure of the amount of oxygen required to oxidise all organic compounds in a unit volume on wastewater.

Sewage sludge contains organic material and nutrients that have an agricultural value, but also some pollutants in the form of heavy metals, organic contaminants and pathogens. Accordingly, the sludge produced in a wastewater treatment plant (WWTP) must be treated and disposed of properly. Nowadays, the treatment and disposal of sludge represents a bottleneck in WWTPs due to environmental, economic, social and legal factors. Specifically, the costs of sludge treatment and disposal can account up to 50% of the total costs of the WWTP (Neptune Project-Deliverable 1.3).

1.2. European legal framework for management of sewage sludge

Several directives have an influence on sludge management, but the ones which have the strongest impact on sludge production, disposal and recycling are Directive 91/271/EEC (CEC, 1991) on urban waste water treatment and Directive 86/278/EEC (CEC, 1986) on the use of sludge in agriculture.

Directive 91/271/EEC prescribes the level of treatment required before wastewater discharge. In this context, collecting systems must be provided for agglomerations of more than 2000 population equivalent (PE) and secondary treatment (biological treatment) must be provided for agglomerations of more than 2000 PE discharging into freshwater and estuaries and agglomerations of more than 10,000 PE discharging into coastal waters. The implementation deadline for Directive 91/271/EEC was 2005 for the 15 older European Union member states (EU-15[2]) and 2015 or 2018 for the countries that joined EU after 2004 (EC, 2009). As a result, an increase of approximately 50% in annual sewage sludge production in EU-15 was noticed, from 6.5 million tons dry solids (DS) in 1992 to 9.8 million tons DS in 2005 (Kelessidis and Stasinakis, 2012). On the other hand, the annual sewage sludge production in the new member states (EU-13[3]) was estimated to be approximately 1.1 million tons DS in 2005,

[2]EU-15: Austria, Belgium, Denmark, Finland, France, Germany, Greece, Ireland, Italy, Luxembourg, the Netherlands, Portugal, Spain, Sweden and the United Kingdom.

[3]EU-13: Bulgaria, Croatia, Cyprus, Czech Republic, Estonia, Hungary, Latvia, Lithuania, Malta, Poland, Romania, Slovakia and Slovenia.

resulting to a total amount of 10.9 million tons DS for all member states (EU-28). The implementation of Directive 91/271/EEC by EU-13 is going to cause a significant increase of annual sewage sludge production in EU during the following years. Estimates indicate that from 2005 to 2020, the total sludge generation may increase by approximately 20% for the EU-15 and by 100% for the EU-13 (Milieu Ltd., WRc and RPA, 2010), thus exceeding 13 million tons DS in 2020.

The biological wastewater treatment leads to the result that pollutants are concentrated in the sludge. Therefore, sludge not only contains much organic matter, but also contains heavy metals, pathogens and persistent organic pollutants, which can cause environment pollution. The Directive 86/278/EEC was adopted with a view to encourage the application of sewage sludge in agriculture and to regulate its use in order to prevent harmful effects on soil, vegetation, animals and humans. This directive sets maximum values of concentrations of heavy metals and bans the spreading of sewage sludge when the concentration of certain substances in the soil exceeds these values. The transposition of this directive into national legislation was carried out without any major difficulty. Nevertheless, this directive is currently under revision. The modifications that should be made, concern mainly the necessity for treatment in sludge before being used, the establishment of lower limits in metal content as well as the introduction of some new criteria (Fytili and Zabaniotou, 2008). Specifically, the Directorate-General for the Environment (DG Environment) of the European Commission has elaborated a working document, called the 3rd official draft from the EU (Environment DG, EU, 2000), considering more restricted parameters for land application of sludge, i.e., lower limit values for heavy metals as well as limit values for pathogens and organic micropollutants. Nonetheless, this document is not a mandatory text and should only be used for consultation purposes.

Finally it is worthwhile mentioning that sewage sludge is regarded as waste, so it is also subject to general waste legislation, i.e., to the Landfill Directive 1999/31/EC, Waste Incineration Directive 2000/76/EC, Waste Framework Directive 2008/98/EC and Industrial Emissions Directive 2010/75/EU.

1.3. Sludge treatment in a wastewater treatment plant

A typical configuration for a WWTP is shown in Figure 1.1.

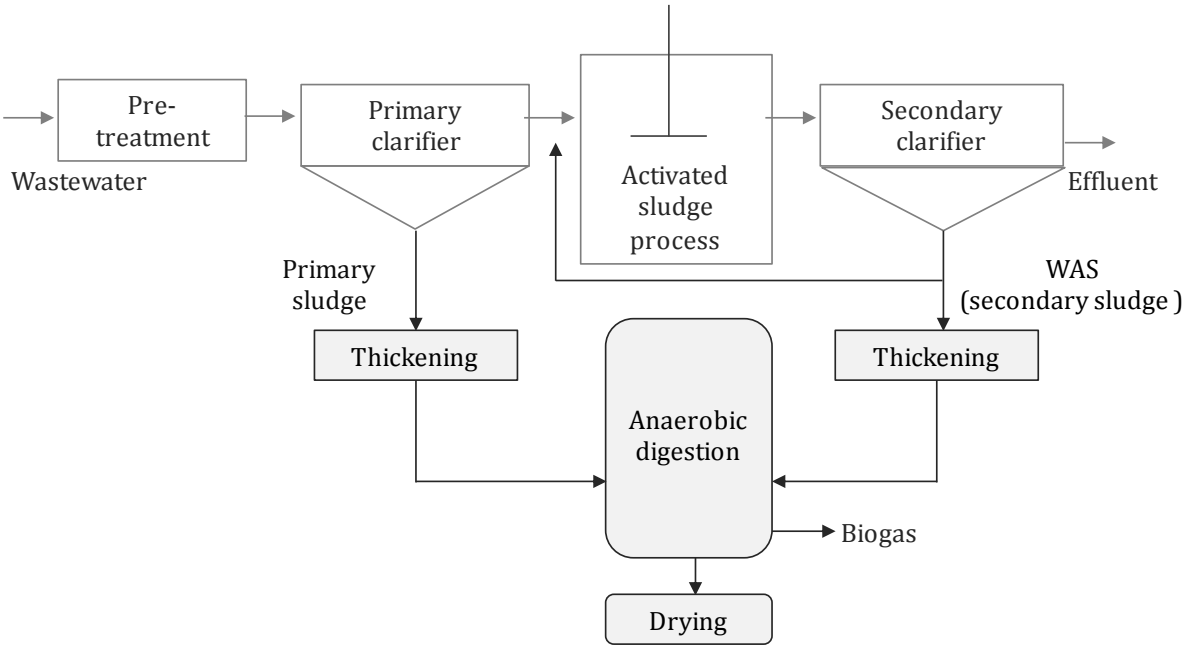

Figure 1.1. Scheme of a WWTP with primary sludge and waste activated sludge (WAS) digested together.

The two main types of sludge produced from the wastewater treatment process are primary sludge and WAS (also called biological sludge or secondary sludge). Primary sludge is a result of the capture of suspended solids and organics in the primary treatment process through gravitational sedimentation, typically by a primary clarifier. Thus, primary sludge consists of a flocculated mixture of organic and inorganic matter and is characterised for being putrescible and easy to dewater when compared to WAS. In turn, WAS is produced during activated sludge process, which consists essentially of an aerobic treatment that oxidises organic matter to CO_2 and H_2O, NH_4^+ and new cell biomass. The microbial cells form flocs that are allowed to settle in a secondary clarifier. Only part of this settled sludge (the excess WAS) is sent to subsequent treatment, whereas the remainder part is recirculated to maintain the bacterial population in the reactor. WAS consists of microorganisms (mainly bacteria), as well as organic and

inorganic matter, held together in a matrix by extracellular polymeric substances (EPSs). Two schematic representations of an activated sludge floc are provided in Figure 1.2. The overall floc structure is negatively charged due to the physicochemical interactions between bacteria, EPSs (primarily proteins, polysaccharides, humic acids and lipids) and inorganic particles (Urbain et al., 1993). The size of a floc typically ranges from 20 to 200 μm.

A

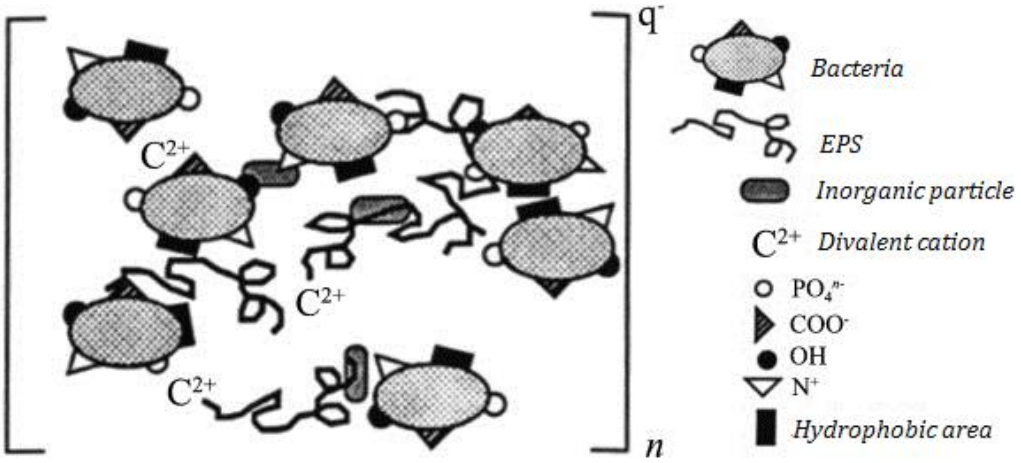

B

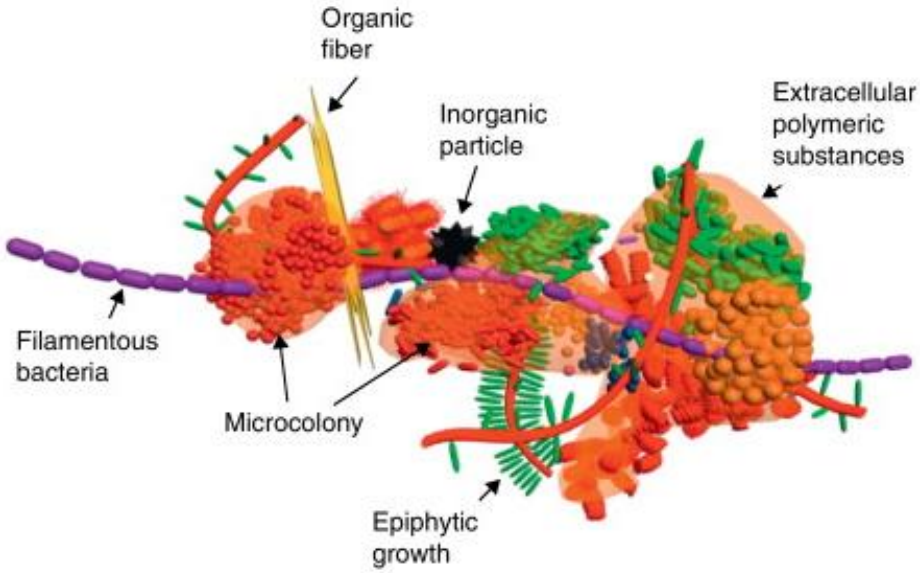

Figure 1.2. Schematic representations of an activated sludge floc from (A) Urbain et al. (1993) and (B) Nielsen et al. (2012). Filamentous bacteria often form a backbone linking the microstructures, all glued together by the extracellular polymeric substances (EPSs).

The general processes for sludge treatment comprises thickening, stabilisation and drying (Figure 1.1). Thickening is the practice of increasing solids content of sludge by the removal of a portion of its water content. The removal of water from sludge allowed the reduction in volume and consequently the size requirements for subsequent treatment units, such as the size of the digester. Thickening is accomplished by gravity thickeners, centrifuges, belt presses and diffused air floatation units. The stabilisation of sludge aims to reduce pathogens, eliminate offensive odours and reduce or eliminate the potential for putrefaction. Anaerobic digestion is currently one of the most widely adopted treatment processes for sludge stabilisation and involves decomposition of organic matter in strict anaerobic conditions. The benefits associated with anaerobic digestion include the sludge mass reduction and the generation of biogas, which is a renewable energy source (Lu et al., 2008). The drying process aims at reducing the water content of sludge, which is generally greater than 95% (Colin and Gazbar, 1995), to less than 10% by evaporation, making sludge suitable for incineration or processing into fertiliser. Mechanical dewatering is usually used prior to thermal drying and allowed to remove the free water. However, the final moisture content reached through this method is not generally sufficient and drying becomes obligatory. During sludge drying almost all water is evaporated, including surface, capillary and cell water, achieving 85-95% dry solids.

Primary sludge and WAS can be treated together, as outlined in Figure 1.1, or separately, depending on the sludge treatment strategy. Segregating primary sludge from WAS allows for better reuse, since the primary sludge can be thickened, digested and mechanically dewatered much easier alone than in a mixture with WAS (Kopp and Dichtl, 2001). In turn, WAS is better suited for agricultural reuse, containing about double concentration in nutrients but significantly less organic contaminants (Neptune Project-Deliverable 1.3). However, WAS is difficult to dewater compared with primary sludge (Chang et al., 2001) due to the existence of colloidal materials and EPSs, which strongly retain water. This behaviour generates high sludge viscosities (Neyens and Baeyens, 2003). WAS is also more difficult to digest under anaerobic conditions due to the presence of glycan strands in microbial cell walls. Numerous disintegration methods (e.g., ultrasound, thermal or alkali) have been employed for WAS conditioning under the

assumption that these methods are capable of disrupting the sludge flocs and cells, thus releasing the water trapped in interstitial spaces of flocs and microorganisms (Vesilind, 1994) and the intracellular organic matter. As a result, the dewaterability and digestibility of WAS can be improved.

1.4. Sludge disposal routes

There is no universal solution to the issue of sludge management, but the solution must be appropriate to local or national, cultural, historical, geographical, legal, political and economic circumstances (Lundin et al., 2004; Fytili and Zabaniotou, 2008). Currently, the most widely available options in the EU for sludge disposal are the agricultural use and incineration. Agricultural use is a cost-effective solution, but the use of sludge in agriculture is limited to its quality. When properly treated and processed, sewage sludge becomes biosolids, which can be safely recycled and applied as fertiliser to sustainably improve and maintain productive soils and stimulate plant growth. However, sludge is being produced all year round, whereas its application on land takes place once or twice a year; consequently the sludge should be stored (Fytili and Zabaniotou, 2008). Conversely, incineration with energy recovery provides a large volume reduction of sewage sludge and results in improved thermal efficiency. Thus, for larger cities where available land is limited and the quality of sludge is questionable, energy recovery is a better alternative. However, the scrubbing costs of the product gases for air pollution control are usually very high. Moreover, incineration does not constitute a complete disposal method since approximately 30% of the solids remain as ash (Malerius and Werther, 2003).

Figure 1.3 shows the common sludge disposal routes for the EU-15 for year 2010 (the most recent available data for the EU-15 are these of 2010). At the moment, the distribution of applied sludge disposal methods in whole European Union (EU-28) is very close to that of EU-15, as the old Member States produce almost 90% of the total amount of sludge (http://epp.eurostat.ec.europa.eu). Sludge reuse (including direct agricultural application and composting) seems to be the predominant choice for sludge management in EU-15 (59% of produced sludge), following by incineration (29% of

produced sludge). This is consistent with the hierarchy set by the Waste Framework Directive 2008/98/EC, where reuse comes before energy recovery. The sludge disposal in landfills presents a significant and continuing decrease due to EU recent legislation and increased costs (Kelessidis and Stasinakis, 2012).

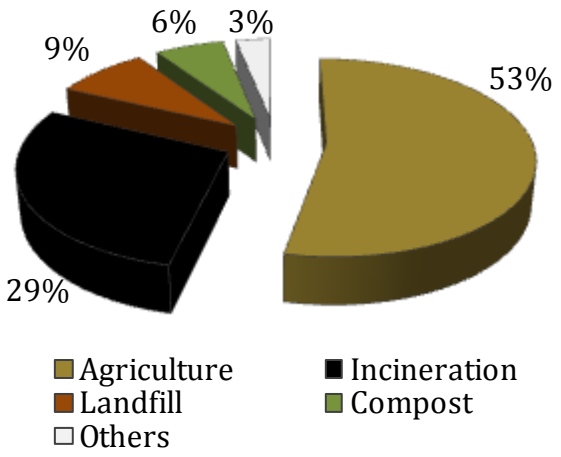

Figure 1.3. Sewage sludge disposal methods in EU-15 for year 2010 (data obtained from http://epp.eurostat.ec.europa.eu/).

Chapter 2 State of the art on sludge disintegration

In addition to the general processes for sludge treatment (thickening, stabilisation and drying), there are also a number of treatments which aims at improving the sludge treatment train. These treatments can be located in a number of places in the WWTP depending on the needs. The objectives of the overall treatment train is to remove organic material and water, thus reducing volume and mass, remove degradable material, which prevents subsequent odours, and remove pathogens (Carrère et al., 2010). As explained in the previous chapter, WAS is difficult to dewater and digest and therefore needs to be broken down in order to release the water trapped within sludge flocs and increase its biodegradability. In this context, a pre-treatment for dewatering and anaerobic digestion is required. On the other hand, those treatments that allow sludge hygienisation can be used as post-treatment.

In this chapter, the major classes of biological, mechanical, thermal and chemical treatments are described, with particular emphasis on the ultrasound, low-temperature thermal and alkali treatments because they are the object of study of this thesis.

2.1. Sludge disintegration methods

2.1.1. Biological treatment

The biological treatment can be considered as a partial digestion, which aims at enhancing the hydrolysis[4] process in an additional stage prior to the main digestion process (Carrère et al. 2010). It is based on the effect of hydrolytic enzymes (also known as hydrolases), which are produced and released by the microorganisms in activated sludge to degrade the complex organic matter. The hydrolytic enzymes that have been detected in sludge are mainly proteases, aminopeptidases, dehydrogenases, galactosidases, glucosidases, lipases and phosphatases (Nabarlatz et al., 2010). These enzymes are useful to improve the degradation of sludge itself and to increase the biogas production during the anaerobic digestion (Yu et al., 2013), since they can break down EPSs through multi-step processes, during which compounds can be transformed from a recalcitrant state to one that is more biodegradable (Gianfreda and Rao, 2004). However, it was demonstrated that the free enzymatic activity present in the activated sludge is almost negligible (Cadoret et al., 2002) and therefore hydrolytic enzymes should be externally added to increase the efficiency.

The biological treatment can be conducted in two ways: (1) adding commercial enzymes (Yang et al., 2010); (2) adding specific bacteria which can secret certain enzymes (Tang et al., 2012). It should be noted that the commercial enzymatic preparation represents a high cost and therefore the inoculation of enzyme producing strains is concerned as the proper way to conduct the treatment (Yu et al., 2013). Another option is the extraction and recovery of the enzymes contained in the own sludge. However, still there is not a unique method allowing to extract the maximum amount of all the enzymes present in the WAS, and therefore further studies must be carried out to optimise the enzyme extraction process.

Temperature and pH have a great influence on hydrolytic enzymes activity. Temperatures in the range of 50-60 °C appear to give the best performance, while temperatures higher than 70 °C cause the inactivation of enzymes (Whiteley et al.,

[4] Hydrolysis is considered the rate-limiting step during waste activated sludge degradation.

2002). Regarding the pH, Whiteley et al. (2002 and 2003) found that the lipases showed optimum activity in a pH range of 6.5 to 8, while the proteases and phosphatases had greatest activity at pH 10 and 4.5, respectively.

The advantage of biological treatment compared to chemical or physical processes is that it does not cause pollution and does not need any special equipment (Parawira, 2012).

2.1.2. Mechanical treatment

Mechanical treatment employs several strategies for physically disintegrating the cells and partially solubilising their content. Some of these techniques are lysis-centrifuge, collision plate, high-pressure homogeniser, stirred ball mills and ultrasonication.

2.1.2.1. Lysis-centrifuge

Lysis-centrifuge is a thickening centrifuge equipped with additional rotating cutting tools for sludge disintegration. Thus, by using this equipment, thickening and partial disintegration of sludge can be obtained simultaneously. This method allows treating large volumes of sludge with moderate energy consumption.

Lysis-centrifuge produced a significant increase in sludge biodegradability, with an increase of biogas production during anaerobic digestion (Foladori et al., 2010). There are several full-scale implementations, which registers an increase in biogas production of 15-26% (Carrère et al., 2010).

Another advantage of this method relates to the significant reduction of sludge viscosity. The pumping limit for thickened sludge is generally held to be around 6% sludge total solids (TS). At higher TS content, clogging problems may occur in the head piping. In this context, disintegration using the lysis-centrifuge allows sludge to be thickened up to 9-11% TS, while maintaining pumpability (Foladori et al., 2010).

2.1.2.2. Collision plate

Sludge is pressurised to 30–50 bar by a high pressure pump and hurled to a collision plate with velocities of 30–100 m/s (Carrère et al., 2010). The sludge that collides with the plate breaks the bacterial cell membranes, thus improving sludge solubilisation and increasing the availability of the degradable matter.

This process has only been applied at laboratory scale and allowed a decrease in the anaerobic digester hydraulic retention time from 13 to 6 days, without major effects on the process performance and on effluent quality (Nah et al., 2000).

2.1.2.3. High-pressure homogeniser

A high-pressure homogeniser consists of (1) a high pressure pump which compresses sludge to pressures up to 900 bar (Carrère et al., 2010) and (2) an adjustable homogenisation valve where sludge decompression to atmospheric pressure takes place (Figure 2.1).

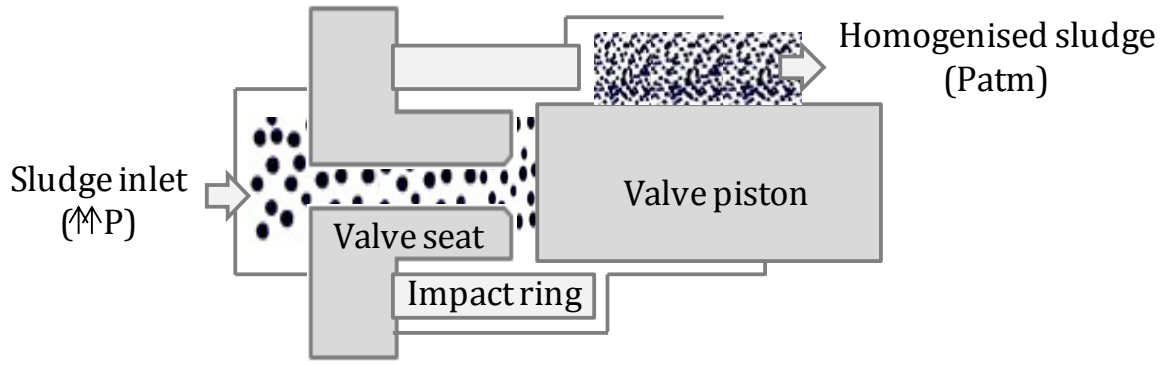

Figure 2.1. Section of a homogenisation valve.

When sludge passes through the homogenisation valve, its speed increases up to fifty times (up to 300 m/s) due to the intense restriction. The speed increase causes a rapid drop of pressure to below vapour pressure (cavitation) and induces collisions among sludge particles. These reactions cause the disaggregation of flocs and the rupture of cells (Foladori et al., 2010).

This process has been tested at full-scale for anaerobic digestion. According to Onyeche (2007), the treatment of a fraction of digested sludge at 150 bar followed by their subsequent reintroduction in the digester, led to an increase of biogas production by 30% and a reduction of sludge volume by 23%. However, sludge dewaterability decreased (Barjenbruch and Kopplow, 2003).

2.1.2.4. Stirred ball mills

Stirred ball mills treatment employs a cylindrical grinding chamber (vertical or horizontal) almost entirely filled with grinding spheres that rotate under the action of a high speed stirrer (Giachino, 2011). The spheres are made of steel or ceramic materials and are forced to collide with each other. A simplified configuration of a stirred ball mill is shown if Figure 2.2.

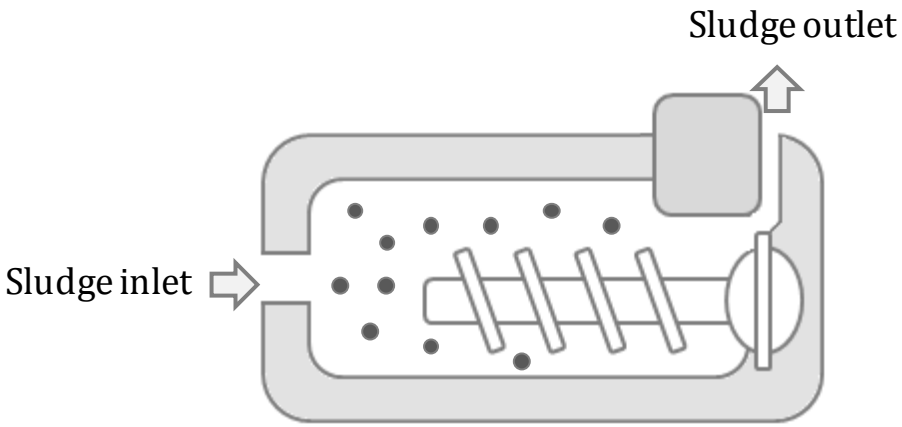

Figure 2.2. A simplified configuration of a stirred ball mill.

Sludge and microbial cells are disrupted in the contact zone of the spheres due to the shearing action and by energy transfer from balls to cells (Foladori et al., 2010). The effectiveness of this treatment improves when the sphere size decreases. Spheres of 0.10-0.15 mm are used to obtain the disaggregation of biological flocs and also the disintegration of microbial cells. However, in full-scale applications, spheres of a greater size (0.4-0.6 mm) are more suitable because it is easier to separate them from the sludge at the sieve. Another important operational factor is the rotational speed; a rotational

speed over 10 m/s is recommended for the disintegration of bacterial cells (Foladori et al., 2010). The contact time of sludge in stirred ball mills is few minutes.

This process has been tested at full-scale (Netzsch and Draiswerke technologies) as pre-treatment before anaerobic digestion. Wett et al. (2010) found that the ball mill technique achieved a solubilisation rate of 28% and increased biogas production by approximately 41%. This treatment also improves sludge dewatering (Foladori et al., 2010). The main drawback of this technique is the high energy demand.

2.1.2.5. Ultrasound treatment

Ultrasound treatment can disrupt the sludge floc matrix due to the hydro-mechanical shear forces produced by cavitation bubbles. This treatment is described in detail in Section 2.2, as it is one of the treatments studied in the research part of this thesis (Chapter 4 onwards).

2.1.3. Thermal treatment

Thermal treatment has been studied using a wide range of temperatures ranging from 60 to 270 ºC (Climent et al., 2007). Temperatures higher than 180 ºC have found to reduce the biodegradability of the sludge, since formation of refractory compounds is observed (Stuckey and McCarty, 1984; Wilson and Novak, 2009). Thus, the most common treatment temperatures are between 60 and 180 ºC (Climent et al., 2007). Treatments applied at temperatures up to 100 ºC are considered as low-temperature thermal treatments (Gavala et al., 2003).

2.1.3.1. Thermal hydrolysis (T >100 ºC)

Thermal hydrolysis partially solubilises the sludge, which enhances anaerobic digestion (Bougrier et al., 2006; Mottet et al., 2009). Specifically, it results in increased hydrolysis rates and the consequent reduction of the hydraulic retention time in the digester. The highest yield of hydrolysis was found to be at temperatures between 160-180 ºC and

treatment times from 30 to 60 min (Carrère et al., 2010). Under these conditions, the increase in biogas production in activated sludge ranged from 40 to 100%.

According to Carrère et al. (2008), the increase in methane production has been linked to sludge COD solubilisation by linear correlations. Nevertheless, Dwyer et al. (2008) found that at temperatures above 150 ºC, the increased solubilisation does not result in an increase in methane conversion. Similarly, Wilson and Novak (2009) found that temperatures higher than 180 ºC lead to the formation of recalcitrant soluble organics or toxic/inhibitory intermediates, thus reducing the biodegradability in spite of achieving high solubilisation efficiencies. This is usually ascribed to the so called Maillard reactions (Dwyer et al., 2008), involving carbohydrates and amino acids in the formation of melanoidins, which are difficult or impossible to degrade (Bougrier et al., 2008).

Thermal hydrolysis also improves sludge dewaterability since it allows degradation of the sludge structure and the subsequent release of trapped water (Neyens and Baeyens, 2003). Other advantages include sludge hygienisation and viscosity reduction, thus enhancing sludge handling. The main disadvantage is the high energy requirement for heating the sludge. Nevertheless, thermal hydrolysis may result in net energy production because of increased biodegradability and reduced digester heating requirements (Carrère et al., 2010).

Sludge thermal hydrolysis is a well-known technology used at labscale and full scale. Some industrial processes such as Cambi and Biothelys have been commercialised. Both processes consist of a treatment at 150–180 ºC during 30–60 min, by vapour injection. The Cambi process doubles digester capacity, reduces sludge volume by increasing biogas production and dewaterability, while converting sludge to a low-odour and disinfected soil conditioner.

2.1.3.2. Low-temperature thermal treatment (T ≤100 ºC)

Low-temperature thermal treatment has been pointed out as an effective treatment for increasing biogas production and reducing pathogen loads. This treatment is described

in detail in Section 2.3, as it is one of the treatments studied in the research part of this thesis (Chapter 4 onwards).

2.1.4. Chemical treatment

The chemical treatment of sludge may be accomplished by using chemical oxidants (such as ozone), acids or alkalis, as discussed below.

2.1.4.1. Oxidation methods

The process of sludge ozonation is generally described by the sequential reactions of floc disintegration, solubilisation and subsequent oxidation of the released organics into carbon dioxide (mineralisation). Ozone (O_3) can be industrially produced with a well established technique, based on ionisation of air or pure oxygen by means of a high voltage electrical discharge. Ozonation is a well proven technology for sludge reduction and is successful in full-scale plants. The main advantages of ozonation include the improvement of sludge settleability and the enhancement of methane production during anaerobic digestion (Chu et al. 2009). The main drawback is the high capital costs related to equipment and high operational costs for ozone production.

Hydrogen peroxide (H_2O_2), Fenton process (Fe^{2+} + H_2O_2) and wet oxidation (a treatment in which oxygen or air is used as oxidant) have also been found effective for disintegration of municipal sludge. Hydrogen peroxide yields no noxious or polluting by-products (its only by-products are water and oxygen). It can oxidise a wide variety of aqueous pollutants, reduce odours and destroy pathogenic organisms (Gogate and Pandit, 2004). According to Pham et al. (2010), Fenton oxidation decreases the apparent viscosity, increases the particle size (due to the reaggregation of sludge particles) and improves the dewaterability and biodegradability of the sludge. Wet oxidation is considered to be an effective alternative for the solubilisation and mineralisation of WAS. Typical conditions for wet oxidation are temperatures between 150 and 320 ºC and pressures between 20 and 150 bar (Hii et al., 2014).

2.1.4.2. Acid hydrolysis

Treating activated sludge with sulphuric acid or together with surfactant is reported to be an effective method to improve its dewaterability and settleability. Chen et al. (2001) illustrate that the optimum pH value for filtration dewatering is 2.5. A further decrease of the pH does not improve the dewatering capacity. One possible explanation for the enhancement of dewatering after sulphuric acid treatment is the solubilisation of EPS in the supernatant, which makes it easy to pack the sludge aggregates.

2.1.4.3. Alkali treatment

Alkali treatment can be effective in solubilising the sludge, but it can diminish sludge dewaterability depending on the alkali added and concentration used. This treatment is described in detail in Section 2.4, as it is one of the treatments studied in the research part of this thesis (Chapter 4 onwards).

2.2. Ultrasound treatment

The ultrasound is cyclic sound pressure (compression and rarefaction) with a frequency greater than 20 kHz (Pilli et al., 2011). The ultrasound range is divided in three regions depending on the frequency: (1) power ultrasound (20–100 kHz), (2) high frequency ultrasound (100 kHz–1 MHz), and (3) diagnostic ultrasound (1–500 MHz). In sludge treatment, low frequencies (20–40 kHz) are the most efficient (Carrère et al., 2010).

2.2.1. Ultrasound disintegration mechanism: the cavitation phenomena

The cavitation phenomena is the formation, growth and violent collapse of cavitation bubbles, caused by alternate compression and rarefaction cycles of ultrasound waves travelling through the liquid (in this case, the sludge medium) (Gallipoli and Braguglia, 2012). The compression cycles exert a positive pressure on the liquid by pushing the molecules together and the rarefaction cycle exerts a negative pressure by pulling the molecules from one another. The cavitation bubbles are formed in the rarefaction region

and then grow in successive cycles until they reach an unstable dimension that make them collapse violently producing shock waves (temperature of around 5000 ºC and pressure of 500 atmospheres at a lifetime of few microseconds) (Pilli et al., 2011). This violent collapse generates powerful hydro-mechanical shear forces in the bulk liquid surrounding the bubbles. Representation of development and collapse of the cavitation bubble is shown in Figure 2.3.

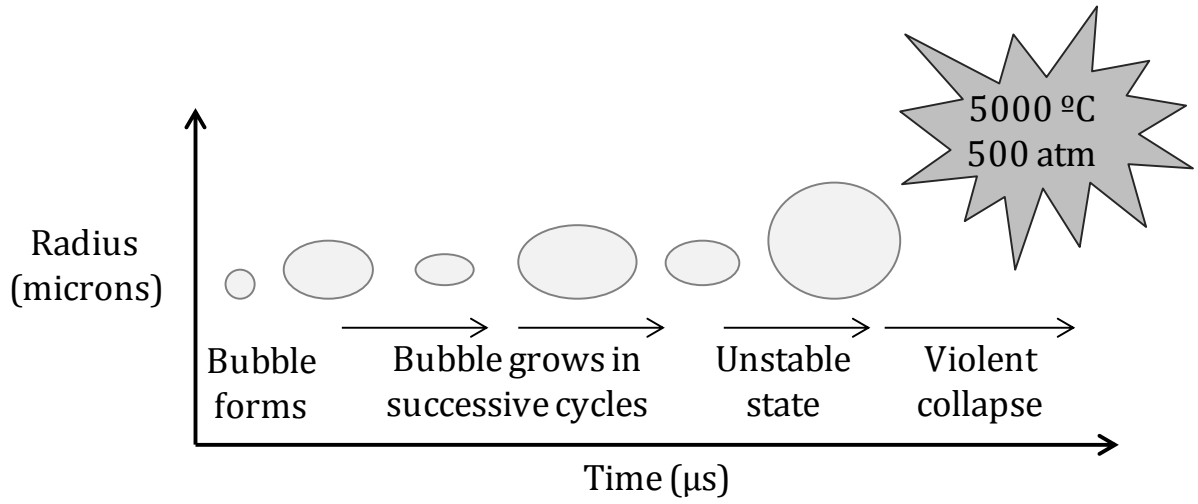

Figure 2.3. Development and collapse of a cavitation bubble (Pilli et al., 2011).

Moreover, the high temperature produced decomposes water into extremely reactive ionised hydrogen atoms (H^+) and hydroxyl (OH•) radicals. In this context, sludge disintegration is expected to occur in two ways: by hydro-mechanical shear forces and by the oxidising effect of OH•. However, Wang et al. (2005) found that the oxidation effect of OH• on sludge disintegration is negligible; they added $NaHCO_3$ to mask the oxidising effect of OH• and obtained similar results with and without adding $NaHCO_3$. Therefore, the disintegration of the sludge occurs mainly by hydro-mechanical shear forces produced by cavitation bubbles.

The cavitation phenomenon is highly dependent on the temperature of bulk solution. With increase in temperature, the solvent reaches the boiling point and produces larger number of cavitation bubbles, which acts as barrier to sound transmission and nullifies the effectiveness of ultrasound energy.

2.2.2. Evaluation of ultrasound disintegration

The most common way to express the energy applied in order to disintegrate the sludge is the specific energy, E_S (kJ/kg TS), which can be calculated as:

$$E_S = \frac{P \cdot t}{V \cdot TS} \tag{2.1}$$

where P is the ultrasonic power of the ultrasonic homogeniser (kW), t is the application time (s), V is the sample volume (L) and TS is the concentration of total solids (g/L).

The ultrasound technique leads to sludge floc disintegration and microorganisms lyses, according to the treatment time and power (Chu et al., 2002). Therefore, the physical and biochemical properties of sludge change during ultrasonication. Some of these changes are detailed below:

- *Changes in particle size*. The particle size reduces gradually with increase in sonication time. For instance, Wang et al. (2014) observed a particle size reduction from 128 μm to 56, 35 and 24 μm after treating with E_S of 7500, 30,000 and 75,000 kJ/kg TS, respectively.
- *Changes in viscosity*. Very few studies are found in the literature regarding the effect of ultrasound on sludge viscosity. Bougrier et al. (2006) found that the apparent viscosity decreases approximately 60% after ultrasonication at an E_S of 6250 kJ/kg TS.
- *Changes in dewaterability*. Experimental results regarding the effect of ultrasound on sludge dewaterability are contradictory, with positive or negative impacts. The dewaterability is often assessed in terms of the capillary suction time (CST), which indicates how quickly sludge releases its water. It is reported that the CST increases gradually with increased in ultrasonication intensity (Quarmby et al., 1999; Chu et al., 2001), which suggests that the dewaterability worsens. Specifically, Feng et al. (2009a) found that application of low E_S (<4400 kJ/kg TS) slightly enhanced sludge dewaterability, whereas larger E_S

(>4400 kJ/kg TS) significantly deteriorated it. On the other hand, Kim and Kim (2003) found that ultrasonication reduced the drying time, resulting in an increase in drying efficiency.

- *Changes in settleability*. According to Feng et al. (2009b), E_S greater than 5000 kJ/kg TS deteriorate the settleability of sludge due to the complete breakdown of flocs.
- *Changes in turbidity*. Due to the release of microparticles into the supernatant, the turbidity of the supernatant drastically increases at E_S greater than 5000 kJ/kg TS (Feng et al., 2009b). Conversely, E_S below 1000 kJ/kg TS cannot disrupt large amounts of sludge into the supernatant and therefore the turbidity does not increase. Thus, the minimum energy required to disrupt the sludge is 1000 kJ/kg TS.
- *Biochemical evaluation*. The soluble COD can be used as a parameter to evaluate the sludge disintegration. The ultrasonication increases the concentration of soluble COD by breaking the sludge flocs, thus releasing the extracellular organic compounds into the supernatant. Salsabil et al. (2009) found that the COD solubilisation increased linearly with increasing E_S. Other parameters, such as the ammonium nitrogen, nitrate nitrogen and EPS concentrations (proteins, polysaccharides, nucleic acids, lipids and other polymeric compounds) are also important parameters in chemical evaluation after sludge ultrasonication.

2.2.3. Effect of ultrasound on sludge anaerobic digestion

Ultrasound has widely been applied as pre-treatment for anaerobic digestion; some results are summarised in Table 2.1. As can be observed, the biogas production increases with the energy input. This increase is because the ultrasound solubilised particulate organic matter from the sludge, making it available for the methanogenic bacteria responsible for digestion. Bougrier et al. (2005) reported that when the supplied energy is higher than 7000 kJ/kg TS, biogas generation is constant and solubilisation is less marked. Specifically, they found that for supplied energies of 7000 and 15,000 kJ/kg TS, biogas production was almost the same. Conversely, Salsabil et al.

(2009) registered an important improvement of anaerobic digestion (an increase of 84% in biogas production) when treating with an E_S of 108,000 kJ/kg TS.

Table 2.1. Overview of some ultrasound treatment studies on anaerobic digestion of WAS.

Ultrasound treatment	**Anaerobic digestion**	**Results**	**Reference**
20 kHz 9690 kJ/kg TS	Batch, 35 days 36 ºC	Increase of biogas production (~44%)	Erden and Filibeli (2009)
20 kHz 7000 and 15,000 kJ/kg TS	Batch, 16 days 35–37 ºC	Increase of biogas production (~40%)	Bougrier et al. (2005)
200 kHz 25,000 kJ/kg TS	Batch, 20 days 37 ºC	Increase of biogas production (~40%)	Braguglia et al. (2012)
20 kHz 108,000 kJ/kg TS	Batch, 50 days 37 ºC	Increase of biogas production (~84%)	Salsabil et al. (2009)

TS: total solids

2.2.4. Full-scale implementation

The ultrasound has been implemented in industry primarily as pre-treatment for anaerobic digestion and also for improving sludge dewaterability. There are currently two approaches on how to employ ultrasound, based on the quantity of the sludge stream to be sonicated: full-stream and part-stream sonication. The full-stream approach involves treating the entire sludge stream with ultrasound, whereas a part-stream approach involves treating only a fraction of the sludge stream (Pérez-Elvira et al., 2010). Most of the suppliers of ultrasound devices use part-stream approach due to lower running costs. Plant-scale ultrasonication is usually implemented by the following four industries (Neptune Project-Deliverable 1.3):

- *IWE Tec Ultrasound System.* This system operated at sonication times of 30 to 60 s and employs “cascade” probes, each installed within a cylindrical reactor

(Khanal, 2008). The commercially available units are commonly equipped with either 2 or 4 kW probes and are designed to operate between 50 and 75% of the maximum power.

- *Sonico*. This system is composed of individual radial horns (of 2, 3 or 6 kW) that are shaped like a ring. Horns are mounted in series in a reactor that typically contains three or five horns. The system is designed to typically run at 70 to 75% of the maximum amplitude sonication and operates at sonication times of around 2 s.
- *UltraWaves Ultrasound System*. The reactor typically contains five probes (of 2 kW each one). The systems typically operate at 50% power draw and sonication times of approximately 2 s.
- *VTA Technology*. This technology developed and patented the reverse flow disintegration unit, which achieves the disintegration effect by means of ultrasound at 25 kHz frequency. By means of an agitator the sludge suspension is treated by continuously being passed through the ultrasonic oscillators.

2.3. Low-temperature thermal treatment

As mentioned in Section 2.1.3.1, thermal hydrolysis (T >100 ºC) implies high energy requirements for bringing the sludge to the disintegration temperature. This largely reduces the overall profitability of the process. In this context, the application of low-temperature thermal treatment (T ≤100 ºC) could form an alternative to overcome this drawback. However, although this treatment implies lower energy consumption, few references are found in the literature, most of them regarding the improvement on sludge biodegradability.

2.3.1. Effect of temperature on sludge anaerobic digestion

Low-temperature thermal treatment has been pointed out as an effective pre-treatment for increasing biogas production from both primary sludge and WAS (Gavala et al., 2003). At low temperatures, treatment time plays a more important role than treatment

temperature. Table 2.2 shows an overview of some low-temperature thermal treatments as pre-treatment for anaerobic digestion.

Table 2.2. Overview of some low-temperature thermal treatment studies on anaerobic digestion of WAS.

Treatment	**Results**	**Reference**
60-100 ºC 30 min	Studied mesophilic digestion. The methane generation increased by approximately 30-52%. Maximum increase of methane generation (52%) was achieved for the temperature of 60 ºC.	Wang et al. (1997)
70 ºC 1-7 days	Studied mesophilic and thermophilic digestion. The net methane production was only increased upon mesophilic digestion; with 1 and 7 days of pre-treatment duration, the methane production increased by 20 and 26%, respectively.	Gavala et al. (2003)
70 ºC 9-72 h	Studied thermophilic digestion. Maximum increase of biogas production (58%) at 9 h. Surprisingly, biogas production at 72 h was almost equal to that of untreated sludge.	Climent et al. (2007)
70-90 ºC 15-60 min	Studied mesophilic digestion. Biogas production increased significantly at 90 ºC (>100%), especially for the 60 min treatment. Biogas production remained constant at 70 ºC.	Appels et al. (2010)
50-95 ºC 20 min	Studied mesophilic digestion. The final biogas production was negligible.	Audrey et al. (2011)
70 ºC 9 h	Studied mesophilic digestion. Biogas production increased by 32%	Xu et al. (2014)

The results reported for mesophilic anaerobic digestion emphasise the importance of selecting the proper treatment time (Table 2.2). Audrey et al. (2011) studied the effect of thermal treatment (50-95 ºC) at a short treatment time (20 min). Under these conditions, it was observed a release of organic components from the particulate to the soluble fraction, but the biogas production barely increased. The particle size distribution revealed that these conditions induced only a deflocculation of macroflocs structure but no significant floc breakage. Thus, according to Audrey et al. (2011), the improvement of WAS biodegradability require both intracellular material release (cell lysis) and complete floc disintegration (EPSs disruption). Wang et al. (1997) used a slightly longer treatment time (30 min) and observed an increase in methane production of approximately 52% at 60 ºC. Similarly, Appels et al. (2010) registered an important increase in biogas production (>100%) for sludge pre-treated at 90 ºC for 60 min. Xu et al. (2014) further increased the pre-treatment time (9 h), but obtained a lower biogas production increase (32%) than the previous authors. Similar results were reported by Gavala et al. (2003). According to Climent et al. (2007), this may be because of the high increase in the volatile fatty acids (VFA) concentration when treatment times are long, which may inhibit the microbial activity to some extent leading to a lower production of biogas. From these results it can be concluded that the proper treatment times are those neither too short nor too long.

Gavala et al. (2003) studied the effect of thermal pre-treatment (70 ºC, 1-7 days) followed by mesophilic and thermophilic digestion and found that the net methane production was only increased upon mesophilic digestion. This may be because thermophilic digestion suffers from a higher degree of product and/or substrate inhibition.

2.3.2. Effect of temperature on sludge viscosity

It is generally agreed that increase in temperature will result in a decrease in sludge viscosity (Battistoni et al., 1993; Baudez et al., 2013; Ruiz-Hernando et al., 2013). However, according to Moreau et al. (2009), the temperature effect is not significant if the temperature range examined is approximately room temperature or even lower. The

relationship of sludge viscosity and temperature can be described with an Arrhenius type equation (Equation 2.2):

$$\eta_\infty = A\ exp\left(\frac{E_a}{RT}\right) \tag{2.2}$$

where η_∞ is limit viscosity, A is empirical constant, T is absolute temperature, R is universal gas constant, and E_a is the activation energy.

Equation 2.2 has been used to describe temperature effect on limiting viscosity of several types of sludge (Eshtiaghi et al., 2013). Other equations, such as the Vogel-Tammann-Fulcher, have also been used. However, it was observed that thermal history may have a strong impact on the viscosity of sludge. Baudez et al. (2013) found that if sludge is heated and cooled before measurement, its rheological behaviour is irreversibly altered due to the conversion of solids into dissolved constituents. Accordingly, the usual laws used to model viscosity-temperature dependence are not entirely valid because such laws can only be used when the composition remains constant.

Farno et al. (2014) studied the effect of temperature (50-80 ºC) at different treatment times (1, 15 and 30 min) on anaerobic digested sludge, and found that the sludge becomes less viscous as the temperature increases. They also found that when increasing the treatment time at a fixed temperature, the sludge becomes less viscous in the low shear rate range (20 s^{-1}) and more viscous in high shear rate range (280 s^{-1}). According to Farno et al. (2014), this is because at low shear rates, the potential energy of mutual interactions depends basically on the spatial configuration of particles, whereas at high shear rates (or hydrodynamic regions), the suspension viscosity strongly depends on the interstitial fluid. Thus, when increasing the duration of thermal treatment, the viscosity of the liquid medium (interstitial fluid) of sludge increased, and consequently, the viscosity of sludge (the mixture of particles and liquid medium) increased at high shear rates.

2.3.3. Effect of temperature on pathogen inactivation

Pathogens are inactivated during exposure to heat, which to be effective and relatively rapid must be above their optimum growth temperature. Pathogens that may be found in sludge include bacteria (e.g., *Salmonella* species (spp.), *Escherichia coli, Clostridium perfringens*), viruses (e.g., rotavirus, hepatitis A-virus), protozoa (e.g., *Giardia lambia*), helminths (e.g., *Taenia saginata*), yeast (e.g., *Candida albicans*) and fungi (e.g., *Aspergillus* spp.) (EC, 2001). The treatment time needed for inactivation of the pathogens is dependent on the temperature and on the species of organisms. Based on the knowledge of typical concentration of pathogenic microorganisms in raw materials and the heat resistance of these pathogens, the minimum time-temperature treatment for inactivation of the pathogens (the "safety zone") can be calculated (Strauch, 1991) (Figure 2.4).

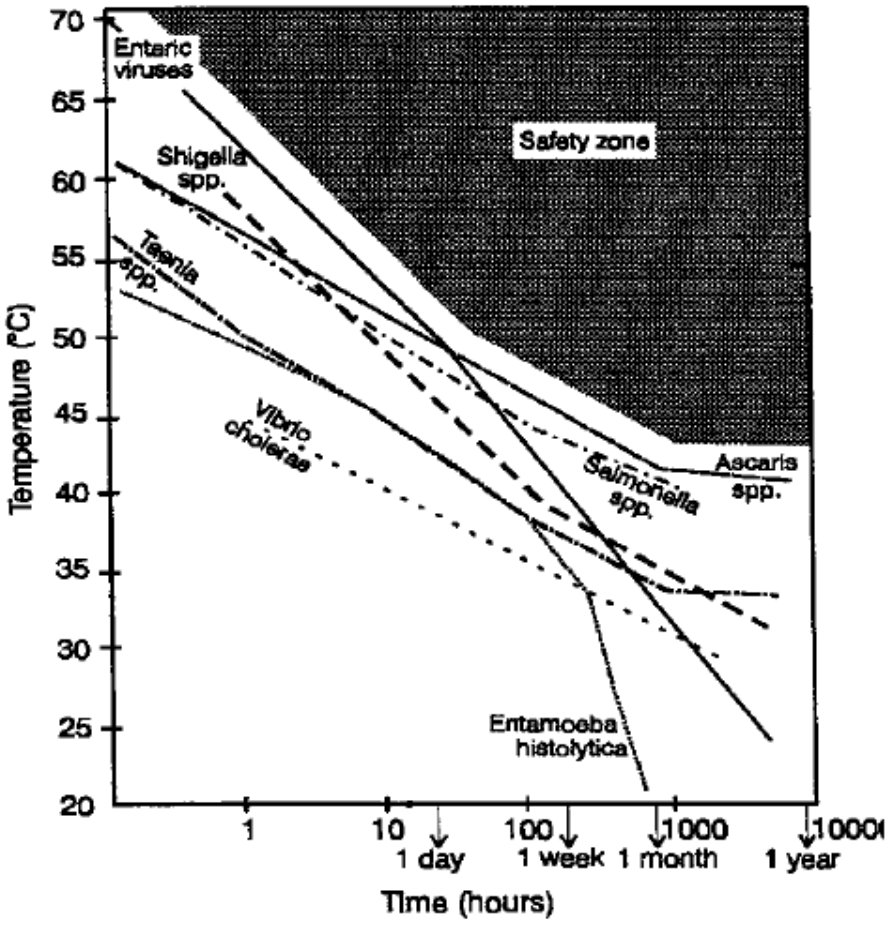

Figure 2.4. Time-temperature requirements to produce a virtually pathogen-free sludge (EC, 2001).

If the operating parameters are above the minimum requirements shown in Figure 2.4, the resultant sludge would be virtually pathogen-free. The data from Figure 2.4 suggest that the operating parameters should be in excess of 7 min at 70 ºC; 30 min at 65 ºC; 2 hours at 60 ºC, 15 hours at 55 ºC or 3 days at 50 ºC. However, plant design constraints indicate that the minimum time for exposure should be 30 min (which means a minimum temperature of 65 ºC).

Finally, it is important to note that some pathogens may be even more heat resistant. Especially, some plant pathogens and spore forming bacteria have been found to be difficult to inactivate (EC, 2001). According to Mocé-Llivina et al. (2003), bacteriophages[5] are significantly more resistant to thermal inactivation than bacterial indicators, with the exception of spores of sulfite-reducing clostridia.

2.3.4. Devices for low-temperature thermal treatment

Since low-temperature treatment occurs below 100 ºC, it is easier to operate compared to thermal hydrolysis, which is usually associated with high pressure. This means that the treatment reactor configuration generally involves standard stirred-tanks (continuous or semi-batch), which are preferred from a process point of view. However, continuous stirred-tanks cannot guarantee a fixed retention time for the entire feed quantity. When a specific retention time must be guaranteed (for instance for ensure pathogen inactivation), bach or plug-flow reactors must be used (Paul and Liu, 2012).

Methods of heating can be divided into either direct heating or heat exchange (with issues similar to those of normal digester sludge heating) (Paul and Liu, 2012). Methods for direct heating may include:

- *Direct hot water injection*.
- *Direct steam injection.*
- *Biochemical production of heat by autothermal aerobic digestion*.

[5] Bacteriophage: a virus that infects and replicates within a bacteria.

Heat exchange based methods include:

- *Heating of the feed steam*. This is commonly used where mixing is by gas or by mechanical impeller. It allows the recovery of the effluent heat and working at a greater ΔT between the hot and cold sides. Disadvantages include low heat transfer coefficients due to high fluid viscosities.
- *Recirculation heating.* This is commonly used where hydraulic mixing is used. It will have a better heat transfer coefficient due to better fluid properties, but normally works at a lower ΔT.

2.4. Alkali treatment

The mechanism of alkali treatment is to induce swelling of particulate organics at high pH, making the cellular substances more susceptible to enzymatic reaction (Baccay and Hashimoto, 1984). It has advantages of simple device, convenient operation and high efficiency.

2.4.1. Effect of alkali treatment on sludge anaerobic digestion

Most investigations have indicated an increase of biogas production and a decrease in volatile solids after alkali pre-treatment. Generally, the preferred chemical is sodium hydroxide (NaOH), which at relatively low dosage level is effective in solubilising nitrocellulose (which is resistant to direct degradation) into soluble organic carbon forms (Lin et al., 2009). Specifically, NaOH yields greater solubilisation efficiency than KOH, $Ca(OH)_2$ or $Mg(OH)_2$ (Kim et al., 2003). In most cases, the optimum dose of NaOH was at a level of 80–160 g/kg TS (Lin et al., 1997; Lin et al., 2009). Lin et al. (2009) registered similar increases (83 and 88%) in methane productivity after treating the sludge with NaOH doses of 80 g/kg and 160 g/kg. On the other hand, Navia et al. (2002) registered the maximum COD solubilisation at a NaOH dose of 250 g/kg TS. Higher doses led to a limited increase in solubilised sludge organic matter, but the residual NaOH would require more HCl for neutralisation and the higher concentration of Na^+ may also inhibit the activity of microorganisms (Li et al., 2012).

2.4.2. Effect of alkali treatment on sludge dewatering

Alkali treatment can disrupt flocs and cells and release the internal water, which cannot be removed by conventional dewatering processes (Li et al., 2009). Alkali treatment with $Ca(OH)_2$ is very useful for improving sludge dewaterability because calcium cations can enhance the reflocculation of soluble organic polymers. On the other hand, the effectiveness of the NaOH treatment in sludge dewatering will depend on the concentration used. According to Li et al. (2008), when the NaOH concentration is lower than 0.2 mol/L, fine particles, hydrophilic organic polymers and vicinal water content all increase, and sludge dewaterability deteriorates significantly. Conversely, when the NaOH concentration is higher than 0.2 mol/L, some disrupted floc fragments can be reflocculated with the help of dissolved organic polymers, thereby leading to obvious improvement in the sludge dewaterability (Li et al., 2008).

2.4.3. Effect of alkali treatment on pathogen inactivation

Alkali treatment can achieve sludge hygienisation, but the reported effectiveness of this treatment varies greatly. Factors that may contribute to this variability include temperature, the type and dose of alkalinising agent, the maximum pH attained, and the pH profile during storage (Pecson et al., 2007). Carrington et al. (1998) suggest that a pH of 12 for 2 hours will reduce many pathogens to insignificant numbers. However, some pathogens are more resistant than others. For instance, faecal coliform counts decreased rapidly after treatment of sludges to obtain a pH between 10.5 and 12, whereas *Salmonella* sp. survived for a month in a sludge at pH 10 (Storm et al., 1981).

Treatment with quicklime (CaO), which brought sludge to a pH of at least 12, caused complete inactivation of viruses, damage of parasite eggs and removal of enteric bacteria (Allievi et al., 1994). Similarly, Graczyk et al. (2008) found that quicklime stabilisation treatments reduced the load of *Cryptosporididium* and *Giardia* to non-detectable levels. On the other hand, the hygienisation effect of NaOH on sludge has not been extensively studied, but some studies reported it is efficient in reducing the pathogen load. For instance, Kato et al. (2001) combined NaOH with $(NH_4)_2SO_4$ and registered an *Ascaris* egg inactivation higher than 99% after 48 h.

2.4.4. Alkaline stabilisation systems

Alkaline stabilisation can be conducted before or after dewatering. In general, alkaline stabilisation systems are quite reliable and flexible; the same equipment can often be used to produce different degrees of hygienisation of biosolids with minor process modifications (US Environmental Protection Agency, 2000). These modifications refer to larger dosages of alkaline material or the addition of supplemental heating (pasteurisation). Figure 2.5 shows a typical flow diagram for alkaline stabilisation. The basic equipment for alkaline stabilisation includes the following:

- Sewage sludge feed/conveyance mechanism.
- Alkaline material storage (silo).
- Lime transfer conveyor.
- Mixer.
- Air emission control equipment to minimise odours and dust.

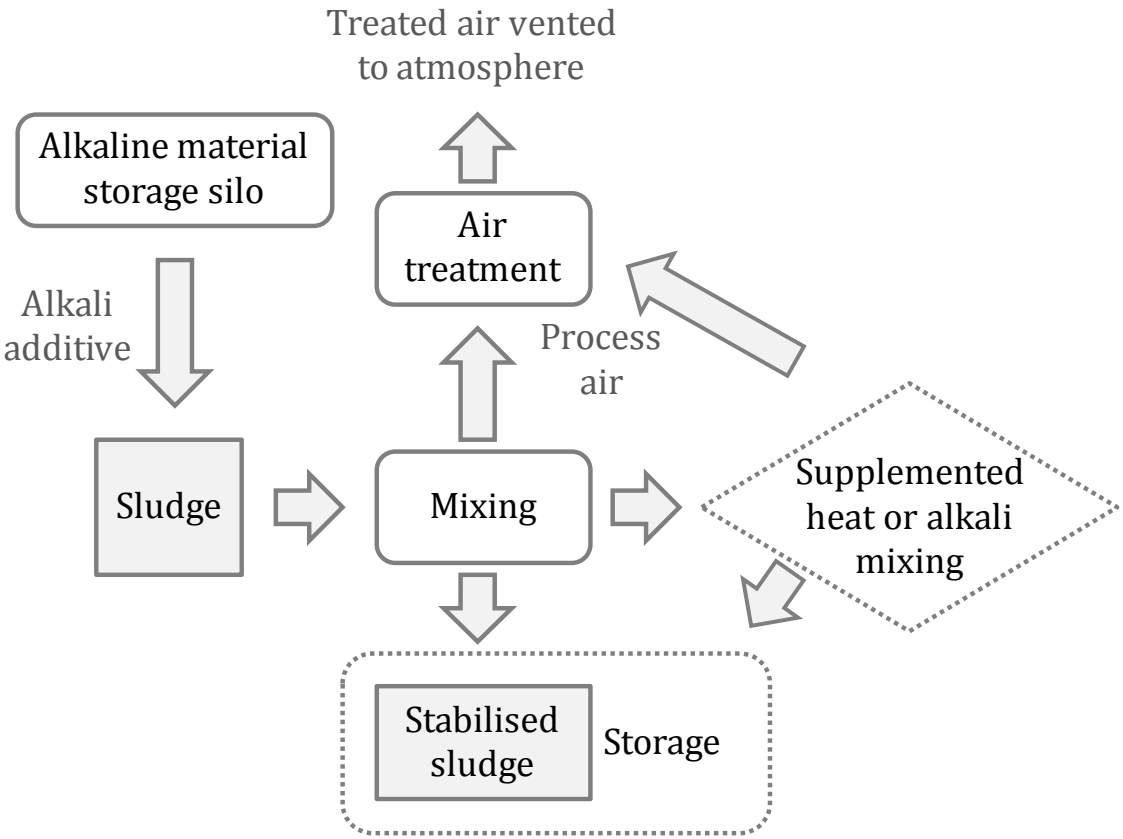

Figure 2.5. Typical flow diagram for alkaline stabilisation. Dashed lines indicate optional equipment.

Quicklime is the most common material used in alkaline stabilisation because it has high heat of hydrolysis and can significantly enhance pathogen destruction. The alkaline stabilised biosolid is suitable for application in many situations, such as landscaping, agriculture, and mine reclamation, but it is unsuitable in alkaline soils due to the high pH material. Alkaline stabilisation is practical at small WWTPs that store sewage sludge for later transportation to larger facilities for further treatment. However, the volume of material to be managed is increased by approximately 15% to 50% in comparison with other stabilisation techniques, such as anaerobic digestion (US Environmental Protection Agency, 2000). This increased volume results in higher transportation costs.

Chapter 3 Objectives and thesis structure

3.1. Objectives

The general objective of this work is to study the influence of ultrasound, low-temperature thermal and alkali treatments on physicochemical and biological properties of WAS, with special attention to the rheology, dewaterability, hygienisation and methane potential. Rheology enables the quantification of viscosity, which is linked to sludge internal structure. The treatments would disrupt the sludge internal structure, thus modifying the rheological profile. These changes would therefore have effect on sludge dewatering, biodegradability and hygienisation. The specific objectives are as follows:

- To examine the influence of the three treatments on the rheological profile of WAS, with measurements performed both within the linear and non-linear viscoelastic region.
- To develop a rheological structural model to examine the variations in the thixotropic behaviour of the WAS before and after the treatments.
- To evaluate the effect of the treatments on WAS dewaterability and water distribution.

- To obtain the optimum treatment conditions in terms of viscosity reduction and dewatering.
- To extract and analyse the EPSs contained in the WAS before and after the treatments.
- To evaluate the effect of the treatments on sludge hygienisation by means of microbial indicators.
- To compare the effect of the three treatments on anaerobic digestion and provide an overall view of feasible scenarios for sludge management.

3.2. Thesis structure

In Chapter 1 are presented the problems associated with sludge generation together with the European legal framework, the general process for sludge management (thickening, stabilisation and drying) and the main disposal routes. In this chapter it is also highlighted that WAS needs to be broken down in order to enhance its dewaterability and biodegradability (Figure 3.1).

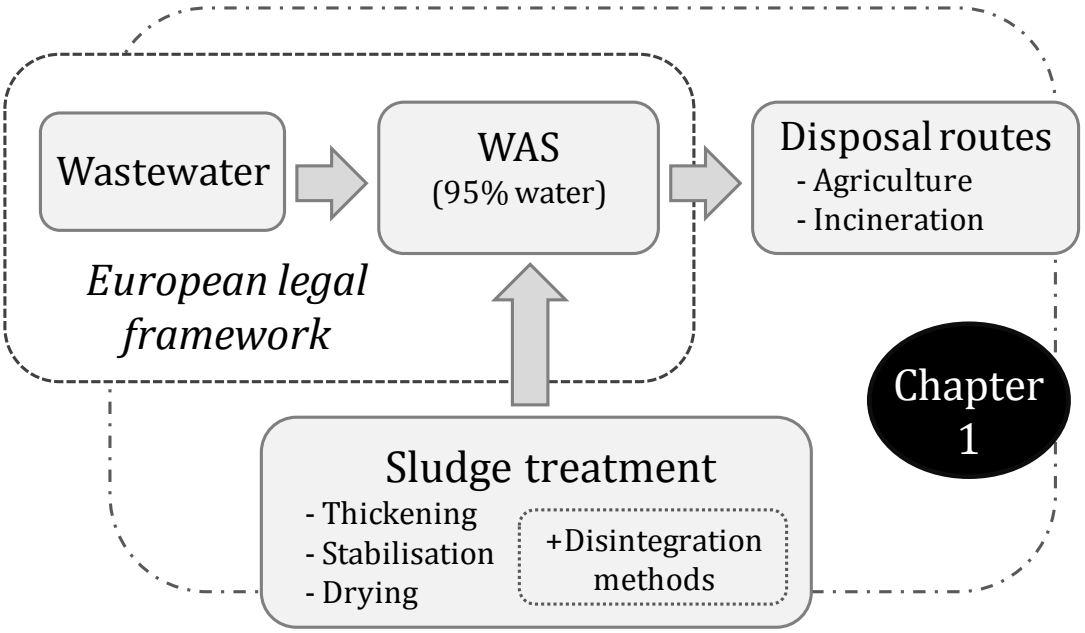

Figure 3.1. Outline of the issues covered in Chapter 1 (WAS: waste activated sludge).

In Chapter 2 are described the major classes of sludge disintegration methods, with particular emphasis on the ultrasound, low-temperature thermal and alkali treatments because they are the object of study of this thesis. The state of the art in terms of sludge dewaterability, biodegradability and hygienisation is provided for the three treatments (Figure 3.2).

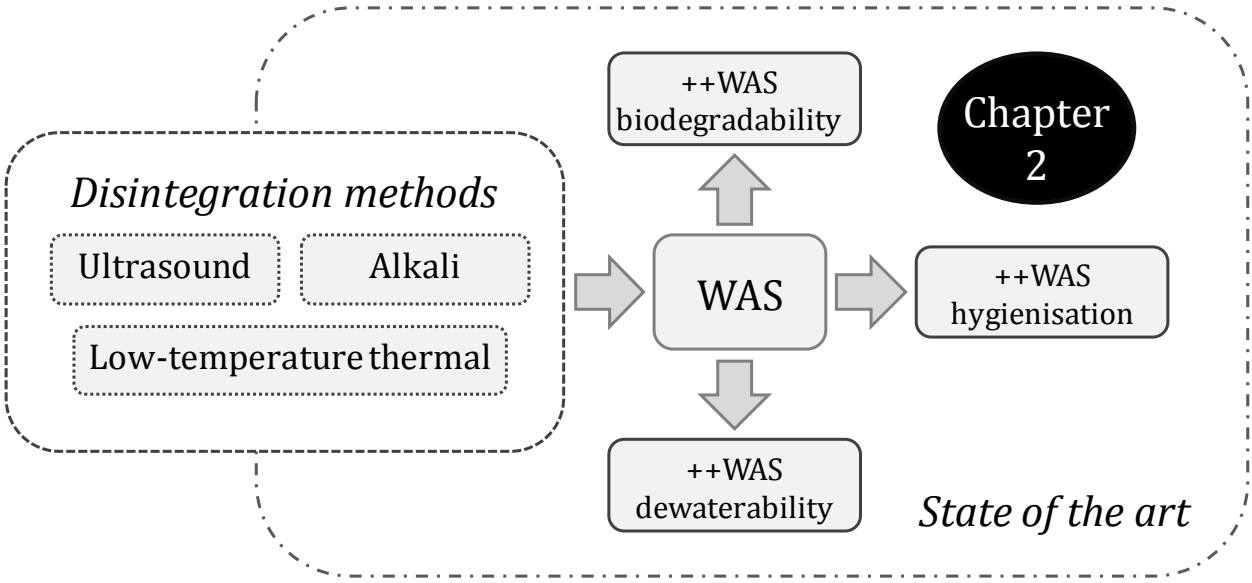

Figure 3.2. Outline of the issues covered in Chapter 2 (WAS: waste activated sludge).

In Chapter 3 is detailed the objective and structure of this work. Some block diagrams have been introduced in order to enable an overview of the study.

In Chapter 4 are described the general materials and methods used in this study. Moreover, the specific materials and methods described in Chapters 5, 7 and 8 are cited (Figure 3.3).

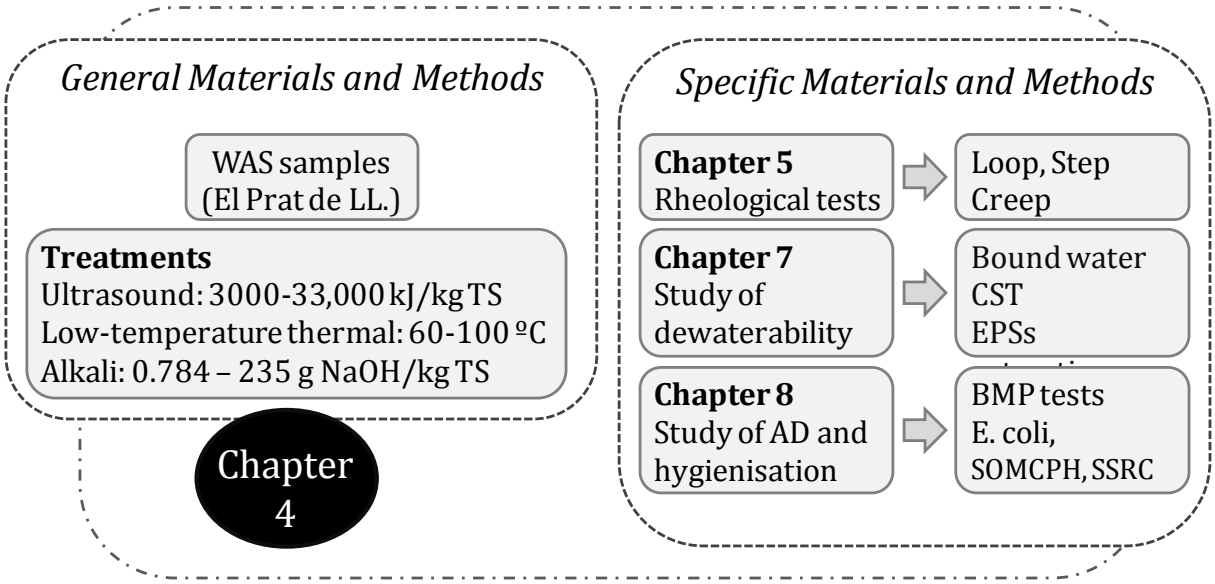

Figure 3.3. Outline of the issues covered in Chapter 4 (AD: anaerobic digestion; BMP: biomethane potential; CST: capillary suction time; EPSs: extracellular polymeric substances; SOMCPH: somatic coliphages; SSRC: spores of sulfite-reducing clostridia; WAS: waste activated sludge).

Chapter 5 deals with the rheological characterisation of the sludge before and after the treatments. The rheological behaviour of sludges was analyzed within the linear viscoelastic region to determine the viscoelastic properties and under flow conditions to determine the apparent viscosity and thixotropy. Specifically, the thixotropy was perceived by (1) measuring the hysteresis area when shear stress is plotted versus shear rate and (2) determined by means of a rheological structural model. The rheological structural model to study the thixotropy is detailed in Chapter 6 (Figure 3.4).

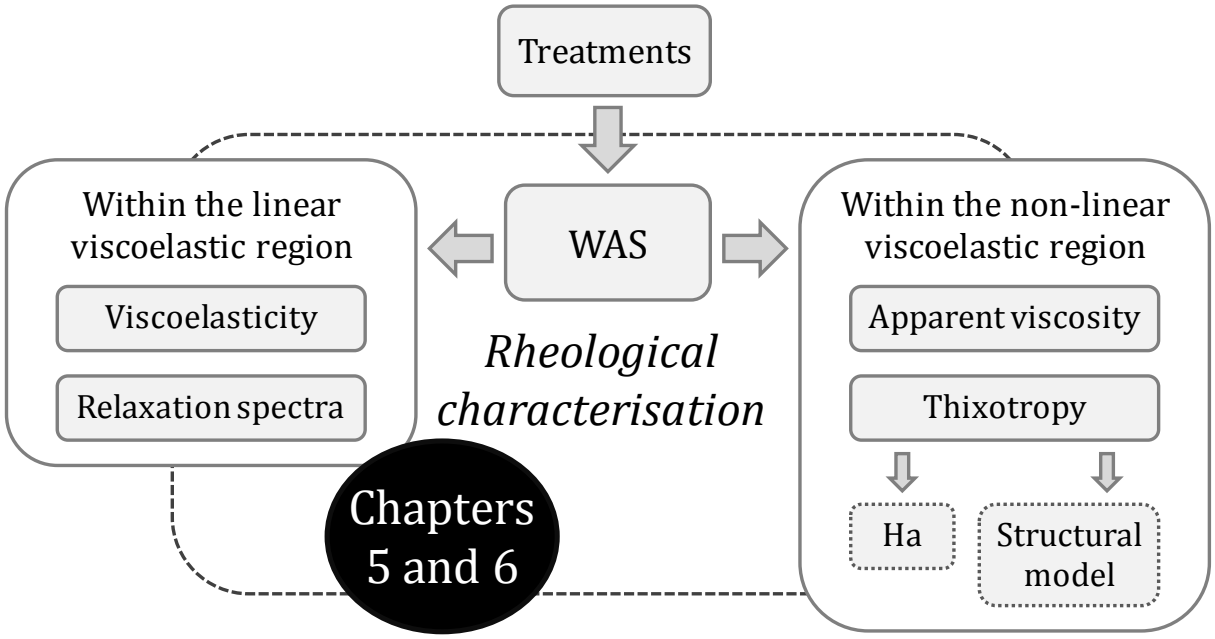

Figure 3.4. Outline of the issues covered in Chapters 5 and 6 (Ha: hysteresis area; WAS: waste activated sludge).

Chapter 7 deals with the effect of the treatments on sludge water distribution and dewaterability. Based on the results obtained for sludge dewatering together with the rheological characterisation (Chapter 5), one condition of each treatment was selected to subsequently extract and analyse the EPSs. As a result, the LB-EPS and TB-EPS fractions were obtained and characterised before and after the treatments (Figure 3.5).

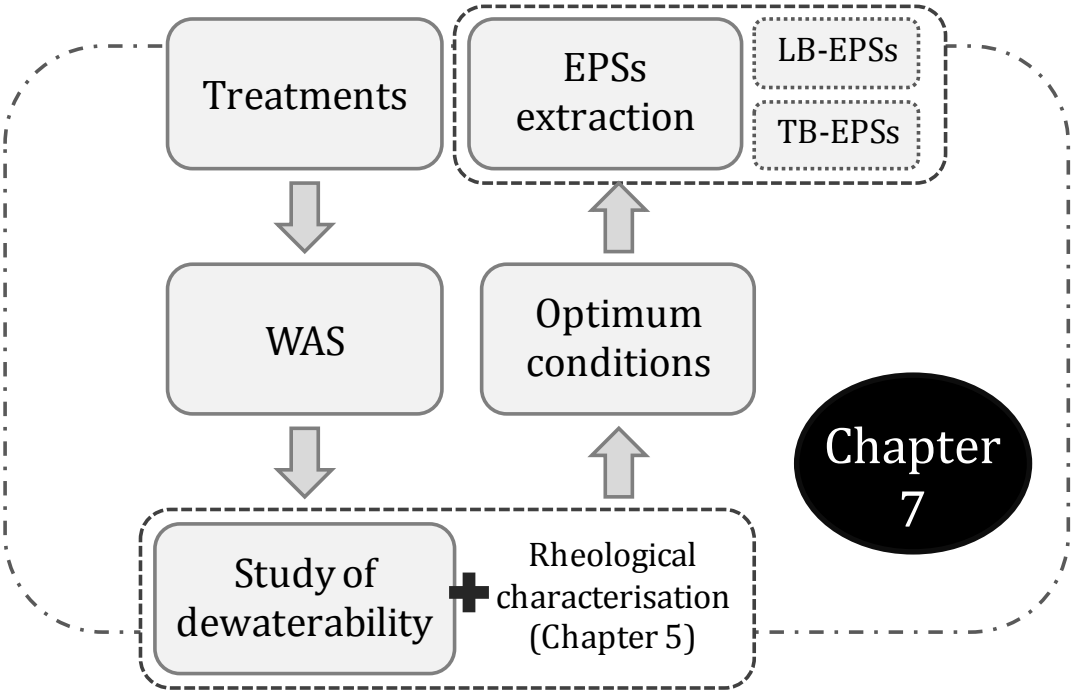

Figure 3.5. Outline of the issues covered in Chapter 7 (EPSs: extracellular polymeric substances; LB-EPS: loosely bound EPSs; TB-EPS: tightly bound EPSs; WAS: waste activated sludge).

Chapter 8 deals with the effect of the treatments on sludge hygienisation and methane potential. The hygienisation effect of the treatments was tested before and after anaerobic digestion. The methane potential was analysed at one condition of each treatment. These conditions were selected in terms of microbial indicators reduction and sludge dewatering improvement (Chapter 7). Finally, an assessment of the different treatment scenarios was conducted considering the results together with an energy balance (Figure 3.6).

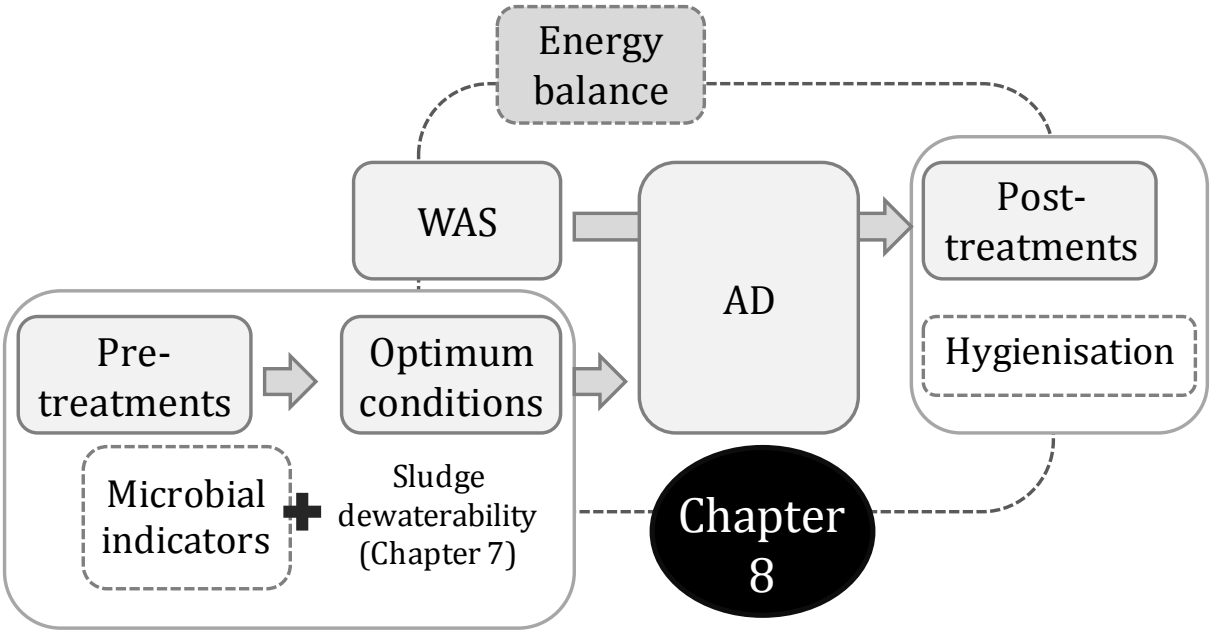

Figure 3.6. Outline of the issues covered in Chapter 8 (AD: anaerobic digestion; WAS: waste activated sludge).

Finally, in Chapter 9 are summarised the main conclusions obtained in this work together with some recommendations.

Chapter 4 General materials and methods

This chapter describes the WAS sampling and the procedures to perform the ultrasound, low-temperature thermal and alkali treatments. Some analytical tools, such as the solids quantification, are also specified. The specific materials and methods are detailed in the following chapters:

- Chapter 5 describes the rheological tests (creep, hysteresis loop and shear rate step tests).
- Chapter 7 describes the procedures for measuring the bound water content, the CST and the water removed by centrifugation. The EPSs extraction and characterisation procedures are also described.
- Chapter 8 describes the procedure to conduct the biomethane potential (BMP) tests and the procedures to determine the occurrence and levels of three microbial indicators (*E. coli*, SOMCPH and SSRC).

4.1. Analytical methods to characterise the sludge

- *Solid content*

Total solids (TS) and volatile solids (VS) contents were determined following the guidelines given by the Standard Methods 2540G (APHA, 2005). Total suspended solids (TSS) and volatile suspended solids (VSS) were determined following the guidelines given by the Standard Methods 2540D and 2540E (APHA, 2005), respectively.

- *Particle size distribution*

Sludge particle size distribution was measured at room temperature by a Beckman Coulter LS 13 320 laser-diffraction particle dimension analyser (Beckman Coulter Corporation, Fullerton, CA), which provided measurements over a particle diameter range of 0.017μm to 2000 μm. Measurements were performed with the sludge diluted in deionised water. This analysis was performed at the scientific and technological centers of the University of Barcelona (CCiTUB).

- *pH and conductivity*

The pH was measured with a Crison 5014T pH probe. The conductivity was measured by a Crison 5070 conductivity probe. pH and conductivity were also measured using a multimeter (Hach Lange HQ 40D multi) with the IntelliCal electrodes (PHC301-01 for pH; CDC401-01 for conductivity).

- *Total and soluble chemical oxygen demand*

Total chemical oxygen demand (tCOD) and soluble chemical oxygen demand (sCOD) were determined following the guidelines given by the standard method 5220D (APHA, 2005). Analysis of the total fraction was performed directly on the whole sample. For the analysis of the soluble fraction, the sample was centrifuged at 1252 x *g* for 10 min and the supernatant was filtered through a regenerated cellulose 0.45 mm filter (CHM® SRC045025Q). Finally, the sCOD analysis was conducted in the filtered supernatant.

- *Volatile fatty acids (VFA)*

Individual VFA (acetate, propionate, butyrate and valerate) were analysed by an HP 5890-Series II chromatograph equipped with a capillary column (Nukol™) and a flame ionisation detector (Astals et al., 2012a).

- *Elemental analysis*

The elemental organic components (total carbon, hydrogen, nitrogen and sulphur) of the sludge were determined with a Carlo Erba 1108 CHNS-O Instrument, equipped with a thermal conductivity detector. This analysis was performed at the CCiTUB.

- *Semi-quantitative metal content*

Prior to quantification, the WAS sample was allowed to dry at room temperature for 72 h. Afterwards, the dried WAS sample was grinded (Figure 4.1).

Figure 4.1. Fresh WAS (on the left) and dried-grinded WAS (on the right).

To semi-quantify the metal contents, 0.5 g of grinded sludge was mixed with 8 g of aqua regia and warmed up to 200 ºC (10 min of heating and 15 min of temperature maintenance). Then, mixture was cooled down and filtered. The semi-quantification was conducted by inductively coupled plasma (ICP-OES and ICP-MS). This analysis was performed at the CCiTUB.

4.2. Waste activated sludge (WAS) samples

The WAS samples analysed in this work came from the Baix Llobregat WWTP (Barcelona, Spain), located in an area with a strong industrial presence. It is one of the largest WWTPs in Europe and can treat 315,000 m^3/day, which is equivalent to the use of water of more than 1,700,000 inhabitants (http://www.aiguesdebarcelona.cat/). As a result, the annual sludge production is approximately 12,000 tons dry matter/year. Figure 4.2 shows an aerial view of the Baix Llobregat WWTP.

Figure 4.2. Aerial view of Baix Llobregat WWTP (Barcelona, Spain).

After leaving the secondary tank, the sludge was thickened by adding a cationic polyelectrolyte (approximately 1 kg/ton dry sludge) before centrifugation. Slight changes in the water content of the sludge could be obtained with higher doses of polyelectrolyte. Before collecting the sample, the sludge circulating through the pipe was allowed to run for a little time to guarantee the homogeneity of the sample. Once in the laboratory, the samples were stored at 4 ºC until their utilisation. A summary of some physicochemical and biological parameters of the WAS sample are detailed in Table 4.1.

Total solids (TS), volatile solids (VS), pH and conductivity were measured for each sampling. The ratio VS/TS was approximately 0.8.

Table 4.1. Physicochemical and biological parameters of the WAS sample.

Parameter	**Units**	**Mean (± SD)**
Physicochemical characterisation		
TS	g/L	56.1 (± 7.0)
VS	g/L	46.5 (± 6.7)
TSS	g/L	52.1 (± 4.7)
VSS	g/L	44.5 (± 4.3)
Average particle size	μm	50.5 (± 35.7)
CST	s	1490 (± 115)
pH	-	6.46 (± 0.21)
Conductivity	mS/cm	5.17 (± 0.16)
tCOD	g O_2/L	80.9 (± 0.4)
sCOD	g O_2/L	0.9 (± 0.1)
VFA	mg/L	223 (± 10)
Microbiological characterisation		
E. coli	$\log_{10}$ CFU/g TS	5.99 (± 0.22)
SOMCPH	$\log_{10}$ PFU/g TS	7.02 (± 0.34)
SSRC	$\log_{10}$ CFU/g TS	6.07 (± 0.16)
Elemental analysis: $C_5H_{8.5}N_{0.9}S_{0.05}$		

TS: total solids; VS: volatile solids; TSS: total suspended solids: VSS: volatile suspended solids; CST: capillary suction time; tCOD: total chemical oxygen demand; sCOD: soluble chemical oxygen demand; VFA: volatile fatty acids; SOMCPH: somatic coliphages; SSRC: spores of sulfite-reducing clostridia; CFU: colony-forming unit; PFU: plaque-forming unit; SD: standard deviation.

Table 4.2 summarises the metals content in the WAS sample.

Table 4.2. Metal contents in the WAS sample. It is a semi-quantification conducted by inductively coupled plasma.

Metal	**Concentration (mg/kg dry sludge)**	**Metal**	**Concentration (mg/kg dry sludge)**
P	22718	Co	4.08
K	16504	U	4.06
Ca	16492	Zr	3.79
S	10105	Ce	2.88
Mg	6669	La	2.46
Al	4064	Sb	2.29
Fe	3629	Bi	1.98
Na	2288	Ga	1.17
Zn	**678**	W	1.11
Si	592	Nd	1.00
Cu	**285**	Sc	0.97
Sr	224	Y	0.94
Ba	155	Th	0.89
Ni	**111**	**Cd**	**0.80**
Mn	71.8	**Hg**	**0.54**
Cr	**67.3**	Nb	0.41
Sn	62.3	Pr	0.31
Pb	**50.9**	Cs	0.30
Ag	15.6	Gd	0.17
Rb	7.50	Sm	0.16
Mo	5.34	Dy	0.11
Li	4.97		

The values highlighted in bold correspond to the heavy metals covered by the Directive 86/278/EEC and the 3rd official draft from the EU.

The values highlighted in bold correspond to the heavy metals covered by Directive 86/278/EEC (CEC, 1986) on the use of sludge in agriculture and the 3rd official draft from the EU (Environment DG, EU, 2000). As aforementioned, this latter document considers lower limit values for heavy metals, but is not a mandatory text and should only be used for recommendation purposes. The limit values for concentrations of heavy metals in sludge for use on land are summarised in Annex I. As shown, the WAS sample used in this work comply with both regulations.

4.3. Treatment conditions

4.3.1. Ultrasound treatment specifications

The ultrasonic apparatus consisted of a HD2070 Sonopuls Bandelin Ultrasonic Homogeniser equipped with a MS 73 titanium microtip probe (Bandelin, Berlin, Germany; 20 kHz). The ultrasonication power was fixed at 70 W (maximum supplied power of the device), and the exposure times were changed to provide a wide range of E_S, from 3000 to 33,000 kJ/kg TS. The E_S applied to the sludge was calculated as specified in Equation 2.1. Table 4.3 summarises the ultrasound treatment specifications.

Table 4.3. Ultrasound treatment specifications.

Ultrasound treatment	
Ultrasonic power	70 W
Ultrasonic frequency	20 kHz
Sample volume	10 mL
Treatment time[1]	25 to 270 s
Specific energies	3000 to 33,000 kJ/kg TS
Beaker	50 mL Schott Duran (42 mm diameter)
Refrigeration	Sample container on ice (see Figure 4.3)

[1]This is an example of the treatment time duration to obtain the desired specific energies according to a sludge TS content of 56.7±0.7 g/L.

Preliminary tests confirmed that a glass vial was not resistant enough to the ultrasound treatment (the base of the vial was broken after few minutes of treatment). Accordingly, a 50 mL Schott Duran beaker of 42 mm of diameter was used. The sludge sample volume was 10 mL.

To minimise the increment of sludge temperature due to the thermal effect of cavitation phenomenon, the beaker containing the samples was submerged in ice. Therefore, the temperature of the sludge samples after ultrasonication never exceeded room temperature. Finally, the sludge sample was manually oscillated during the treatment to ensure that the ultrasonic waves reached the entire sample volume. Figure 4.3 shows the ultrasound experimental device used.

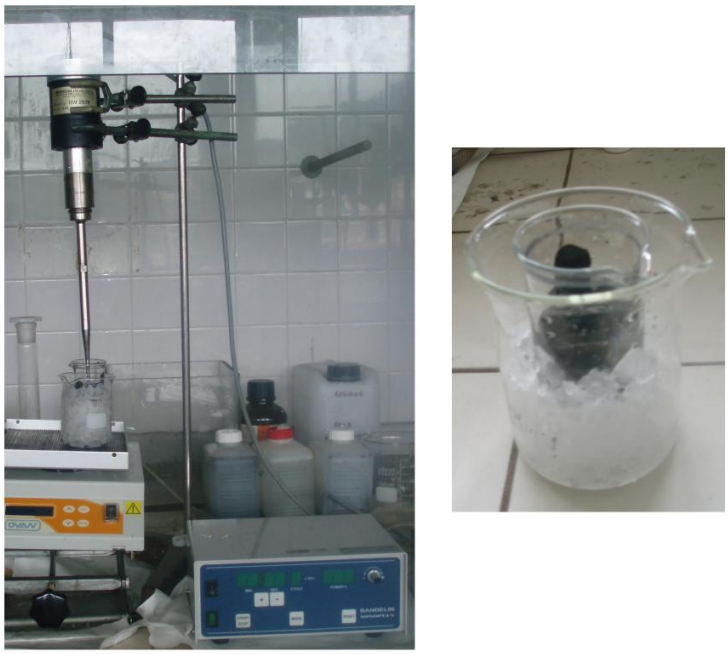

Figure 4.3. Ultrasound treatment experimental device.

4.3.2. Low-temperature thermal treatment specifications

The reactor (Autoclave-Engineer, bolted-closure stirred reactor) used for the thermal treatment operates in sequencing batch mode and essentially consists of a closed tank subjected to pre-set temperatures between 60 and 100 ºC. The reactor was well-sealed

to avoid significant loss of water during treatment. A heating jacket provided the heat to increase the temperature of the sludge sample (100-150 mL) contained inside the tank. Treatment lasted until the temperature reached the desired value (approximately 30 min) and then was kept at this temperature for 30 min. Finally, the samples were cooled to room temperature before the reactor was opened. Figure 4.4 shows the experimental device used for the low-temperature thermal treatment.

Figure 4.4. Low-temperature thermal treatment experimental device.

The energies supplied to the sludge were calculated considering the heat required for heating the sludge until the desired temperature and the heat required for temperature maintenance (the explanation for this calculation is provided in Annex II). The apparent specific energies (called specific energy, E_S, for simplicity) were obtained by dividing the supplied thermal energy by the total solid content of the sludge. For instance, for a sludge TS content of 56.7±0.7 g/L and a sample volume of 100 mL, the E_S applied were 12,000 (60 ºC), 15,000 (70 ºC), 17,000 (80 ºC), 20,000 (90 ºC) and 22,000 (100 ºC) kJ/kg TS. The WAS was mechanically agitated during thermal treatment to

ensure the temperature homogeneity of the sample. Table 4.4 summarises the low-temperature treatment specifications.

Table 4.4. Low-temperature thermal treatment specifications.

Low-temperature thermal treatment	
Heating ramp	~30 min
Temperature maintenance	30 min
Sample volume	100 to 150 mL
Application temperatures	60 to 100 ºC
Specific energies[1]	12,000 to 22,000 kJ/kg TS
Agitation during treatment	Yes
Cooling	At room temperature

[1]These specific energies have been calculated for a sludge TS content of 56.7±0.7 g/L and a sample volume of 100 mL.

4.3.3. Alkali treatment specifications

The alkali treatment was conducted at room temperature (~25 ºC) by adding different concentrations of NaOH (NaOH pellets, Sigma-Aldrich, ref. no. 221465). A NaOH stock solution (5 M) was used. The sludge sample volume was 100 mL. The concentrations studied included values within a wide range, from 0.784 to 235 g NaOH/kg TS. The treatment lasted 24 h and after that time the samples were neutralised with $HCl_{37\%}$ (Sigma-Aldrich, ref. no. 258148) in the pH range of 6.5-7.5. The reason of working with concentrated reagents (NaOH 5M and HCl 37%) is for minimising the sludge dilution.

The pH values varied widely depending on the NaOH concentration. For instance, the pH values (± confidence interval 95%) just after adding the NaOH concentrations of 35.3, 70.6 and 157 g NaOH/kg TS were 9.9±0.9, 11.2±0.6 and 12.5±0.2, and after 24 h (before neutralisation) were 6.9±0.2, 9.1±0.7 and 12.3±0.2, respectively. The increase in

salinity due to the alkali addition was not corrected. Table 4.5 summarises the alkali treatment specifications.

Table 4.5. Alkali treatment specifications.

Alkali treatment	
Stock solution	NaOH (5 M)
Sample volume	100 mL
Temperature	Room temperature (~25 ºC)
Alkali concentration range	0.784 to 235 g NaOH/kg TS
pH value just adding the NaOH	35.3 g NaOH/kg TS: 9.9±0.9 70.6 g NaOH/kg TS: 11.2±0.6 157 g NaOH/kg TS: 12.5±0.2
Duration of treatment	24 h
pH value after 24 h of treatment	35.3 g NaOH/kg TS: 6.9±0.2 70.6 g NaOH/kg TS: 9.1±0.7 157 g NaOH/kg TS: 12.3±0.2
Neutralising agent	HCl (37%)
pH neutralisation range	6.5-7.5

Chapter 5 Effect of the treatments on WAS rheological profile

5.1. Introduction

Rheology is the science that studies the relationships between stress, strain (deformation) and time of viscoelastic materials. The rheological properties of a material are noted when a force (stress) is exerted on it, because of which, it deforms or flows. The extent to which a material deforms under a certain force depends strongly on its properties (Vliet and Lyklema, 2005). When a force is applied, some materials basically only deform (elastic behaviour), others basically only flow (viscous behaviour) and others deform and flow simultaneously (viscoelastic behaviour).

The rheological properties of a **purely elastic material** are described by the Hooke's equation (Equation 5.1); accordingly, the strain is directly proportional to the stress.

$$\tau = G \cdot \gamma \tag{5.1}$$

where τ is the shear stress (Pa), G is the shear modulus (Pa) and γ is the shear strain (-).

The shear stress, τ, is defined as the magnitude of the force per unit cross-sectional area of the face being sheared (F/A) (Figure 5.1). The shear strain, γ, is defined as the tangent of the angle caused by the shear stress (Δx/L). The shear modulus, G, relates to the relationship between the shear stress and strain.

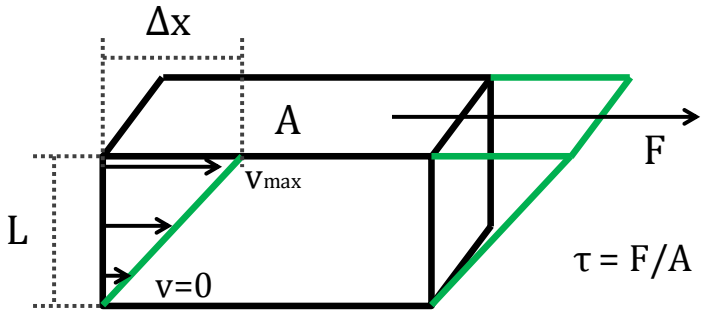

Figure 5.1. Flow velocity of a fluid between two parallel flat plates under the influence of a shear stress. The bottom plate is motionless.

Conversely, a **purely viscous fluid** subjected to an external stress is continuously deformed (strained) until the stress ceases; when the stress has ceased the deformation lasts indefinitely. For the simplest case, the rheological properties of a purely viscous material are described by the Newton's equation (Equation 5.2), which states that shear rate and shear stress are directly proportional and is independent on the deformation itself:

$$\tau = \eta \cdot \dot{\gamma} \tag{5.2}$$

where η is the viscosity (Pa·s) and $\dot{\gamma}$ is the shear rate (s^{-1}), which is generated by the strain rate (Figure 5.1) at laminar flow.

A graph of shear stress, τ, vs. shear rate, $\dot{\gamma}$, (the so-called rheogram) for a Newtonian fluid is a straight line of slope η that passes through the origin (Figure 5.2).

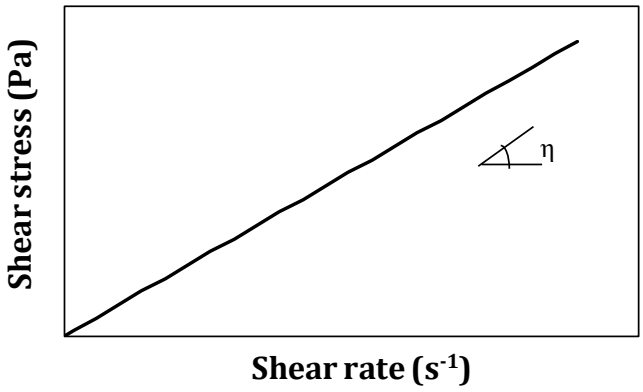

Figure 5.2. Typical rheogram for a Newtonian fluid.

Equation 5.2 is accomplished in two main cases: (1) when the material is not structured (this is the case of fluids as water or simple organic solvents) or (2) when the material is structured but it is exposed to low stresses and strains that cannot modify its structure. Conversely, when a structured material is subjected to high stresses that modify its structure, the linear dependence between shear rate and shear stress is not accomplished (non-Newtonian behaviour).

The purely elastic and purely viscous behaviours are two ideal models and between them are the real **viscoelastic materials**. A viscoelastic fluid will be simultaneously viscous and elastic, being more viscous or more elastic depending on the characteristics of the material and the type of test performed (Labanda, 2003).

5.1.1. Classification of rheological behaviours

It can be distinguished two major fields into the rheology, depending if the analysed material is flowing with its original structure unchanged due to the low shear stresses applied (linear viscoelastic region) or is flowing with their structure changed due to the higher shear stresses (non-linear viscoelastic region). Rheological measurements performed within the linear viscoelastic region, far away from the normal flow conditions, gives information about the organisation of the internal structure of the material because the applied stress does not change the internal structure. Conversely, when the stress changes the internal structure of the material, the measurements are

performed within the non-linear viscoelastic region, and viscosity is dependent on the applied stress (non-Newtonian behaviour).

5.1.1.1. Rheological behaviour within the linear viscoelastic region

The rheological response of a viscoelastic fluid measured in the linear viscoelastic region is independent of the applied shear stress. The linear viscoelastic region is operative at very low shear stresses. Above a critical shear stress, the strain increases significantly and the internal structure breaks down. Below a critical shear stress, the applied shear stress does not alter the internal structure and therefore the rheological response is directly related with the conformation of this internal structure at rest. The internal structure of colloidal dispersions is constituted by the union of small particles, aggregates or flocs. This structure can be extended to all dispersion, leading to the formation of a network or gel. The measurement of deformation of a viscoelastic fluid under this linear regime allows identifying the viscoelastic properties of the undisturbed internal structure (Labanda and Llorens, 2006).

The linear viscoelastic properties can be measured using the oscillatory sweep test or the creep test. For instance, in a creep test, a constant stress in the linear viscoelastic region is applied, τ, and the time-related strain, $\gamma(t)$, is measured. The two can be mathematically interrelated by:

$$\gamma(t) = J(t) \cdot \tau \tag{5.3}$$

where $J(t)$ is the compliance (Pa^{-1}).

The compliance defines how compliant a sample is: the higher the compliance the easier the sample can be deformed by a given stress. Sometimes, when the creep test is finished, the shear stress is kept to zero and the compliance is recorded to follow the recovery process. Figure 5.3 shows the creep and recovery response for three different

materials: purely elastic (ideal solid), purely viscous (ideal liquid) and viscoelastic material.

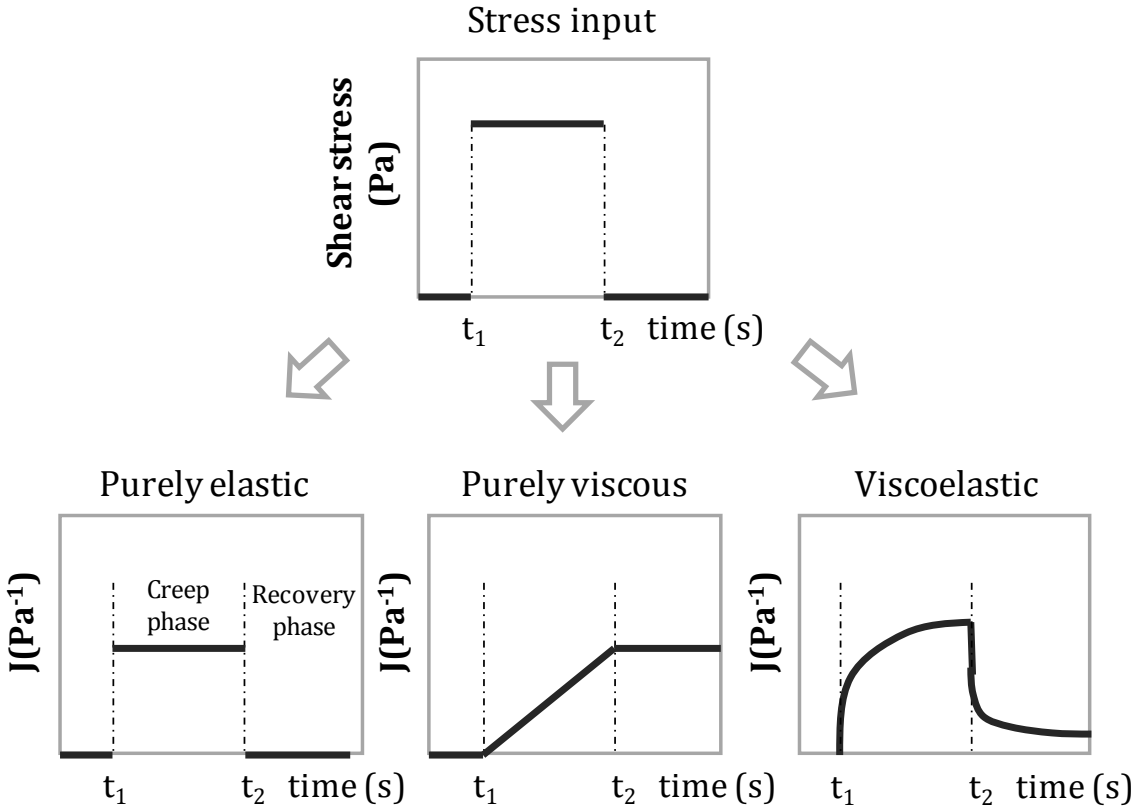

Figure 5.3. Rheological response of a purely elastic, purely viscous and viscoelastic material when a creep-recovery test is applied.

As can be observed, for a purely elastic material, the application of a force or stress is instantaneously followed by a deformation/strain, which is linearly proportional to the force applied: doubling the stress means doubling the deformation, which remains constant as long as that stress is applied. A spring is used as a model to characterise an ideal elastic body. For a purely viscous material, the deformation is linearly increased with time and the final deformation is maintained when the stress has been removed. A dashpot is used to characterise the behaviour of a Newtonian liquid. Viscoelastic materials exhibit an intermediate behaviour between these two extremes:

the compliance increases rapidly at the beginning of creep test due to elastic behaviour and afterwards the viscous behaviour becomes more significant and the compliance increases more slowly. During the recovery phase, a viscoelastic material exhibits a progressive decrease of deformation.

As aforementioned, as long as the tested sample is subjected to test conditions within the linear viscoelastic region, the compliance will be independent of the applied stress. This fact is shown in Figure 5.4, where the same sample is subjected to different stresses being constant each time during the creep phase. Notice that the four applied shear stresses are very low ($\tau \leq 3$ Pa).

A

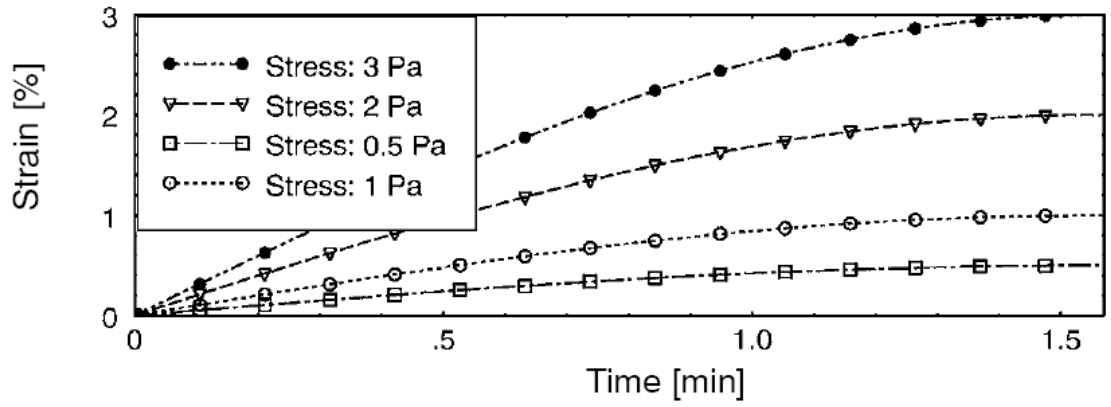

B

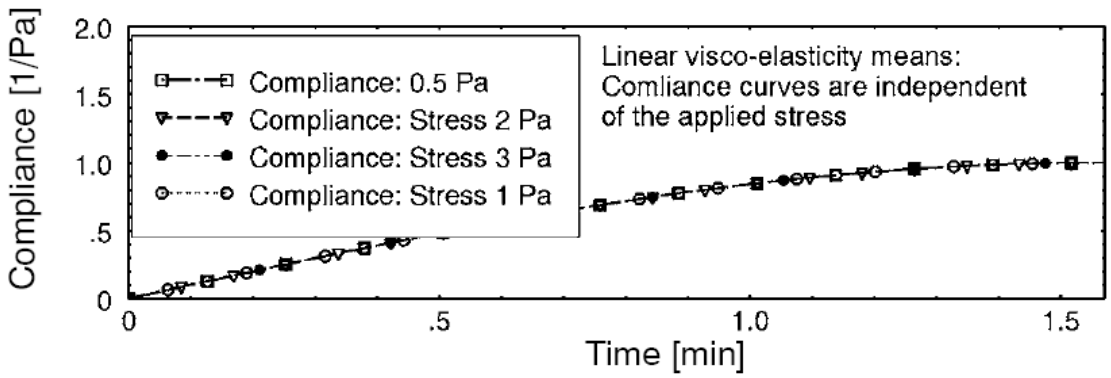

Figure 5.4. Creep tests: (A) strain and (B) compliance curves for viscoelastic samples subjected to variable stresses within the boundaries of linear viscoelasticity (Schramm, 2004).

Figure 5.4a shows the strain/time curves within the linear viscoelastic region, which are proportional to the stresses used. If the strain values are divided by the relevant stresses, this will result in the corresponding compliance data. When plotting those as a function of time, all compliance curves collapse into a single curve (Figure 5.4b). When much higher stresses are used, the individual particles will start to disentangle and permanently change position with respect to each other. Thus, these higher stresses lead to a lower viscosity with the consequence that the deformation is more than proportionally increased. When this happens the compliance curves will start to deviate from those that had collapsed, indicating that the chosen test conditions will exclusively provide non-linear viscoelastic data.

The viscoelastic behaviour can be modelled using combinations of springs and dashpots models in series (Maxwell model for viscoelastic liquids; Equation 5.4) or in parallel (Kelvin–Voigt model for viscoelastic solids; Equation 5.5).

$$J(t) = J_0 + \frac{t}{\eta_0} \tag{5.4}$$

$$J(t) = J_i \left[1 - exp\left(\frac{-t}{\lambda_i}\right)\right] \tag{5.5}$$

where $\lambda = \frac{\eta}{G}$ is the relaxation time (s), which is the time needed in order that the deformed structure of the material vanishes when the stress ceases. Large structures have large relaxation times than small ones.

However, these two models are too simple to characterise real viscoelastic materials. Instead, a Burger model with a Kelvin-Voigt solid and a Maxwell liquid linked in series to each other represents viscoelastic materials much better. The general expression for Buger model is the following:

$$J(t) = J_0 + \sum_i J_i \left[1 - exp\left(\frac{-t}{\lambda_i}\right)\right] + \frac{t}{\eta_0} \quad (5.6)$$

5.1.1.2. Rheological behaviour within the non-linear viscoelastic region

Within the non-linear viscoelastic region, the fluid flows with the application of moderate or high shear stress. Then, the network is disrupted into smaller structures or aggregates. At these conditions, the elasticity is notably reduced and viscosity governs the rheological behaviour (Labanda and Llorens, 2006). As the shear stress is increased, the internal structure becomes less connected and viscosity, now called apparent viscosity, tends to decrease noticeably. The variation of viscosity (or internal structure) with the applied shear stress enables to classify the non-Newtonian behaviour into two groups:

- **Time-independent viscosity**. This behaviour is characteristic of all non-Newtonian fluids and viscosity only depends on the shear stress.
- **Time-dependent viscosity**. Some non-Newtonian fluids show that viscosity depends on the shear stress and time. This behaviour is called thixotropy.

5.1.1.2.1. Non-Newtonian time-independent fluids

The relationship between the shear stress and the shear rate in these fluids is independent of the recent deformation history of the material. Under flow conditions, these fluids do not exhibit neither elasticity nor thixotropy.

5.1.1.2.1.1. Bingham plastic

The relationship between the shear stress and the shear rate is linear, but exhibits a yield stress, τ_0. Thus, the rheogram does not pass through the origin, as it is shown in Figure 5.5. Therefore, a Bingham fluid does not begin to flow until the stress magnitude exceeds the yield stress. The mathematic form for a Bingham plastic is expressed as:

$$\tau = \tau_0 + \eta \cdot \dot{\gamma} \tag{5.7}$$

where τ_0 is the yield stress (Pa).

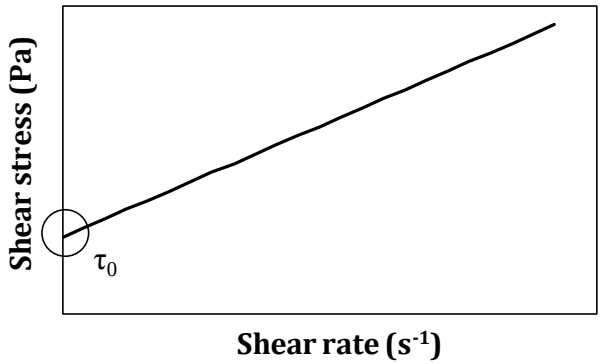

Figure 5.5. Typical rheogram for a Bingham fluid.

5.1.1.2.1.2. Pseudoplastic and dilatant fluids

Both pseudoplastic and dilatant fluids (also called shear thinning and shear thickening fluids, respectively) follow a potential relationship between shear stress and shear rate (Figure 5.6). Consequently, they are also referred as fluids governed by the power law.

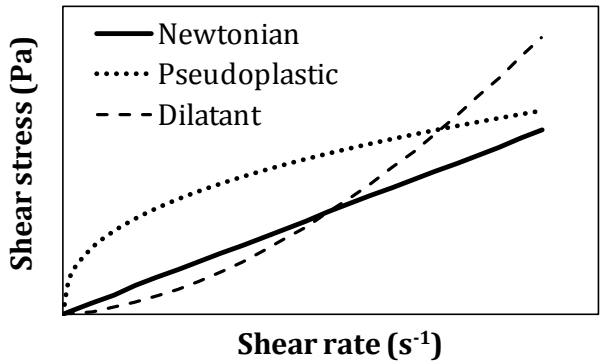

Figure 5.6. Typical rheogram for a pseudoplastic, dilatant and Newtonian fluid.

The mathematical form for these fluids is described by the Ostwald–de Waele model:

$$\tau = K \cdot \dot{\gamma}^{n} \tag{5.8}$$

where K is the consistency index (Pa·s^n) and n is the power law index (-).

The consistency index is a measure of the average firmness of the sample. Power-law fluids can be subdivided into three different types of fluids based on the value of their power law index: n=1 for a Newtonian fluid, n>1 for a dilatant fluid, and n<1 for a pseudoplastic fluid. The parameters K and n are determined directly from double logarithmic representation of the rheogram τ vs. $\dot{\gamma}$.

5.1.1.2.1.3. General-plastic fluids

The general plastics have characteristics of both Bingham plastic and fluids that follow the power law (Figure 5.7). Thus, they are characterised by the presence of a yield stress and usually behave as a solid at low shear rates. Conversely, when increasing the shear rate, these forces can be offset, which implies a decrease in viscosity.

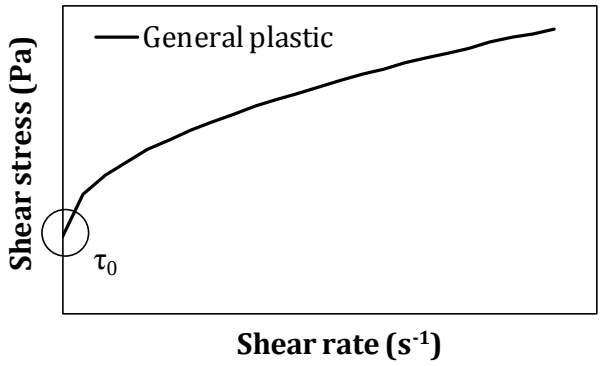

Figure 5.7. Typical rheogram for a general-plastic fluid

The mathematical form of a general plastic can be described by the Herschel-Bulkley model:

$$\tau = \tau_0 + K \cdot \dot{\gamma}^{\mathrm{n}} \tag{5.9}$$

The parameters K and n are determined directly from double logarithmic representation of the rheogram $\tau - \tau_0$ vs. $\dot{\gamma}$. The yield stress, τ_0, is usually quantified separately. Thus, its determination is not univocal and can vary over a wide range depending on the equation used and the shear rates applied. The τ_0 value can be determined using the Casson equation in the range of lower values of $\dot{\gamma}$:

$$\sqrt{\tau} = \sqrt{\tau_0} + \sqrt{\eta_\infty} \cdot \sqrt{\dot{\gamma}} \tag{5.10}$$

where η_∞ is the high shear rate viscosity (limit viscosity).

5.1.1.2.1.4. Determination of the apparent viscosity

The apparent viscosity at each shear rate can be calculated for each type of fluid using Newton's equation ($\eta = \tau/\dot{\gamma}$). The viscosity curves (viscosity vs. shear rate) for different flow behaviours are shown in Figure 5.8.

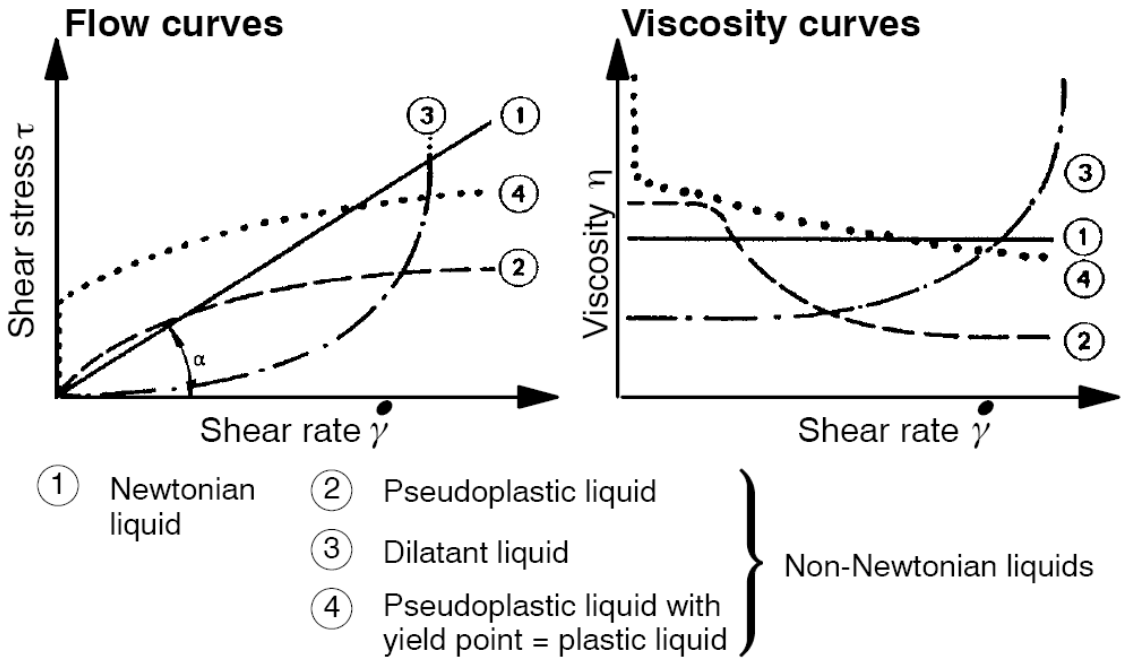

Figure 5.8. Various types of common flow behaviours (Schramm, 2004).

The viscosity curve for a pseudoplastic fluid is shown in more detail in Figure 5.9. η_0 is the viscosity at very low shear rates (when shear rate tends to zero) and η_∞ is the viscosity at very high shear rates, where the reduction in size of the elements is total. For a pseudoplastic fluid, the viscosity decreases with increasing the shear rate because the internal structure is modified in order to facilitate the flow. Accordingly, there is a decrease of the internal friction of the fluid. At low shear rates, molecular Brownian motion maintains the molecules or particles in a random order, although these elements begin to orientate and reduce in size because of the shearing. At very low shear rates, the fluid exhibits Newtonian behaviour with a constant viscosity, η_0. Conversely, at very high shear rates, viscosity achieve a constant level, η_∞. Dilatant fluids exhibit an opposite behaviour to pseudoplastic fluids; dilatant fluids increase the viscosity when increasing shear rate (Figure 5.8).

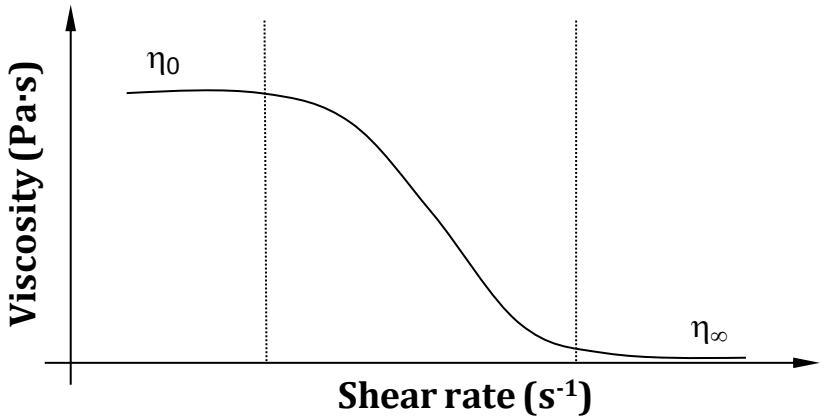

Figure 5.9. Viscosity vs. shear rate for a pseudoplastic fluid.

5.1.1.2.2. Non-Newtonian time-dependent fluids (thixotropy)

The rheological behaviour of thixotropic fluids is influenced by their recent deformation history. The internal structure of thixotropic fluids changes when changing the shear rate, but does not suit instantaneously to the current shear rates. Thus, in these systems, time appears as a new variable and the transient shear stresses do not follow Equations 5.7-5.9. However, if the fluid stays enough time at a fixed shear rate, the final shear stress follows the aforementioned equations. This is a very frequent behaviour in colloidal systems such as activated sludge. Therefore, a thixotropic fluid can behave as a Bingham plastic, pseudoplastic, dilatant or general-plastic fluid in steady state conditions.

There is quite a general agreement in the scientific community that thixotropy should be defined as: the continuous decrease of shear stress (or viscosity) with time when shear rate is applied to a fluid that has been previously at rest and the subsequent recovery of shear stress (or viscosity) in time when the flow is decreased (Mewis and Wagner, 2009). The opposite effect to thixotropy is known as negative thixotropy (also known as rheopexy), which is a property of certain fluids to show a time-dependent increase in shear stress (or viscosity). The shear rate step test is commonly used for measuring the thixotropy. This test consist of applying a constant shear rate for a certain

time and suddenly moves to another shear rate (Figure 5.10). For a positive thixotropic fluid, when the shear rate is increased and then kept constant, the network breaks down and the shear stress decreases over time. Conversely, the network builds up and the shear stress increases over time when the shear rate is decreased and then kept constant.

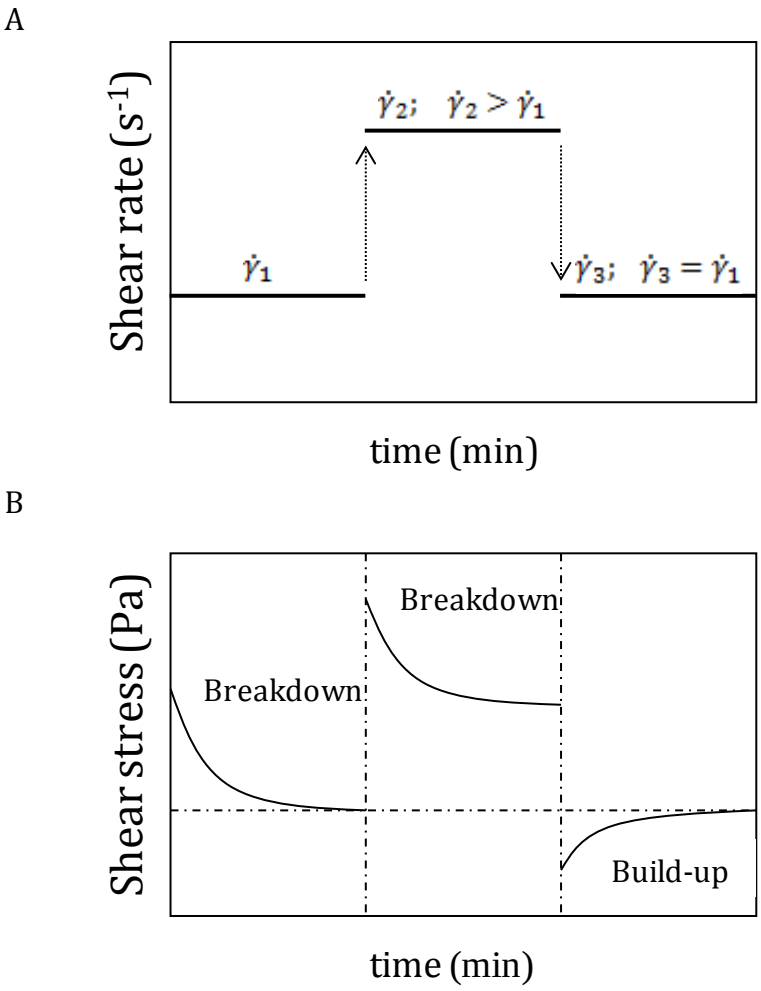

Figure 5.10. Shear rate step test: (A) shear rate input and (B) shear stress response for a material with positive thixotropic behaviour.

Another method for exploring thixotropy is the hysteresis loop area (Perret et al., 1996), which consists of measuring the enclosed area between the up-curve and down-

curve in a plot of shear stress vs. shear rate (Figure 5.11). This plot is obtained by (i) linearly increasing the shear rate from zero to a maximum shear rate over a period of time and (ii) linearly decreasing the shear rate from the maximum shear rate to zero over the same period of time (Green and Weltmann, 1946; Perret et al., 1996). The hysteresis area, *Ha*, is calculated as follows:

$$Ha = \int_0^{\dot{\gamma}} \tau\,(\dot{\gamma}) \cdot d\dot{\gamma} \tag{5.11}$$

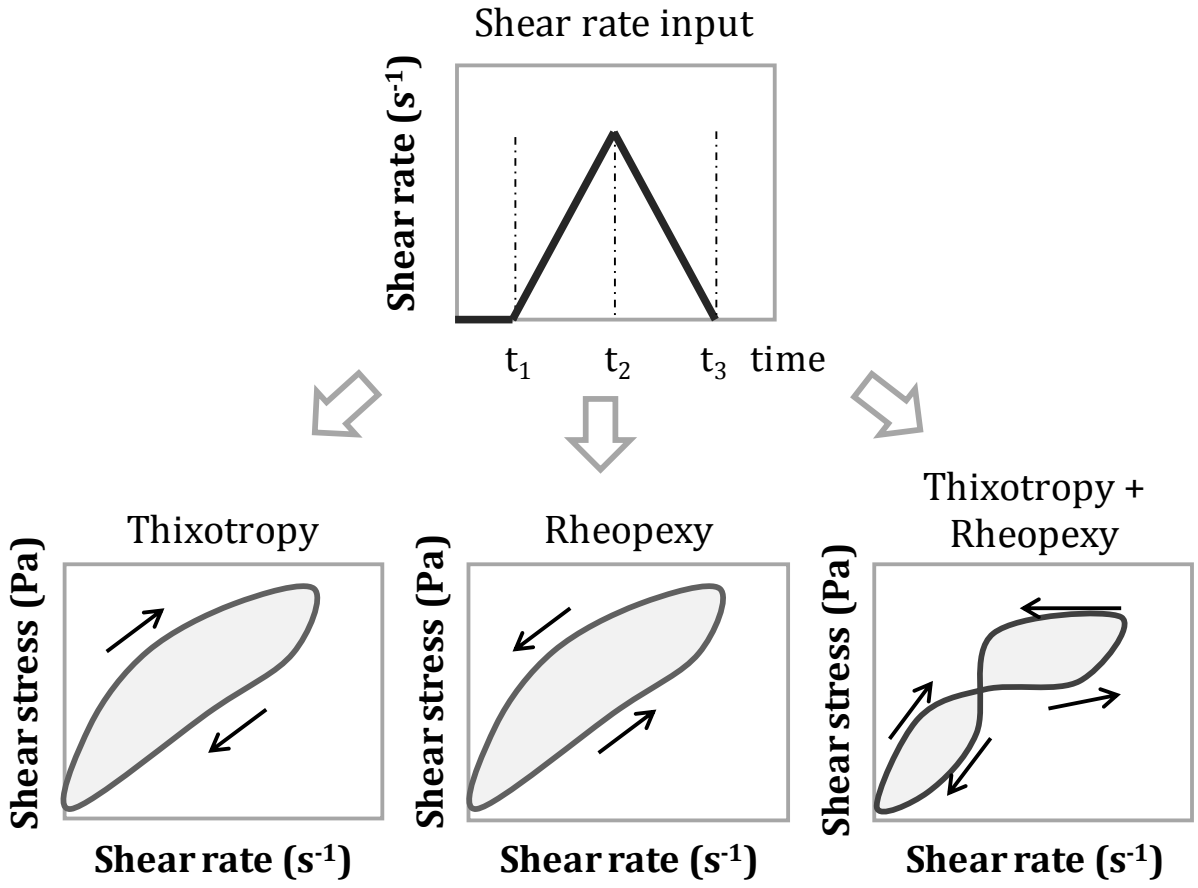

Figure 5.11. Hysteresis loop for a material with positive thixotropic behaviour, a material with negative thixotropic behaviour (rheopexy) and a material with both positive and negative thixotropic behaviour.

A slow breakdown kinetic process suggests that the shear stress (or viscosity) slowly reaches the steady state value and therefore the hysteresis area becomes large. However, the hysteresis area is only a method for detecting thixotropy and does not reveal the individual kinetic behaviours of the breakdown and build-up processes (Labanda and Llorens, 2005). Thixotropy can be better quantified using mathematical equations known as structural models. These models describe the time dependence of viscosity by means of the time dependence of a structural parameter, which is a numerical scalar measurement of the internal structure level (Moore, 1959). Moreover, these models define the time evolution of the structural parameter as a function of the kinetic coefficients for the breakdown and build-up processes. Thereby, the thixotropic behaviour is determined based on the magnitude of both kinetic coefficients instead of the general parameter (hysteresis area). A more complete explanation regarding the structural models is provided in Chapter 6.

5.1.2. WAS rheology

The rheological behaviour of WAS is very complex, since it is composed of water and dissolved wastewater constituents as the continuous phase and sludge flocs, particulate wastewater constituents and biological products (i.e., EPSs) as the dispersed phase. Viscosity interferes with (1) sludge pumping (i.e., recycle flows), (2) bioreactor hydrodynamics (i.e., mixing), (3) oxygen transfer, (4) secondary settler hydrodynamics, (5) membrane filtration and (6) sludge dewatering (Ratkovich et al., 2013). Therefore, a proper understanding of rheology is essential for WAS management in WWTPs, especially in transportation for the calculation of pressure losses in pipes and pump selection and for the design of aeration systems (Ratkovich et al., 2013).

In steady state laminar flow, WAS generally behaves as a non-Newtonian pseudoplastic fluid (Seyssiecq et al., 2008), which indicates that the viscosity decreases following a power law with the applied shear rate. This behaviour arises because the internal sludge structure changes to suit the prevailing shear rates. According to the literature, the Ostwald–de Waele model, i.e., a power-law model with no yield stress, is the most commonly used equation to represent the non-Newtonian behaviour of sludge,

most likely due to its simplicity and good fitting (Bougrier et al., 2006; Ayol et al., 2006; Seyssiecq et al., 2008). Other models, such as the Herschel-Bulkley model or the Bingham model, are also valid. As aforementioned, in opposition to the Ostwald–de Waele equation, these models are characterised by the presence of yield stress, below which the sample to analyse is not flowing. Generally, for a given suspension, the value of the yield stress increases with increasing the solid volume fraction (Seyssiecq et al., 2003). However, one fundamental problem with the concept of yield stress is the difficulty in determining the true yield stress (Labanda et al., 2007) because its determination is not univocal and can vary over a wide range depending on the equation used. Similarly, the shear banding effect at low shear rates may also mask the true yield stress (Baudez et al., 2013).

WAS also exhibits thixotropic behaviour (Tixier et al., 2003a), which means that internal sludge structure is formed by a complex network based on the union of flocs and macroflocs that breaksdown slowly for adapting their structure to the shear. However, very few studies concerning the sludge thixotropy can be found in the literature and most of them rely exclusively on the measurement of the hysteresis area (Tixier et al., 2003a; Guibaud et al., 2005; Baudez, 2006). According to Tixier et al. (2003b), the filamentous bacteria lead to a strong internal structure and therefore a filamentous sludge shows high viscosity and hysteresis area. Similarly, Guibaud et al. (2005) compared the hysteresis areas of two sludges with similar solid contents but different filamentous bacteria contents and found that the obtained rheogram for the filamentous sample exhibited a larger hysteresis area.

The aim of this chapter is to examine the influence of the ultrasound, low-temperature thermal and alkali treatments on the rheological profile of WAS, based on the assumption that the treatment will modify the rheological features of WAS. The rheological behaviour of the WAS has been analysed within the linear viscoelastic region by the creep test and within the non-linear viscoelastic region using the hysteresis loop and shear rate step tests.

5.2. Materials and methods

5.2.1. WAS characteristics

The rheological characterisation was performed at a constant TS content (45.9±0.9 g/L) because the rheological properties of sludge are highly conditioned by this parameter (Pollice et al., 2006; Mori et al., 2006; Laera et al., 2007). Nevertheless, at the end of this chapter, it is shown that the effect of the treatments on different sludges (with different TS contents) is reproducible.

5.2.2. Rheometer

The rheometer used in this work was a Haake RS300 control stress rheometer (Germany) (Figure 5.12) equipped with HAAKE RheoWin Software.

Figure 5.12. Rheometer Haake RS300.

This rheometer works great when operates in strain-controlled mode due to a fast feedback control loop. The rheometer is equipped with a temperature control system (thermostatic bath) and is connected to a computer that allows programming the

rheological assays and recording the data in real time. The software used for programming the rheological assays and obtaining the data were the RheoWin JobManager and the RheoWin DataManager, respectively. Measurements were conducted at 22 ± 0.1 ºC.

Different sensor geometries can be coupled to the rheometer. The choice of the proper geometry will depend on the nature of the sample and the type of experiment. Figure 5.13 shows the different types of sensor geometries commonly used in rheological assays.

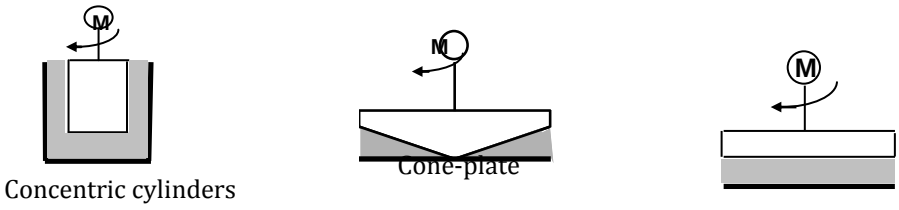

Figure 5.13. Different types of sensor geometries used in rotational viscometers and rheometers (Labanda, 2003).

The concentric cylinders are suitable for samples with very low viscosity because of its large shearing surface. The cone-plate sensor geometry is commonly used in non-Newtonian regime (under flow conditions), since it guarantee the homogeneity of shear rate in all cone points. Conversely, the plate-plate geometry is used in Newtonian regime.

5.2.3. Rheological assays

5.2.3.1. Creep test

The rheological behaviour within the linear viscoelastic region was analysed by the creep test, where a constant shear stress is applied and the time-related strain is measured. Before starting the creep test, the sludge samples were kept at rest for 10 min to relax their structures. The limiting stress in the linear viscoelastic region was

determined by conducting a shear sweep test from 0 to 100 Pa at a frequency of 1 Hz (Ruiz-Hernando et al., 2010). The stresses that did not exceed 5 Pa assured that no changes were produced in the internal structure of the WAS. Therefore, the creep tests were conducted at 5 Pa. The compliance (strain divided by shear stress), $J(t)$, (Equation 5.12) was monitored for 2 h.

$$J(t) = \frac{\gamma(t)}{\tau_a} \tag{5.12}$$

where $\gamma(t)$ is the time-related strain (-) and τ_a is the applied shear stress (Pa).

The obtained compliance data were fitted to a Burger model, which consists of three Kelvin-Voigt elements (with their corresponding relaxation times) and a Maxwell element in series (Equation 5.13):

$$J(t) = J_0 + J_1\left[1 - exp\left(\frac{-t}{\lambda_1}\right)\right] + J_2\left[1 - exp\left(\frac{-t}{\lambda_2}\right)\right] + J_3\left[1 - exp\left(\frac{-t}{\lambda_3}\right)\right] + \frac{t}{\eta_0} \tag{5.13}$$

where J_0 is the instantaneous elastic compliance of the Maxwell spring (Pa^{-1}); J_1, J_2 and J_3 are the retarded compliances (Pa^{-1}) associated to the respective relaxation times λ_1, λ_2 and λ_3 (s) of the the Kelvin–Voigt elements; and η_0 is the zero shear rate viscosity of the Maxwell dashpot (Pa·s).

A serrated plate-plate sensor geometry (20 mm in diameter) was used. Preliminary rheological experiments conducted using non-serrated parallel plates did not allow the proper recording of the creep test. The sample was isolated from the environment to prevent evaporation of water from the sample during the test (Figure 5.14).

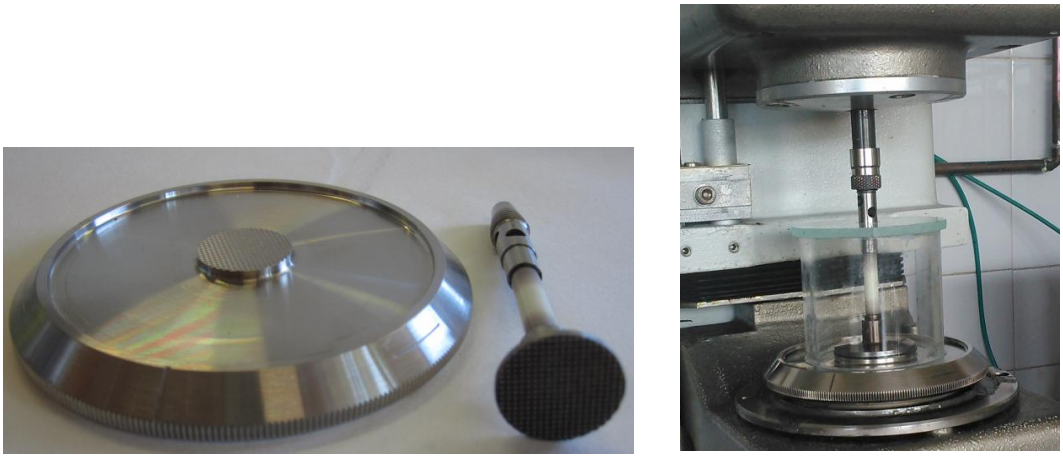

Figure 5.14. Serrated plate-plate sensor geometry used for the creep test (on the left) and isolation system (on the right).

5.2.3.2. Hysteresis loop and shear rate step tests

The rheological behaviour within the non-linear viscoelastic region was analysed by the hysteresis loop and shear rate step tests. The sensor geometry used for these assays was a 4º cone and a flat stationary plate of 35 mm diameter (Figure 5.15). The average gap of the cone-plate geometry is 888 μm and the maximum centripetal acceleration at a shear rate of 300 s^{-1} (maximum shear rate applied) is 0.78 x *g*. Under such settings, the particles trapped in the gap and the movement of particles towards the edges is minimal.

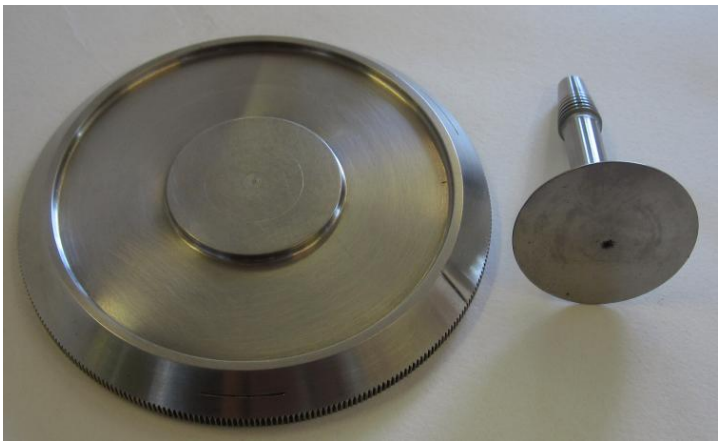

Figure 5.15. Cone-plate sensor geometry used for the hysteresis loop and shear rate step tests.

The hysteresis loop test allowed the quantification of the hysteresis area (Equation 5.11). This test was performed by linearly increasing the shear rate until reach a maximum shear rate over 5 min (up-curve); this maximum shear rate was maintained for 10 min to attain a steady state. Finally, the shear rate was decreased linearly to 0 s^{-1} over 5 min (down-curve). The maximum tested shear rates were 30, 125 and 300 s^{-1}. Previously, the stress history was minimised by pre-shearing the sludge at 5 s^{-1} for 10 min (Figure 5.16). Therefore, the tests always began with the steady state corresponding to a shear rate of 5 s^{-1}.

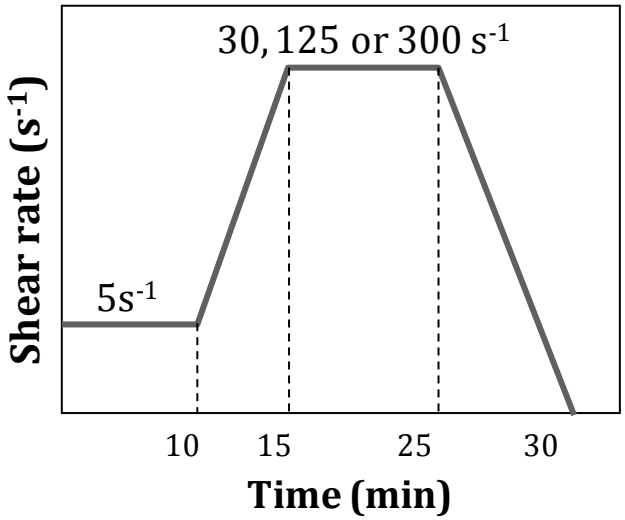

Figure 5.16. Hysteresis loop test performed.

The shear rate step test allowed the steady state viscosity, η_e, to be determined at different shear rates (5, 30, 125 and 300 s^{-1}). The test consisted of pre-shearing the sludge at a fixed shear rate of 5 s^{-1} for 10 min. Then, the shear rate was suddenly changed to 30, 125 or 300 s^{-1} for 10 min to achieve steady states (Figure 5.17). This test also allowed the quantification of the kinetic process (this is further explained in Chapter 6). As the sequences of shear rate were always increased, all the experimental data of this test corresponds to the kinetic breakdown process.

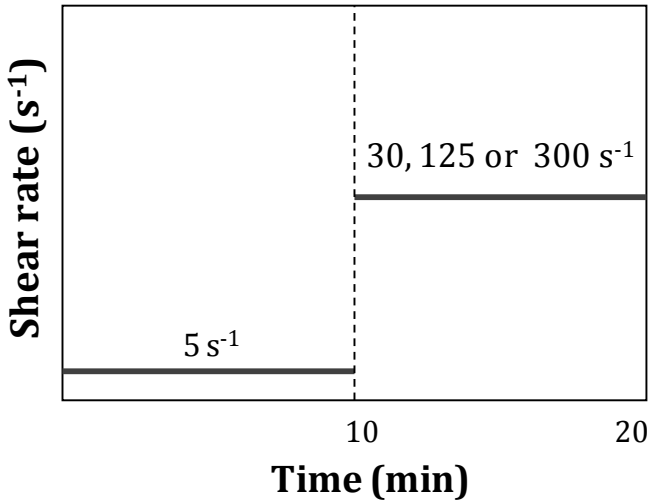

Figure 5.17. Shear rate step test performed.

The steady state viscosity, η_e, was determined from the experimental data and following a first-order kinetic equation (the explanation of this equation is provided in the next chapter and corresponds to Equation 6.8). Then, the steady state viscosities measured for each shear rate were fitted to the Ostwald-de Waele equation (Equation 5.14, which is Equation 5.8 in terms of viscosity), which is valid for pseudoplastic fluids.

$$\eta_e = K \cdot \dot{\gamma}^{n-1} \tag{5.14}$$

5.3. Results and discussion

5.3.1. Rheological characterisation within the linear viscoelastic region

5.3.1.1. The creep compliance

Figures 5.18, 5.19 and 5.20 show the creep compliance data corresponding to the untreated and treated sludge samples (ultrasound: 5000, 11,000 and 27,000 kJ/kg TS; thermal: 11,000 (60 ºC), 15,000 (80 ºC) and 18,000 (90 ºC) kJ/kg TS; alkali: 70.6 and 157 g NaOH/kg TS) and their respective best fits to the Burger model (Equation 5.13). Note that the maximum value for the y-axis is not the same for the three treatments in order to facilitate the visualisation of the simulation. The good fit of the experimental

data showed the capability of the model to reproduce the viscoelastic response of the sludge.

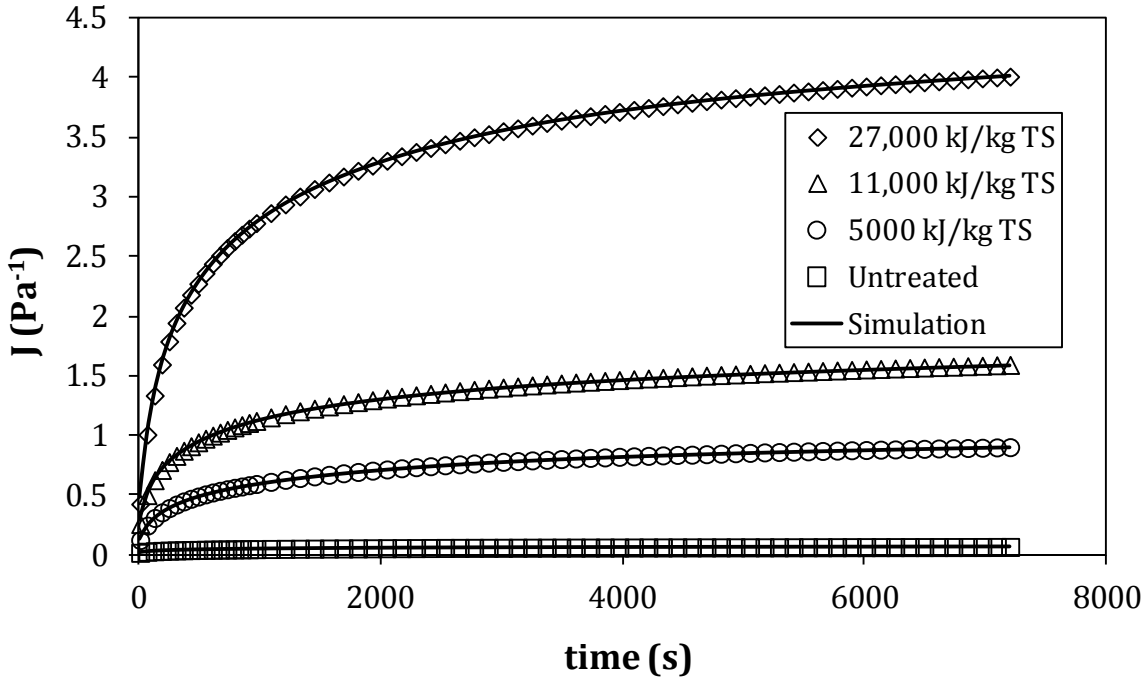

Figure 5.18. Creep assay for the untreated and three ultrasonicated sludge samples. The solid black lines correspond to the best fit to the Burger model described in Equation 5.13.

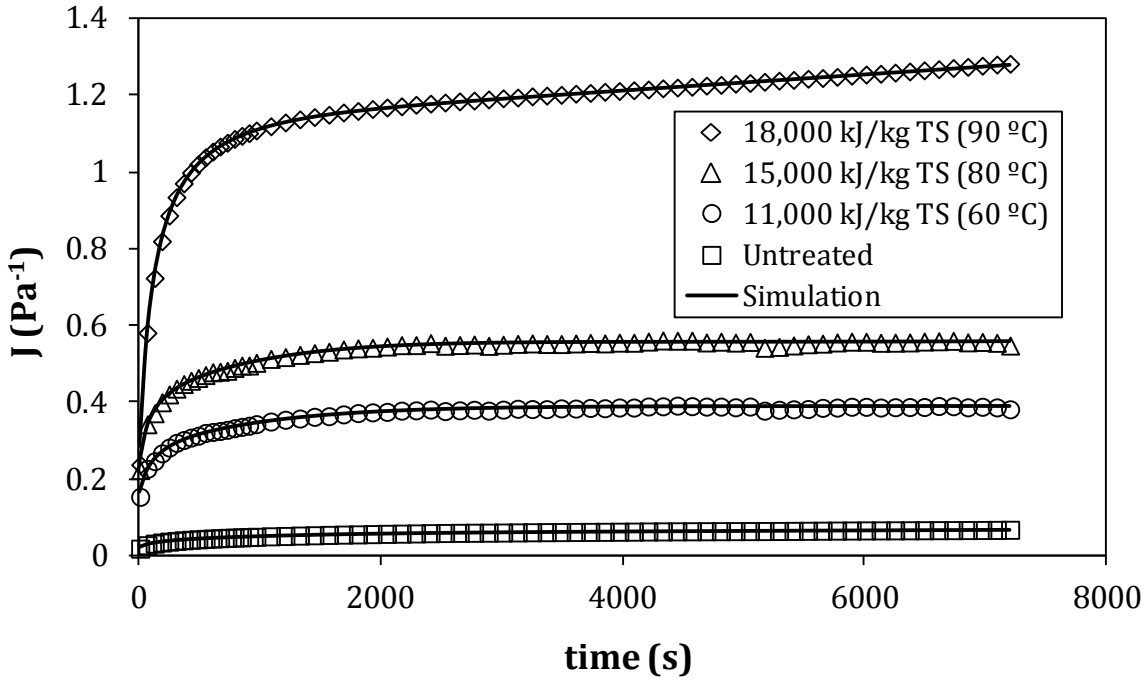

Figure 5.19. Creep assay for the untreated and three thermally treated sludge samples. The solid black lines correspond to the best fit to the Burger model described in Equation 5.13.

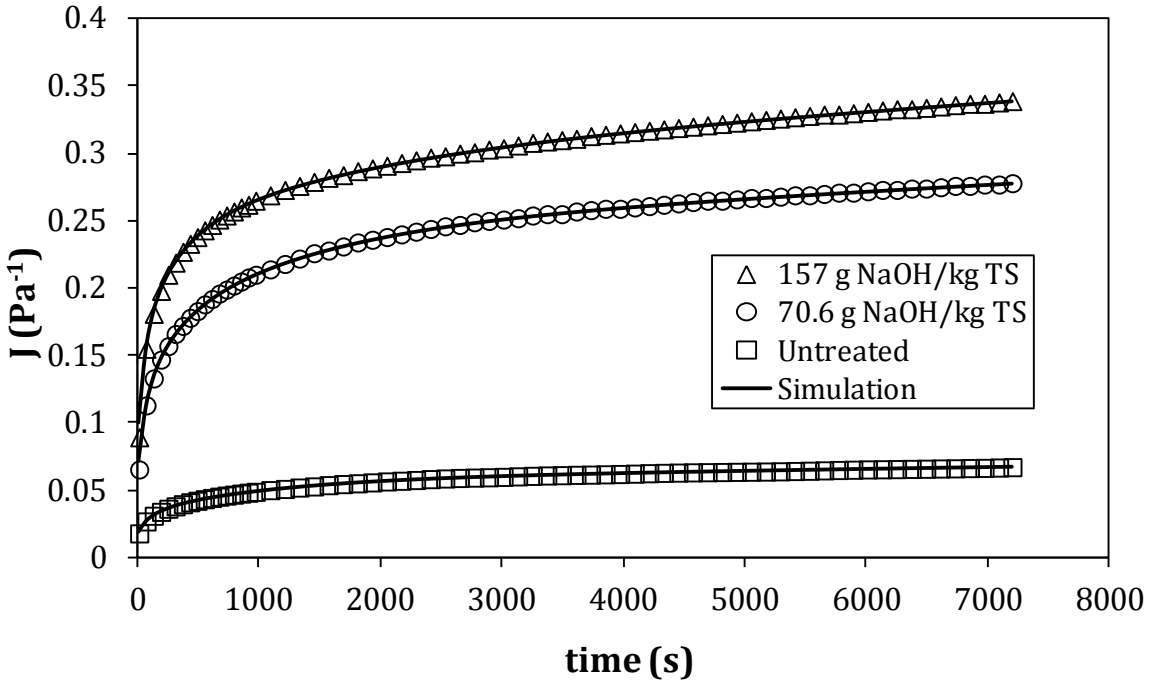

Figure 5.20. Creep assay for the untreated and two alkali-treated sludge samples. The solid black lines correspond to the best fit to the Burger model described in Equation 5.13.

In a typical creep test for a viscoelastic material, the strain (or compliance) shows three different behaviours in time. Initially, a sudden increase of strain is observed, which corresponds to a pure elastic behaviour of the sample. This behaviour can be quantified with the parameter G_0, which is the inverse of J_0 and measures the initial elasticity of the sample. Then, the strain increases at a variable rate over a long period of time, which corresponds to the viscoelastic behaviour of the sample. This behaviour can be quantified with the following parameters: elasticity modulus, $G_i = 1/J_i$, and relaxation times, λ_i, i = 1, 2 and 3, (Equation 5.13). Finally, the strain increases at a constant rate, which corresponds to the pure viscous behaviour of the sample. This behaviour can be quantified with the parameter η_0 (Equation 5.13), which corresponds to the zero shear rate viscosity (Schramm, 2004).

The creep compliance increased when increasing the treatment intensity, which suggested that the treated sludge was more easily deformed by a given stress (Figures 5.18, 5.19 and 5.20). Specifically, the ultrasound treatment resulted in the greatest

deformation. Table 5.1 shows the values of the parameters $G_0$and η_0, obtained with the model described in Equation 5.13. High values of G_0 indicated mechanically strong and rigid structures, and high values of η_0 indicated large structures. All of the treatments decreased the G_0 and η_0 values compared to the untreated sludge. Therefore, all treatments loosened and disrupted the internal structure of the sludge.

Table 5.1. Initial elasticity, G_0, and zero shear rate viscosity, η_0, obtained using the Burger model described in Equation 5.13.

	G_0 (Pa)	$\eta_0 \cdot 10^{-4}$ (Pa·s)
Untreated	58.8	78.1
Ultrasound (kJ/kg TS)		
5000	8.77	5.98
11,000	4.20	4.08
27,000	2.70	1.96
Thermal (kJ/kg TS; ºC)		
11,000 (60 ºC)	6.71	30.9
15,000 (80 ºC)	4.57	18.9
18,000 (90 ºC)	3.88	3.58
Alkali (g NaOH/kg TS)		
35.3	20.8	n.a.
70.6	16.1	21.0
157	11.6	16.9

n.a.: not available. The $\eta_0$value corresponding to the concentration of 35.3 g NaOH/kg TS is not available because data were inconsistent with the model for creep, possibly due to the evaporation of water during the creep assay.

5.3.1.2. The relaxation spectra

Figures 5.21, 5.22 and 5.23 show the relaxation spectra of the untreated and treated sludge samples. These spectra were obtained from the creep test fit to Equation 5.13, and corresponded to the period of time when the samples exhibited viscoelastic behaviour (response of the Kelvin-Voigt elements). The G_i modules and relaxation times

associated, λ_i, are related to the viscoelastic structures of the sample. The relaxation time of a structure is closely related to the size of this structure and the modulus G_i is related to the number of these structures. These relationships are well known in the field of polymeric materials (Llorens et al., 2003). The three treatments decreased the number of structures in all the relaxation times analysed (Figures 5.21, 5.22 and 5.23). When the maximum intensity used in each treatment is compared, the maximum decrease in the number of structures was observed after the ultrasound treatment (Figure 5.21).

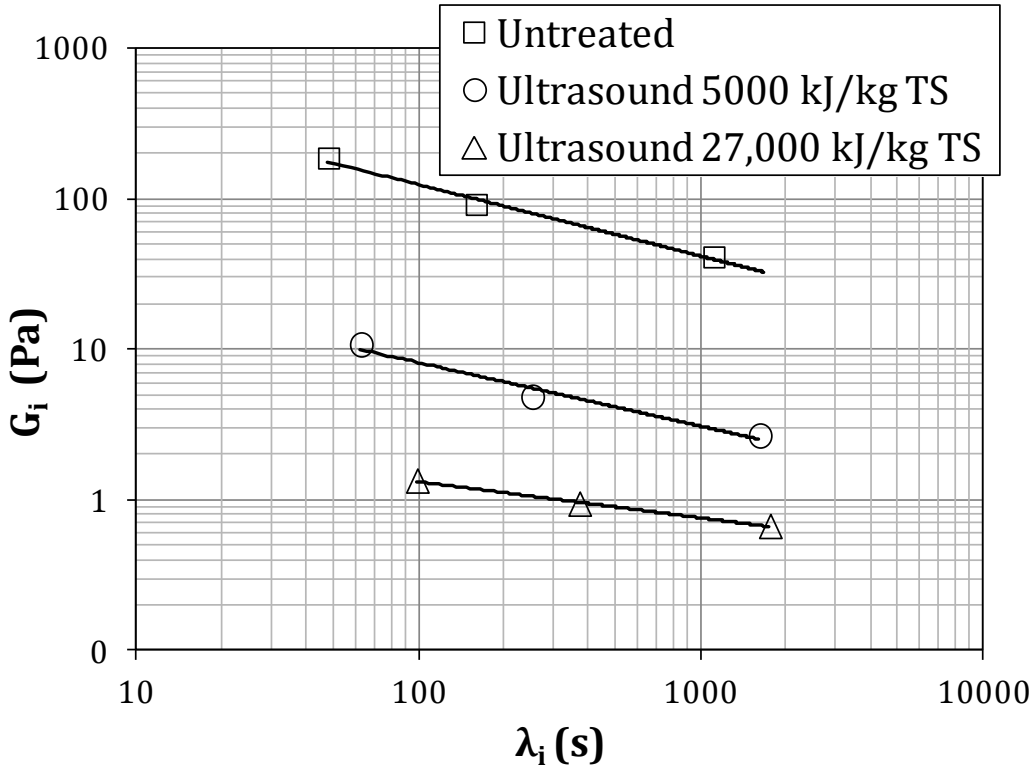

Figure 5.21. Relaxation spectra for the untreated and two ultrasonicated sludge samples.

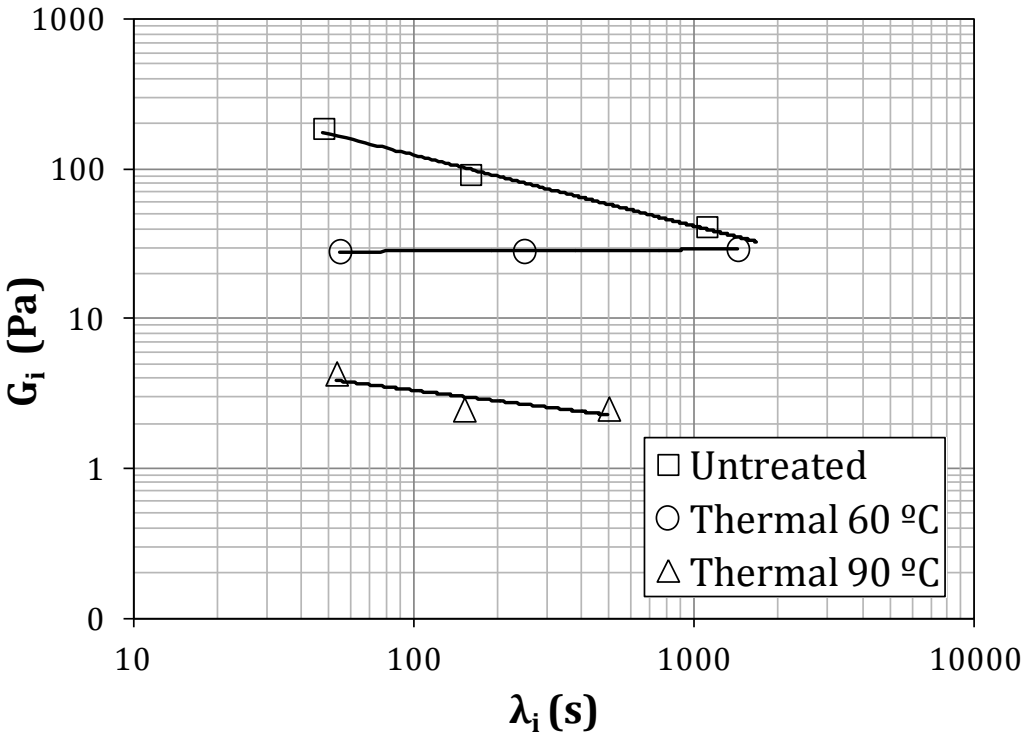

Figure 5.22. Relaxation spectra for the untreated and two thermally treated sludge samples.

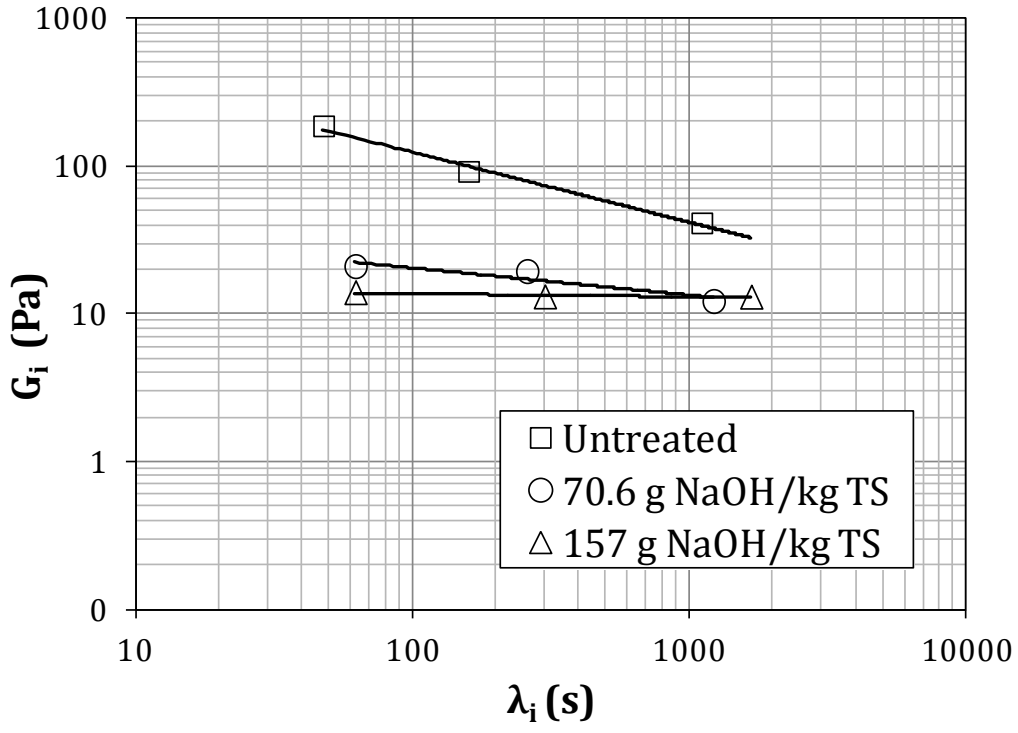

Figure 5.23. Relaxation spectra for the untreated and two alkali-treated sludge samples.

5.3.2. Rheological characterisation within the non-linear viscoelastic region

5.3.2.1. Steady state viscosity

Figures 5.24, 5.25 and 5.26 show the evolution of steady state viscosity with applied shear rate for the untreated and treated sludges. As can be observed, the viscosities decrease when increasing shear rate. It was observed for all the sludge samples that shear stresses always tend to zero as shear rates tend to zero (extending the range of view in the very low shear rates). Therefore, the steady state viscosity followed the pseudoplastic behaviour defined by Ostwald's equation (Equation 5.14), following power law dependence with the shear rate. The good fit of the experimental data showed the capability of the Ostwald–de Waele model to reproduce the pseudoplastic response of the WAS.

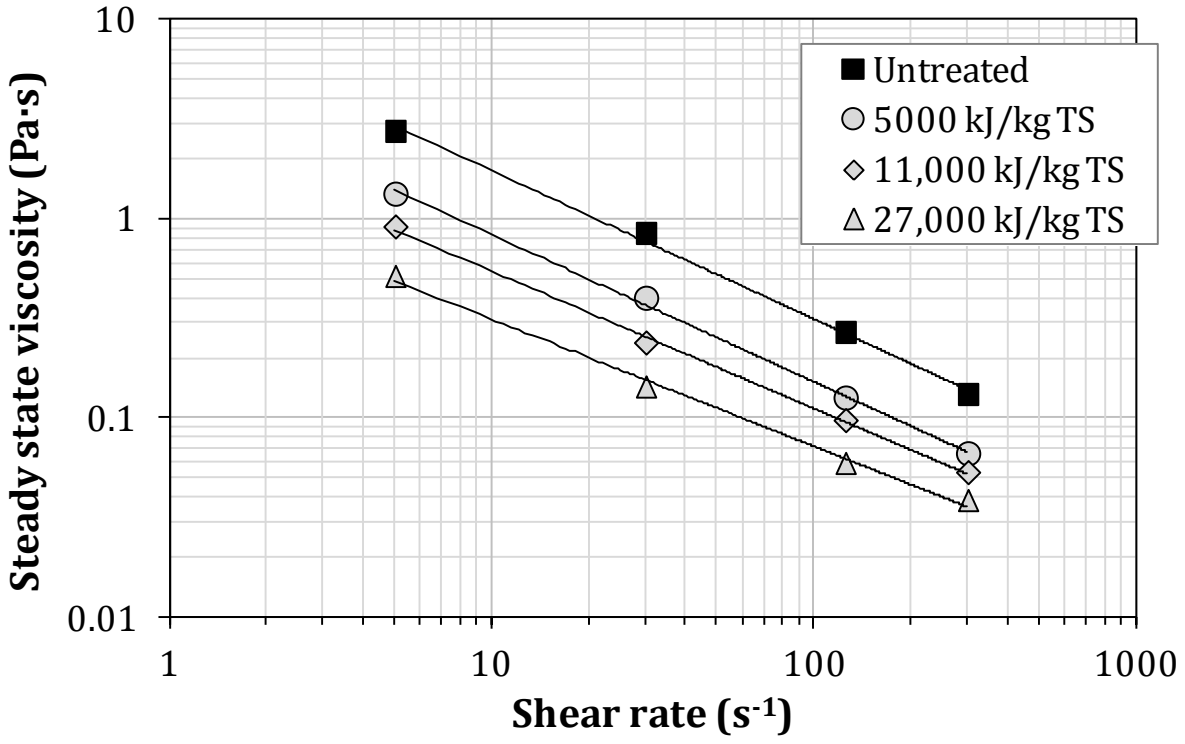

Figure 5.24. Steady state viscosity as a function of shear rate for the untreated and three ultrasonicated sludge samples. The solid black lines correspond to the fit to the Ostwald-de Waele power-law model.

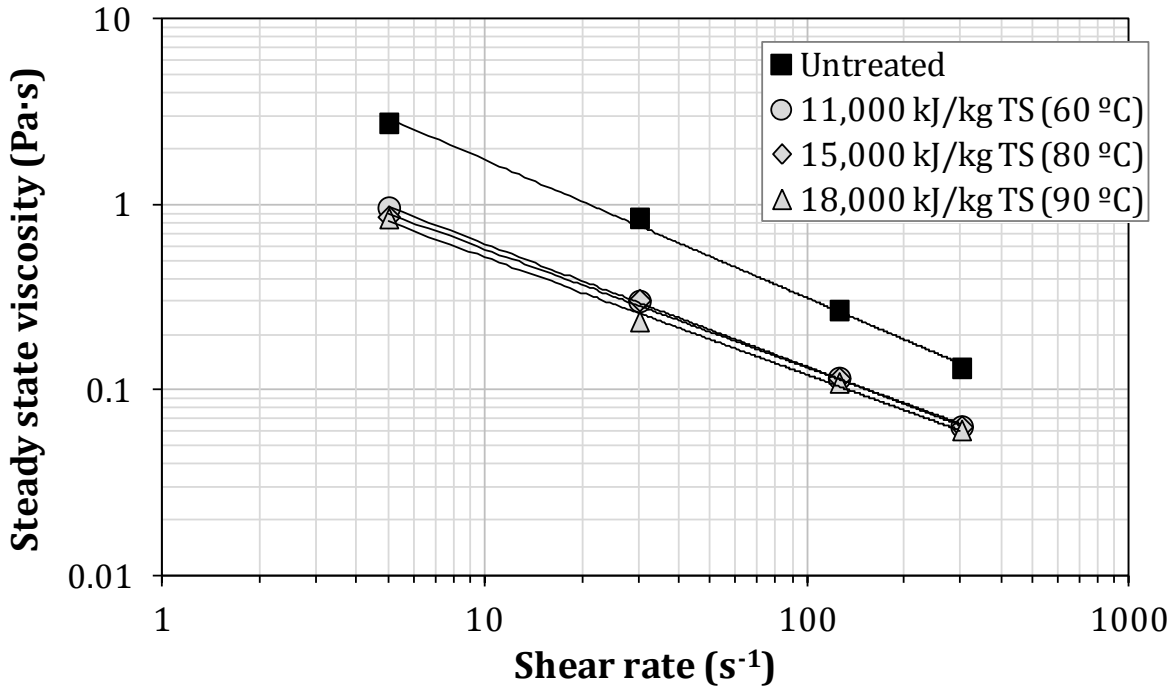

Figure 5.25. Steady state viscosity as a function of shear rate for the untreated and three thermally treated sludge samples. The solid black lines correspond to the fit to the Ostwald-de Waele power-law model.

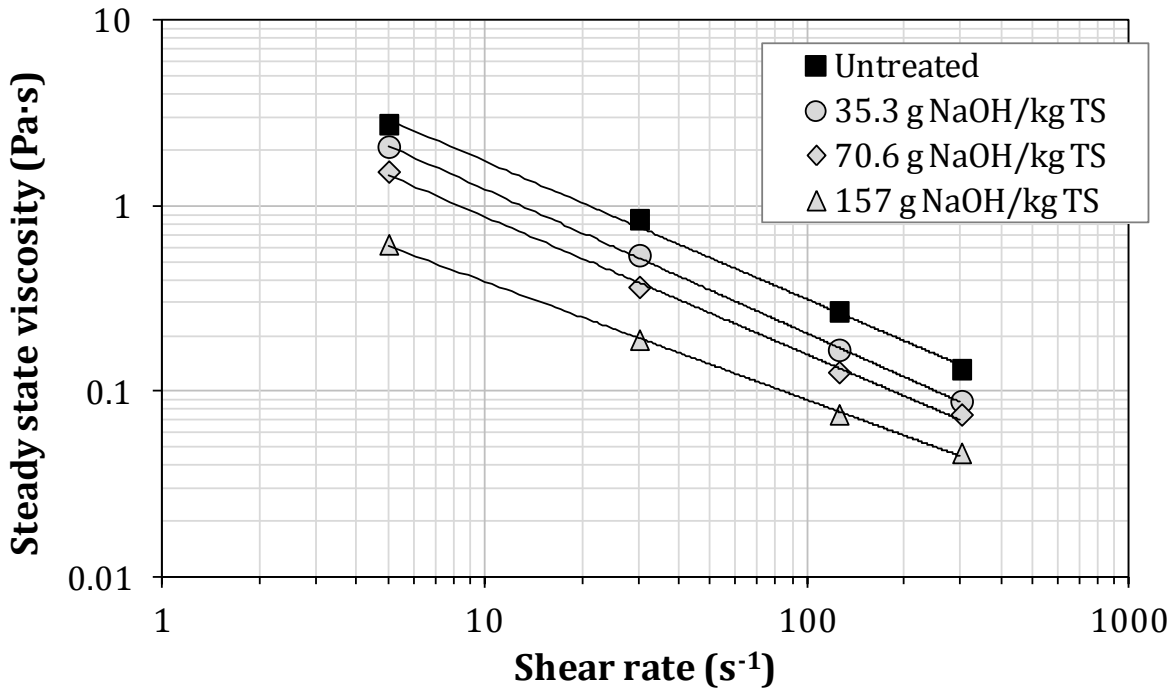

Figure 5.26. Steady state viscosity as a function of shear rate for the untreated and three alkali-treated sludge samples. The solid black lines correspond to the fit to the Ostwald-de Waele power-law model.

To better visualise the effect of the treatments on sludge viscosity reduction, the values of the steady state viscosity corresponding to a shear rate of 5 s^{-1} are shown in Figure 5.27. The steady state viscosity was reduced with the treatments. In the case of the ultrasound and alkali treatment, this reduction was higher when increasing treatment intensity, whereas the reduction of viscosity after the thermal treatment was very similar between the three tested temperatures. Specifically, the ultrasound treatment at 27,000 kJ/kg TS resulted in the highest viscosity reduction, which represented a reduction of approximately 80% (0.515 Pa·s). In contrast, the low doses of alkali treatment (35.3 and 70.6 g NaOH/kg TS) showed the lowest reductions of steady state viscosities. Similar results were observed on the other tested shear rates. However, the differences in viscosity were less significant at higher shear rates because of the pseudoplastic behaviour of the sludge. The reduction in the sludge viscosity after the application of the treatments may be due to the weakening of connections between sludge flocs.

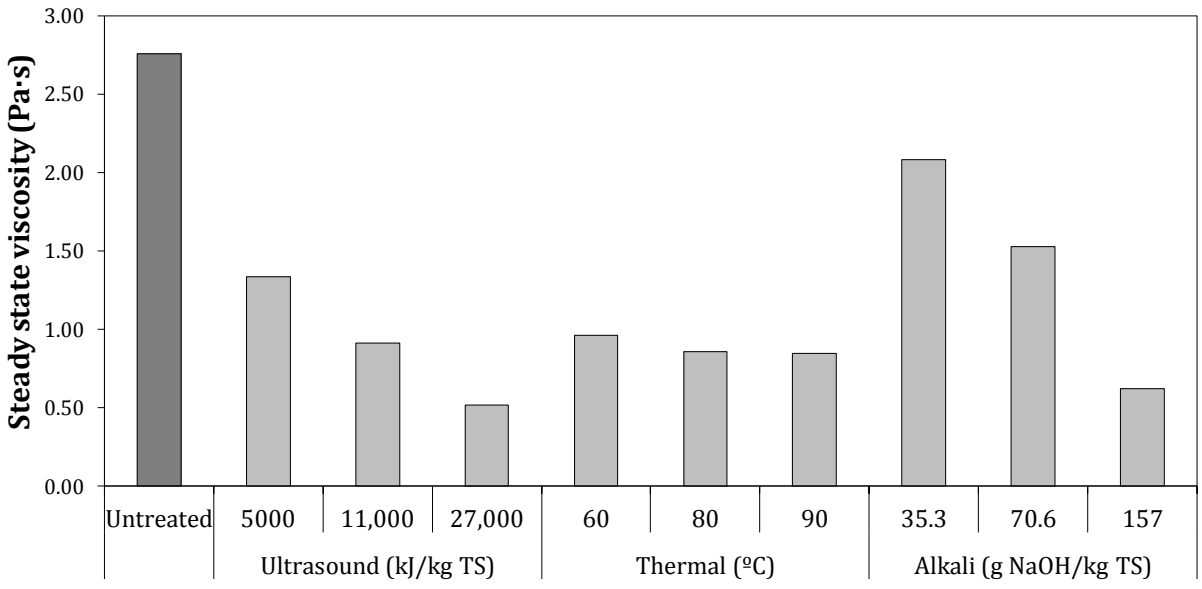

Figure 5.27. Steady state viscosity of the untreated and treated sludge samples at a shear rate of 5 s^{-1}.

The parameters of the Ostwald–de Waele equation and the correlation of the coefficients are shown in Table 5.2.

Table 5.2. Ostwald-de Waele parameters. *K* is the consistency index and *n* the power law index.

	K (Pa·s^n)	**n (-)**	**R^2[1]**
Untreated	9.67	0.256	0.9971
Ultrasound (kJ/kg TS)			
5000	4.56	0.261	0.9983
11,000	2.67	0.311	0.9985
27,000	1.36	0.392	0.9954
Thermal (kJ/kg TS; ºC)			
11,000 (60 ºC)	2.83	0.337	0.9998
15,000 (80 ºC)	2.50	0.362	0.9981
18,000 (90 ºC)	2.15	0.371	0.9904
Alkali (g NaOH/kg TS)			
35.3	7.38	0.222	0.9996
70.6	4.84	0.257	0.9975
157	1.70	0.363	0.9990

[1]Correlation coefficients for the Ostwald-de Waele parameters.

The consistency index, *K*, is a measure of the average firmness of the sample; the higher the value of the *K*, the greater the apparent steady state viscosity (Moeller and Torres, 1997). The power law index, *n*, is linked to the apparent steady state viscosity dependence on shear rate: *n* is equal to 1 for Newtonian fluids, higher than 1 for dilatant fluids and lower than 1 for pseudo-plastic fluids. The tested treatments caused a reduction in *K* and an increase in *n* (although the value of *n* remained always below unity). The reduction in *K* suggested that the internal structure of the material decreased in size with treatments, which is consistent with the results obtained for the particle size distribution (this is explained below). The small structures (with lower *K*) were less pseudoplastic than the larger structures because the small structures were less

deformable. The simultaneous decrease of the consistency index and increase of the power law index with increased temperature has been observed by other authors (Hammadi et al., 2013; Feng et al., 2014).

5.3.2.2. Particle size distribution

Figure 5.28 shows the profiles of the particle size distribution of the untreated and three treated sludge samples. The conditions analysed for the ultrasound and alkali treatments were the highest intensities tested for these treatments (27,000 kJ/kg TS and 157 g NaOH/kg TS, respectively). The condition analysed for the thermal treatment was the temperature of 80 ºC, since the differences in viscosity reduction between 80 and 90 ºC were minimal.

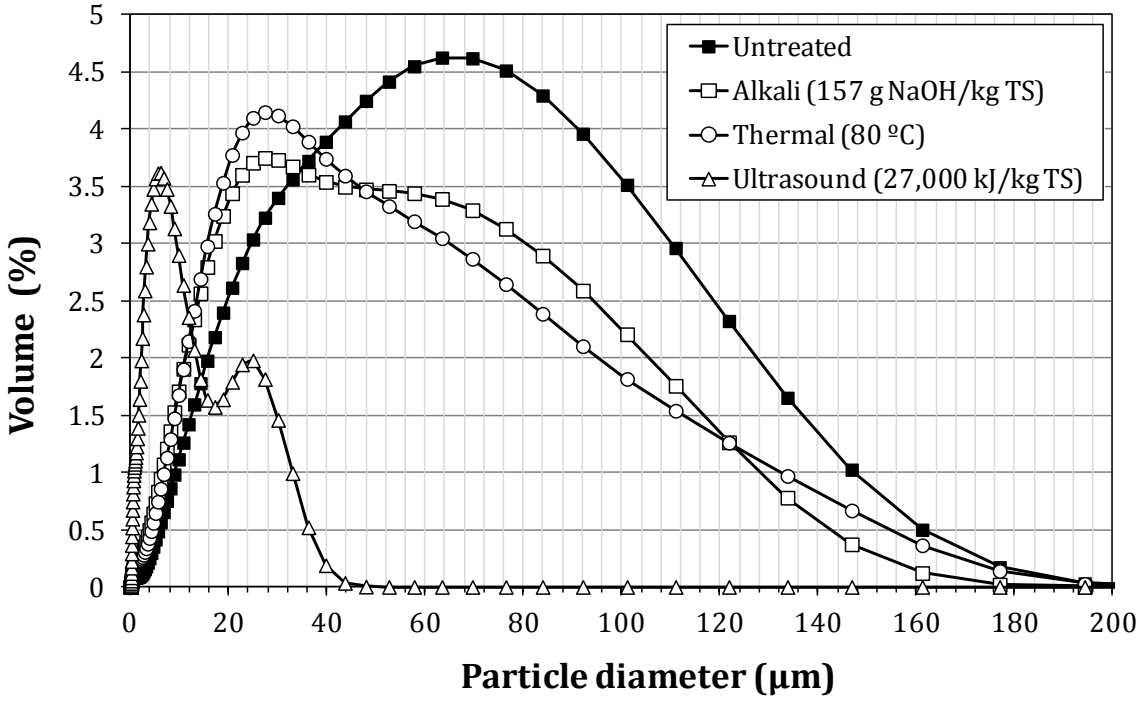

Figure 5.28. Particle size distribution.

All sludge particles were smaller than 200 µm. The average particle size for the untreated sludge was 50.5 µm. The particle size profiles of treated sludges vary widely,

depending on the treatment. The results given in Table 5.3 express the particle sizes that correspond with 10%, 50% and 90% of the size histogram; i.e., in the case of untreated sludge, 90% of the volume consists of particles smaller than 101 μm, 50% consist of particles smaller than 39.8 μm, and 10% consist of particles smaller than 10.8 μm. The maximum reduction in particle size was observed after the ultrasound treatment, which resulted in the highest viscosity reduction. Specifically, in the case of ultrasound treatment, the particle size decreased by over 80%, with an average particle size of 7.82 μm. The reduction in particle size by the application of ultrasonic waves was observed by other authors (Bougrier et al., 2006; Pham et al., 2010). Of course, this reduction depends not only on the specific ultrasonic energy supplied, but also on the sludge properties. The thermal and alkali treatments decreased the particle size by approximately 25% and their mean sizes were 38.0 μm and 38.3 μm, respectively.

Table 5.3. Particle sizes for the untreated and three treated sludge samples.

	d10 (μm)	**d50 (μm)**	**d90 (μm)**	**Average particle size (μm)**	**SD (μm)**	**CV (%)**
Untreated	10.8	39.8	101	50.5	35.7	70.5
Ultrasound (27,000 kJ/kg TS)	0.791	5.11	20.7	7.82	7.94	101
Thermal (80 ºC)	6.76	27.4	83.9	38.0	32.1	84.6
Alkali (157 g NaOH/kg TS)	6.16	27.4	83.9	38.3	31.4	82.0

SD: standard deviation.

CV: coefficient of variation= SD/average particle size·100.

5.3.2.3. Pumping costs

The reduction in sludge viscosity will reduce the energy for pumping and mixing when the flow is away from the highly turbulent region. A rough estimate of the energy consumption required for pumping the untreated and treated sludges throughout a pipeline of 500 m is summarised in Table 5.4. The head loss throughout the length of the pipeline was calculated using a mechanical energy balance for non-Newtonian fluids that follows the power law.

Table 5.4. Energy consumption for pumping the sludge.

	Energy for pumping (kJ/kg TS)
Untreated	11.8
Ultrasound (kJ/kg TS)	
5000	5.65
11,000	3.71
27,000	2.27
Thermal (kJ/kg TS; ºC)	
11,000 (60 ºC)	4.17
15,000 (80 ºC)	3.90
18,000 (90 ºC)	3.43
Alkali (g NaOH/kg TS)	
35.3	8.34
70.6	5.94
157	2.66

The highest intensities of ultrasound, alkali and thermal treatments reduced the energy of pumping from 11.8 kJ/kg TS (no treatment) to 2.27, 3.43 and 2.66 kJ/kg TS, which corresponds to a reduction of approximately 80, 70 and 75%, respectively. This approach was obtained assuming a sludge flow velocity of 0.2 m/s, a pipeline length of 500 m and a pipeline internal diameter of 150 mm. These specifications were obtained from the Baix Llobregat WWTP. Clearly, the energy required for pumping the untreated sludge (11.8 kJ/kg TS) is considerably lower than the cost of conducting the ultrasound (27,000 kJ/kg TS) or thermal (18,000 kJ/kg TS) treatments. Nevertheless, on an industrial scale, these differences would be lower due to the higher efficiency of commercial ultrasonic devices or the use of a combined heat and power (CHP) unit. Finally, although it was not quantified, it is conceivable that the decrease in viscosity improved the mixing in the digester and allowed the realisation of high solids anaerobic digestion, thus enhancing the final biogas production and the energy balance.

5.3.2.4. Hysteresis area

Under non steady state conditions, the sludge samples exhibited thixotropic behaviour, as observed by the presence of the hysteresis area (Figures 5.29, 5.30 and 5.31). Indeed, the presence of the hysteresis area indicated that the sludges showed positive thixotropic behaviour. Thus, shear stresses during the up-curves were higher than shear stresses during the down-curves at the same shear rate. Figures 5.29, 5.30 and 5.31 show the hysteresis loops for the untreated and treated sludges at a shear rate of 300 s^{-1}. As can be observed, the hysteresis area is reduced when increasing treatment intensities. This effect is also observed in Table 5.5, where the value of the hysteresis area is provided for the untreated and treated sludge samples for all the tested shear rates. As in the case of the steady state viscosity, the maximum reduction of the hysteresis area (approximately 95%) was observed after ultrasonication at 27,000 kJ/kg TS. Similarly, the lower reduction was observed after alkali addition of 35.3 g NaOH/kg TS. The hysteresis area reduction after thermal treatments was similar for the three tested temperatures.

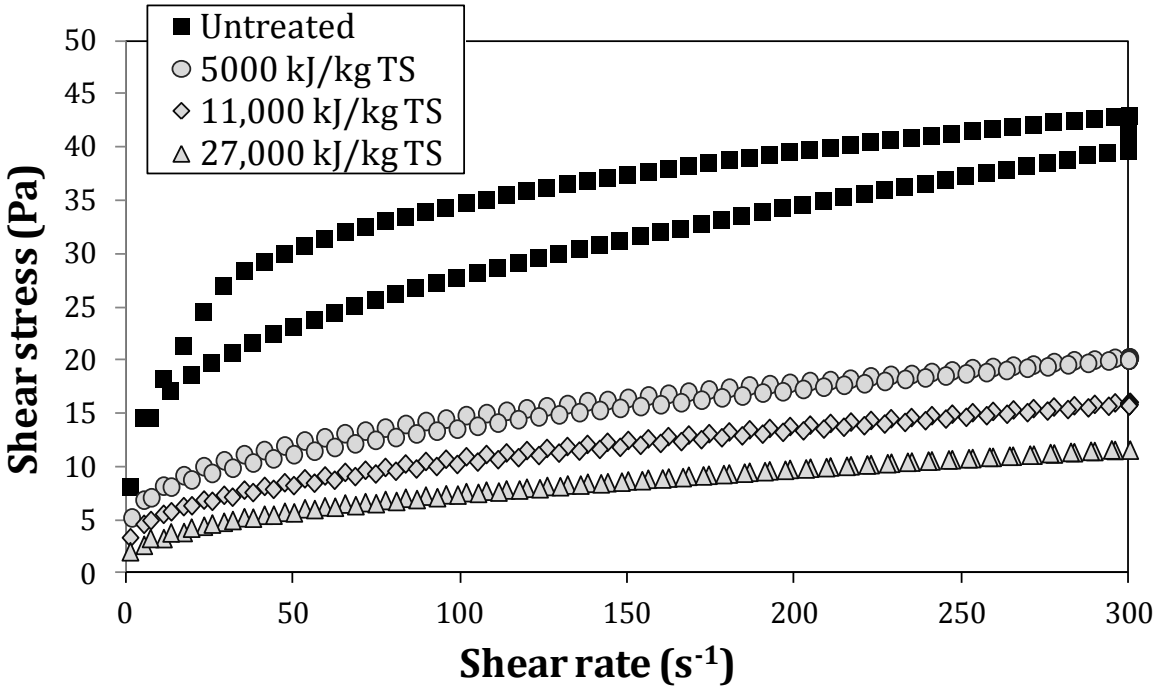

Figure 5.29. Hysteresis loops obtained for the untreated and three ultrasonicated sludge samples at a maximum shear rate of 300 s^{-1}.

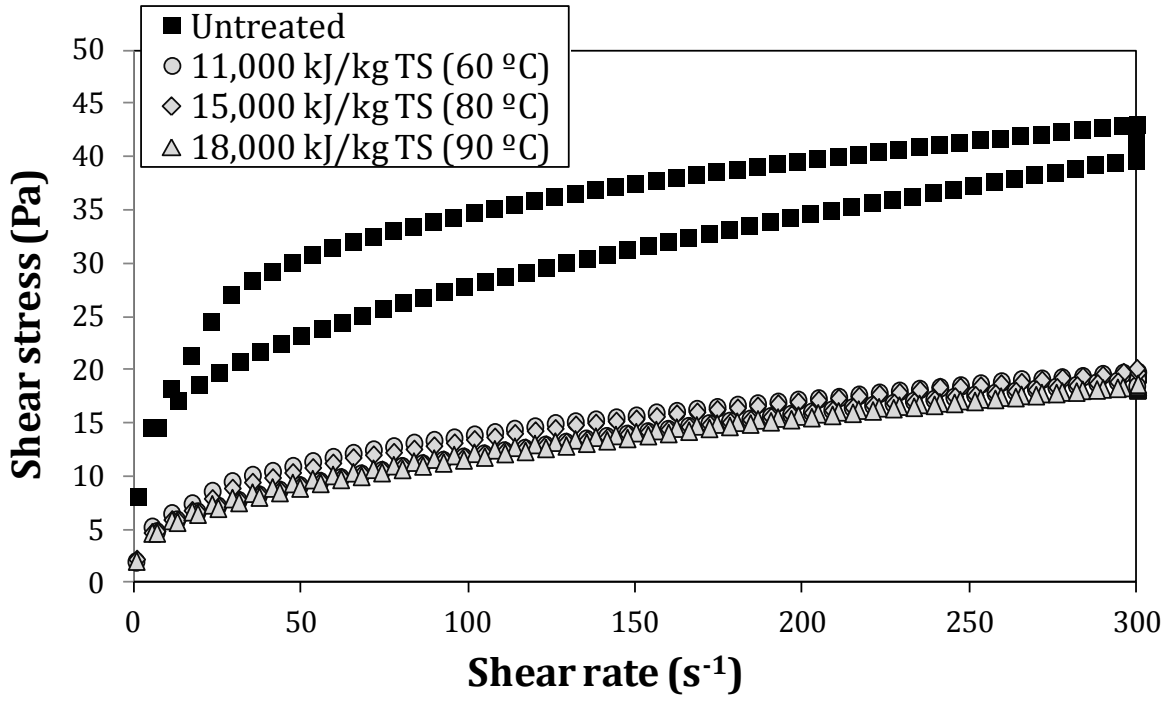

Figure 5.30. Hysteresis loops obtained for the untreated and three thermally treated sludge samples at a maximum shear rate of 300 s^{-1}.

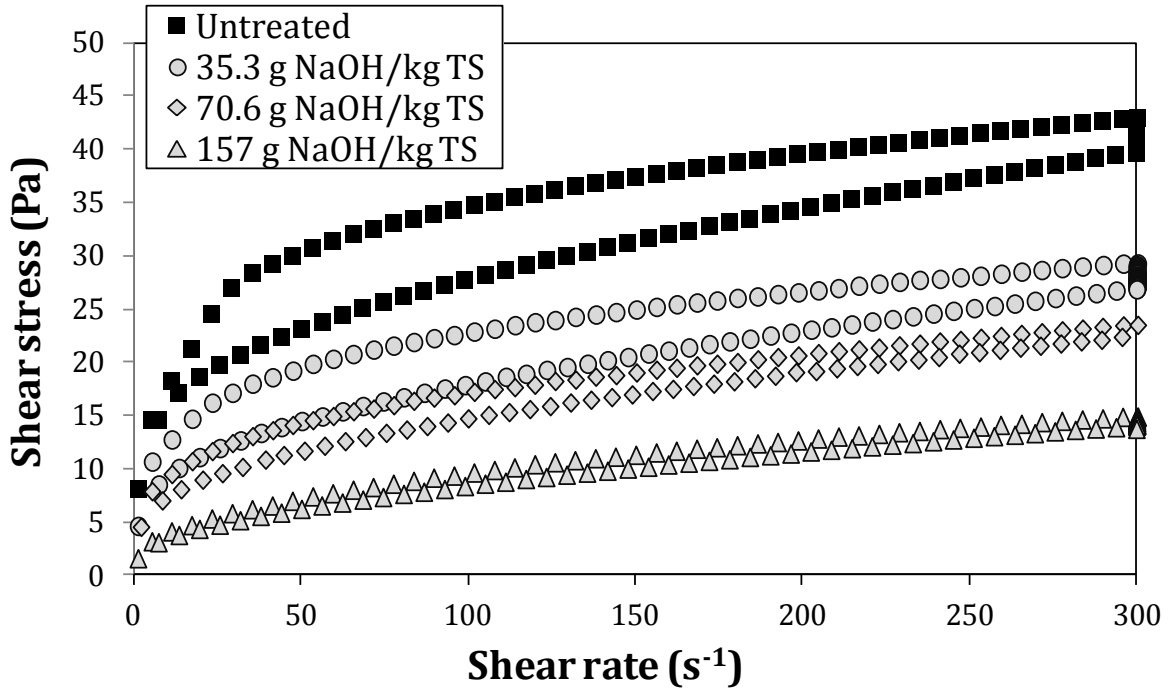

Figure 5.31. Hysteresis loops obtained for the untreated and three alkali-treated sludge samples at a maximum shear rate of 300 s^{-1}.

Table 5.5. Hysteresis area values of all the sludges at the three maximum shear rates analysed: 300, 125 and 30 s^{-1}.

	Hysteresis area (Pa s^{-1})		
	Maximum shear rate of 300 s^{-1}	Maximum shear rate of 125 s^{-1}	Maximum shear rate of 30 s^{-1}
Untreated	1569	368	68.9
Ultrasound (kJ/kg TS)			
5000	198	27.5	17.0
11,000	120	24.5	13.2
27,000	44.3	22.1	10.6
Thermal (kJ/kg TS; ºC)			
11,000 (60 ºC)	420	72.6	44.9
15,000 (80 ºC)	335	33.8	23.2
18,000 (90 ºC)	89.1	32.8	15.1
Alkali (g NaOH/kg TS)			
35.3	1161	278	53.5
70.6	558	165	40.0
157	306	60.7	12.6

5.3.2.5. Reproducibility of the treatments on sludge rheology

As aforementioned, the rheological properties of sludge are highly conditioned by the solid content. This means that, in absolute value, the values of both the viscosity and hysteresis area varied widely depending on the total solid content. For instance, the absolute value of the hysteresis area corresponding to a shear rate of 300 s^{-1} is 1569 Pa·s^{-1} for an untreated sludge with a TS content of 45.9±0.9 g/L, 3102 Pa·s^{-1} for an untreated sludge with a TS content of 50.8±0.3 g/L and 4176 Pa·s^{-1} for an untreated sludge with a TS content of 56.7±0.7 g/L. Thus, the hysteresis area is higher for concentrated sludges and, accordingly, the effect of the treatments will be reflected in proportion to this. Nevertheless, if we compare the effect of treatments in terms of hysteresis area reduction (% of reduction in comparison with the untreated sludge), the results are very similar regardless of the TS content of the sample. This idea is summarised in Table 5.6, which shows the hysteresis area reduction after one condition

of each treatment and for different TS contents. The hysteresis area is a very good parameter to do this comparison because its value takes into account all the shear stresses of the rheogram.

Table 5.6. Hysteresis area reduction after one condition of each treatment and for different total solid contents.

	Hysteresis area reduction (%)[1]			
	TS = 45.9±0.9 g/L	TS = 50.8±0.3 g/L	TS = 56.7±0.7g/L	Mean (±SD)
Ultrasound: 27000 kJ/kg TS	97%	94%	88%	93±5
Thermal: 15,000 kJ/kg TS	79%	73%	81%	78±4
Alkali: 157 g NaOH/kg TS	80%	77%	83%	80±3

[1]Data for a shear rate of 300 s^{-1}.

Chapter 6 Rheological structural model to study the thixotropic behaviour of WAS

6.1. Theory

In this chapter, it has been analysed the variations in the thixotropic behaviour of WAS before and after the treatments by means of a rheological structural model. The model proposed is defined following the classical description of thixotropic structural models. The breakdown and build-up of the internal network with shear-time is demonstrated with an equation of state (called the constitutive equation) and two kinetic equations, which consider the time dependence of the viscosity at constant shear rate conditions. The model is based on the definition of the structural parameter, *S*, which quantifies the structural level of the internal structure at any time and shear rate (Labanda and Llorens 2006; Ruiz-Hernando et al., 2015a). The structural parameter goes to zero when the internal structure is completely broken down and produces the lowest viscosity, while a complete build-up structure corresponds to the highest value of *S* and yields the highest viscosity. The proposed constitutive equation for a pseudoplastic fluid is:

$$\eta(S,\dot{\gamma}) = S \cdot \dot{\gamma}^{-m} \tag{6.1}$$

where η is the viscosity (Pa·s), S is the structural parameter (Pa·s^{1-m}), $\dot{\gamma}$ is the shear rate (s^{-1}) and m is a parameter that quantifies viscosity changes when a shear rate is applied (-).

Equation 6.1 shows that viscosity can arise not only from structural changes due to changes in the shear rate but also due to the change in the shear rate itself. The power law exponent is negative because the viscosity decreases with the shear rate for pseudoplastic fluids. After a sudden change in the share rate, the viscosity value only changes because of the shear rate effect (called start-up viscosity). This change occurs due to the instantaneous variations in the alignment and deformation of flocs and can be quantified via the m parameter. Despite this change, the structural level remains constant in size. After alignment and deformation, the structure breaks down or builds up, and the viscosity value changes following the kinetic processes that characterise the thixotropic behaviour of sludge.

The time dependence of the non-equilibrium structural parameter is defined as the net breakdown and net build-up kinetic processes because of shear forces and particle interactions. Thus, the net breakdown process at a fixed shear rate depends on the destruction of internal structure due to the imposed shear and the restructuration of internal structure, which is almost shear rate independent (Coussot, 2005):

$$\frac{dS}{dt} = k_R \cdot (S_0 - S) - k_D \cdot (S - S_\infty) \tag{6.2}$$

where k_R and k_D are the kinetic coefficients (s^{-1}) for restructuration and destruction processes, respectively, and S_0 and S_∞ are the limiting values of the structural parameter at zero and infinite shear rate, respectively.

At steady state conditions, Equation 6.2 can be solved to find the equilibrium structural parameter as follows:

$$Se = \frac{k_R \cdot S_0 + k_D \cdot S_\infty}{k_R + k_D} \tag{6.3}$$

where S_e is the steady state structural parameter.

By combining Equations 6.2 and 6.3, the net kinetic equation is defined by the driving force for the net kinetic process, which is the difference between the steady state and current structural state (Cheng, 2003):

$$\frac{dS}{dt} = -K \cdot (S - S_e) \tag{6.4}$$

where K is a characteristic thixotropic kinetic coefficient (s^{-1}), which is related to the time needed to reach the steady-state structural parameter.

Importantly, both thixotropic kinetic processes can show different kinetic coefficients because the time to break down the structure is usually faster than the time to build up the structure (Abu-Jdayil, 2003). However, if the applied shear rate is very low, the rate of restructuration could predominate and, as a result, the build up process could be faster than the breakdown process (Coussot, 2005). The kinetic process then features two kinetic coefficients: the thixotropic kinetic coefficient for the net build-up of the structure, K_{up}, and the thixotropic kinetic coefficient for the net breakdown of the structure, K_{down}. The evolution of the structural parameter with time is obtained by integrating the kinetic equation:

$$S = (S' - S_e) \cdot exp(-K \cdot \Delta t) + S_e \quad (6.5)$$

where S' is the structural parameter at time $t' = t\text{-}\Delta t$.

Thus, the current structural parameter, S, depends on the previous structural parameter, S', the steady state structural parameter at the current shear rate, S_e, and the kinetic coefficient, K.

Under steady state conditions, the viscosity reaches the steady state viscosity at the shear rate applied, and most sludges exhibit pseudoplastic behaviour. Thus, the steady state viscosity, η_e, obeys an empirical power law model (the Ostwald–de Waele model) under typical shear rates:

$$\eta_e(S_e, \dot{\gamma}) = a \cdot \dot{\gamma}^{n-1} \quad (6.6)$$

where a is the consistency index ($Pa \cdot s^n$) and n the power law index (-).

The combination of Equations 6.1 and 6.6 leads to the determination of the steady state structural parameter:

$$S_e = a \cdot \dot{\gamma}^{n+m-1} \quad (6.7)$$

Finally, the shear stress can be determined using Newton's equation ($\tau = \eta \cdot \dot{\gamma}$). The model contains a total of five parameters (m, K_{up}, K_{down}, a and n) that characterise the complete rheological behaviour of sludge. In order to minimise mathematical coupling, the parameter values have been obtained using different experimental data; the equilibrium values (a and n) have been obtained from the equilibrium data, the K_{down} value from the step data, and the K_{up} and m from the loop data.

6.2. Model implementation

The rheological model was implemented for a WAS sample with a TS content of 56.7±0.7 g/L. The WAS was ultrasonicated (3000; 7000; 17,000; 27,000 and 33,000 kJ/kg TS), thermally treated (12,000 (60 ºC); 15,000 (70 ºC); 17,000 (80 ºC); 20,000 (90 ºC) and 22,000 (100 ºC) kJ/kg TS) and alkali-treated (0.784; 7.84; 78.4; 157 and 235 g NaOH/kg TS). The results shown below correspond to the experimental and simulated data obtained from the model described above.

At steady state conditions, both the untreated and treated sludges showed pseudoplastic behaviour (Figures 6.1, 6.2 and 6.3). Thus, the steady state viscosity decreased with the shear rate following a power law equation (Equation 6.6). The good fit of the experimental data showed the capability of the Ostwald-de Waele model to reproduce the pseudoplastic response of the WAS. In this case, the reduction of viscosity after the ultrasound treatment was lower than that presented in Chapter 5 possibly because the higher TS content hindered the transmission of ultrasonic waves.

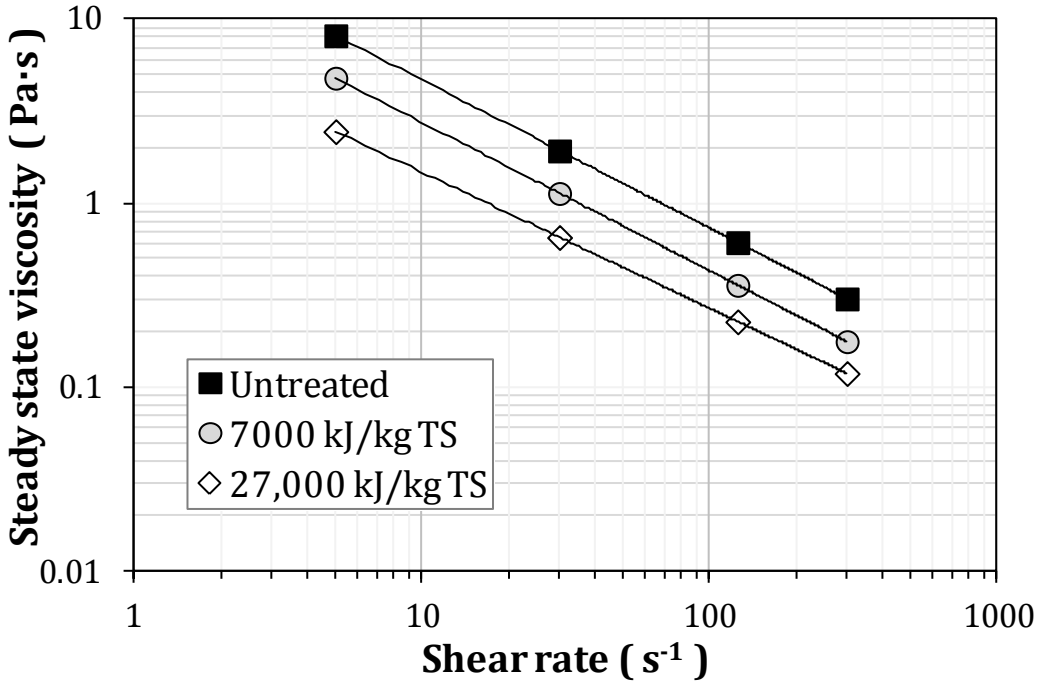

Figure 6.1. Steady state viscosity as a function of shear rate for the untreated and two ultrasonicated sludge samples. The solid lines correspond to the fit to the Ostwald-de Waele power-law model.

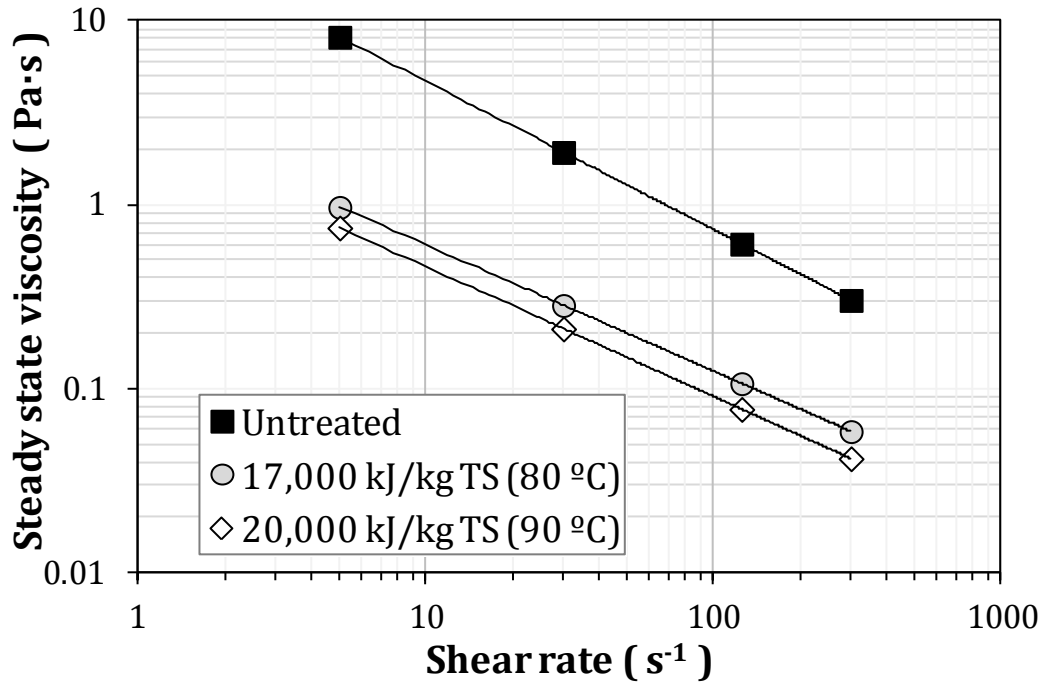

Figure 6.2. Steady state viscosity as a function of shear rate for the untreated and two thermally treated sludge samples. The solid lines correspond to the fit to the Ostwald-de Waele power-law model.

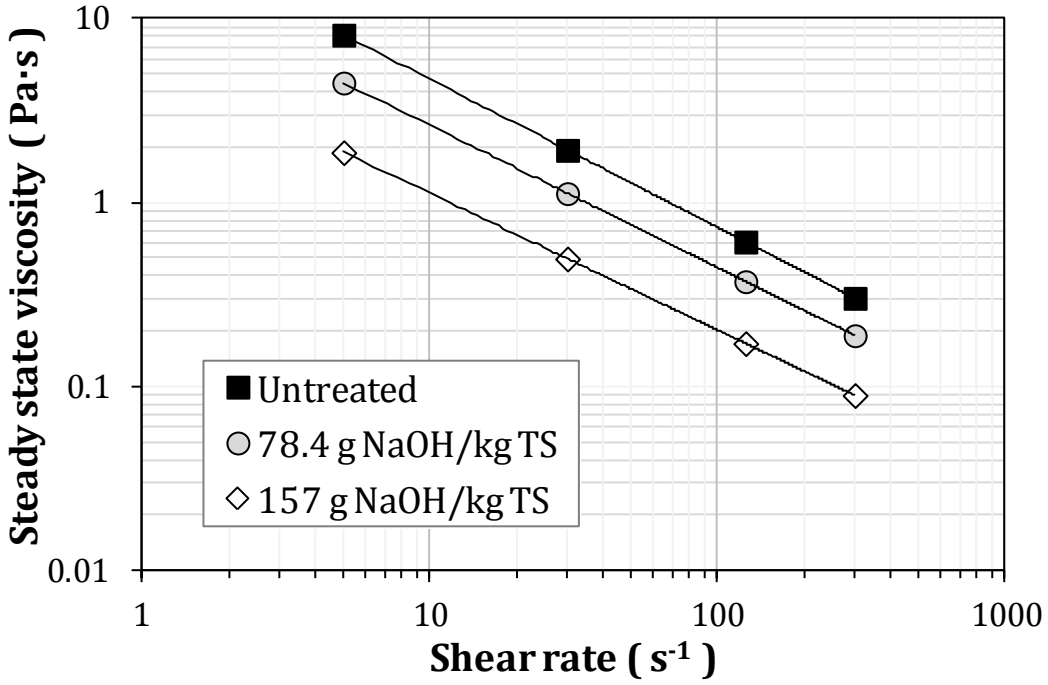

Figure 6.3. Steady state viscosity as a function of shear rate for the untreated and two alkali-treated sludge samples. The solid lines correspond to the fit to the Ostwald-de Waele power-law model.

Table 6.1 shows the values of the consistency index, *a*, and the power law index, *n*, for the untreated and treated sludges as a function of the treatment intensities. The explanation regarding the pseudoplastic behaviour of WAS is not detailed in this chapter, since it has already been discussed in Chapter 5.

Table 6.1. Ostwald-de Waele parameters.

	a (Pa·s^n)	**n (-)**
Untreated	29.7	0.196
Ultrasound (kJ/kg TS)		
3000	19.6	0.206
7000	17.5	0.195
17,000	15.6	0.188
27,000	8.06	0.261
33,000	7.84	0.266
Thermal (kJ/kg TS; ºC)		
12,000 (60 ºC)	8.83	0.259
15,000 (70 ºC)	4.33	0.314
17,000 (80 ºC)	2.92	0.315
20,000 (90 ºC)	2.33	0.295
22,000 (100 ºC)	1.43	0.355
Alkali (g NaOH/kg TS)		
0.784	29.9	0.156
7.84	21.4	0.216
78.4	15.5	0.228
157	6.18	0.258
235	3.46	0.316

The time evolution of viscosity obtained from the step changes in the shear rate allowed determining and quantifying the breakdown kinetic process. The thixotropic behaviour is connected to the evolution over time of the internal network configuration after rapid changes in shear rate. When the shear rate is increased and then kept constant, the network breaks down and the viscosity decreases over time. Conversely, the network builds up and the viscosity increases over time when the shear rate is decreased and then kept constant. Considering Equation 6.1, it can be observed that the

evolution of viscosity is equal to the evolution of structural parameter. Thus, to better visualise the variation of the viscosity with time at a fixed shear rate, Equation 6.5 has been rewritten and normalised as follows:

$$\frac{\eta - \eta_e}{\eta_i - \eta_e} = \frac{S - S_e}{S_i - S_e} = \exp(-K \cdot t) \tag{6.8}$$

where t is the time of shearing and η_i is the initial viscosity just when the constant shear rate begins (t = 0).

Remarkably, Equation 6.8 is independent of the m parameter and represents a pure kinetic thixotropic process. Thus, the kinetic coefficient, K, can be determined directly from the experimental data. Figure 6.4 shows the evolution of the normalised viscosity over time for the untreated sludge. The figure shows data obtained at three shear rates (30, 125 and 300 s^{-1}), which were applied after pre-shearing the sludge at 5 s^{-1} (in order to reach equilbrium at 5 s^{-1}) and represent the breakdown kinetic process. The solid lines correspond to the first-order kinetic equation (Equation 6.8), which correlates with the time needed to reach the equilibrium.

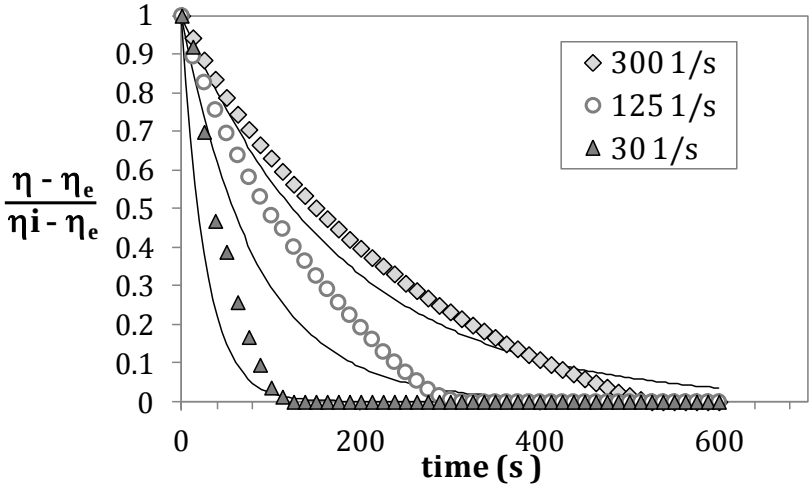

Figure 6.4. Evolutions of the normalised viscosities over time for the untreated sludge sample when the shear rates are 30, 125 and 300 s^{-1}. The solid lines correspond to the first-order kinetic equation (Equation 6.8).

As can be observed, the shear rates do not all simultaneously reach the steady state viscosity value, which corresponds to a normalised viscosity equal to 0. For example, for the untreated sludge, the steady state viscosity is reached in 120 s at 30 s^{-1}, in 300 s at 125 s^{-1} and in 550 s at 300 s^{-1} (Figure 6.4). Indeed, it has been observed that the kinetic coefficients, *K,* depend on the shear rate in accordance with a potential equation:

$$K = \alpha \cdot \dot{\gamma}^{\beta} \tag{6.9}$$

where α ($s^{\beta-1}$) and β (-) are kinetic parameters, designed as α_{down} and β_{down} for the breakdown process and α_{up} and β_{up} for the build-up process.

The kinetic parameters of the breakdown process were easily determined from K_{down} data calculated from the step test experimental data and Equation 6.9. Table 6.2 shows the obtained kinetic parameters for the breakdown process, α_{down} and $\beta_{down,}$ with regression coefficient higher than 0.98. The kinetic coefficient for the breakdown process significantly depended on the shear rate ($\beta_{down} \neq 0$). The negative value of β_{down} parameter means that the time to reach the equilibrium is higher at high shear rates. The shear rate dependency was minimised as the treatment intensity was increased, especially in the case of the thermal treatment.

Table 6.2. Kinetic parameters for the breakdown process.

	α_{down} ($s^{\beta down-1}$)	β_{down} (-)	R^2 [1]
Untreated	2.6945	-0.848	0.994
Ultrasound (kJ/kg TS)			
3000	1.5419	-0.761	0.985
7000	1.4175	-0.757	0.987
17,000	1.3083	-0.752	0.988
27,000	1.1720	-0.743	0.988
33,000	1.0703	-0.733	0.991
Thermal (kJ/kg TS; ºC)			
12,000 (60 ºC)	1.4394	-0.744	0.987
15,000 (70 ºC)	1.0769	-0.697	0.995
17,000 (80 ºC)	0.6779	-0.622	0.995
20,000 (90 ºC)	0.3441	-0.512	0.999
22,000 (100 ºC)	0.1693	-0.401	0.995
Alkali (g NaOH/kg TS)			
0.784	2.4652	-0.840	0.996
7.84	2.0000	-0.810	0.986
78.4	1.6596	-0.784	0.984
157	1.5989	-0.754	0.987
235	1.3828	-0.750	0.992

[1] Correlation coefficients for the kinetic parameters for breakdown process.

Figures 6.5a, 6.6a and 6.7a show the kinetic coefficient for breakdown process as a function of the shear rate for the ultrasound, thermal and alkali treatments, respectively. As can be observed, K_{down} decreases when increasing both the treatment intensity and shear rate, which means that the viscosity takes more time to reach the steady state value (more thixotropy). In the case of the thermal treatment, the reduction of K_{down} with treatment intensity is mainly observed at low shear rates, whereas at high shear rates the K_{down} values tend to be independent of the E_S. In comparison with the thermal treatment, the K_{down} values of the ultrasound and alkali treatments were less dependent on the E_S in all shear rates.

A

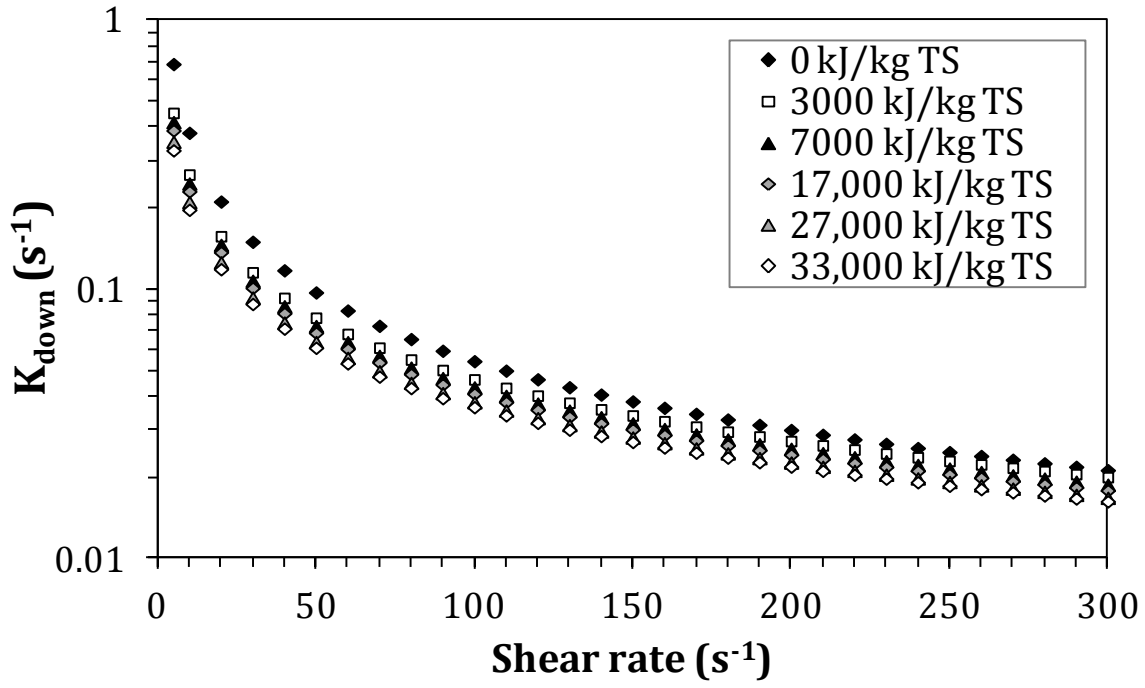

B

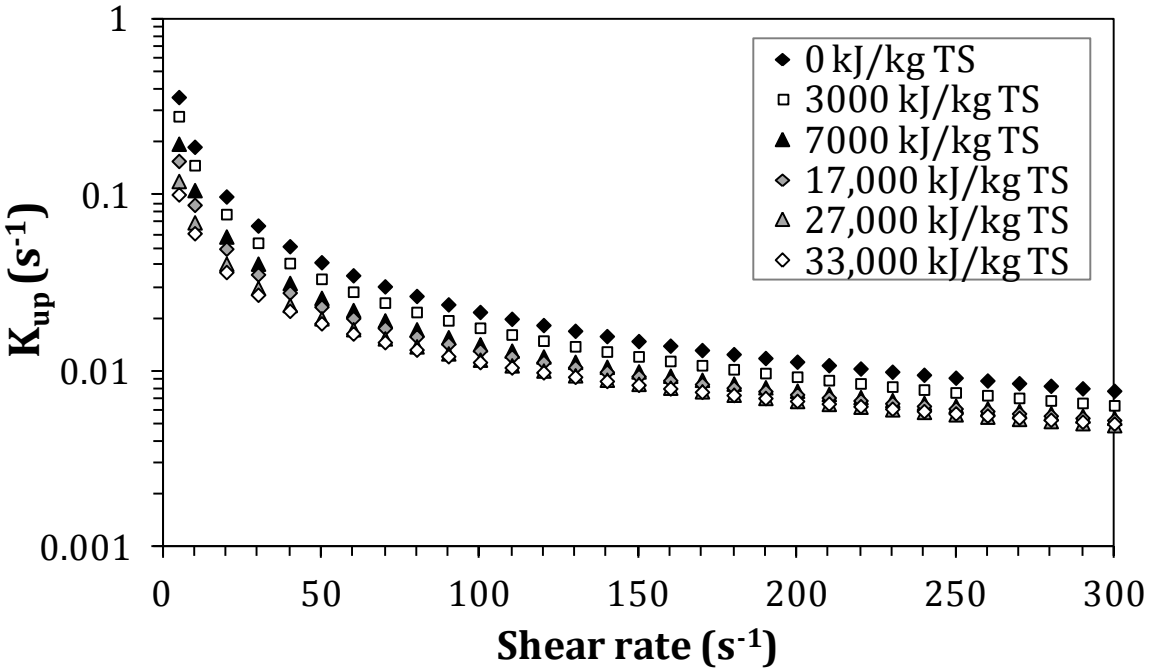

Figure 6.5. Kinetic coefficients for (A) breakdown and (B) build-up processes for the untreated and ultrasonicated sludge samples.

A

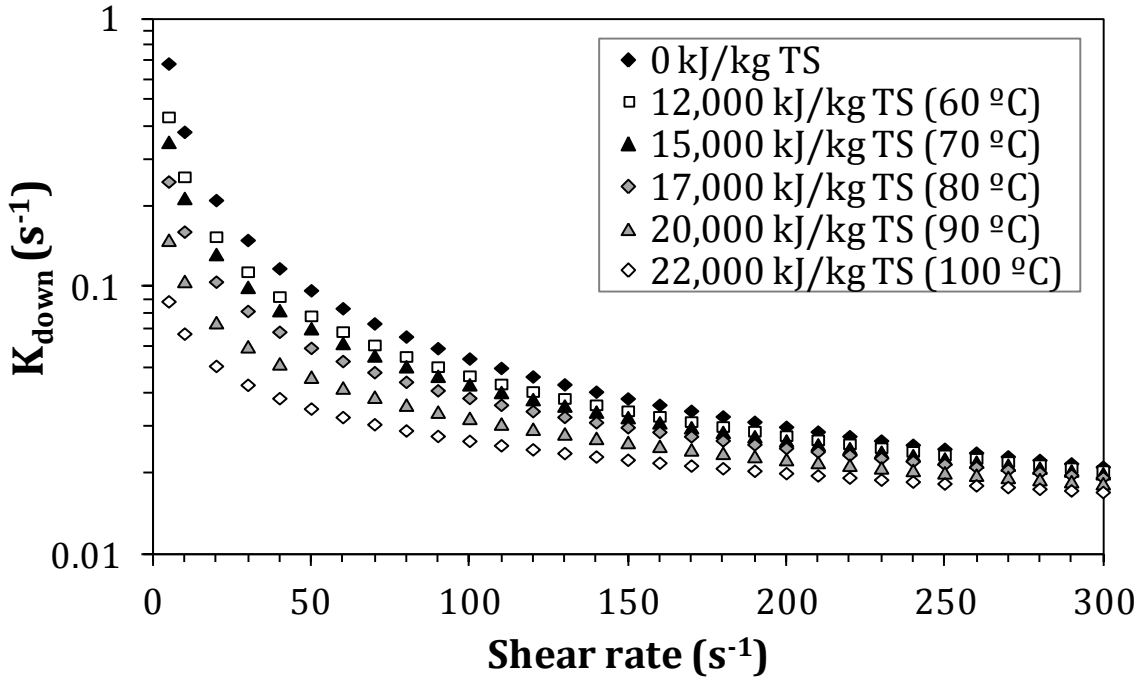

B

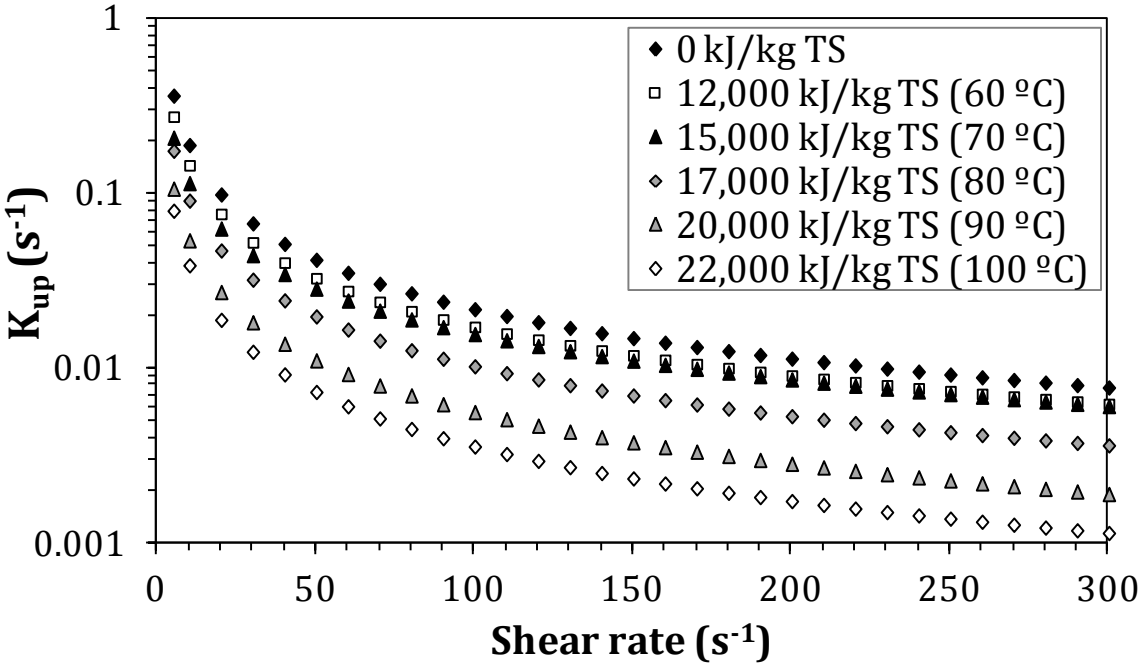

Figure 6.6. Kinetic coefficients for (A) breakdown and (B) build-up processes for the untreated and thermally treated sludge samples.

A

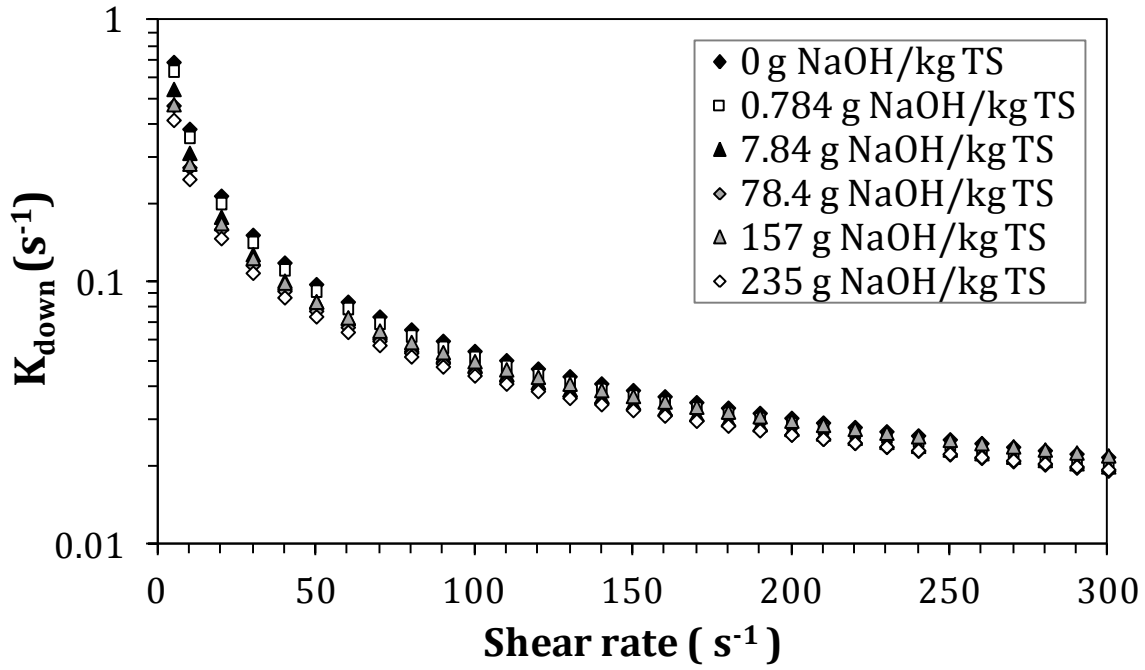

B

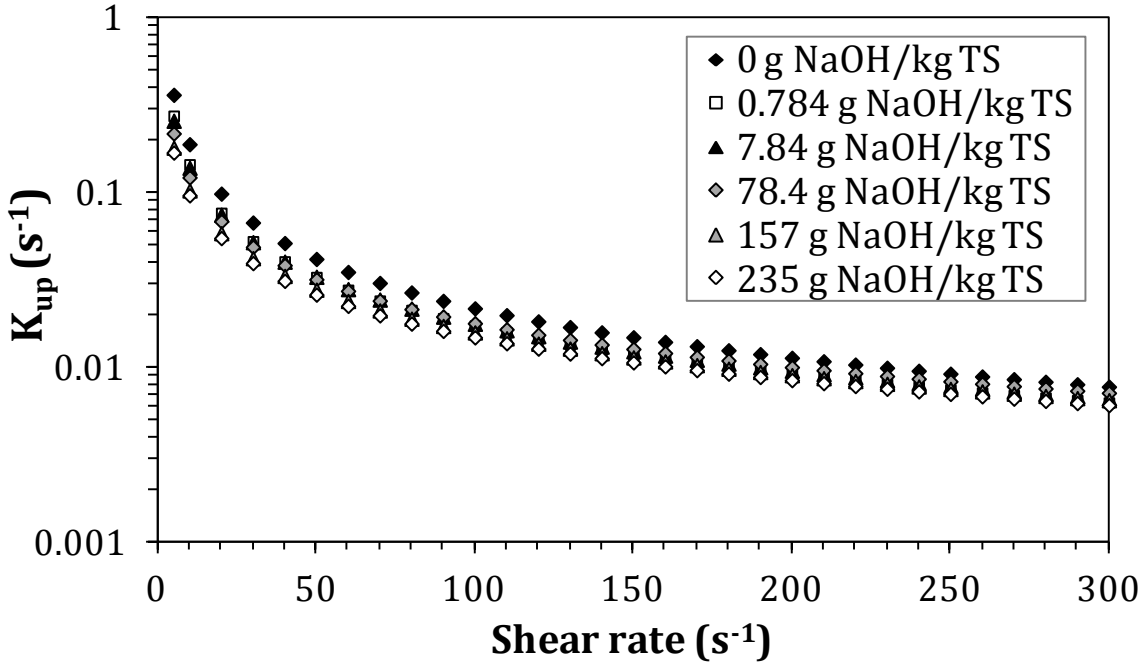

Figure 6.7. Kinetic coefficients for (A) breakdown and (B) build-up processes for the untreated and alkali-treated sludge samples.

Figures 6.8, 6.9 and 6.10 show the hysteresis loops for the ultrasound, thermal and alkali treatments, respectively. The solid lines correspond to the data fitted with the proposed model (Equations 6.1-6.7). The *m* parameter and the kinetic parameters of the build-up process, α_{up} and β_{up}, were obtained from the loop data, i.e., these parameters were varied to match the calculated and experimental data using the steady state and kinetic breakdown parameters (step data) determined previously and by minimising the average relative error (ARE). In this context, the coupling effect among the adjusted parameters is reduced. The experimental data of the two loop tests were fitted simultaneously, with maximum shear rates of 125 and 300 s^{-1}. All the sludges displayed positive thixotropic behaviour, which means that the shear stresses during the up-curves are higher than those at the same shear rate during the down-curves. The hysteresis loops do not show evidences of elastic behaviour, which is represented by a stress overshoot in the up-curve (Baudez, 2006).

A

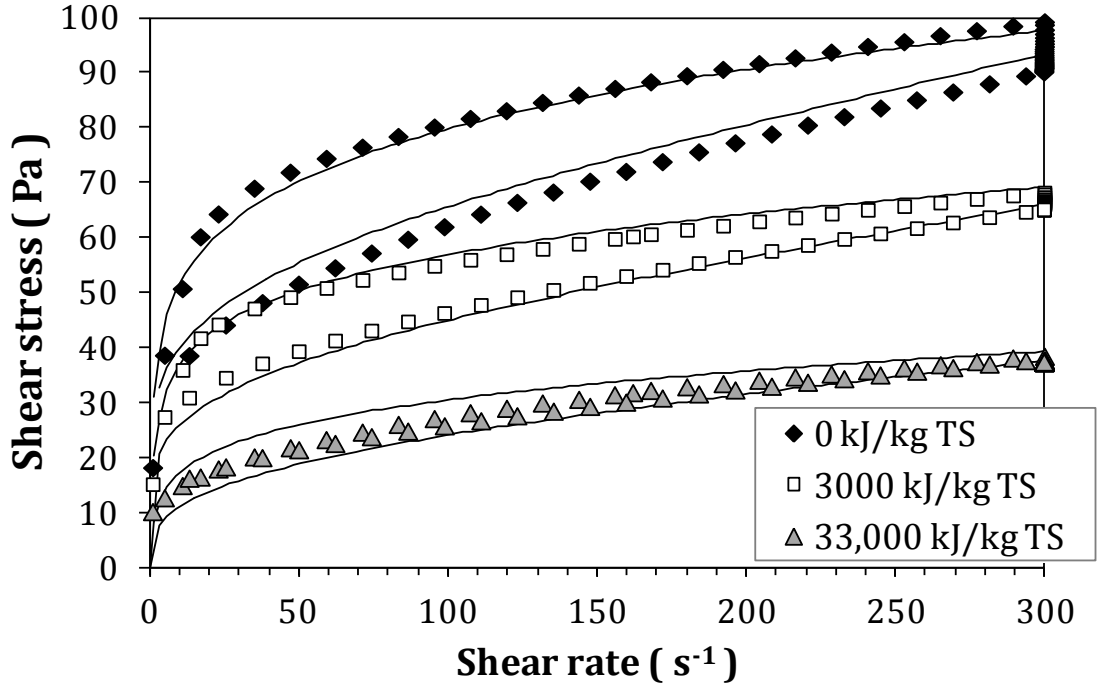

B

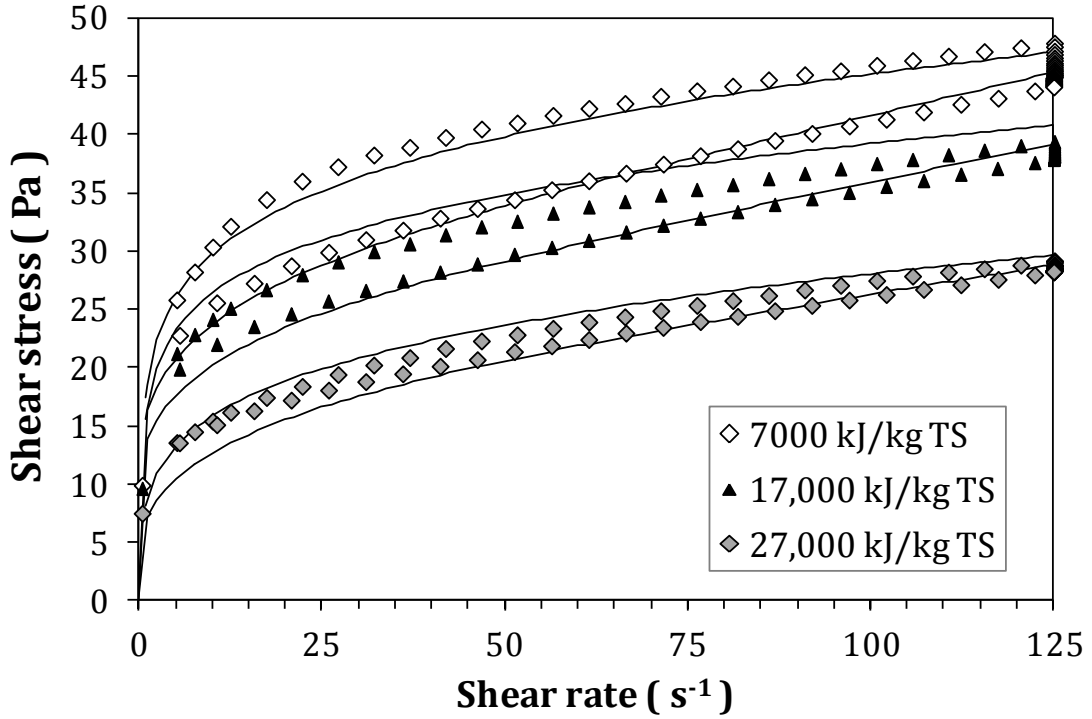

Figure 6.8. Hysteresis loops obtained for the untreated and ultrasonicated sludge samples at a maximum shear rate of (A) 300 s^{-1} and (B) 125 s^{-1}. Solid lines correspond to the data predicted using the proposed model.

A

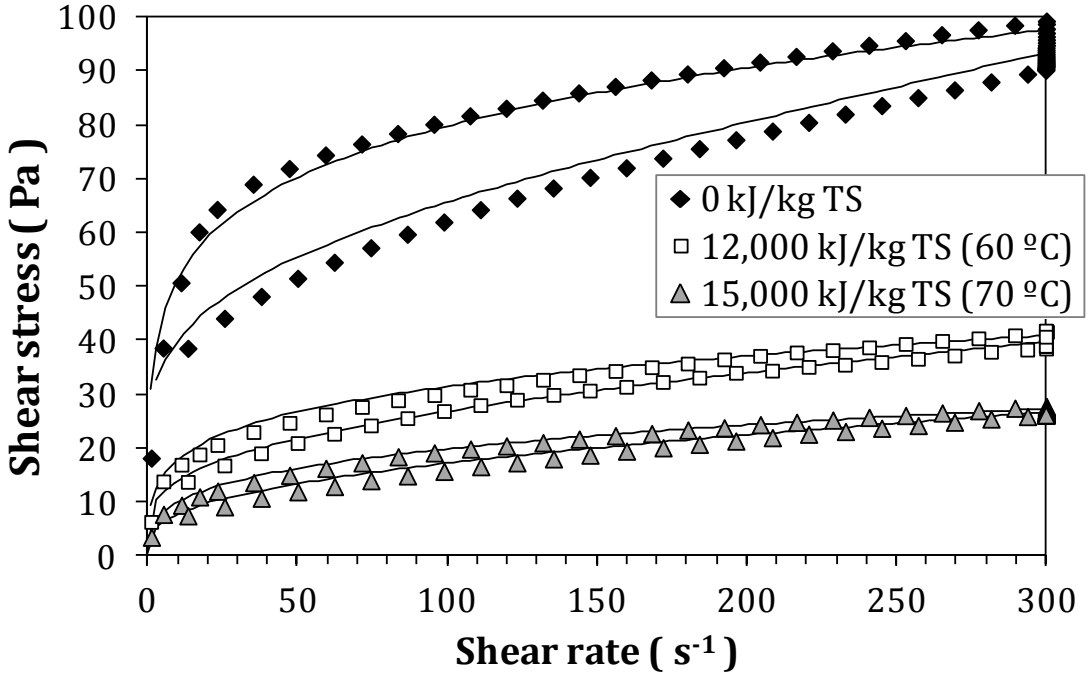

B

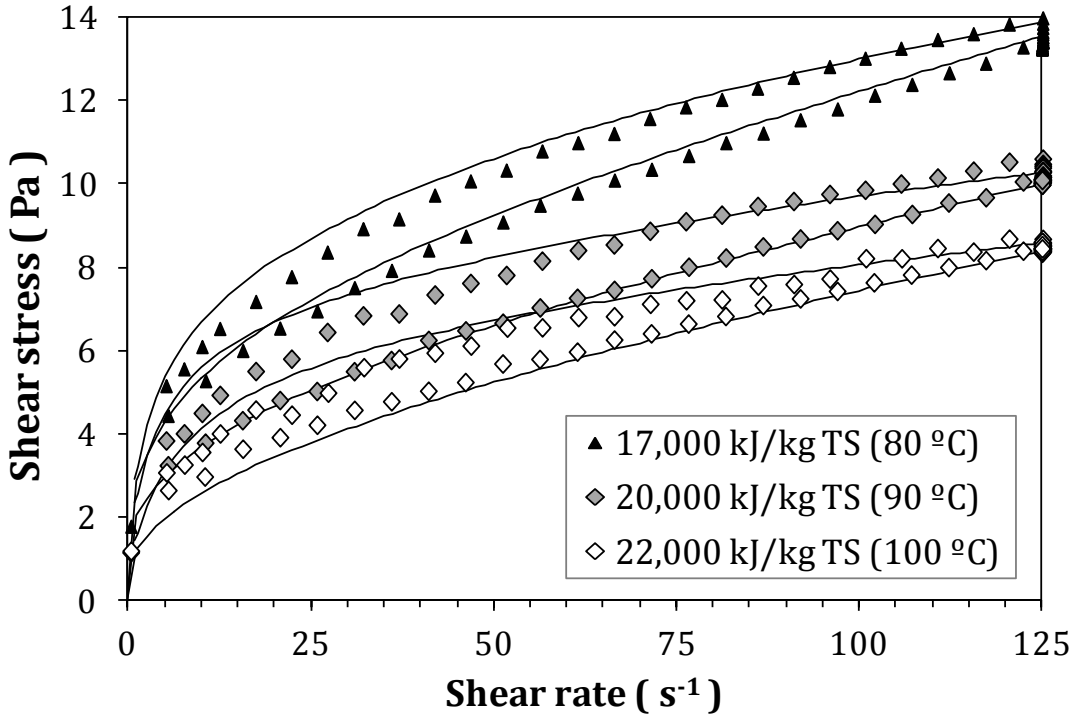

Figure 6.9. Hysteresis loops obtained for the untreated and thermally treated sludge samples at a maximum shear rate of (A) 300 s^{-1} and (B) 125 s^{-1}. Solid lines correspond to the data predicted using the proposed model.

A

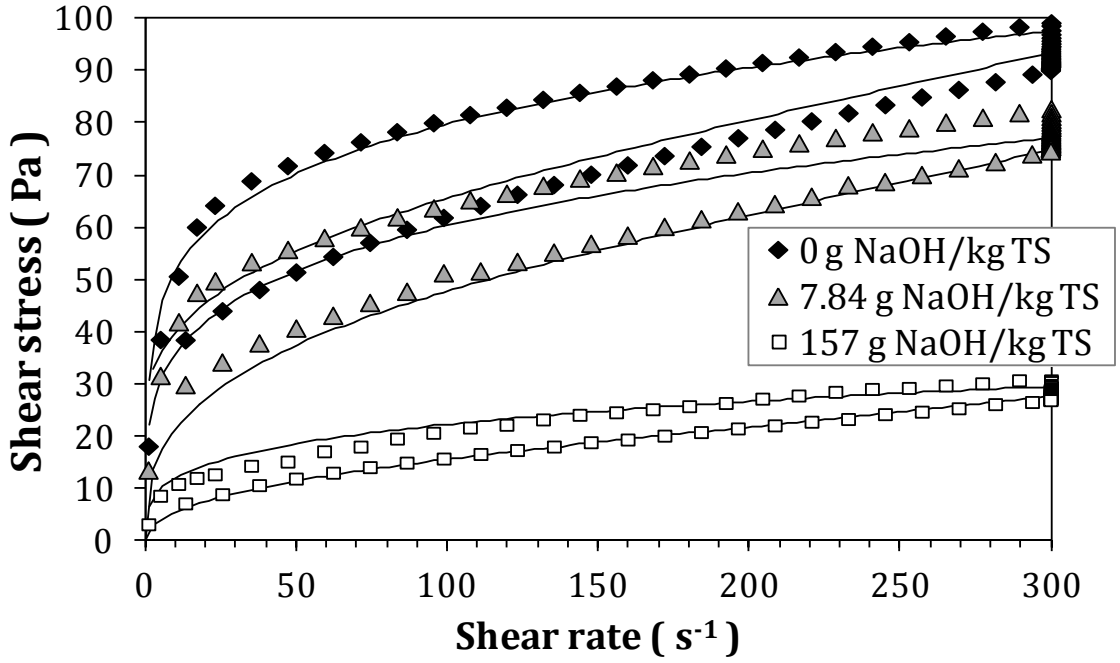

B

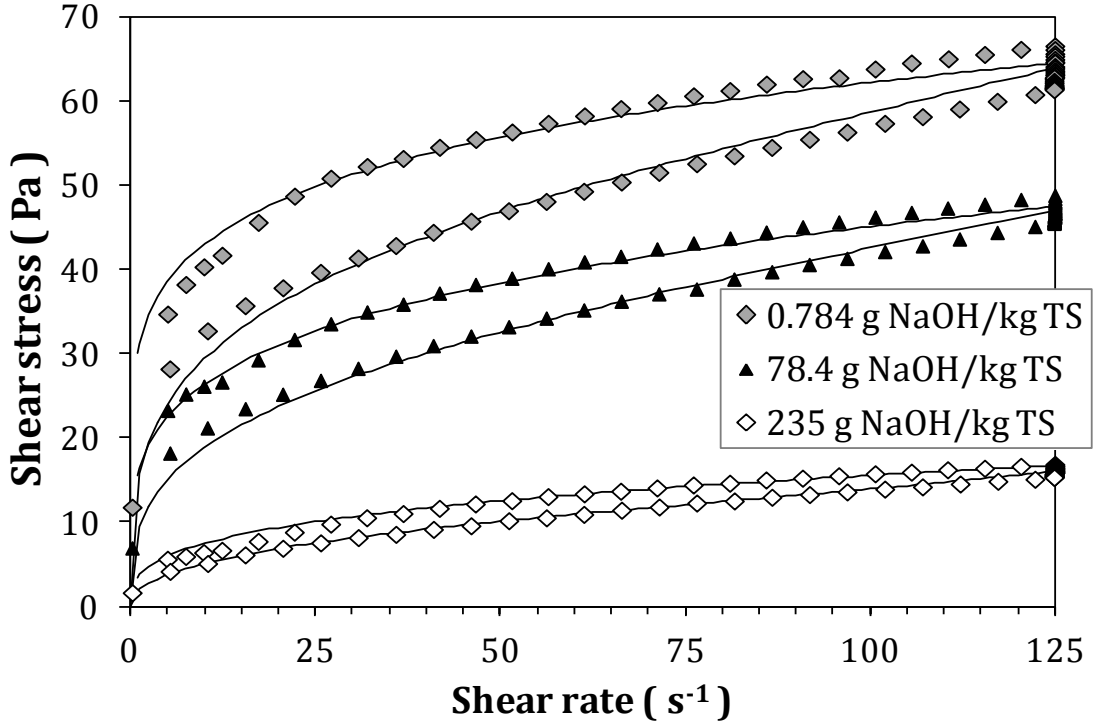

Figure 6.10. Hysteresis loops obtained for the untreated and alkali-treated sludge samples at a maximum shear rate of (A) 300 s^{-1} and (B) 125 s^{-1}. Solid lines correspond to the data predicted using the proposed model.

The *m* parameter and the kinetic parameters of the build-up process, α_{up} and β_{up} that better adjust the experimental loop data are presented in Table 6.3. The equations of the proposed model were observed to satisfactorily fit the experimental data with an ARE lower than 0.24. The *m* parameter negatively correlated with the E_S value, but never reached values close to zero. Therefore, sludge structures always experienced alignment in the shear rate fields. These alignments are more significant when E_S and NaOH concentration are low (large structures). The kinetic coefficients for the build-up process (Figures 6.5b, 6.6b and 6.7b) were always lower than the coefficients for the breakdown process (Figures 6.5a, 6.6a and 6.7a). Therefore, building structures is slower than collapsing.

Table 6.3. Alignment and kinetic parameters for the build-up process.

	m **(-)** [1]	**α_{up}** **($s^{\beta up-1}$)** [1]	**β_{up}** **(-)** [1]	**ARE** **(-)**
Untreated	0.622	1.641	-0.940	0.148
Ultrasound (kJ/kg TS)				
3000	0.604	1.246	-0.925	0.105
7000	0.593	0.805	-0.877	0.132
17,000	0.590	0.594	-0.829	0.238
27,000	0.580	0.423	-0.781	0.160
33,000	0.573	0.328	-0.733	0.226
Thermal (kJ/kg TS; ºC)				
12,000 (60 ºC)	0.602	1.214	-0.925	0.104
15,000 (70 ºC)	0.577	0.834	-0.864	0.175
17,000 (80 ºC)	0.543	0.805	-0.949	0.159
20,000 (90 ºC)	0.517	0.516	-0.983	0.138
22,000 (100 ºC)	0.474	0.421	-1.038	0.222
Alkali (g NaOH/kg TS)				
0.784	0.594	1.212	-0.924	0.065
7.84	0.552	1.082	-0.894	0.123
78.4	0.532	0.833	-0.835	0.103
157	0.483	0.667	-0.813	0.132
235	0.452	0.625	-0.813	0.112

[1] These parameters where obtained by minimising the average relative error, ARE, between the experimental and calculated loop data.

Table 6.4 shows the value of the hysteresis areas corresponding to the two maximum shear rates of 300 and 125 s^{-1}.

Table 6.4. Hysteresis areas at maximum shear rates of 300 and 125 s^{-1}.

	Hysteresis area (Pa s^{-1})	
	Maximum shear rate of 300 s^{-1}	Maximum shear rate of 125 s^{-1}
Untreated	4176	1251
Ultrasound (kJ/kg TS)		
3000	2007	750
7000	1359	511
17,000	580	217
27,000	502	96
33,000	276	20
Thermal (kJ/kg TS; ºC)		
12,000 (60 ºC)	939	244
15,000 (70 ºC)	801	243
17,000 (80 ºC)	580	116
20,000 (90 ºC)	544	104
22,000 (100 ºC)	224	62
Alkali (g NaOH/kg TS)		
0.784	1802	421
7.84	1505	338
78.4	925	243
157	723	73
235	573	124

The hysteresis area noticeably decreased with the treatment intensities (this same effect was also observed in Chapter 5). This may seem to disagree with the theoretical results obtained with the model, since a large value of the hysteresis area might suggest a higher thixotropy (and vice versa). However, the absolute value of the hysteresis area is not a good parameter to compare the thixotropy of different samples with different viscosities. A large absolute value of the hysteresis area can represent low thixotropy if the viscosity of the fluid is very high. Conversely, a small absolute value of the hysteresis area can represent high thixotropy if the viscosity of the fluid is very low.

K_{down} decreased when increasing both the treatment intensity and shear rate (Figures 6.5a, 6.6a and 6.7a), which means that viscosity takes longer to achieve the steady state value (more thixotropy). This could be linked to the fact that the smaller flocs take longer to reach the equilibrium, either by the effect of the treatment or shear rate.

Chapter 7 Effect of the treatments on WAS dewaterability

7.1. Introduction

The purification of domestic and industrial wastewaters produces large quantities of sludges, whose water content is generally greater than 95% (Colin and Gazbar, 1995). The dewatering of these sludges is therefore necessary to obtain a product dry enough to allow a reduction in storage volume, facilitate the transportation or limit the energy used in case of incineration. However, WAS is generally difficult to dewater mainly due to the presence of EPSs; although a part of the water in WAS is intracellular and thus trapped within cell walls, most of the water is trapped in EPSs, which hinders the dewatering process (Jin et al., 2004).

As shown in the previous chapters, the viscosity of the sludge can be reduced by ultrasound, thermal and alkali treatments. In this chapter, it has been analysed the effect of these treatments on sludge dewatering, i.e., on the water that can be removed from the sludge after centrifugation, in order to obtain a more concentrated but also less viscous sludge.

7.1.1. Distribution of water in WAS

The dewatering efficiency will depend on the treatment protocol and on the type of water in the sludge. Thus, the representation of the moisture distribution within the sludge is considered to be essential for the examination of dewatering problems. Vaxelaire and Cézac (2004) reported that the behaviour of a molecule of water during the dewatering process is widely dependent on its proximity to the solid. Usually, two primary types of water are identified: the free (or bulk) water, which is not influenced by the solid particles and can be easily removed, and the bound water, whose properties are modified due to the presence of particles (bound water does not behave as pure water). However, simply classifying water into two categories is often insufficient to fully understand the mechanisms of dewatering. Accordingly, Vesilind (1994) suggested that the water in the sludge can be classified into four categories:

- Free (or bulk) water: water that is not attached to solid particles and can be separated easily by simple gravitational settling. It freezes at the normal freezing point of water.
- Interstitial water: water that is trapped within the floc structure or within a cell. It can be released (and therefore becomes free water) by breaking up the floc or disruption of the cell. Only small amounts of interstitial water might be removed by mechanical dewatering systems such as centrifugation or vacuum filtration. Due to high dissolved solid concentrations, this type of water freezes at temperatures lower than normal freezing point (Mowla et al., 2013).
- Vicinal (or surface) water: water molecules which are physically bound to solid particles surface by adsorption and adhesion and cannot be separated by any mechanical means. Actually, vicinal water can only be removed by changing the surface quantity able to adhere water. Vicinal water can also be located within the microbial cells, as long as it is associated with a solid surface. It could be frozen only at very low temperature.
- Water of hydration: water molecules that are chemically bound to the solid particles. The water of hydration can only be removed by thermal dehydration above 105 ºC.

Figure 7.1 represents a schematic model of water distribution in WAS.

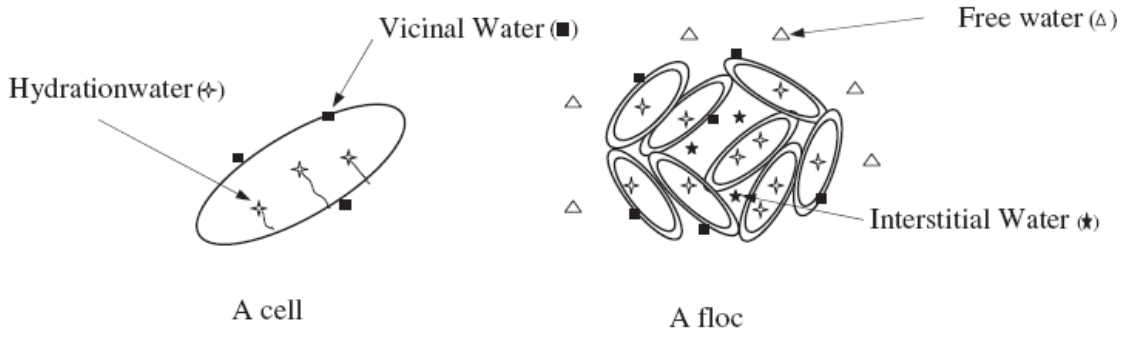

Figure 7.1. Schematic model of various forms of water in WAS (Mowla et al., 2013).

The distribution of each water type will depend on the nature and composition of the internal sludge structure, which is stabilised primarily by the EPSs. It is reasonable to think that the main limitation in sludge dewatering is the presence of vicinal water and water of hydration, whose properties are modified due to the presence of solids. In contrast, the interstitial water is free to move when physical confinement is eliminated (Erdincler and Vesilind, 2003) and therefore relatively easy to separate by the application of treatments (which cause floc disintegration) and subsequent mechanical dewatering. However, Vesilind (1994) reported that the effect of particles on interstitial water is unclear and suggested that some part of the interstitial water may not physically behave as free water. Consequently, bound water is generally considered a gross estimate of several states of water including vicinal water, water of hydration and some fraction of interstitial water (Erdincler and Vesilind, 2003).

There are various methods for measuring the bound water based on the principle that free water, but not bound water, has the same thermodynamic properties of pure water (Katsiris and Kouzeli-Katsiri, 1987; Lee and Lee, 1995; Erdincler and Vesilind, 2003; Yin et al., 2004; Deng et al., 2011). For example, bound water does not freeze at temperatures below the normal freezing point of water. Actually, a widely accepted definition of bound water is water that does not freeze at some given temperature,

usually -20 ºC. According to Büchi et al. (2009), the chemically bound water does not freeze all the way down to −120 °C. The differential scanning calorimetry (DSC) test is a suitable technique for measuring bound water by permitting a direct thermal analysis of phase changes of free water.

7.1.2. Extracellular polymeric substances (EPSs) in WAS

It is accepted that the EPSs are mainly responsible for sludge floc formation (Bitton, 2005) and therefore are the main component of the WAS floc matrix (Frølund et al., 1996). EPSs bind with cells through complex interactions to form a vast net-like structure with plenty of water that protects cells against dewatering (Wingender et al., 1999) and toxic substances (Sutherland, 2001).

EPSs are primarily composed of high-molecular-weight secretions from microorganisms and the products of both cellular lysis and macromolecule hydrolysis (Sheng et al., 2010). Moreover, some of the organic matter from wastewater can also be adsorbed into the EPS matrix (Nielsen and Jahn, 1999; Liu and Fang, 2003). Proteins, humic substances and polysaccharides are usually the major components of EPSs (Frølund et al., 1995; Frølund et al., 1996). Lipids, nucleic acids, uronic acids, and inorganic components have been found in smaller quantities (Sheng et al., 2010). Figure 7.2 shows the composition of organic matter in WAS, with emphasis on EPSs.

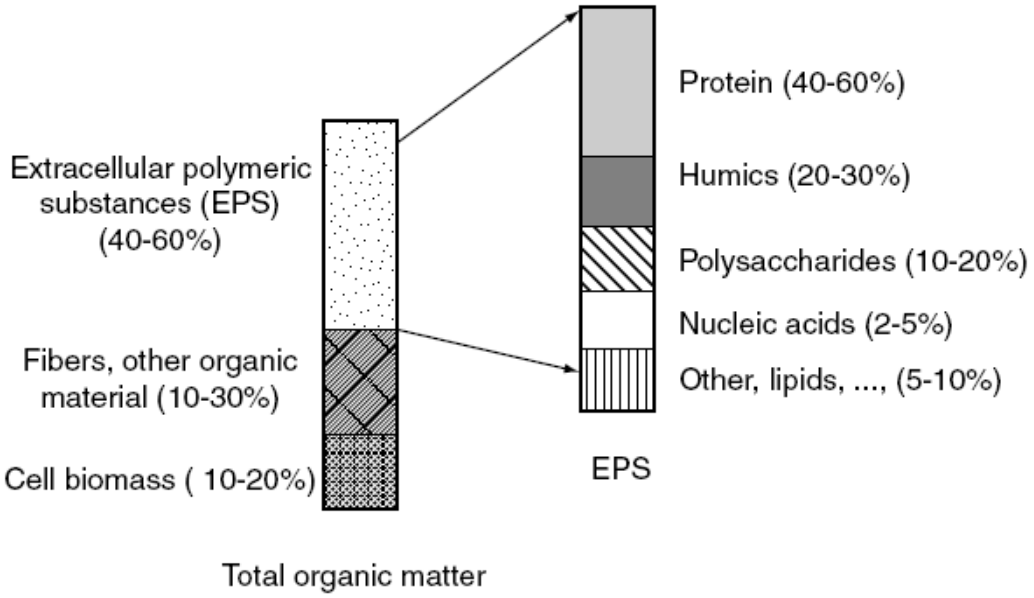

Figure 7.2. Composition of the organic part of sludge (Nielsen, 2002).

The floc matrix is generally represented by a dynamic double-layered EPS structure: the inner layer consists of tightly bound EPSs (TB-EPSs), and the outer layer consists of loosely bound EPSs (LB-EPSs) (Li and Yang, 2007). The inner layer has a certain shape, and it is bound tightly and stably to the cell surface, while the outer layer does not exhibit an obvious boundary (Sheng et al., 2010). Therefore, LB-EPSs may function as the primary surface for cell attachment and flocculation.

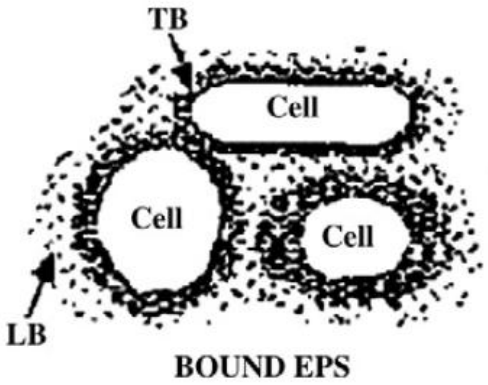

Figure 7.3. Sketch of EPSs structure (Sheng et al., 2010).

The content of the LB-EPSs in microbial aggregates is always less than that of the TB-EPSs (Li and Yang, 2007). To study the composition and characteristics of the LB-EPSs and TB-EPSs in a WAS sample, the two fractions may be extracted separately. As the LB-EPSs bound with cell loosely, a mild method (e.g., high-rate shear, heating at low temperatures, or high speed centrifugation) should be chosen to avoid the inclusion of the TB-EPS. Subsequently, a harsh method (e.g., heating at high temperatures, ultrasonication or chemical extraction methods) should be applied for the TB-EPS extraction (Sheng et al., 2010).

The structural and functional integrity, and therefore the physicochemical and biological properties of flocs are mainly controlled by the EPSs. Indeed, the presence of EPSs in WAS can cause difficulties in dewatering (Nelson et al., 1998). Accordingly, rupturing of EPSs by means of treatments, such as ultrasound, thermal or alkali, can improve dewaterability of the treated sludge.

The aim of this chapter is to compare the effect of the ultrasound, low-temperature thermal and alkali treatments on WAS dewaterability and water distribution. The bound water content was quantified by DSC. The effect of the treatments on sludge-water separation was evaluated by directly measuring the water removed by centrifugation. Moreover, the LB-EPS and TB-EPS were extracted and subsequently analysed by colorimetric methods, gel permeation chromatography and other techniques.

7.2. Materials and methods

7.2.1. Analysis on the sludge samples

7.2.1.1. Differential scanning calorimetry (DSC) analysis for bound water measurement

The amount of free water in the sludge was quantified from the peaks of the crystallisation/melting data from the DSC graphs. The heat released by freezing the free water was equal to the latent heat needed to melt the ice (Lee and Lee, 1995). To perform the DSC test, a weighted amount of sludge (4-6 mg) was added to the thermal

analyser (Mettler Toledo DSC 30) with pure N_2 as the carrying gas. The instrument was calibrated using melting point standards (indium and zinc). The temperature of the sludge sample was first decreased at a rate of 2 ºC/min from 25 ºC to -40 ºC and then raised back to 40 ºC at the same rate. In the DSC test, the heat absorbed and released by the sample was recorded. The phase transition from water to ice was detected and measured and was assumed to correspond to free water (Lee and Lee, 1995; Erdincler and Vesilind, 2003). Then, the amount of free water was determined by dividing the heat absorbed by the sample by the water's latent heat of melting ice (334.4 kJ/kg). Afterwards, the bound water content was determined by calculating the difference between the total water content (measured by drying the sample at 105 ºC) and the free water measured by DSC (Katsiris and Kouzeli-Katsiri, 1987). Finally, the bound water content was expressed as kg bound water/kg dry solids.

7.2.1.2. Centrifugation test and soluble total organic carbon measurement

A centrifugation method was used to measure the amount of water that could be removed from the WAS after the treatments. Initially, the centrifuge tubes contained approximately a 12 ml volume of sludge. The samples were centrifuged at 2500 x *g* for 15, 30 and 45 min. After each centrifugation, the supernatant was removed, and the centrifugal tubes were weighed again. The difference between the initial weight and the weight obtained after removing the supernatant corresponded to the amount of water removed from the sludge by centrifugation. The measurements were performed in triplicate. The amount of water removed at the different centrifugation times was expressed as percentage:

$$\%_{w,t} = \frac{W_0 - W_t}{W_0} \cdot 100 \qquad (7.1)$$

where $\%_{w,t}$ is the percentage of the water removed at time t (15, 30 or 45 min), W_0 is the initial weight of the WAS sample and W_t is the weight of the sample after the supernatant was removed following centrifugation for a time t.

The soluble total organic carbon (sTOC) was measured in triplicate using a TOC-VCSN Analyser (Shimadzu). The measurement was performed on the resulting supernatants after centrifugation of the untreated and treated sludge at 2500 x *g* for 45 min. Before the analysis, the samples were filtered through a 0.45-µm low protein-binding syringe with polyvinylidene difluoride (PVDF) membranes.

7.2.1.3. Capillary suction time (CST) test

The CST measurement was conducted by the Type 304M Capillary Suction Time (Triton Electronics Ltd., UK) device. This method consists of a sludge column contained in a metal cylinder centered in the middle of two concentric electrodes located at diameter D1 and D2 (Figure 7.4). The cylinder rests on a filter paper. The test starts when the water (contained in the sludge) advancing through the filter reaches the first electrode and ends when it reaches the second one. The time elapsed between the two electrodes is the CST.

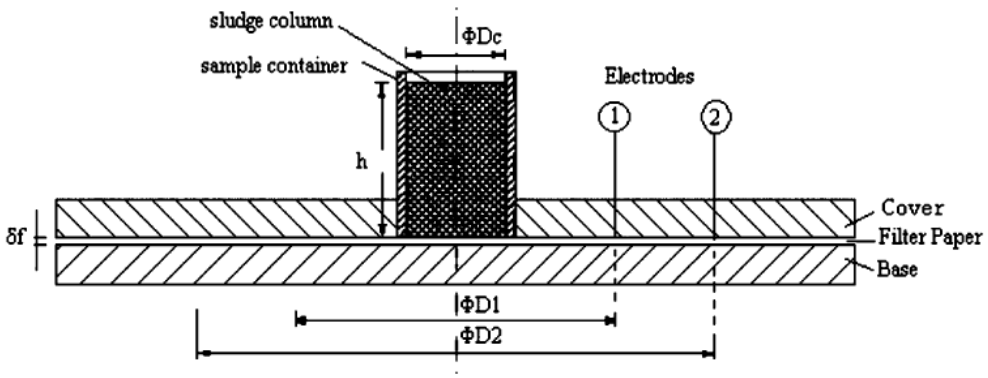

Figure 7.4. Schematic representation of CST apparatus (Huisman and Kesteren, 1998).

Because of its simplicity, the CST test only characterises the filtration phase of the dewatering process. Despite this limitation it is widely used and lower CST values are associated with better dewaterability (Cobbledick et al., 2014).

7.2.2. EPSs extraction protocol

The EPSs extraction was conducted on the untreated sludge and three treated sludges (one condition for each treatment). The fractionation protocol followed in the present work was very similar to that presented by Yu et al. (2009) and is described below. The WAS sample was dewatered by centrifugation at 2000 x *g* for 10 min. The supernatant was discarded, and the bottom sediments were resuspended to the original volume using a buffered solution (pH 7) consisting of Na_3PO_4 (Sigma-Aldrich, ref. no. 222003), NaH_2PO_4 (Sigma-Aldrich, ref. no. S9638), NaCl (Sigma-Aldrich, ref. no. S9888), and KCl (Sigma-Aldrich, ref. no. P3911) at a molar ratio of 2:4:9:1 (Frølund et al., 1995). The conductivity of the buffer was adjusted to match the conductivity of the WAS samples. The suspension was centrifuged at 5000 x *g* for 15 min, and the bulk solution and solid phase were collected separately. The soluble organic matter in the bulk solution was the LB-EPS fraction. The collected bottom sediments were resuspended using the aforementioned buffer solution and centrifuged again at 5000 x *g* for 15 min to eliminate the LB-EPS that impregnated these sediments. Subsequently, the collected sediments were resuspended in the buffer solution and later ultrasonicated for 10 min using an HD2070 ultrasonic homogeniser (Sonopuls Bandelin). The resulting suspensions were centrifuged at 20,000 x *g* for 20 min. The soluble organic matter in the bulk solution was the TB-EPS fraction. All of the EPS fractions were filtered through 0.45-μm low protein-binding polyvinylidene difluoride (PVDF) membranes. The centrifuge used was an Avanti® J-25 I High-Performance Centrifuge. The rotor used was a Rotor Beckman JA-25.50.

Therefore, once the extraction protocol was completed, 8 EPS fractions were obtained: two fractions (LB-EPS and TB-EPS) for each of the four analysed sludge samples (untreated, ultrasonicated, thermally treated and alkali-treated). The fractionations of the untreated sludge and the three treated sludge samples were performed in triplicate.

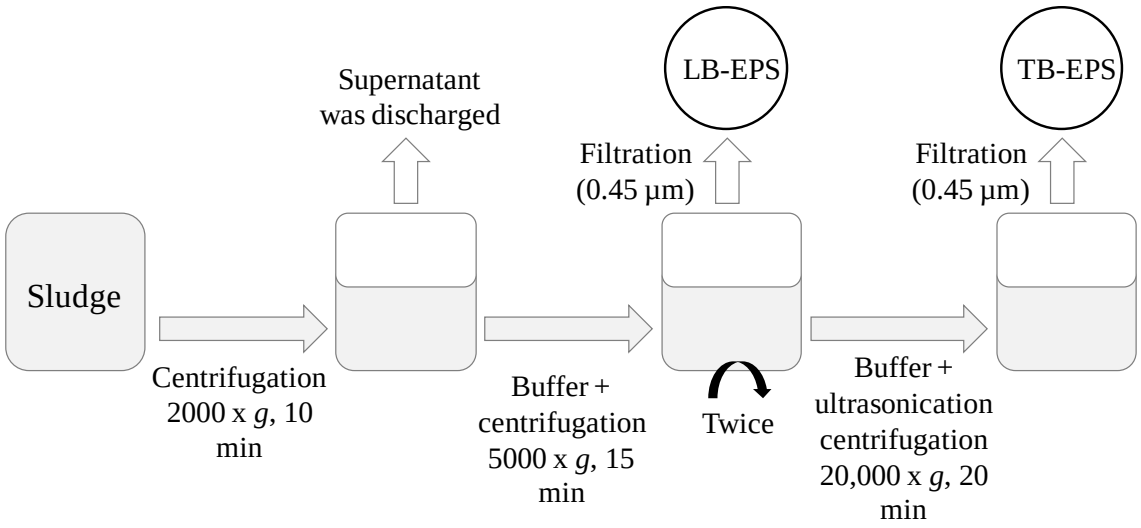

Figure 7.5. Scheme of the EPSs extraction protocol.

7.2.3. Analysis on the EPS fractions

7.2.3.1. Viscosity and zeta potential measurements

The viscosity of the EPS bulk solution was quantified by measuring the relationship between the shear rate and the shear stress on a Brookfield Viscometer (model LVF). The viscosimeter was equipped with a geometry specially designed for the measurement of very low viscosities (Figure 7.6). Specifically, the instrument consisted of a concentric cylinder with a diameter of 26.57 mm, a length of 93.4 mm and a cup diameter of 27.62 mm. The sample volume was 9.2 mL. The rheological test was based on the measurement of torque under stepwise changes of three different rotational velocities, which corresponded to shear rates of 16, 32, and 81 s^{-1}. Shear rates were maintained until the torque reached the steady-state value, at which point a sudden change in rotational velocity was imposed. All of the measurements were performed at 20 ± 0.1 ºC. The torque of the viscosimeter was calibrated with water at 20 ± 0.1 ºC.

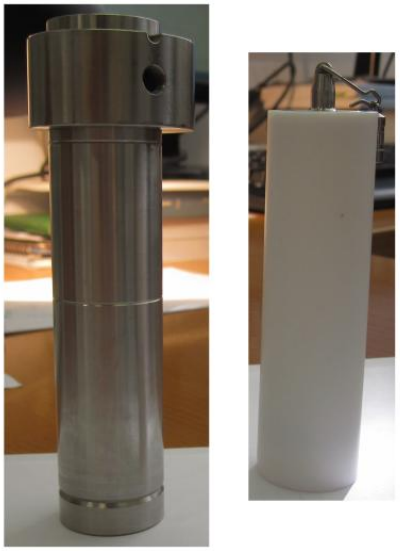

Figure 7.6. Concentric cylinders sensor geometry used for measuring the viscosity of the EPSs bulk solutions.

To quantify the charge of the EPS bulk solution, the zeta (ζ) potential was measured using a Malvern Zetasizer instrument (Nano-Z, Malvern) and the Smoluchowski equation:

$$v_E = 4\pi\varepsilon_0\varepsilon_r \frac{\zeta}{6\pi\mu}(1 + \kappa r) \tag{7.2}$$

where v_E is the particles mobility, ε_0 and ε_r are the relative dielectric constant and the electrical permittivity of a vacuum, respectively, μ is the solution viscosity, r is the particle radius and $\kappa = (2n_0z^2e^2/\varepsilon_r\varepsilon_0k_BT)^{1/2}$ is the Debye-Hückel parameter (n_0 is the bulk ionic concentration, z is the valence of the ion, e is the charge of an electron, k_B is the Boltzmann constant and T is the absolute temperature).

The zeta potential values were obtained from the average of approximately six measurements at the stationary levels of a cylindrical cell equilibrated at 20 ± 1 ºC. All solutions were diluted 1:10 to obtain a clear signal.

7.2.3.2. Total organic carbon, protein and polysaccharide analysis

Different parameters were measured to characterise the EPS content. The total organic carbon (TOC) of the EPS was measured with a TOC-V_{CSN} analyser (Shimadzu). The biochemical composition was studied through colorimetric methods using a Perkin Elmer UV/vis Lambda 20 spectrophotometer. The polysaccharides were quantified through an anthrone-based method (anthrone 98%, Panreac, ref. no. 162441.1606) using glucose (Panreac, ref. no. 131341.1211) as the standard (Frølund et al., 1996). The protein content was measured through the Lowry method using bovine serum albumin (BSA) (Sigma-Aldrich, ref. no. A3299) as the standard (Lowry et al., 1951). The Lowry method relies on the reaction of copper ions with peptide bonds to quantify proteins and peptides. Nevertheless, when referring to the Lowry measurement, the term protein was used for simplicity. Each of these analyses was performed in triplicate for each extraction (three extractions); the standard deviation of the nine measurements was calculated.

7.2.3.3. Amino acid analysis

The analysis of the total and free amino acid content present in EPSs was performed using a Biochrom 30 amino acid analyser (Biochrom Ltd., Cambridge, UK) equipped with a PEEK manufactured column containing a cation-exchange resin (Ultrapac, polystyrene/divinylbenzene sulfonate, 5 μm, 200 x 4 mm; Biochrom Ltd.). The method uses a post-column derivatisation of the amino acids with ninhydrin to produce coloured amino acid derivatives that can be determined spectrophotometrically at 570 and 440 nm. The amino acid peaks were identified according to the retention times of the corresponding standards. The quantification was conducted using an internal standard, which was a known amount of norleucine. The amount of analyte was calculated using the area responses of the analyte and the internal standard.

To quantify the free amino acids, the samples were allowed to dry in a desiccator under vacuum (24 h), resuspended in lithium citrate loading buffer (pH 2.20, Biochrom Ltd.), and filtered using a compact laboratory centrifuge with Microcon centrifugal filters. To quantify the total amino acids, the samples were hydrolysed with 12 N HCl

and subsequently dried at 105 ºC for 24 hours. Amino acid standards were used for the hydrolysates (Sigma Products, ref. no. A2908) and for the free amino acids (a mixture of Sigma Products, ref. no. A6282 and A6407).

7.2.3.4. Gel permeation chromatography (GPC) analysis

GPC was carried out to complement the conventional colorimetric EPS measurements and to quantify the humic substances through fluorescence. During GPC, a lower retention time usually implies a higher molecular weight. However, proteins may occur in various shapes and sizes and need to be folded into their three-dimensional forms (tertiary structure) to become functional. Therefore, despite being heavier, a folded protein can exhibit a larger retention time than an unfolded protein. The chromatographic operating conditions were conducted at pH 7 to ensure that the proteins remained in their natural state.

The EPSs extracted from the WAS were separated using a Waters Alliance 2695 chromatograph. Two serially linked columns (Ultrahydrogel 500, 10 µm, 7.8 x 300 mm and Ultrahydrogel 250, 6 µm, 7.8 x 300 mm) were used to obtain a wide selective permeation range to improve the EPS fingerprint differentiation. The Ultrahydrogel 500 column was placed before the Ultrahydrogel 250 column. The mobile phase was a 50 mM phosphate buffer solution containing 0.9% NaCl. The measurements were performed using an isocratic method at 0.3 mL/min, corresponding to an operating pressure of 450 psi. The detector was adjusted by passing the mobile phase through the chromatography column for 2 h before the measurements to obtain a proper baseline. The injection volume was 50 µL. Each chromatogram was collected over 115 min for the EPS samples and 90 min for the standards. The chromatograms for the samples were slightly longer to avoid all of the possible impurities from the previously punctured sample. The device was coupled to three different detectors: a Waters 2996 photodiode array (PDA) detector (190-800 nm), a Waters 2414 refractive index (RI) detector (sensibility of 256; the measurement was performed at 37 ºC) and a Jasco FP 1520 detector.

Protein-like substances absorb strongly at 280 nm due to their conjugated character (Garnier et al., 2006; Simon et al., 2009). However, although nucleic acids maximally absorb UV light at 260 nm, they also absorb at 280 nm (Stephenson, 2010). Accordingly, the reading at 280 nm (A_{280}) was corrected by subtracting the contribution from nucleic acids (A_{260}) (Layne, 1957):

$$Protein\ concentration\ \left(\frac{mg}{mL}\right) = 1.55 \cdot A_{280} - 0.76 \cdot A_{260} \quad (7.3)$$

The polysaccharides were analysed through RI detection (Ni et al., 2009). Because the proteins did not provide a signal during RI detection, the polysaccharide measurements were not affected by the presence of proteins. The molecular weight (MW) calibration was performed using five standards (Sigma Products, ref. no. MWGF200 and D9503) for the protein-like substances (beta-amylase: 200,000 Da; bovine serum albumin: 66,000 Da; carbonic anhydrase: 29,000 Da; cytochrome c: 12,400 Da; and amino acid 3,4-dihydroxy-DL-phenylalanine: 197 Da) and four standards (Sigma Products, ref. no. 49297, 31425, D5251, D4876) for the polysaccharides (1,400,000 Da, 670,000 Da, 503,000 Da, and 185,000 Da). Some protein-like substances with low MW were detected. Therefore, the aforementioned standard amino acid (3,4-dihydroxy-DL-phenylalanine, 197 Da) was introduced to obtain a calibration curve that allowed quantifying these small substances. A good correlation was found between the MW and retention times for the proteins and polysaccharides.

The humic acids were quantified via fluorescence using a Jasco FP 1520 detector. The excitation and emission wavelengths were 345 nm and 492 nm, respectively. These wavelengths were optimised using a standard humic acid supplied by Sigma-Aldrich (53680 Humic Acid). In fact, the standard was a mixture of humic substances with several different molecular weights. Consequently, the standard exhibited a broad peak with high polydispersity. This effect was also observed in the EPS samples. The calibration was performed using six different concentrations of the aforementioned standard humic acid mixture.

7.3. Results and discussion

7.3.1. Bound water content

The DSC thermogram for the untreated sludge is shown in Figure 7.7. A non-recurring large amount of heat was released in the range -6 to -12 ºC. The area above the baseline was found to be 269 J/g. When the temperature was below -12 ºC, no clear exothermic peak was observed. When heating from -40 ºC to +40 ºC at the same rate, the heat absorption occurred in the range of -5 to 7 ºC. The amount of energy absorbed in this region (275 J/g) was slightly larger than the energy released in the cooling stage. This may have been caused by the simultaneous melting of water and other frozen organic compounds, a permanent change of moisture distribution, or both (Lee and Lee, 1995). The bound water measurements were conducted on a WAS sample with a TS content of 48.2 g/L.

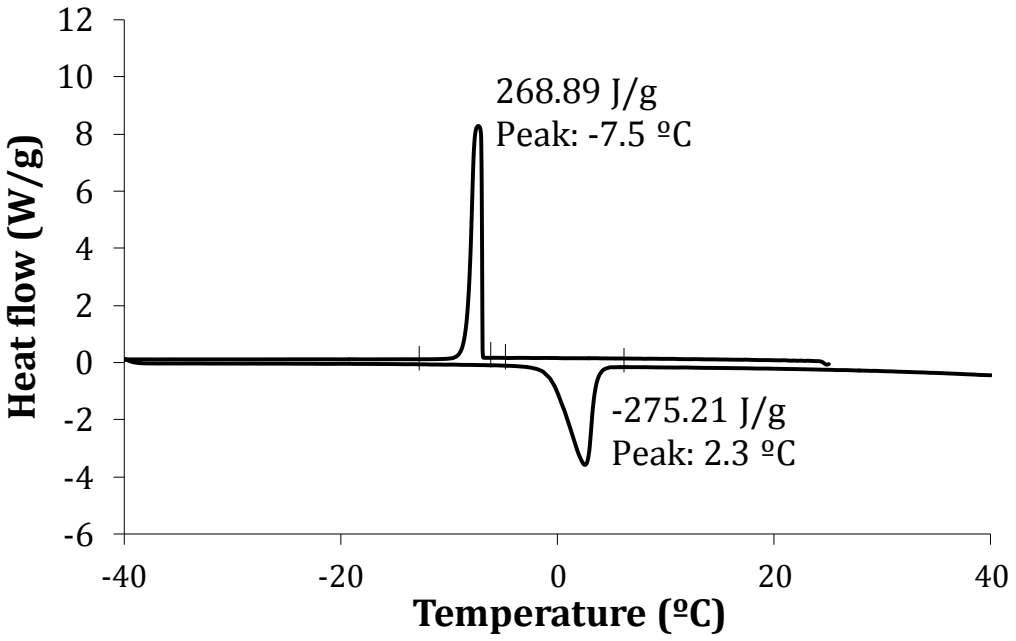

Figure 7.7. DSC thermogram for the untreated sludge. Cooling and heating rate of 2 ºC/min. Sample weight of 5.15 mg.

From the free water content measured in the DSC test and the total water content from drying at 105 ºC for 24 h, the bound water content for the untreated and treated sludge samples was determined and listed in Table 7.1.

Table 7.1. Bound water content calculated from DSC measurements and sTOC measured on the supernatant obtained after centrifugation.

	Bound water (vicinal and hydration water) (kg/kg dry solid)	**sTOC (mg/L)[1]**
Untreated	3.06	355 ± 1
Ultrasound (kJ/kg TS)		
5000	3.05	1692 ± 16
11,000	3.23	2149 ± 15
27,000	3.83	3197 ± 32
Thermal (kJ/kg TS; ºC)		
11,000 (60 ºC)	4.00	5646 ± 66
15,000 (80 ºC)	3.55	5704 ± 86
18,000 (90 ºC)	4.37	5717 ± 55
Alkali (g NaOH/kg TS)		
35.3	4.23	1991 ± 22
70.6	4.28	5398 ± 127
157	4.29	7009 ± 114

[1]The sTOC was measured in the supernatant, obtained after centrifugation at 2500 x *g* for 45 min and filtered through 0.45-µm. Errors represent the confidence interval (95%).

The untreated WAS contained approximately 3 kg bound water per kg of dry sludge. Similar values for the bound water of the WAS were reported by Heukelekian and Weisberg (1956), Colin and Gazbar (1995) and Chu et al. (2001). Considerably higher bound water values in the range of 6-7 kg bound water per kg of dry sludge were found by Lee and Lee (1995) in WAS samples. The bound water content increased with

the treatments intensity, except in the case of thermal conditioning at 80 ºC (3.55 kg/kg of dry sludge), whose water content was lower than that registered after thermal conditioning at 60 ºC (4.00 kg/kg of dry sludge). This may have been related to the non-uniformity of the WAS sample when performing the DSC (Lee and Hsu, 1995). The increase in the bound water content after treatment was also observed by other authors (Chu et al., 2001; Erdincler and Vesilind, 2003). An increase of bound water may suggest a more difficult dewatering; however, the opposite was true, as discussed below. This could be explained if frozen water measured in DSC was free and interstitial water. Thus, what increased with treatments was the set of vicinal water and water of hydration.

Table 7.1 also shows the sTOC concentration, which was measured on the supernatant obtained after centrifuging the sludge at 2500 x *g* for 45 min. The sTOC concentration may be an indication of the degree of cell rupture and solubilisation of EPSs. An increase in the sTOC (always over 100% with respect to the untreated WAS) was observed when increasing treatment intensity, which suggested that a large amount of organic material, including primarily protein, polysaccharide, lipids and other molecules were released into the liquid phase due to sludge floc disruption and cell rupture. Specifically, the maximum disruption was observed after the alkali treatment of 157 g NaOH/kg TS. Jin et al. (2004) found that proteins and polysaccharides, which are the primary constituents of EPSs, actively contributed to the water-binding capacity of the sludge floc matrix. Thus, it is conceivable that the material released after cell wall disruption increased the available surface for the vicinal water (Ruiz-Hernando et al., 2014b).

7.3.2. WAS dewatering by centrifugation

Figures 7.8, 7.9 and 7.10 show the amount of water removed from the untreated and treated sludge samples (ultrasound: 5000, 11,000 and 27,000 kJ/kg TS; thermal: 11,000 (60 ºC), 15,000 (80 ºC) and 18,000 (90 ºC) kJ/kg TS; alkali: 35.3, 70.6 and 157 g NaOH/kg TS) after centrifugation at 2500 x *g* for 15, 30 and 45 min. The sludge flocs were deformed under centrifugal pressure, and the sludge became more compact by increasing the centrifugation time. According to Lee (1994), at a certain centrifugation

speed, the sludge cannot be compressed anymore and it contains only the solid phase and the bound water. However, the relationship between the equilibrium sediment height for WAS and the rotational speed is nonlinear for rotational speeds higher than 3500 rpm; therefore, the centrifugal settling method would not be entirely accurate to calculate the bound water content. Accordingly, the centrifugal method primarily provided information about the compressibility of the sludge.

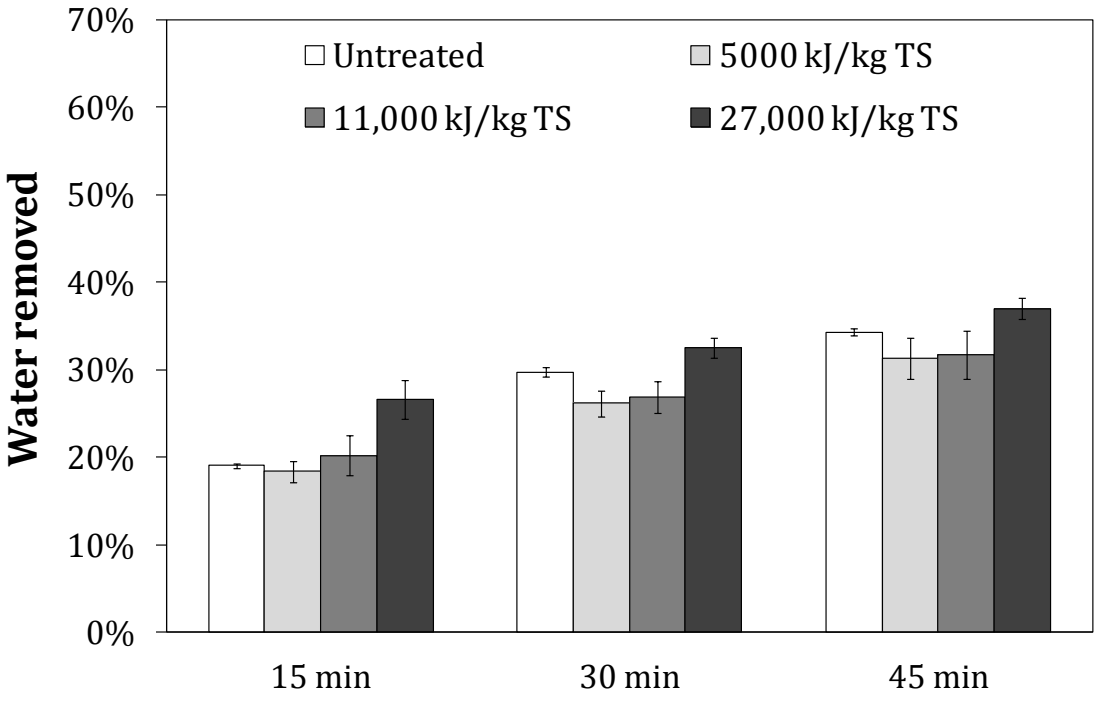

Figure 7.8. Water removed from the ultrasonicated sludges after centrifugation at 2500 x *g* for 15, 30 and 45 min. Error bars represent confidence interval (95%).

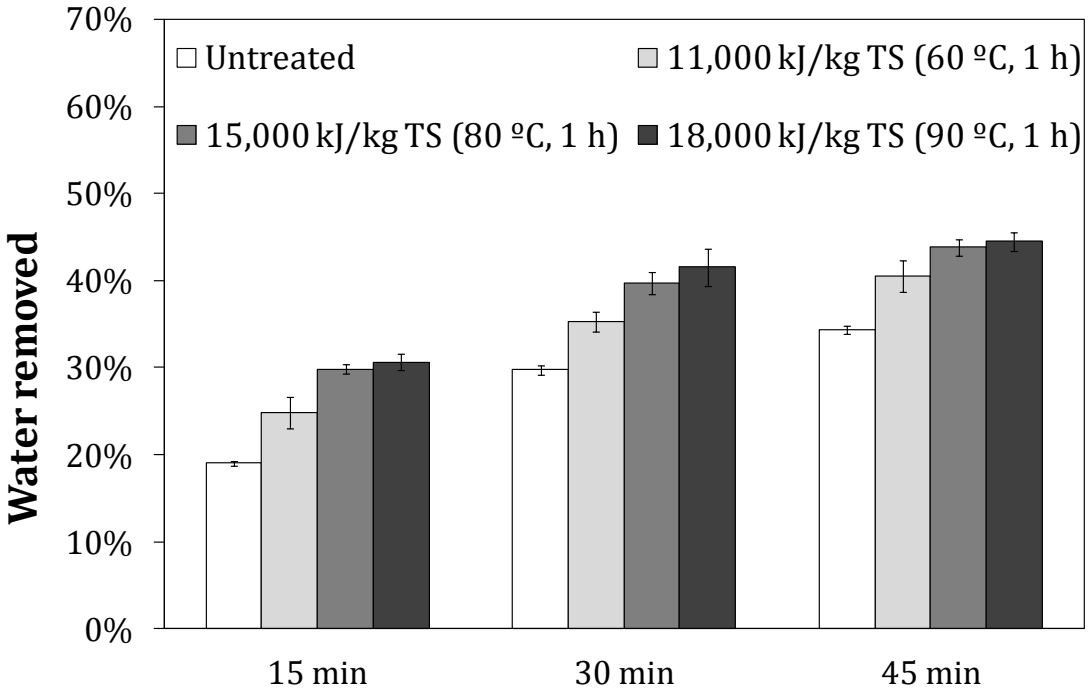

Figure 7.9. Water removed from the thermally treated sludges after centrifugation at 2500 x *g* for 15, 30 and 45 min. The time of treatment include the heating ramp (~30 min). Error bars represent confidence interval (95%).

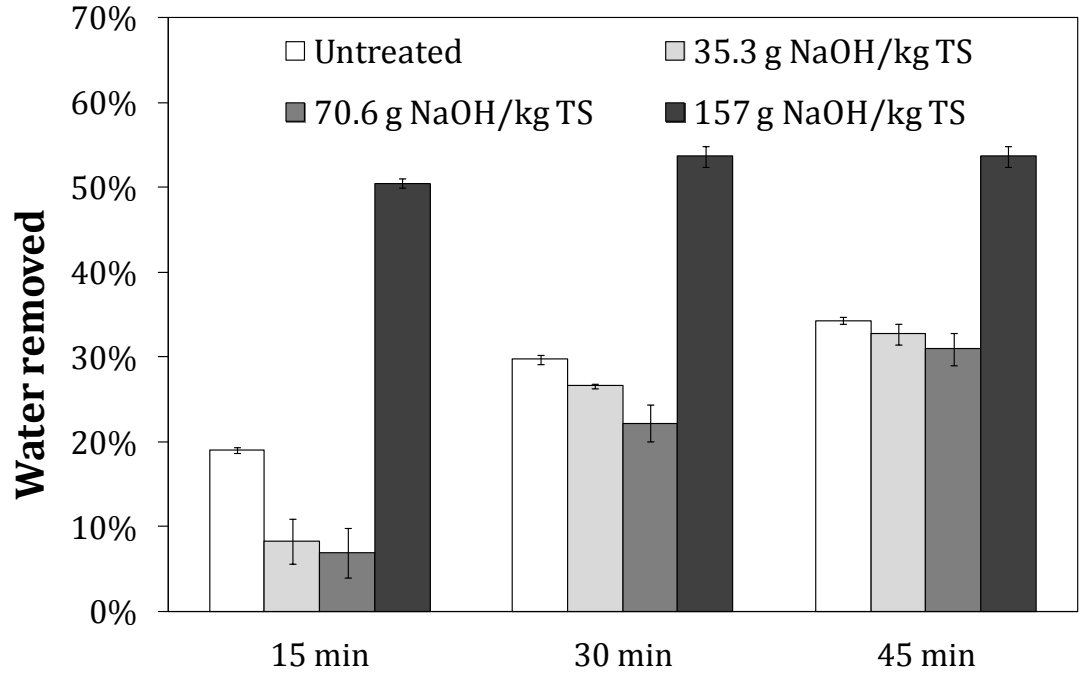

Figure 7.10. Water removed from the alkali-treated sludges after centrifugation at 2500 x *g* for 15, 30 and 45 min. Error bars represent confidence interval (95%).

By comparing the amount of water removed from the treated sludges with respect to the untreated sludge, it was possible to identify the treatment conditions that improved or worsened the dewatering of the sludge. As in the case of the apparent viscosity reduction (Figure 5.27), the thermal treatment resulted in a different pattern in comparison with the ultrasound and alkali treatments. The three conditions of the thermal treatment decreased the viscosity of the sludge at similar levels and resulted in a better dewatering, especially the higher temperatures. In contrast, although all the conditions tested for the ultrasound and alkali treatments were able to reduce the viscosity of the sludge, only the stronger conditions (27,000 kJ/kg TS and 157 g NaOH/kg TS, respectively) resulted in an improvement of the sludge dewatering. The results were similar for the three centrifugation times studied. Therefore, despite the increase in the bound water content, treatments were able to improve sludge dewatering by centrifugation. As already said, it is conceivable that the bound water measured by DSC may have been primarily vicinal and not interstitial water. Thus, the improvement of sludge dewatering with treatments may be because the interstitial water was removed and passed to the supernatant fraction.

Under the tested conditions, the ultrasound treatment only improved the sludge dewatering at high E_S, whereas in the literature it is widely accepted that high E_S deteriorates sludge dewatering because it sharply increases the CST (Chu et al., 2001; Feng et al., 2009a). Nevertheless, several investigators have criticised the use of CST to characterise the sludge dewaterability and have highlighted some experimental problems, such as the influence of the sludge concentration and the influence of the filter paper structure (La Heij, 1994; Herwijn, 1996). In particular, the viscosity, surface tension and contact angle of the water flowing through the capillaries of the paper greatly affects the CST result. All of these variables can be significantly altered by released organic material induced by treatments. Despite these limitations, the CST has been registered because it is widely used in the field of sludge dewatering. Figure 7.11 shows the evolution of the CST with the E_S applied by the ultrasound and thermal treatments. An increase in CST with an increase in specific ultrasound energy is clearly observed. This could be attributed to the amount of water attached (vicinal water) to the new surfaces provided by the small particles after ultrasonication (Figure 5.28).

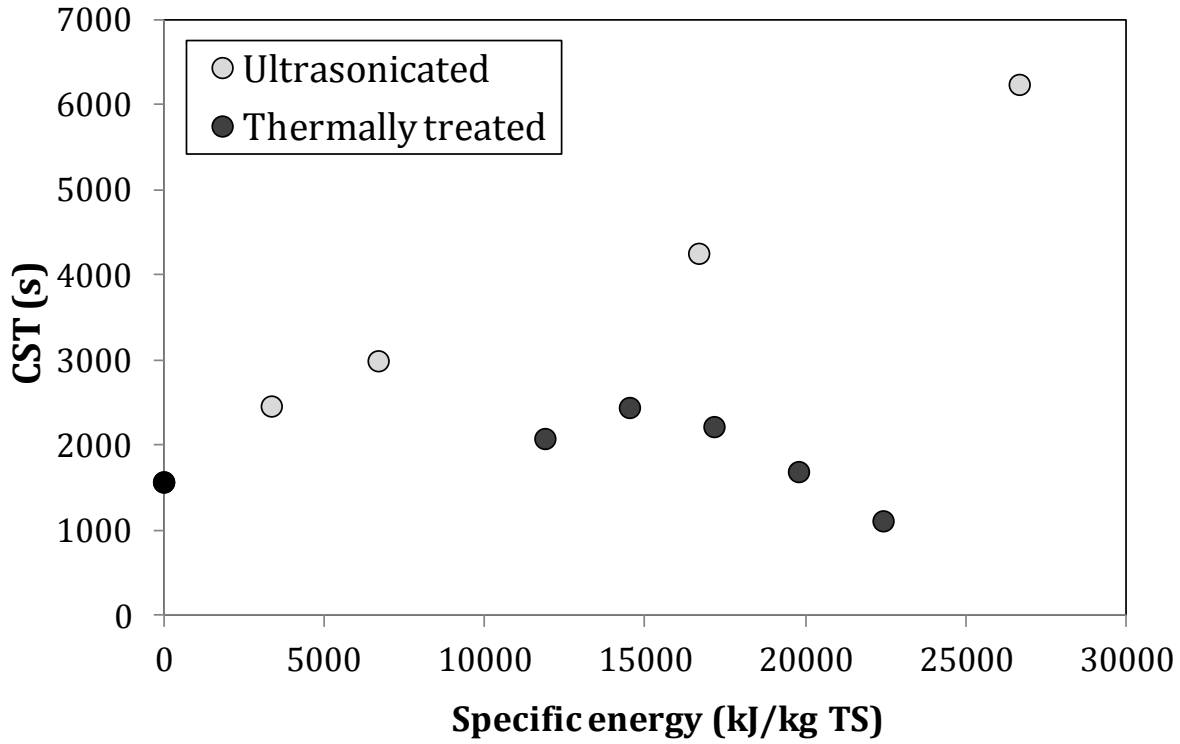

Figure 7.11. Capillary suction time (CST) for the ultrasonicated and thermally treated sludges.

The three conditions of the thermal treatment improved sludge dewatering. A possible explanation for the effectiveness of this treatment may be the release of interstitial water due to sludge disruption and deflocculation (this is explained below, in Section 7.3.3.3). Furthermore, the CST was observed to initially increase with the thermal E_S, but it began to decrease above 15,000 kJ/kg TS (80 ºC) (Figure 7.11). Specifically, the CST value was 1100 s for a thermal E_S of 22,000 kJ/kg TS, which was below the value obtained for the untreated sludge (1500 s). Similar results were reported by Bougrier et al. (2008), who found that the CST value increased at low temperatures and decreased at temperatures higher than 130 ºC.

The results obtained for the alkali treatment are consistent with those reported by Li et al. (2008), who concluded that doses of NaOH lower than 0.2 mol/L deteriorated sludge dewaterability, while this ability could be restored to some extent by treatment with a high dose. The concentrations of 35.3 and 70.6 g NaOH/kg TS corresponded to

0.05 and 0.10 mol/L, which were below the limit found by Li et al. (2008) to improve sludge dewatering with NaOH. As a result, these concentrations worsened sludge dewatering. On the other hand, the level of neutralisation after alkali treatment affects the dewaterability of the sludge. Indeed, dewatering was very sensitive to the final pH. After several trials, it was concluded that a dose greater than 0.2 mol NaOH/L was required with a final neutral pH of 7 after 24 h of aging. Otherwise, the quantity of water extracted would have been much lower, or even negligible, above a neutralisation pH of 8.5. The CST value for alkali conditioning was too high to be recorded.

7.3.3. EPSs fractionation

To further evaluate the effect of treatments on the sludge dewatering, the EPSs contained in sludge were extracted and characterised. The EPS analyses were conducted on the untreated sludge and on a unique condition of each treatment. These conditions were selected based on rheological (Chapter 5) and dewatering criteria. Thus, the condition selected for the ultrasound treatment was 27,000 kJ/kg TS, since it was the only ultrasound E_S that improved sludge dewatering by centrifugation (Figure 7.8) and registered the highest viscosity reduction (Figure 5.27). Similarly, the condition selected for the alkali treatment was the concentration of 157 g NaOH/kg TS (Figure 7.10 and Figure 5.27). For the thermal treatment, the temperature selected was 80 ºC (15,000 kJ/kg TS), since both sludge dewatering and viscosity reduction was similar to the temperature of 90 ºC (Figure 7.9 and Figure 5.27).

Before presenting the results, it should be noted that the designation used for EPSs, LB-EPSs and TB-EPSs, would only be strictly appropriate for the untreated sludge. The treatments disrupt the sludge, releasing some organic material that was previously confined in sludge flocs and cells. Consequently, measuring the EPS content after treatment does not correspond exclusively to the EPS but also to some other organic compounds released into the bulk solution. Nevertheless, the LB-EPS and TB-EPS nomenclature has been maintained throughout the study to facilitate exposition of the results.

7.3.3.1. EPS bulk solutions characterisation: viscosity and zeta potential

Table 7.2 shows the viscosity of the EPS bulk solutions interpolated at a shear rate of 10 s^{-1} for the untreated and treated (ultrasound: 27,000 kJ/kg TS; thermal: 80 ºC (15,000 kJ/kg TS); alkali: 157 g NaOH/kg TS) sludge samples. The LB-EPS fractions exhibited the greatest differences in viscosity between the untreated and conditioned sludges. Specifically, the ultrasound, thermal and alkali treatments increased the viscosity of the LB-EPS fraction approximately 65%, 600% and 700%, respectively. In contrast, the viscosities of the TB-EPS fractions were reduced as a result of the treatments, especially after the thermal treatment. Similarly, Farno et al. (2014) found that the increase in the level of solubility induces that some particulate organic matter inside the sludge changed their phase and solubilised into liquid medium (interstitial liquid), thus increasing the viscosity of liquid medium. Thus, the bulk solutions of treated sludges are more complex fluids comprised of EPSs, which increase the available surface for water binding. This could possibly explain the increased CST value for the treated sludges (Figure 7.11).

Table 7.2. Viscosity and zeta potential of the EPS bulk solutions.

		Viscosity (Pa·s)	**Zeta potential (mV)**
Untreated	LB-EPSs	1.35	-30.5±0.8
	TB-EPSs	3.88	-30.6±0.5
Ultrasound (27,000 kJ/kg TS)	LB-EPSs	2.23	-27.2±0.4
	TB-EPSs	2.72	-31.4±0.3
Thermal (80 ºC; 15,000 kJ/kg TS)	LB-EPSs	9.48	-22.7±0.3
	TB-EPSs	1.79	-29.6±0.6
Alkali (157 g NaOH/kg TS)	LB-EPSs	10.7	-20.2±0.9
	TB-EPSs	3.53	-30.6±1.1

Table 7.2 also show the values of the zeta potential of the EPS bulk solutions. The ultrasound, thermal and alkali treatments increased the zeta potential of the LB-EPS

fractions from -30.5±0.8 (untreated sludge) to -27.2 ± 0.4, -22.7 ± 0.3 mV and -20.2 ± 0.9, respectively. Conversely, the TB-EPS fractions remained almost unchanged. According to DLVO theory, the increase of zeta potential makes the colloid particle unstable and improves the flocculation of sludge. As a result, the dewaterability of sludge is improved (Guan et al., 2012).

7.3.3.2. EPS composition

The TOC, protein, humic acid and polysaccharide contents of the LB-EPS and TB-EPS fractions in the untreated and treated sludge were analysed (Figures 7.12, 7.13, 7.14 and 7.15). The evolution of the four parameters followed a similar pattern. Note that the maximum value for the y-axis is the same for the TOC and protein contents, but not for the humic acid and polysaccharide contents. As can be observed, the measurements of the viscosity of the EPS bulk solutions (Table 7.2) were strongly correlated with the EPS contents (Figure 7.12).

The analysis of the untreated WAS revealed that proteins were the major constituents of the EPS; proteins were found primarily in the TB-EPS fraction (92%, w/w), with a small percentage in the LB-EPS fraction (8%). This result agreed with the literature data (Li and Yang, 2007; Yu et al., 2009). Humic substances were the second largest constituent and had distribution patterns similar to the proteins. Specifically, 88% was found in the TB-EPS fraction, and 12% was found in the LB-EPS fraction. Polysaccharides accounted for a small proportion of the EPS, but their trends were similar to those of the proteins and humic substances (TB-EPS = 93.1% and LB-EPS = 6.9%). This finding is expected because polysaccharides are highly biodegradable. The predominance of proteins in the EPSs may be attributed to the presence of a large quantity of exoenzymes (Frølund et al., 1995). Accordingly, the large concentration of humic acids may be explained by the role that these compounds play in immobilising the exoenzymes through reversible complexation (Wetzel, 1991). The distribution of the TOC in the different EPS fractions was consistent with that of proteins; this result is unsurprising because proteins were the primary organic components.

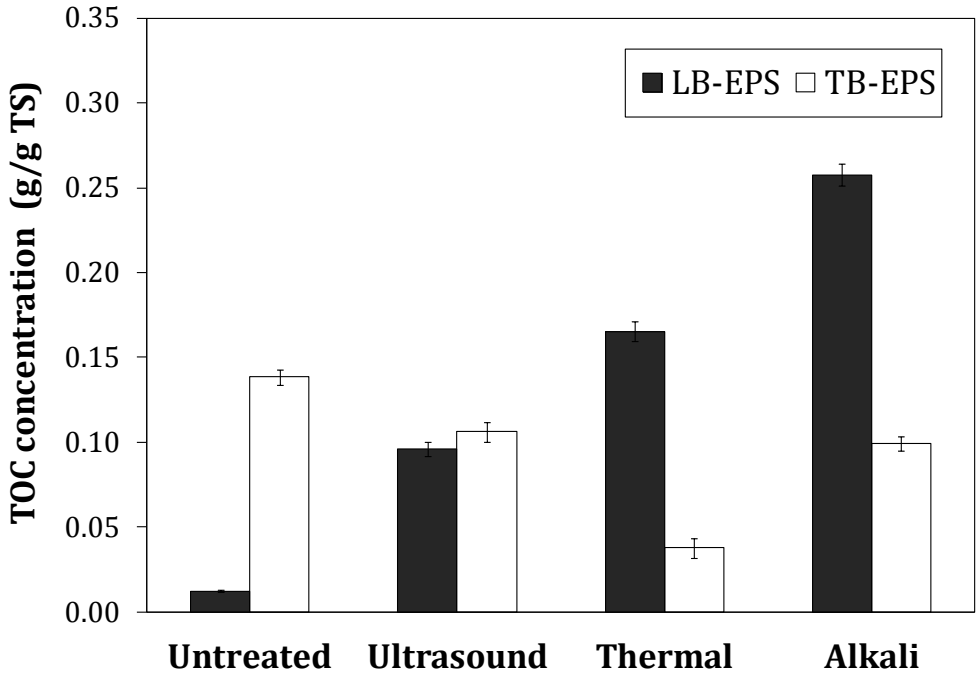

Figure 7.12. LB-EPS and TB-EPS in terms of TOC content. Ultrasound treatment: 27,000 kJ/kg TS. Thermal treatment: 80 ºC. Alkali treatment: 157 g NaOH/kg TS. The error bars represent the confidence interval (95%).

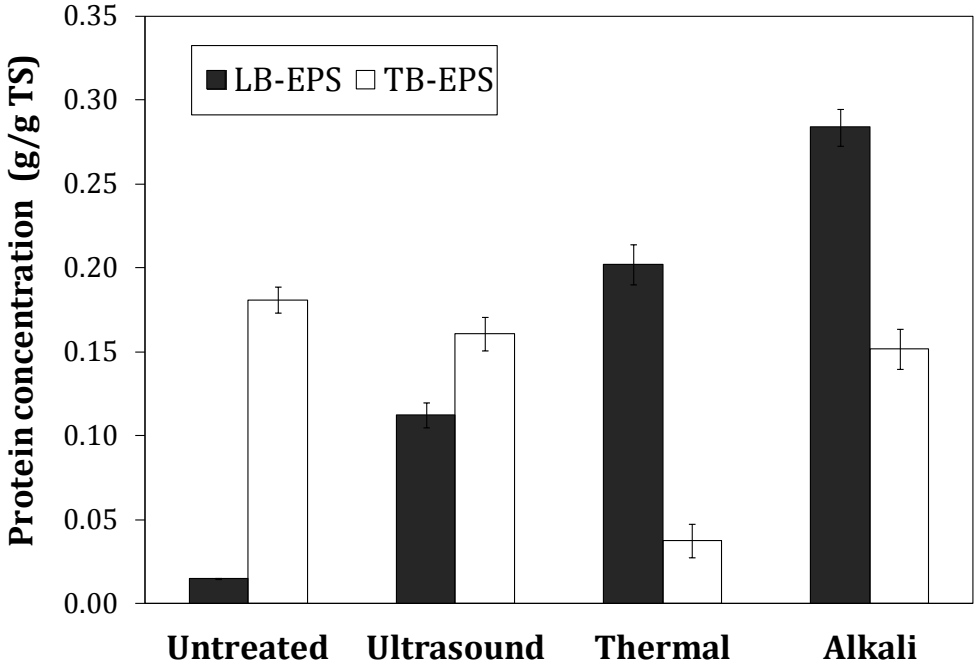

Figure 7.13. LB-EPS and TB-EPS in terms of protein content. Ultrasound treatment: 27,000 kJ/kg TS. Thermal treatment: 80 ºC. Alkali treatment: 157 g NaOH/kg TS. The error bars represent the confidence interval (95%).

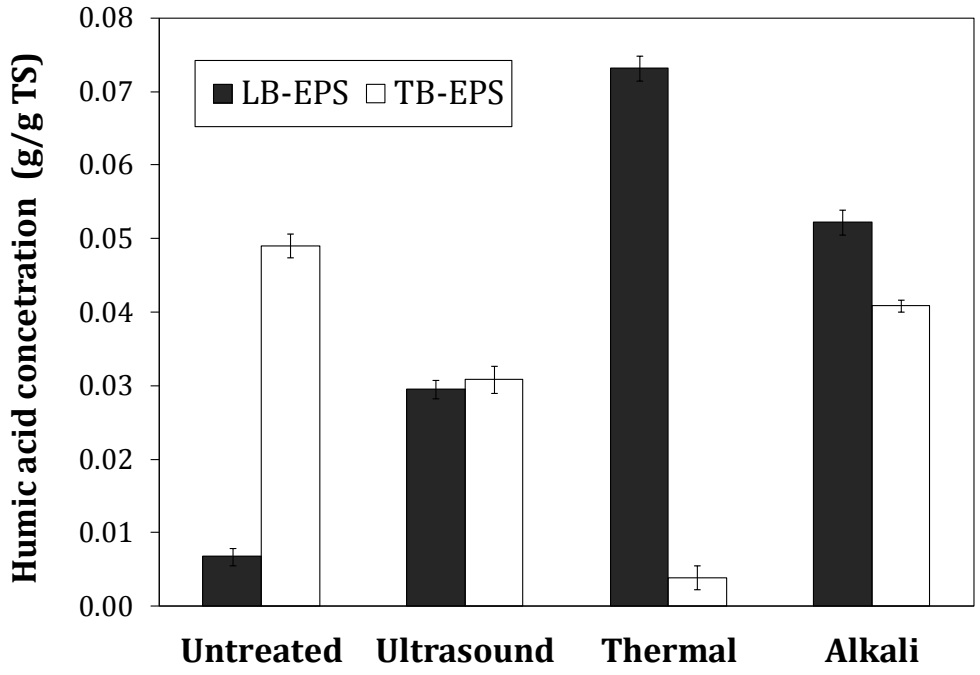

Figure 7.14. LB-EPS and TB-EPS in terms of humic acid content. Ultrasound treatment: 27,000 kJ/kg TS. Thermal treatment: 80 ºC. Alkali treatment: 157 g NaOH/kg TS. The error bars represent the confidence interval (95%).

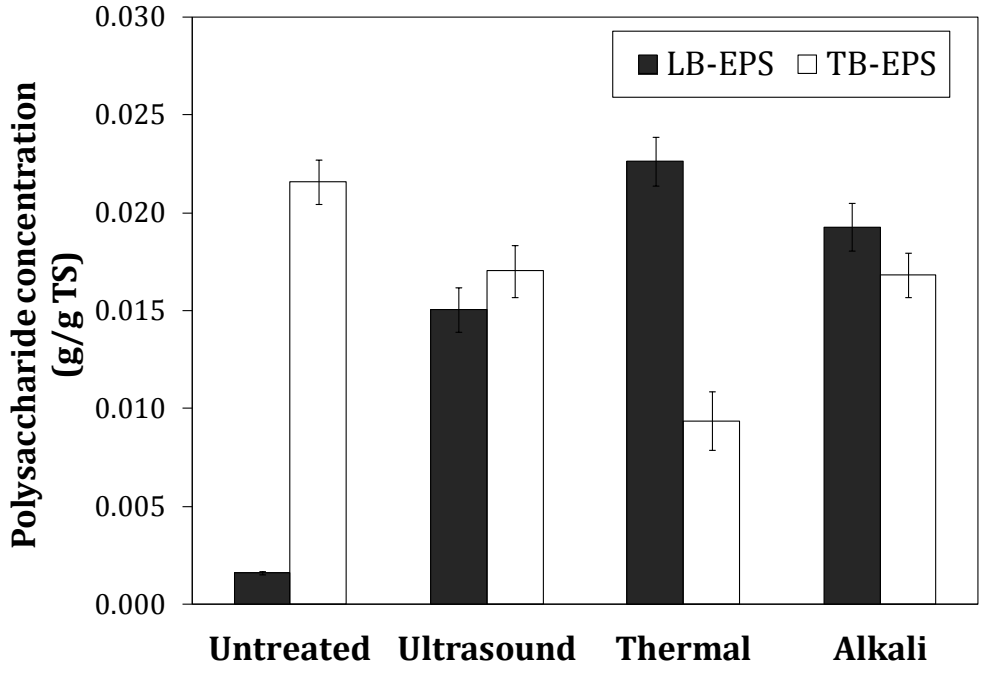

Figure 7.15. LB-EPS and TB-EPS in terms of polysaccharide content. Ultrasound treatment: 27,000 kJ/kg TS. Thermal treatment: 80 ºC. Alkali treatment: 157 g NaOH/kg TS. The error bars represent the confidence interval (95%).

The treated sludge showed higher levels of EPSs in the form of LB-EPSs compared to the untreated sludge. Therefore, the treatments solubilised the EPSs, as indicated by the increased LB-EPS content. The largest increase in the LB-EPS content was observed after the alkali treatment; the second largest increase was observed after the thermal treatment. Although ultrasonication was expected to disrupt the flocs and cellular membranes, the LB-EPS content did not increase as much as it did during the alkali or thermal treatments. This is consistent with the results described in Chapter 8, where the ultrasound treatment was effective enough to dissipate sludge flocs but not for killing bacteria and spores or for inactivating bacteriophages (Ruiz-Hernando et al., 2014a). The TB-EPS fraction was slightly decreased after the ultrasound and alkali treatments and noticeably decreased after the thermal treatment. Specifically, the thermal treatment noticeably increased the protein content of the LB-EPS fraction and reduced the protein content of the TB-EPS fraction by 80% compared to the untreated sludge.

The protein-like molecules were characterised further by measuring the amino acid content in both EPS fractions, as shown in Figure 7.16. The term "total amino acids" refers to the sum of the free amino acids and the amino acids that form proteins.

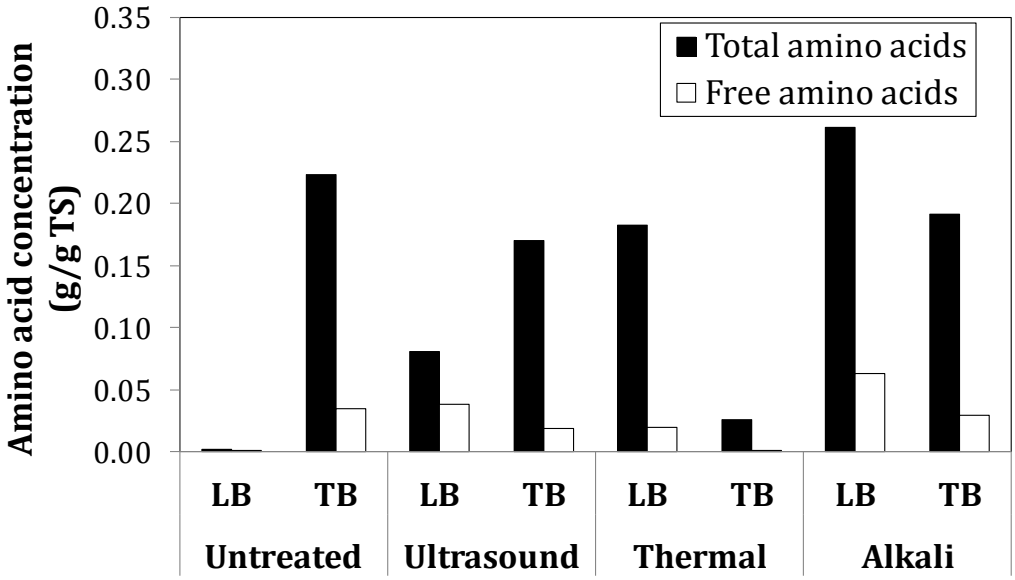

Figure 7.16. Total and free amino acid concentrations of the EPS fractions from the untreated and treated sludges. Ultrasound treatment: 27,000 kJ/kg TS. Thermal treatment: 80 ºC. Alkali treatment: 157 g NaOH/kg TS.

Both the total and free amino acid contents exhibit trends similar to those observed with the proteins measured using the Lowry method (Figure 7.13). Thereby, the total and free amino acid contents in the LB-EPS fraction of the untreated sludge were very low, while the TB-EPS fraction contained a remarkable level of total amino acids. Similar to the proteins, the treatments strongly increased the amount of amino acids in the LB-EPS fractions, particularly after the alkali treatment. Likewise, the treatments decreased the amino acid contents in the TB-EPS fractions, especially after the thermal treatment. The thermally treated sludge exhibited the lowest proportion of free amino acids for both EPS fractions: 11% (free amino acid/total amino acid) for the LB-EPS fraction and 1% for the TB-EPS fraction.

7.3.3.3. Molecular weight distributions of the EPS fractions

The gel permeation chromatography experiments were conducted using a multi-detector that could differentiate between the three types of organic matter: protein-like substances, polysaccharides and humic acids. Figures 7.17, 7.18, 7.19 and 7.20 show the molecular weight distributions (MWDs) of the LB-EPS and TB-EPS fractions for the untreated, ultrasonicated, thermally treated and alkali-treated sludges, respectively.

As specified in the section of materials and methods of this chapter, the absorbance reading at 280 nm, which is commonly used to measure proteins, was corrected by subtracting the contribution from nucleic acids, which maximally absorb UV light at 260 nm (Equation 7.3). The MWDs of the EPS fractions with proteins measured at 280 nm (without correction) are summarised in Annex III. Notably, the size boundary between a protein and a peptide overlaps and is somewhat arbitrary. In the present study, the smallest compound to be called a protein was similar in size to insulin (5800 Da), and those below 5800 Da were considered protein building blocks. The MWDs are presented as dW/dLog M vs. Log M, where W is the weight of organic matter of molecular weight M (M is expressed in Daltons). The total weight (the sum of LB-EPS and TB-EPS) for each analysed organic component has been normalised (100%). Each LB-EPS and TB-EPS fractions has a partial weight in accordance to the measured quantities of protein, humic acid and polysaccharide (Figures 7.13, 7.14 and 7.15).

A

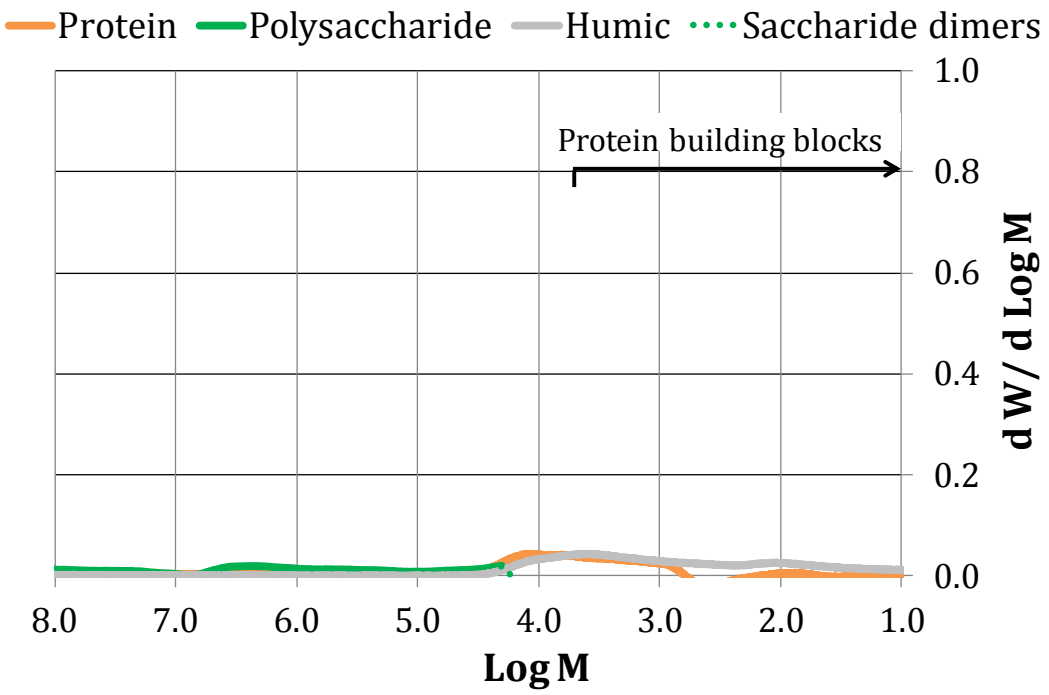

B

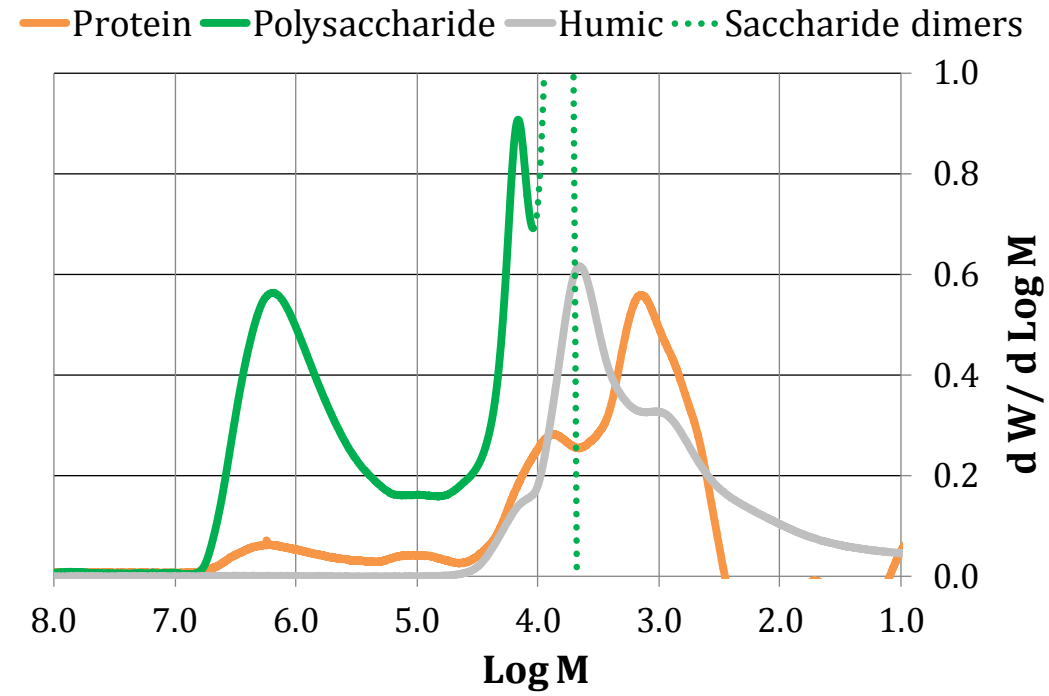

Figure 7.17. Molecular weight distributions determined by gel permeation chromatography of the (A) LB-EPS and (B) TB-EPS fractions for the untreated sludge. *W* is the weight of the organic matter with a molecular weight of *M* (*M* is expressed in Daltons).

A

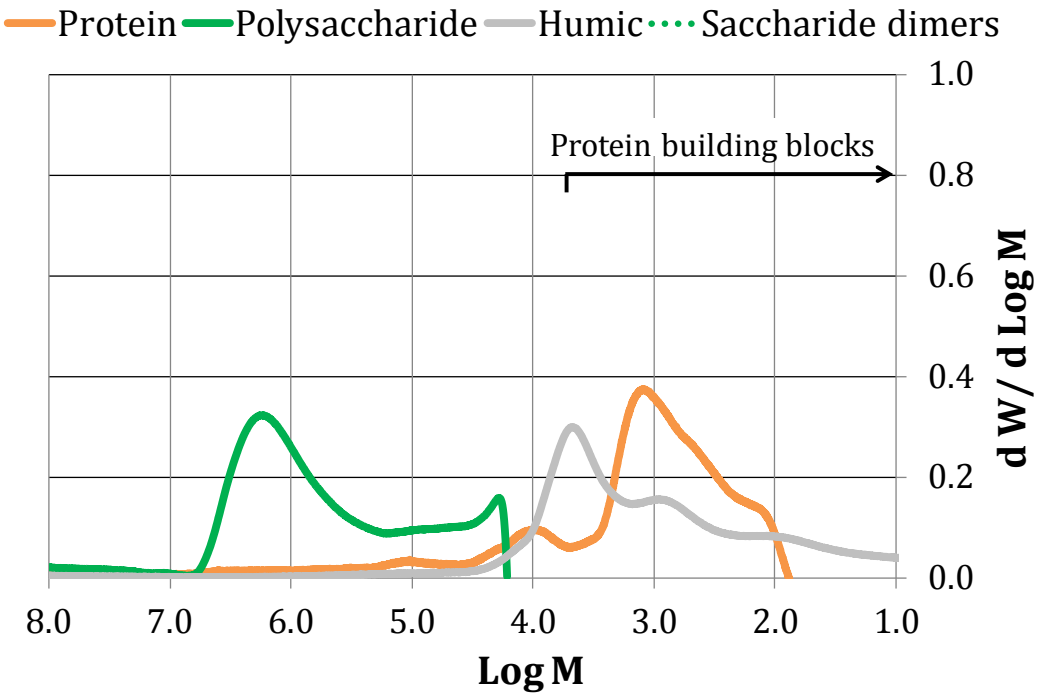

B

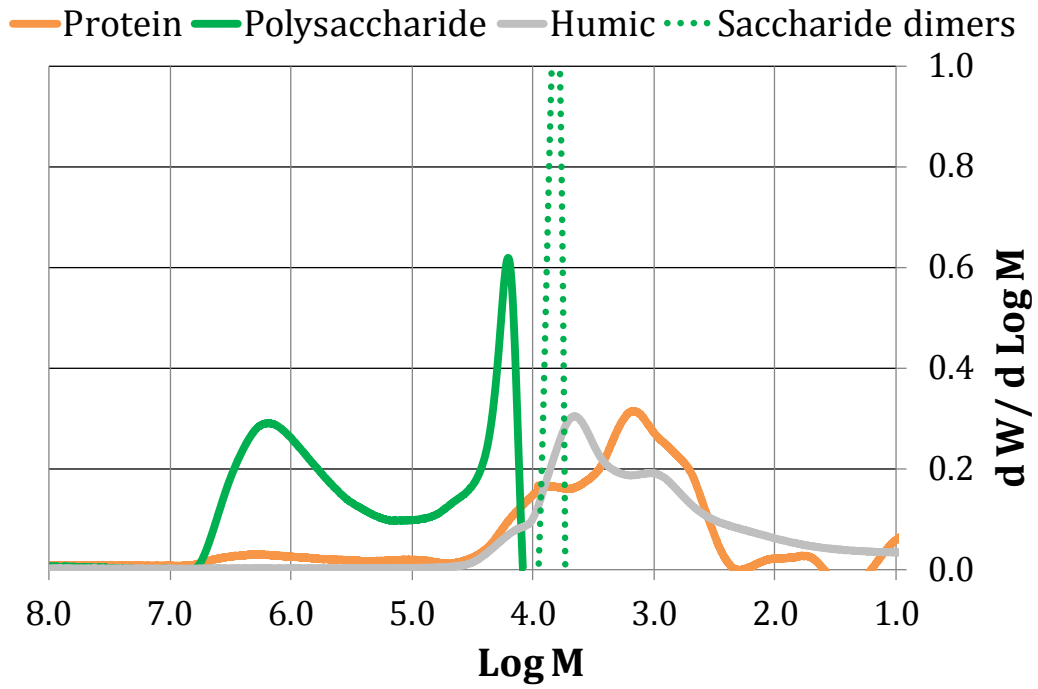

Figure 7.18. Molecular weight distributions determined by gel permeation chromatography of the (A) LB-EPS and (B) TB-EPS fractions for the ultrasonicated sludge (27,000 kJ/kg TS). *W* is the weight of the organic matter with a molecular weight of *M* (*M* is expressed in Daltons).

A

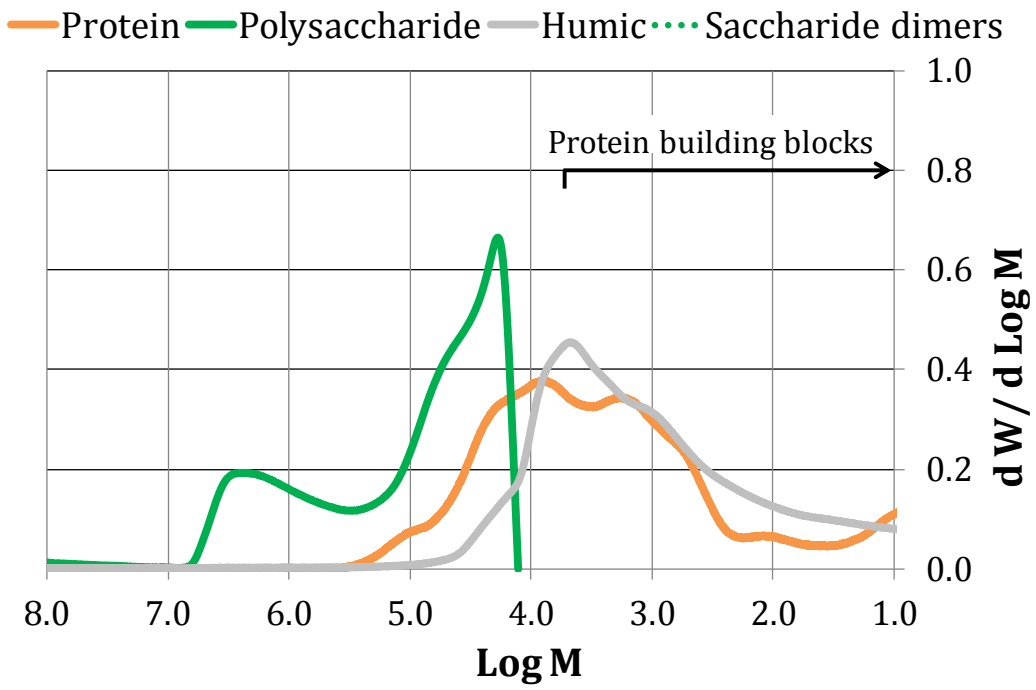

B

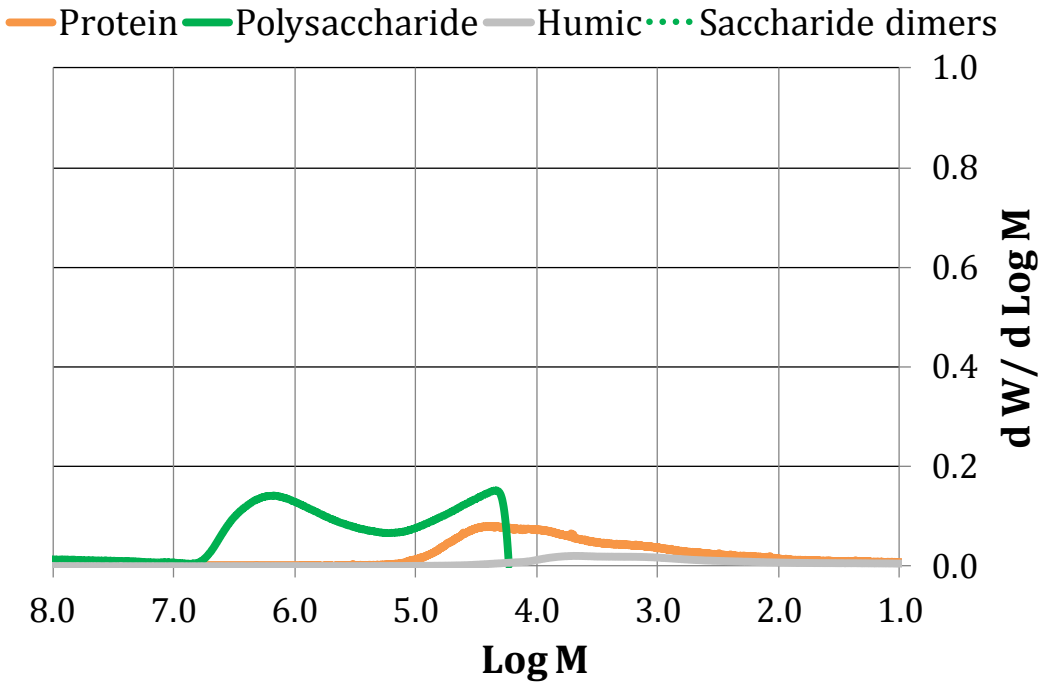

Figure 7.19. Molecular weight distributions determined by gel permeation chromatography of the (A) LB-EPS and (B) TB-EPS fractions for the thermally treated sludge (80 ºC). *W* is the weight of the organic matter with a molecular weight of *M* (*M* is expressed in Daltons).

A

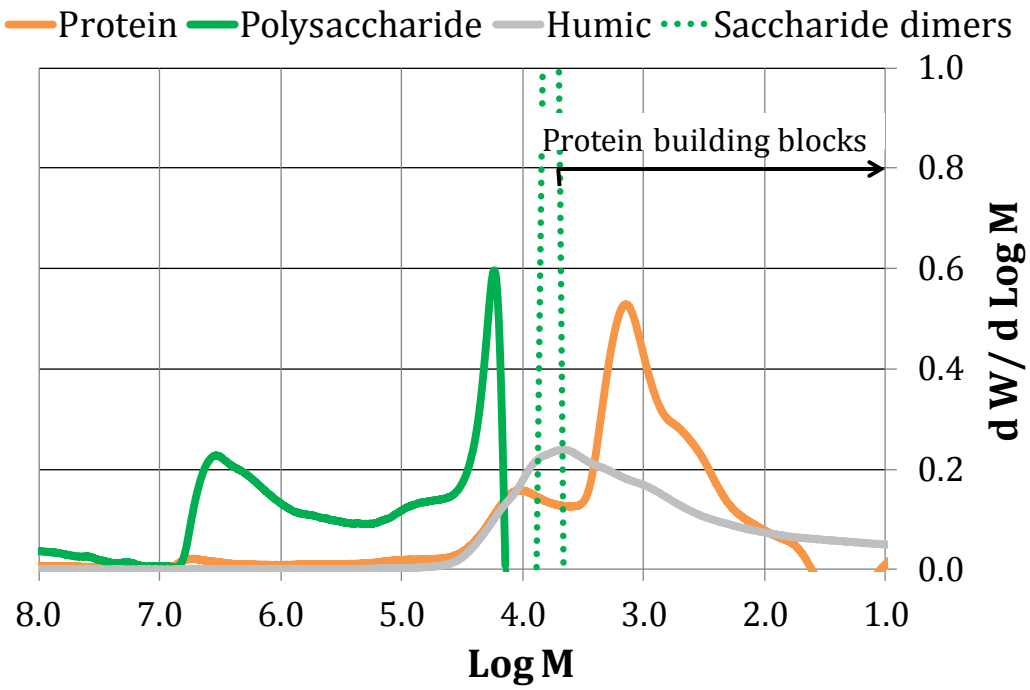

B

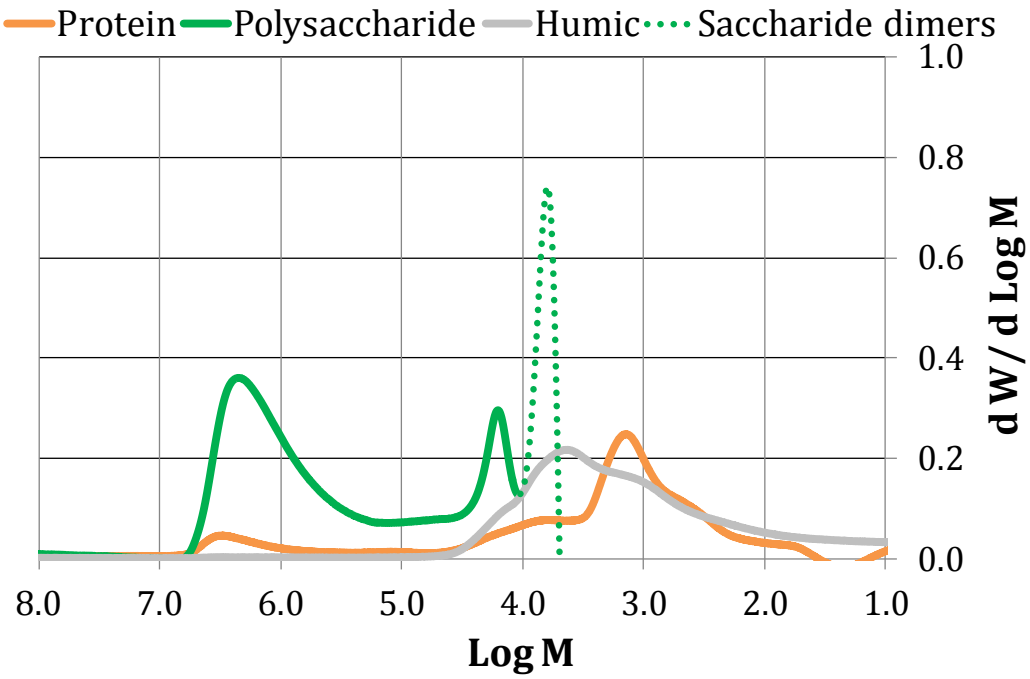

Figure 7.20. Molecular weight distributions determined by gel permeation chromatography of the (A) LB-EPS and (B) TB-EPS fractions for the alkali-treated sludge (157 g NaOH/kg TS). *W* is the weight of the organic matter with a molecular weight of *M* (*M* is expressed in Daltons).

For the untreated sludge, most of the EPSs were found in the TB-EPS fraction (Figure 7.17b), while very small amounts of protein-like substances, polysaccharides and humic acids were found in the LB-EPS fraction (Figure 7.17a). In contrast, all of the conditioned sludge samples contained substantial amounts of LB-EPS (Figures 7.18a, 7.19a and 7.20a), as also shown in Figure 7.12. The GPC chromatograms show that three groups of polydisperse protein-like substances were present: peptides (protein building blocks), low-molecular-weight proteins (approximately 10 kDa) and high-molecular-weight proteins (approximately 1500 kDa). Regarding polysaccharides, two groups are observed: one with a low polydispersity and weights of approximately 15 kDa, and another with a high polydispersity and weights of approximately 1500 kDa. The hatched line corresponds to saccharide dimers and other substances that are detected through RI. Polydisperse humic substances form two major groups with very similar average molecular weights (approximately 1 and 5 kDa). It is necessary to note that the column might absorb some material; therefore, the low molecular weights obtained (~ 10 Da) might actually be higher. Nevertheless, despite this small retention, the comparative analysis between the LB-EPSs and TB-EPSs is valid because all of the samples are affected by the same degree of retention.

The ultrasound treatment solubilised a portion of the peptides and low-molecular-weight proteins, as can be observed in the MWD of the LB-EPS fraction (Figure 7.18a). Notably, this treatment solubilised mostly high-molecular-weight polysaccharides. Separately, the humic substances were solubilised without a preference for molecular weight. The alkali treatment solubilised most of the peptides and proteins of low molecular weights, as well as a small portion of high-molecular-weight proteins (Figure 7.20a). In contrast to the ultrasound treatment, the alkali treatment solubilised more low-molecular-weight polysaccharides than those with high molecular weights. This treatment solubilised half of the humic substances. The thermal treatment solubilised most of the protein-like substances, but the high-molecular-weight proteins were absent from both GPC chromatograms (Figures 7.19a and 7.19b). This fact could be explained by this treatment's ability to change the tertiary structure of these proteins (denaturation). Therefore, the external surface hydrophilicity of these high-molecular-weight proteins decreases while coagulation or gelation occurs (Edelhoch

and Osborne, 1976; Tornberg, 2005; Paulsen et al., 2006). Fundamentally, high-molecular-weight proteins may act as flocculants, providing multiple hydrophilic binding points. Therefore, it is conceivable that the thermal treatment destroyed the flocculating ability of these proteins, resulting in lower water-holding capacity. Consequently, the water retained by the sludge floc matrices was released. The thermal treatment also solubilised most of the low-molecular-weight polysaccharides and humic substances.

7.3.3.4. Correlation between dewatering and EPSs concentration

As shown in Figures 7.8, 7.9 and 7.10, the three conditions selected for the EPSs extraction improved sludge dewatering by centrifugation. This improvement was more important in the case of the alkali treatment (which registered the highest value of LB-EPSs), followed by the thermal treatment and the ultrasound treatment. This fact could be explained by the release of interstitial water after EPS solubilisation. Clearly, it was observed a direct correlation between the soluble protein in the LB-EPS fraction and the water removed by centrifugation (Figure 7.21).

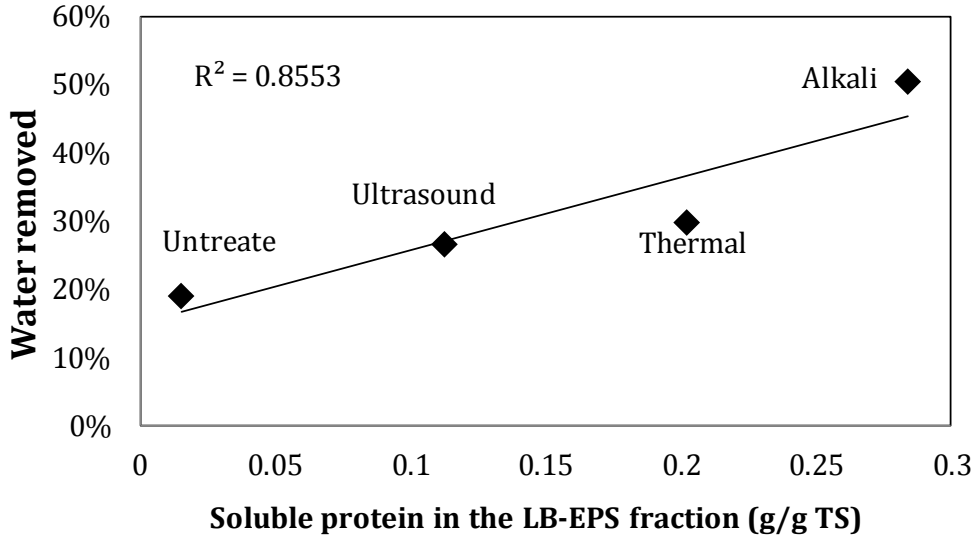

Figure 7.21. Relationship between the water removed from the sludge by centrifugation and soluble protein concentration in the LB-EPS fraction.

Although the thermal treatment denatured the high-molecular-weight proteins, the water removed by centrifugation was higher after the alkali treatment, which solubilised the largest portion of EPSs. Thus, evidence suggests that the solubilisation of EPS is decisive for WAS dewatering (Ruiz-Hernando et al., 2015b). The ultrasound treatment solubilised fewer EPSs than the other two treatments. Accordingly, the ultrasound treatment was less efficient for removing water from the sludge.

7.3.4. Rheological behaviour of dewatered sludges

The observed variations in the EPS matrix affect the rheological profile of the sludge, as demonstrated in Chapters 5 and 6. In this section, it is compared the rheological changes between untreated and dewatered sludges. For this purpose, one condition of each treatment was selected to treat the sludge. These conditions corresponded to the treatment conditions used for the EPS extraction (ultrasound: 27,000 kJ/kg TS; thermal: 80 ºC (15,000 kJ/kg TS); alkali: 157 g NaOH/kg TS). Dewatered sludges were obtained by centrifugation (2,500 x *g* for 30 min) of the aforementioned treated sludges, following by the removal of the bulk water by decantation. Figure 7.22 shows the hysteresis loops (corresponding to a maximum shear rate of 300 s^{-1}) of the untreated and dewatered sludges.

As demonstrated above, the three conditions of treatment resulted in the improvement of sludge dewatering by centrifugation (Figures 7.8, 7.9 and 7.10). In other words, the treatments increased the TS content of the sludge after removing the supernatant resulting from centrifugation (Table 7.3). Nevertheless, despite the increase in the TS content, the dewatered sludges corresponding to the ultrasound and thermal treatments exhibited a reduction in the shear stress (and therefore the viscosity) (Figure 7.22). Therefore, as the solid content of both dewatered sludges was higher than that of untreated sludge, the sludges resulting from dewatering were more concentrated, but also easier to handle. For instance, this would enable a high-solid anaerobic digestion with the advantage of lower power consumption for agitation. The dewatered sludge corresponding to the alkali treatment exhibited a higher viscosity than the untreated

sludge, possibly because of the increased interaction between sludge flocs as a result of the increased TS content.

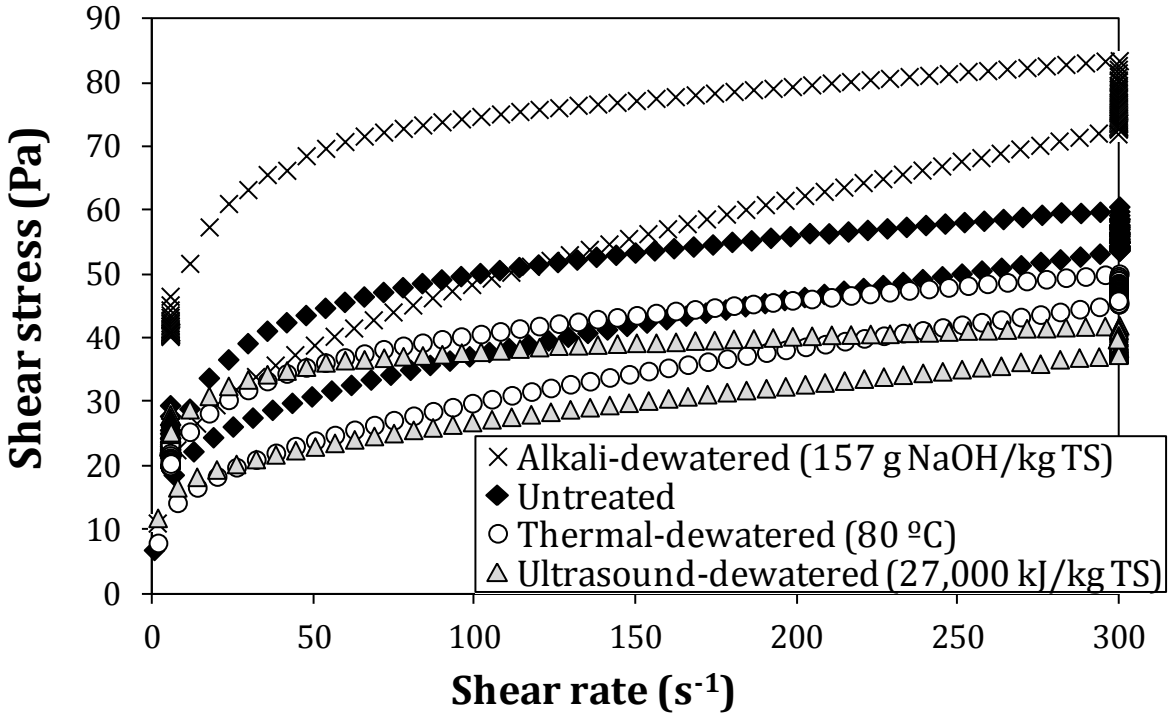

Figure 7.22. Hysteresis loops for the untreated and dewatered sludges obtained by centrifugation of the previously treated sludges.

Table 7.3. Total solid content of the untreated and dewatered sludges. The dewatered sludges were obtained by centrifugation of the treated sludges (ultrasound: 27,000 kJ/kg TS; thermal: 15,000 kJ/kg TS (80 ºC); alkali: 157 g NaOH/kg TS).

	TS (g/L)
Untreated	50.8 ± 0.3
Ultrasound-dewatered	75.3 ± 0.6
Thermal-dewatered	84.2 ± 0.5
Alkali-dewatered	110 ± 0.7

When comparing the power law indexes (the exponent of the Ostwald-de Waele power law model, *n*), it was noticed that the dewatered sludges resulting from the ultrasound and alkali treatments were very similar (n=0.1), suggesting that these treatments have comparable structures. In turn, the dewatered sludge resulting from the thermal treatment has a very similar power law index to the untreated sludge (n=0.2). This effect is better visualised in Figures 7.23 and 7.24, where the hysteresis loops of these sludges are presented with different y-axis values. Lower power law index means more deformable and easy to break down structures with the shear rate. Therefore the untreated and thermally-dewatered sludges have more stable structures than the ultrasonicated and alkali-dewatered sludges.

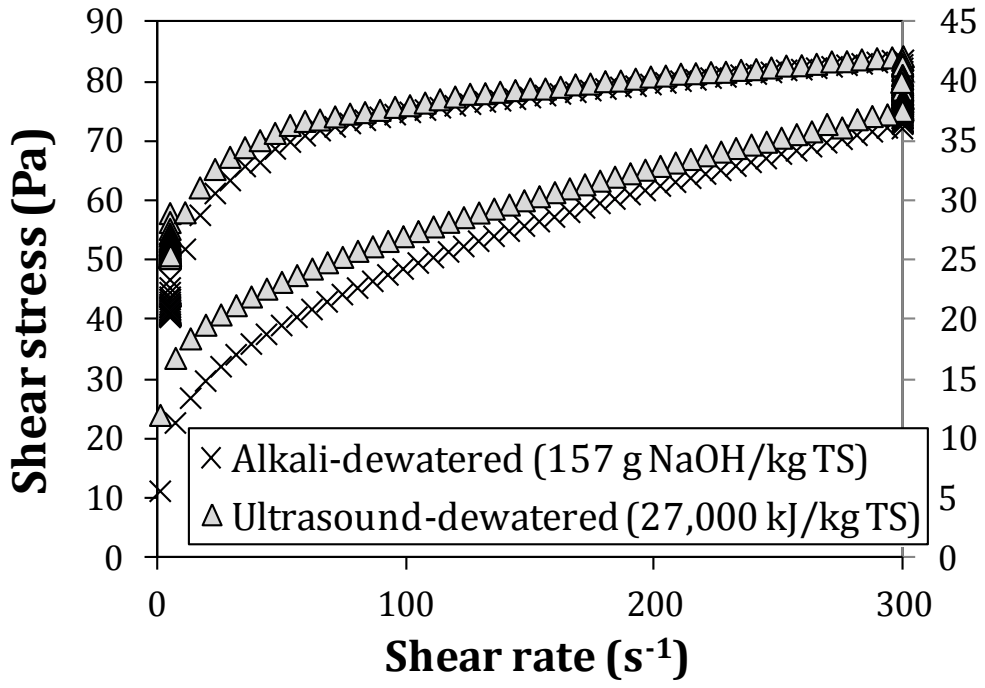

Figure 7.23. Comparison of the loops of the alkali-dewatered (primary y-axis) and ultrasound-dewatered (secondary y-axis) sludges.

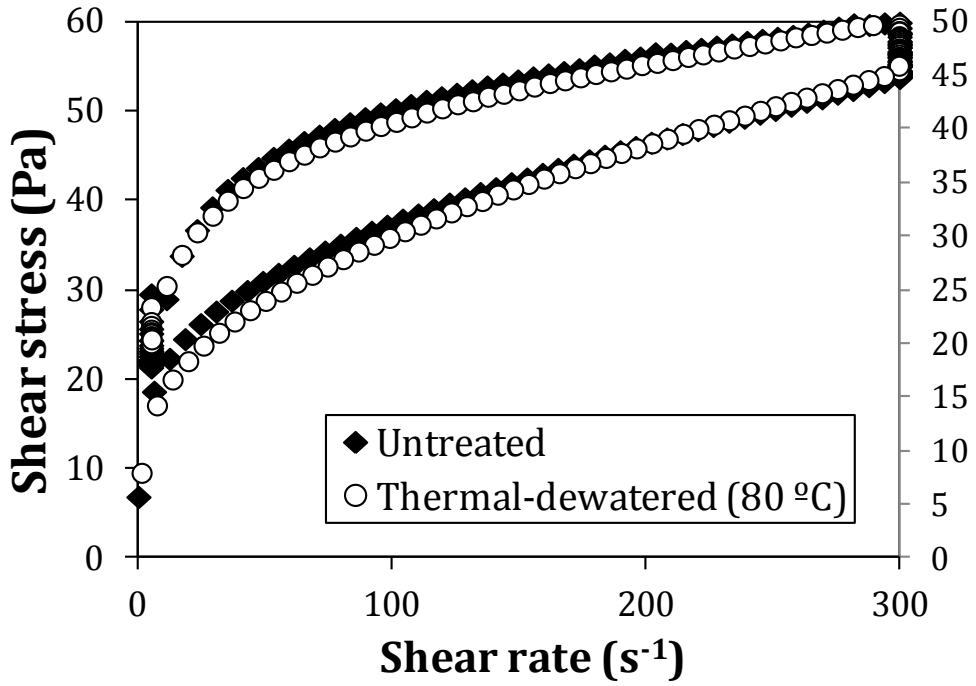

Figure 7.24. Comparison of the loops of the untreated (primary y-axis) and thermal-dewatered (secondary y-axis) sludges.

Chapter 8 Effect of the treatments on WAS hygienisation and methane potential

8.1. Introduction

8.1.1. Evaluation of sludge hygienisation: the use of microbial indicators

8.1.1.1. Land application of biosolids

Land application of biosolids is considered as a way of maintaining or restoring the quality of soils because of the fertilising or improving properties of the organic matter contained in these materials (Lepeuple et al., 2004). The term biosolid refers to the sewage sludge that has been carefully treated and monitored to be used in accordance with regulatory requirements. As already mentioned in Chapter 1, although untreated sewage sludge has beneficial plant nutrients and soil conditioning properties, it may also contain pathogenic microorganisms that can cause disease. Accordingly, an inadequate application of sludge to the land could potentially lead to the contamination of surface water, groundwater, soil and even the food chain. Therefore, the hygienisation of the sludge is of uttermost importance.

8.1.1.2. Pathogens in sludge

In sludge, the most part of pathogens comes from human populations, companion animals and livestock. The main classes of pathogens found in sludge are bacteria, viruses, yeast, fungi and parasites (in this class, two groups can be distinguished: protozoa and helminths). Pathogens can be found directly under infectious form, such as bacteria or virus, but also under a resistance form (spores for bacteria or cysts and eggs for parasites), which will become pathogenic inside human (Lepeuple et al., 2004). Table 8.1 summarises the typical concentrations of microorganisms in untreated sewage sludge.

Table 8.1. Typical concentrations of microorganisms (wet weight) in untreated sewage sludge (EC, 2001).

Type of microorganisms		**Concentration (wet weight)**
Bacteria	*Escherichia coli*	10^6/g
	Salmonella	10^2-10^3/g
Viruses	Enterovirus	10^2-10^4/g
Protozoa	*Giardia*	10^2-10^3/g
Helminths	*Ascaris*	10^2-10^3/g
	Toxacara	10-10^2/g
	Taenia	5/g

The conventional sludge treatment processes are designed to achieve certain reduction in the numbers of infectious microorganisms depending upon intended uses of biosolids in order to safeguard public health. However, a complete sterilisation is difficult to achieve. Most bacteria are inactivated at temperatures in excess of 70 ºC over a relatively short period of time. Lower temperatures over longer time periods are equally effective. However, some that produce spores, e.g., *Clostridium* spp., require higher temperatures for complete kill (EC, 2001). Another factor influencing the survival of pathogens is the pH; survival times are generally shorter at low (<4) or high (>10) pH values.

8.1.1.3. Legal regulation

As explained in Chapter 1, the European directive that is currently in effect concerning the application of sludge in agriculture (Directive 86/278/EEC) does not require the hygienisation of the sludge. However, this directive is currently under revision. The DG Environment has elaborated a working document on sludge (3rd official draft) (Environment DG, EU, 2000) that proposed more restricted parameters for land application of sludge, such as lower limit values for heavy metals (Annex I) and limit values for pathogens. Specifically, this document restricts the concentrations of *E. coli* in <500 CFU[6]/g wet weight (ww). Nevertheless, this document is not a legal text and should only be used for consultation purposes.

The United States have stricter standards for the application of sludge in land and currently take into account microbiological parameters in their legal regulation. For example, the United States Environmental Protection Agency (EPA) restricts the faecal coliform bacteria levels in <1000 MPN[7]/g dry weight (dw, which is equivalent to TS) for class A biosolids[8] (US Environmental Protection Agency, 2003).

8.1.1.4. Conventional and new bacterial indicators

It is not possible monitoring all the microorganisms present in sludge because of their high number and because there are not always specific techniques for their quantification or identification (Lepeuple et al., 2004). It is therefore necessary to define specific microorganisms (known as indicator organisms or surrogates for a pathogen) for the evaluation of the efficiency of the different treatments in terms of microbiological quality. An indicator organism should ideally (1) be consistently present in the raw sludge in large numbers, (2) be not less resistant to the lethal aspects of the sludge treatment processes, but also not be significantly more resistant than the pathogens for

[6] CFU stands for colony-forming unit and is a rough estimate of the number of viable bacteria cells in a simple.

[7] MPN stands for most probable number and is a way of statistically enumerating organisms.

[8] Class A biosolids contain no detectible levels of pathogens.

which it is being used to monitor, and (3) be relatively easy to cultivate, and preferably have characteristics that make it easy to identify and confirm (EC, 2001).

In most of the European countries, the selected microbial indicators are the following: Coliforms, *E. coli, Salmonella, Enterococcus, Enterobacteria* and *Clostridium*. However, it has been reported that conventional bacterial indicators may not provide a precise indication of the fate of viruses and protozoa during sludge treatments because such pathogens survive the environmental stresses more successfully than the conventional indicators (Lucena et al., 1988; Payment and Franco, 1993). Therefore, the availability of new microorganisms able to overcome the limitations of conventional indicators is of major importance. Spores of sulfite-reducing clostridia (SSRC) have been proposed as alternative indicators of protozoan oocysts in water treatment (Payment and Franco, 1993) while bacteriophages of enteric bacteria (as somatic coliphages; SOMCPH) have been proposed as surrogates of waterborne viruses in water quality control processes (IAWPRC, 1991).

8.1.2. Anaerobic digestion process

8.1.2.1. Basic principles of anaerobic digestion

Anaerobic digestion (AD) is a biochemical process which, in the absence of oxygen, decomposes biodegradable organic matter into biogas (mainly methane and carbon dioxide) and a digestate (a mixture of partially degraded organic matter, anaerobic biomass and inorganic matter) (Ferreira, 2013). The conversion of the organic matter into biogas is a process which involves several serie-parallel reactions and different groups of microorganisms. The AD process has been classified in four steps: hydrolysis, acidogenesis, acetogenesis and methanogenesis (Figure 8.1).

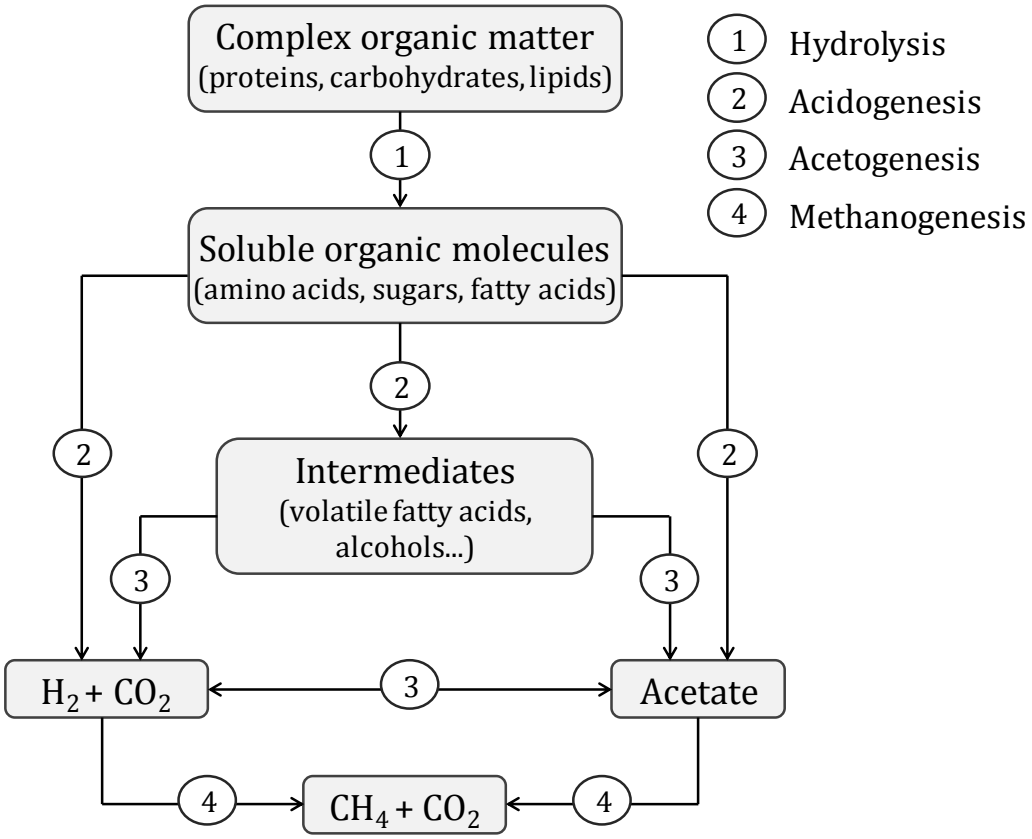

Figure 8.1. Simplified scheme of the anaerobic degradation pathway (adapted from Chen et al., 2014).

- *Hydrolysis*. During hydrolysis, a consortia of bacteria break down the complex organic matter (i.e., proteins, carbohydrates and lipids) from the influent into soluble monomers such as amino acids, simple sugars and fatty acids. Hydrolysis of these complex polymers, some of which are insoluble, is catalyzed by extracellular enzymes such as cellulases, proteases, and lipases (Chen et al., 2014). Many studies have concluded, due to the large fraction of organic matter that must be solubilised before its methanisation, that the hydrolysis step is the rate-limiting step of solid and semisolid wastes (Astals, 2013).
- *Acidogenesis.* Acidogenesis, also known as fermentation, is carried out by a large group of facultative fermentative bacteria. In this stage, the soluble compounds obtained from the hydrolysis step are able to be transported inside the bacteria and then converted to volatile fatty acids (i.e., acetate,

propionate, butyrate, valerate), alcohols and ketones, carbon dioxide, and hydrogen. The main product of all acidogenesis reactions is acetate.

- *Acetogenesis*. Acetogenic bacteria convert the volatile fatty acids (excluding acetate) and other products from the acidogenesis stage into acetate, hydrogen, and carbon dioxide, which are used by the methanogenic biomass. It is well known that acetogenesis reactions are only thermodynamically possible when the hydrogen concentration in the digester medium is low.
- *Methanogenesis*. The last stage of the AD process is carried out by methanogenic microorganisms, which convert the end products of the previous reactions into methane and carbon dioxide (biogas).

Within the anaerobic environment, various important parameters affect the rates of the different steps of the digestion process, i.e., pH, temperature and retention times. Regarding the pH, each group of microorganisms has a different optimum pH range. Specifically, methanogenic bacteria are extremely sensitive to pH with an optimum between 6.5 and 7.2 (Appels et al., 2008). Regarding the temperature, AD can take place between 10 and 65 °C, but most digesters are operated under two optimal ranges: mesophilic (around 35°C) or thermophilic (around 55°C) conditions. Although an increasing temperature (thermophilic conditions) has several benefits (such as the increasing solubility of the organic compounds and the increasing death rate of pathogens), it also has counteracting effects: there will be an increase of the fraction of free ammonia, which plays an inhibiting role for the microorganisms. At present, most digesters operate at mesophilic conditions because of the higher process stability and the lower energy requirements. Finally, the steps of the digestion process are directly related to the solid retention time (SRT), which is the average time the microorganisms spend in the digester. A decrease in the SRT decreases the extent of the reactions and vice versa (Appels et al., 2008).

8.1.2.2. Anaerobic digestion of WAS

AD has been used to stabilise the sewage sludge produced by WWTPs and, eventually, to eliminate pathogens for more than a century (Astals et al., 2012b). However, the application of AD to sludge is often limited by very long retention times (20–30 days) and a low overall degradation efficiency of the organic dry solids (30–50%). Those limiting factors are generally associated with the hydrolysis stage. During hydrolysis, cell walls are ruptured and EPSs are degraded, resulting in the release of readily available organic material for the acidogenic microorganisms (Appels et al., 2008).

Mesophilic anaerobic digestion of sewage sludge (the term "sewage sludge" should be understood as a mixture of primary sludge and WAS) is a commercial reality, due to the high biodegradability of primary sludge. However, WAS, which is primarily formed by microorganisms, is more difficult to degrade through AD due to the glycan strands present in the microbial cell walls (Appels et al., 2008). Accordingly, numerous disintegration methods (e.g., thermal hydrolysis) have been employed for pre-treatment under the assumption that these methods are capable of disrupting cell walls and therefore to release the intracellular organic material into the liquid phase (Appels et al., 2008; Farno et al., 2014). In this context, slowly degradable, particulate organic material is converted to low molecular weight, readily biodegradable compounds, thus bypassing the rate-limiting hydrolysis stage.

The aim of this chapter is to compare the effect of ultrasound, low-temperature thermal and alkali pre-treatments on WAS hygienisation and methane potential. The hygienisation was evaluated before and after digestion. Moreover, the economic feasibility of each treatment has been conducted and the various scenarios for sludge management have been discussed.

8.2. Materials and methods

8.2.1. WAS and inoculum origin

As specified in the general materials and methods (Chapter 4), the WAS samples were collected from the Baix Llobregat WWTP. The samples were collected weekly to guarantee the reliability of the microbiological tests.

The digested sludge sample used as inoculum to conduct the biomethane potential tests was obtained from Gavà-Viladecans WWTP (Barcelona, Spain). This WWTP can treat 64,000 m^3/day, which is equivalent to the use of water of more than 375,000 inhabitants (http://www.aiguesdebarcelona.cat/). Experimentally, it was observed that the digested sludge collected from the Baix Llobregat WWTP exhibited a lower concentration of microbial indicators and therefore a lower concentration of bacteria responsible of methanogenesis in comparison with the digested sludge collected from the Gavà-Viladecans WWTP (Table 8.2). Thus, the digested sludge used as inoculum to conduct the biomethane potential tests was obtained from Gavà-Viladecans WWTP, which exhibited a higher concentration of these organisms. The sludge samples were stored below 4 ºC until their utilisation.

Table 8.2. Levels of *E. coli*, somatic coliphages (SOMCPH) and spores of sulfite-reducing clostridia (SSRC) in digested sludges.

Inoculum (digested sludge) origin	***E. coli*** **(log_{10} CFU/g TS)**	**SOMCPH (log_{10} PFU/g TS)**	**SSRC (log_{10} CFU/g TS)**
Baix Llobregat	3.49	5.73	5.89
Gavà-Viladecans	4.84	6.77	6.63

CFU: colony-forming unit; PFU: plaque-forming unit

8.2.2. Treatment conditions

The low-temperature thermal treatment conducted in this chapter is different to that specified in the general materials and methods (Chapter 4). Specifically, the thermal treatment was performed in a heating bath (Huber Polystat CC2) at two fixed temperatures, 70 and 80 ºC. The exposure times were 10, 20 and 30 min at 70 ºC, and 10, 15 and 30 min at 80 ºC. The time required to reach both temperatures were 10 min and was included in the exposure time, i.e., the exposure time of 15 min corresponds to 10 min heating ramp up + 5 min heating at 80 ºC. For the temperature of 80 º and considering a sludge TS content of 57.9±0.4 g/L, the E_S applied were: 4400, 4500 and 4600 kJ/kg TS. As can be appreciated, these E_S are well below the E_S applied for the thermal treatment described in Chapter 4 (Table 4.4). The ultrasound and alkali treatments are the same as those specified in Chapter 4.

The effect of the optimum condition of each treatment on WAS solubilisation was determined by: (i) the soluble chemical oxygen demand (sCOD) to total chemical oxygen demand (tCOD) percentage ratio (sCOD/tCOD×100) and (ii) the COD solubilisation degree (SD) (Equation 8.1; Table 8.3).

$$SD\ (\%) = \frac{sCOD_f - sCOD_0}{tCOD_0 - sCOD_0} \cdot 100 \qquad (8.1)$$

where $sCOD_f$ is the soluble COD after the treatment, $sCOD_0$ is the soluble COD before the treatment and $tCOD_0$ is the total COD before the treatment.

8.2.3. Microbiological tests

The occurrence and levels of two bacterial indicators (*E. coli* and SSRC) and one viral indicator (SOMCPH) were controlled in this research, by evaluating their indigenous populations in the sludge during the different treatment processes.

8.2.3.1. Bacterial enumeration

5 to 10 g of sludge were mixed in a 1:10 (w/v) ratio with phosphate buffered saline (PBS) solution at pH 7.2, homogenised with a wrist action shaker at 900 osc/min for 30 min at room temperature and centrifuged at 300 x *g* for 3 min at 4 ºC. The resulting supernatant was utilised for analyzing both the *E. coli* and the SSRC present in the sample. For this purpose, serial dilutions were made.

E. coli was tested by the pour plate procedure on Chromocult agar (Merck, Germany) supplemented with *E. coli*/coliforms-Selective Supplement (Merck, Germany). Plates were incubated at 44 ºC overnight (O/N), and dark-blue/purple *E. coli* colonies were counted.

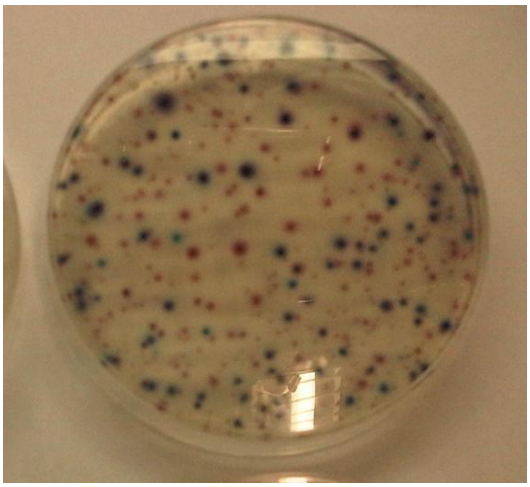

Figure 8.2. The dark-blue/purple colonies correspond to *E. coli*. The remaining colonies correspond to other coliform.

For the SSRC present in the sample, the supernatant and dilutions were subjected to a thermal shock of 80 ºC for 10 min. Then, the samples were anaerobically cultured by mass inoculation in Clostridium perfringens selective agar (Scharlab, Spain) and finally incubated at 44 ºC O/N. The typical black spherical colonies with black halos were counted as SSRC. The analyses were performed in duplicate.

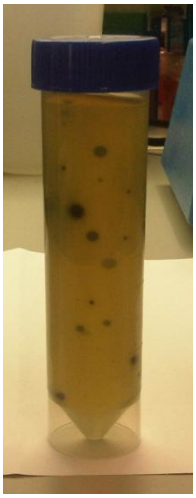

Figure 8.3. The black spherical colonies with black halos correspond to spores of sulfite-reducing clostridia (SSRC).

8.2.3.2. Bacteriophages enumeration

SOMCPH were extracted from sludge as described by Guzmán et al. (2007). Briefly, 5 to 10 g of the sludge sample was mixed in a 1:10 (w/v) ratio with a solution (pH 7.2) containing 10% beef extract powder (Becton Dickinson, France) and homogenised with a wrist action shaker at 900 osc/min for 30 min at room temperature. Next, the sample was centrifuged at 4,000 x *g* for 30 min at 4 ºC. The supernatant was filtered through a 0.22 µm pore size polyethersulfone non-protein binding membrane filter (Millipore, USA). The permeate was analyzed for the presence of SOMCPH as indicated in the ISO 10705-2 standard (Anonymous, 2000). The analyses were performed in duplicate.

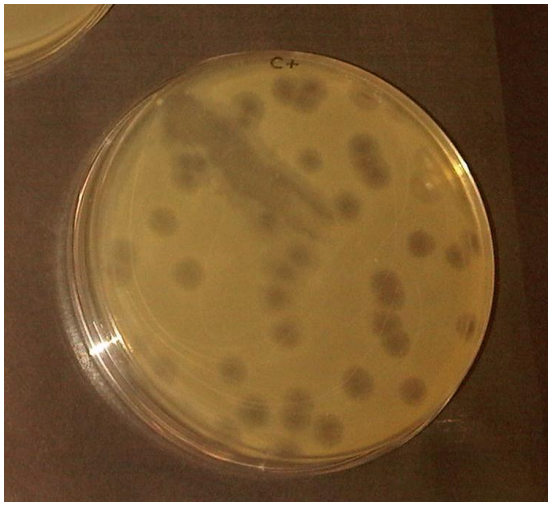

Figure 8.4. The somatic coliphages (SOMCPH) appears as a clear halo around the spot in the surrounding *E. coli* lawn.

8.2.4. Biomethane potential test

Biomethane potential (BMP) tests were carried out at mesophilic temperature conditions following the stages defined by Angelidaki et al. (2009). The BMP tests were performed in 115 mL serum bottles, closed with a PTFE/butyl septum, which was fixed by an aluminium crimp cap. The bottles were filled in with 60 mL of inoculum and 13 mL of WAS sample (untreated or treated), which met an inoculum to substrate ratio of 2 in VS-basis considering the untreated WAS VS value. A control blank with only inoculum was measured to determine the background effect of the inoculum. Before sealing the bottles, all digesters were flushed with nitrogen for one minute (3 L/min). Finally, digesters were placed in a water bath at 37 ± 1 ºC. The bottles were manually mixed by swirling twice daily. All samples were tested in triplicate.

The biogas production during the running test was measured by using a vacuumeter (Ebro – VAM 320) after discarding the overpressure generated during the first hour. The methane content of the biogas accumulated in the bottle headspace was analyzed at each sampling event by a Shimadzu GC-2010+ gas chromatograph equipped with a capillary column (Carboxen®-1010 PLOT) and a thermal conductivity detector. Finally, methane production over time was obtained by multiplying the biogas production,

subtracting the vapor pressure and converted to standard temperature and pressure conditions (i.e., converted to 0 ºC and 1 atm) by the percentage of methane in the biogas.

8.2.4.1. Model implementation and data analysis

Mathematical analysis of the BMPs was based on the IWA Anaerobic Digestion Model No. 1 (ADM1; Batstone et al., 2002). WAS degradation was modeled using first-order kinetics because the hydrolysis step is considered the rate-limiting step during WAS degradation (Appels et al., 2008) (Equation 8.2).

$$r_{WAS} = f_{WAS} \cdot k_{hyd,WAS} \cdot X_{WAS} \quad (8.2)$$

where r_{WAS} is the hydrolysis process rate (mL CH_4/L·day), f_{WAS} is the substrate biodegradability (-), $k_{hyd,WAS}$ is the first order hydrolysis rate constant of the WAS (day^{-1}), and X_{WAS} is the WAS concentration (g COD/L).

The model was implemented in Aquasim 2.1d. Parameter estimation and uncertainty analysis were simultaneously estimated, with a 95% confidence limit, as was the case for Batstone et al. (2003 and 2009). Uncertainty parameters (f_{WAS} and $k_{hyd,WAS}$) were estimated based on a one-tailed t-test with standard error around the optimum, and non-linear confidence regions were also tested to confirm that the linear estimate was representative of true confidence (Jensen et al., 2011). The objective function was the sum of squared errors (χ^2) of averaged data from triplicate experiments.

8.3. Results and discussion

8.3.1. Effect of the treatments on microbial indicators levels

Different microbiological results were obtained with the three treatments conducted (Figures 8.5, 8.6, and 8.7). For the ultrasound, small changes in the levels of microbial indicators were found, even at the highest E_S applied (27,000 kJ/kg TS) (Figure 8.5). Thus, the ultrasonication conditions tested in this research were not effective enough to achieve hygienisation. Because the effect of temperature was nullified by the ice bath, the disinfection mechanism was exclusively related to cell wall disruption due to cavitation, a phenomenon that is influenced by several factors (Pilli et al., 2011). According to Foladori et al. (2007) and Cui et al. (2011), ultrasonication appeared to have two effects: a first step, in which the sludge flocs were dissipated, and the microbial cells attached to the solids were released; and a second step, in which the walls of the exposed cells were disrupted. Thus, it is conceivable that the specific energies applied were effective enough to dissipate sludge flocs but not for killing bacteria and spores or for inactivating bacteriophages. However, to confirm this, more research is required.

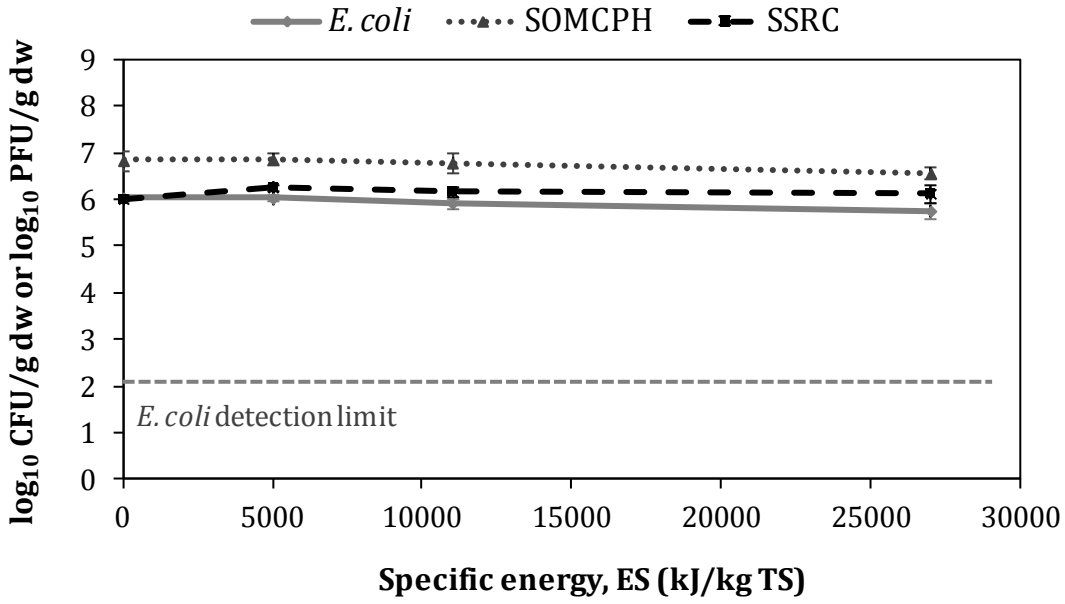

Figure 8.5. Effect of the ultrasound treatment on indicator populations (*E. coli*, SOMCPH and SSRC). Error bars represent standard deviations.

For thermal treatments, better results were obtained at 80 ºC (Figure 8.6b) compared with 70 ºC (Figure 8.6a). At 80 ºC, the three microbial indicators behaved differently: there was a slight reduction for SSRC (0.84 $\log_{10}$ of reduction), approximately 5 $\log_{10}$ of reduction for SOMCPH and a very high grade of hygienisation for *E. coli* (> 4.01 $\log_{10}$ of reduction). In fact, after 15 min, the *E. coli* population significantly dropped below the detection limit of the technique (2.02 $\log_{10}$ CFU/g dw or 4.00 CFU/g ww), satisfying normal levels accepted by the EPA (US Environmental Protection Agency, 2003) and the 3rd official draft from the EU (Environment DG, EU, 2000) for land application of the biosolids. These behaviours are similar to those described by Mocé-Llivina et al. (2003), showing a great sensitivity of *E. coli*, a moderate sensitivity of SOMCPH and a good resistance of SSRC toward thermal treatment. In this context, the use of the three microbial indicators may offer a complete interpretation of the effect of thermal treatments on the microbial population of the WAS.

A

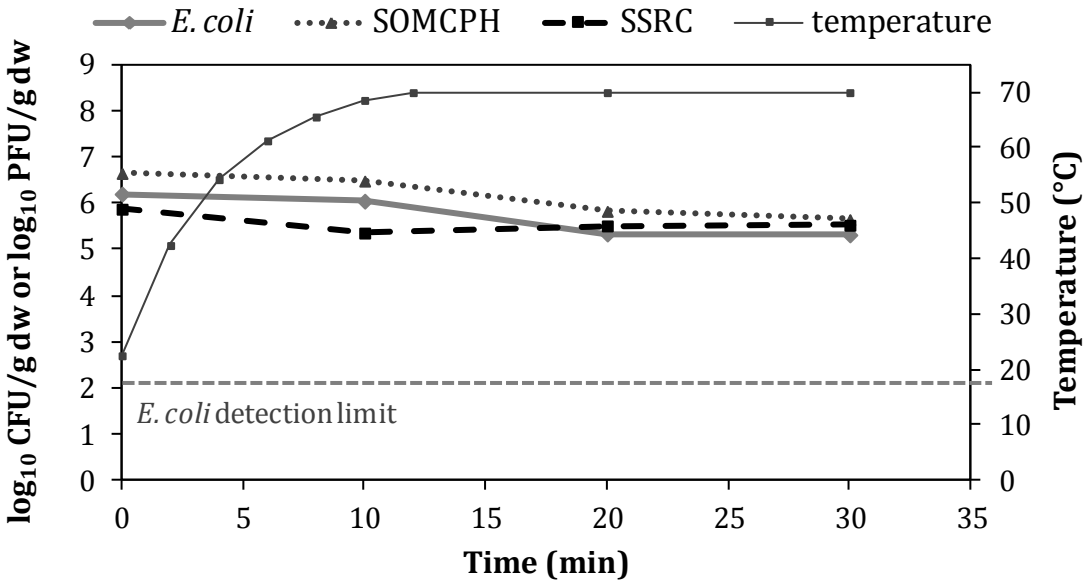

B

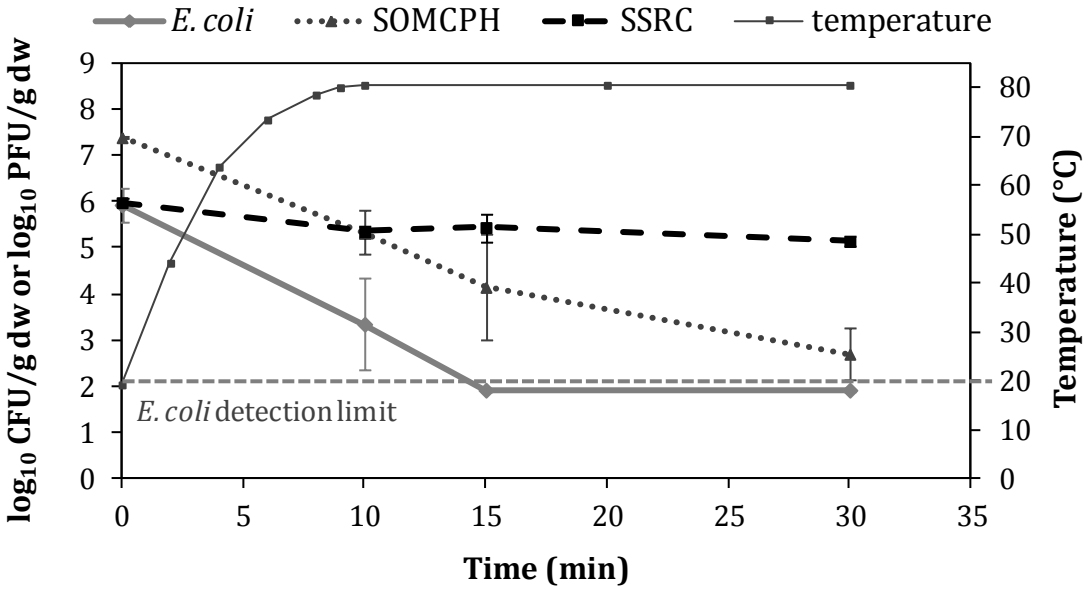

Figure 8.6. Effect of the low-temperature thermal treatment at (A) 70 ºC and (B) 80 ºC on indicator populations (*E. coli*, SOMCPH and SSRC). Error bars represent standard deviations.

For alkali treatment, the disinfecting effect of high pH was previously confirmed (Allievi et al. 1994; Bujoczek et al. 2002). In the present work, a similar pattern of inactivation in the three indicators was found after alkali treatment (Figure 8.7). The highest concentration of NaOH (157 g/kg TS) exhibited an extreme pH (approximately 12) during the 24 h treatment and was lethal for all three microorganisms. Therefore, the required hygienisation levels for *E. coli* were accomplished, with a value of 3.20 $\log_{10}$ CFU/g dw (95.6 CFU/g ww) for a reduction of 2.57 $\log_{10}$. Likewise, SOMCPH and SSRC levels were reduced by 2.79 and 1.72 $\log_{10}$, respectively. Unexpectedly, increases in SSRC and *E. coli* levels (1.04 $\log_{10}$ and 0.87 $\log_{10}$, respectively) were observed with the application of 35.3 g NaOH/kg TS. This reproducible result is not described in this thesis and is currently being investigated.

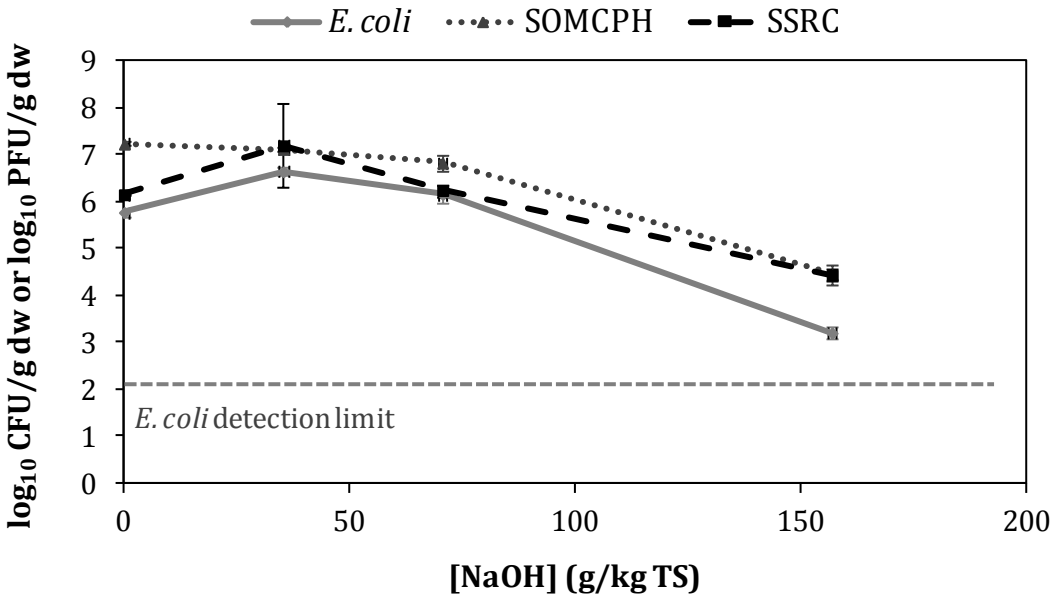

Figure 8.7. Effect of the alkali treatment on indicator populations (*E. coli*, SOMCPH and SSRC). Error bars represent standard deviations.

It is important to note that bacteria could experience multiple physiological states; this fact may prevent the measurement of actual concentrations. In contrast, viruses can only be infective or not infective, simplifying their use as indicators.

8.3.2. Effect of the treatments on anaerobic digestion

8.3.2.1. Selection of the optimum condition of each treatment

The biomethanisation studies were analysed at one condition of each treatment. These optimum conditions were selected based on the hygienisation and dewaterability (Chapter 7) of the sludge. Because no ultrasonication condition resulted in a noticeable reduction of microbial indicators (Figure 8.5), the optimum condition for this treatment responded exclusively to dewatering criteria. Accordingly, an optimum E_S of 27,000 kJ/kg TS was selected because it was the unique ultrasound condition that improved sludge dewatering (Figure 7.8). For alkali treatments, the optimum condition selected was 157 g NaOH/kg TS (252 meq/L; pH 12.4) because it allowed the hygienisation of the sludge (Figure 8.7) and noticeably improved sludge dewatering (Figure 7.10). As can be seen in Figure 8.8, the thermal treatments conducted in this chapter did not improve the sludge dewatering, possibly due to the shorter contact time. Thus, the optimum condition for the thermal treatment was 80 ºC for 15 min because it resulted in sludge hygienisation (Figure 8.6b).

The optimum conditions have been abbreviated as US-WAS (ultrasonicated WAS), T-WAS (low-temperature thermally treated WAS) and NaOH-WAS (alkali-treated WAS).

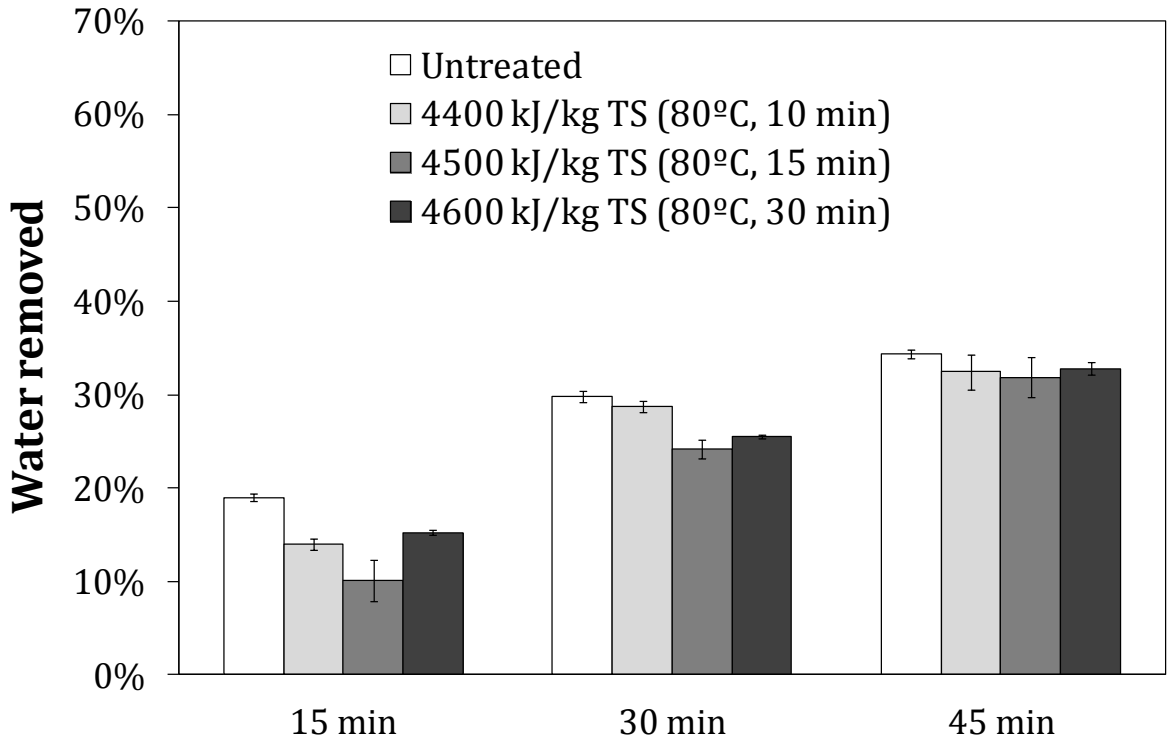

Figure 8.8. Water removed from the thermally treated sludges (treatment in a heating bath) after centrifugation at 2500 x *g* for 15, 30 and 45 min. The time of treatment include the heating ramp (10 min). Error bars represent confidence interval (95%).

8.3.2.2. Physicochemical characterisation

The previously determined optimum conditions were employed for pre-treatment before AD. The untreated and pre-treated sludges were analysed by physicochemical characterisation (Table 8.3). As shown by the sCOD/tCOD ratio and the SD (Equation 8.1), all pre-treatments were able to solubilise particulate organic matter from the WAS. Specifically, ultrasound and low-temperature thermal pre-treatments presented similar efficiencies (approximately 11%) which were lower than the efficiency obtained by the alkali pre-treatment (approximately 15%). Nevertheless, the alkali pre-treatment presented a loss of 5 g COD/L due to organic matter mineralisation, a phenomenon not detected in the ultrasound and low-temperature thermal pre-treatments. The SD obtained by ultrasound pre-treatment is lower than that reported by Bougrier et al.

(2006), who used a lower E_S (6,250 and 9,350 kJ/kg TS) and reached an SD of 15 ± 3%. The differences between the SD values may be related to the pre-treatment performance (e.g., no cooling during ultrasonication) and the sludge TS concentration (Carrère et al., 2010). Regarding the low-temperature thermal pre-treatment, the SD reached in the present study is lower than that reported by Kim et al. (2013a), likely due to the lower exposure time. The authors reported an SD of 23 and 27% when pre-treating WAS for 6 h at 60 and 75 ºC, respectively. The SD achieved through alkali pre-treatment was significantly lower than the values found in the literature, where an SD of approximately 30% was reported for WAS pre-treated with alkali at pH 12 and room temperature. Specifically, 1 h after dosing with 65 meq KOH/L (at a sample pH 12), Valo et al. (2004), recorded an SD of 31%. This value is similar to the result reported in Navia et al. (2002), in which an observed SD of 32% was obtained after dosing with 80 meq/L NaOH for 24 h (WAS from a kraft mill). Similarly, Jiang et al. (2010), evaluated the effect of the treatment time and pH on WAS solubilisation. At pH 12, the authors recorded increases of the SD of 21 and 33% after 0.5 h and 24 h, respectively, of pre-treatment time.

Table 8.3. Characterisation of the untreated and treated WAS. Errors represent standard deviations. Ultrasound pre-treatment: 27,000 kJ/kg TS; thermal pre-treatment: 80 ºC, 15 min; alkali pre-treatment: 157 g NaOH/kg TS.

	Units	**Untreated**	**US-WAS**	**T-WAS**	**NaOH-WAS**
			WAS characterisation		
TS[1]	g/L	64.2 ± 0.2	65.7 ± 0.1	64.6 ± 0.1	72.3 ± 0.1
VS[1]	g/L	52.9 ± 0.2	53.9 ± 0.1	53.0 ± 0.1	49.5 ± 0.2
tCOD	g O_2/L	80.9 ± 0.4	80.5 ± 0.3	81.6 ± 0.5	75.7± 0.4[2]
sCOD	g O_2/L	0.9 ± 0.1	10.3 ± 0.2	9.6 ± 0.2	12.1± 0.1[3]
pH	-	6.5 ± 0.1	6.4 ± 0.2	6.4 ± 0.2	7.5 ± 0.1
VFA	mg/L	223 ± 10	952 ± 16	293 ± 21	560 ± 18
Acetate	mg/L	165 ± 4	634 ± 5	249 ± 18	481 ± 14
Propionate	mg/L	22 ± 5	197 ± 9	25 ± 8	22 ± 3
Butyrate	mg/L	23 ± 1	53 ± 4	19 ± 2	31 ± 2
Valerate	mg/L	13 ± 1	68 ± 1	n.d.[4]	26 ± 2
			Pre-treatment solubilisation efficiency		
sCOD/tCOD	%	1.1 ± 0.1	12.8 ± 0.2	11.7 ± 0.2	16.0 ± 0.2
SD	%	-	11.8 ± 0.4	10.8 ± 0.6	14.0 ± 0.6

[1]The losses of VFA compounds during the solids determination were taken into account and combined to give the final TS and VS values (Astals et al., 2012b).

[2]Obtained by multiplying the VS by 1.53 g COD/g VS due to chloride interference in the COD analysis.

[3]Obtained after removing the chloride COD determined in tCOD analysis.

[4]n.d. non-detected (<10 mg/L).

8.3.2.3. Biomethane potential tests

Although the optimum pre-treatment conditions, in terms of methane production, may be those that present a high COD solubilisation and low organic matter mineralisation, increased solubilisation does not always lead to an enhanced methane potential (Kim et al., 2013b). Therefore, BMP tests are needed to assess the effect of the pre-treatments on AD (Figure 8.9a). Specifically, the effect of the pre-treatments on methane production was evaluated through the modeling of the BMP tests (Figure 8.9b). The 95% confidence region for biodegradability (x-axis) and apparent hydrolysis rate (y-axis) indicated that each pre-treatment had a different effect on WAS biodegradability. T-WAS (0.38 ± 0.1) presented similar biodegradability as WAS (0.37 ± 0.3), whereas US-WAS (0.42 ± 0.2) and NaOH-WAS (0.49 ± 0.1) presented increases of 13% and 34%, respectively, on WAS biodegradability and their final methane potential. The low increase of WAS biodegradability after pre-treatment, when compared with the literature, may be related to the selection of the pre-treatment conditions. In the present study, the strength and exposure time of each pre-treatment was based on dewatering and hygienisation criteria, rather than on the increase of the methane yield. For instance, through low-temperature thermal pre-treatments (60-80 ºC), increases of the biogas production by 20-40% have been reported when pre-treating WAS over 0.5 to 1.5 h (Hiraoka et al., 1984; Li and Noike, 1992; Wang et al., 1997). Likewise, increases of the biogas production between 40 and 50% have been achieved through ultrasound pre-treatment, even though lower E_S (5,000-9,350 kJ/kg TS) were applied (Bougrier et al., 2006; Braguglia et al., 2008). This may be related to the TS concentration (64.2 ± 0.2 g/L) and viscosity of the WAS because increased viscosity (linked to a higher TS concentration) hinders the formation of cavitation bubbles (Carrère et al., 2010). Moreover, in the present study, the WAS sample was cooled down during ultrasonication, thereby avoiding the thermal effect. The literature is less consistent regarding the effect of alkali pre-treatment on the biogas potential at room temperature. Penaud et al. (1999) demonstrated an increase in biodegradability by approximately 40% after adding 125 meq NaOH/L. In contrast, Valo et al. (2004), reached a pH of 12 after adding 65 meq KOH/L, but did not observe any significant improvement on WAS biodegradability.

A

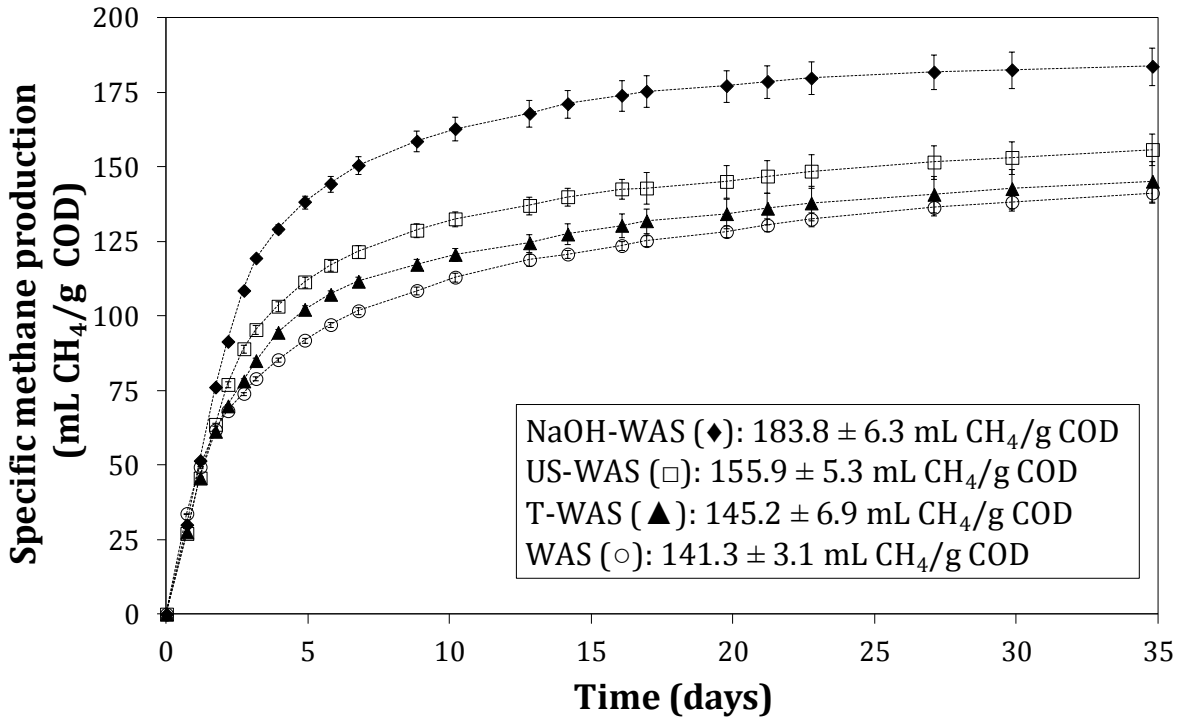

B

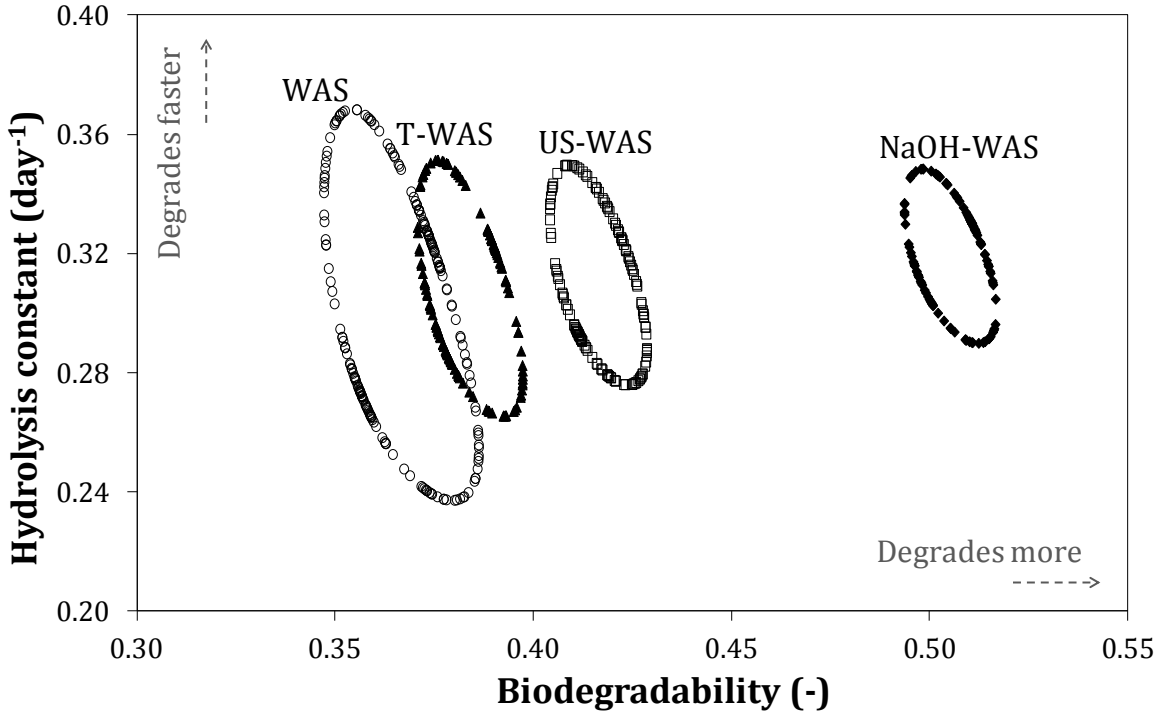

Figure 8.9. Results obtained from the BMP tests: (A) Cumulative methane production curves and (B) Confidence regions for biodegradability (f_{was}) and hydrolysis constant ($k_{hyd,\ was}$). Ultrasound pre-treatment: 27,000 kJ/kg TS; thermal pre-treatment: 80 ºC, 15 min; alkali pre-treatment: 157 g NaOH/kg TS. Error bars represent standard deviations.

Similar SDs, but different biodegradabilities, reached by T-WAS and US-WAS showed that some parts of the cell wall were weakened but not solubilised during the pre-treatments. However, because the pre-treatment conditions applied to the WAS did not affect the hydrolysis rate, it can be understood that most of the methane production still came from the particulate organic matter. Finally, a possible inhibitory effect due to a high sodium concentration (3.6 g Na^+/L) on NaOH-WAS digestion, which is reported within the moderate inhibition sodium concentrations for mesophilic methanogens (Chen et al., 2008), may had been masked by the dilution effect (approximately 1/4) of the inoculum.

8.3.3. Hygienisation effect of the mesophilic anaerobic digestion aided by pre- and post-treatments

Although AD has been designed for increasing biogas production and solids destruction, it also plays a role in pathogen inactivation (Ziemba and Peccia, 2011), and pre-treatment optimisation may help in this purpose. The occurrence of indicators after the BMP tests in the pre-treated sludges is shown in Figures 8.10, 8.11 and 8.12. It is worth remembering that, in order to perform the BMP tests, the untreated and the pre-treated WAS were mixed with digested sludge and therefore the microbiological tests were made on these mixtures. For *E. coli*, the reductions achieved by the entire processes (i.e., pre-treatments + mesophilic AD) provided results below the detection limit of the technique (< 2.02 $\log_{10}$ CFU/g dw or < 4.00 CFU/g ww), successfully overcoming the levels of hygienisation established by the EPA and EU. Specifically, for ultrasound pre-treatment, *E. coli* reduction was due to the single effect of the AD because this pre-treatment did not sanitise the sludge (relevant data corresponding to the single effect of AD are shown in Figure 8.13). For the SOMCPH, the three configurations generated similar results: 2.32, 2.45 and 2.47 $\log_{10}$ reductions for ultrasound, low-temperature thermal and alkali, respectively. Finally, as was observed in Section 8.3.1, unexpected results for SSRC were found after digestion of the ultrasonicated and alkali pre-treated sludge, resulting in an increase of 1.62 $\log_{10}$ and 1.80 $\log_{10}$, respectively (Figures 8.10 and 8.12). However, SSRC did not experience similar changes with the low-temperature

thermal pre-treatment. This increase in the SSRC concentration after AD is currently being investigated. From the three configurations studied in this section, the thermal pre-treatment followed by mesophilic AD seems to be the best option in terms of hygienisation.

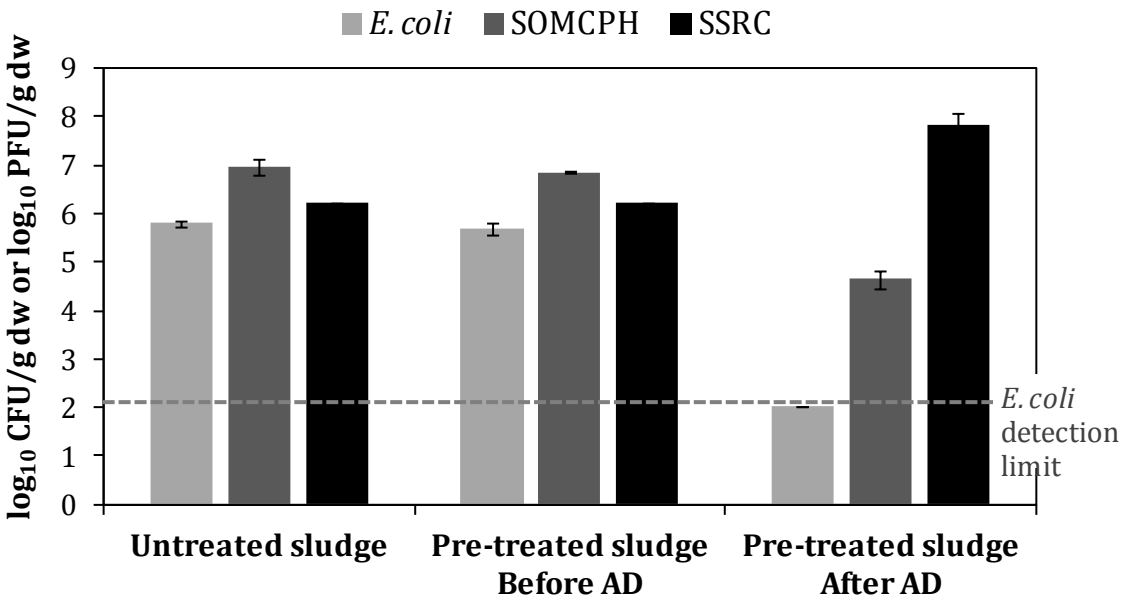

Figure 8.10. Effect of the ultrasound pre-treatment (27,000 kJ/kg TS) and the AD on the microbial populations present in sludge. Error bars represent standard deviations.

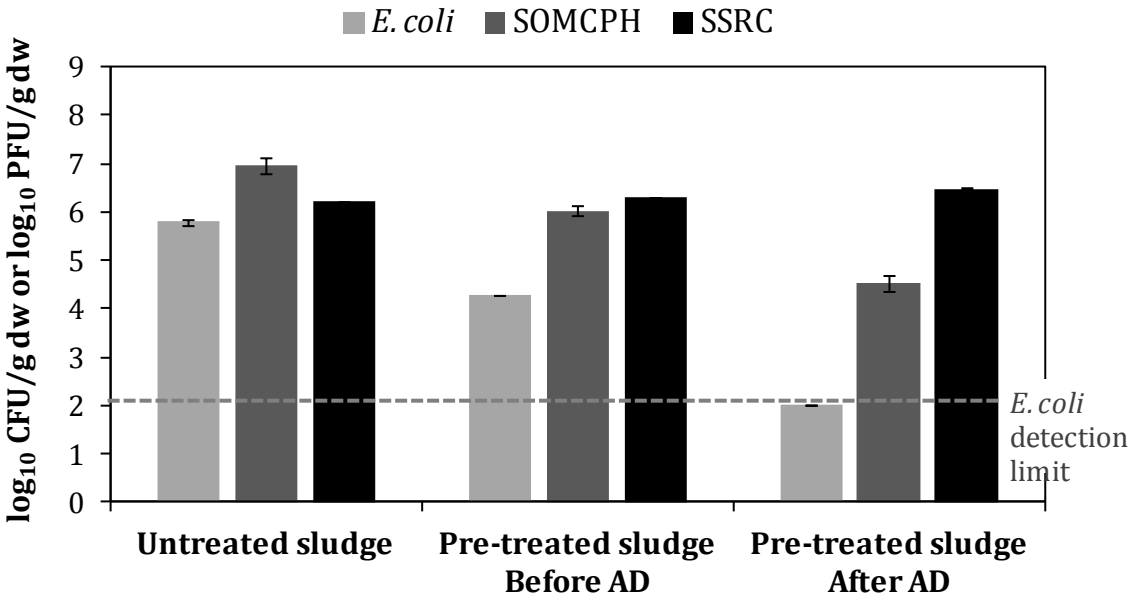

Figure 8.11. Effect of the low-temperature thermal pre-treatment (80 ºC, 15 min) and the AD on the microbial populations present in sludge. Error bars represent standard deviations.

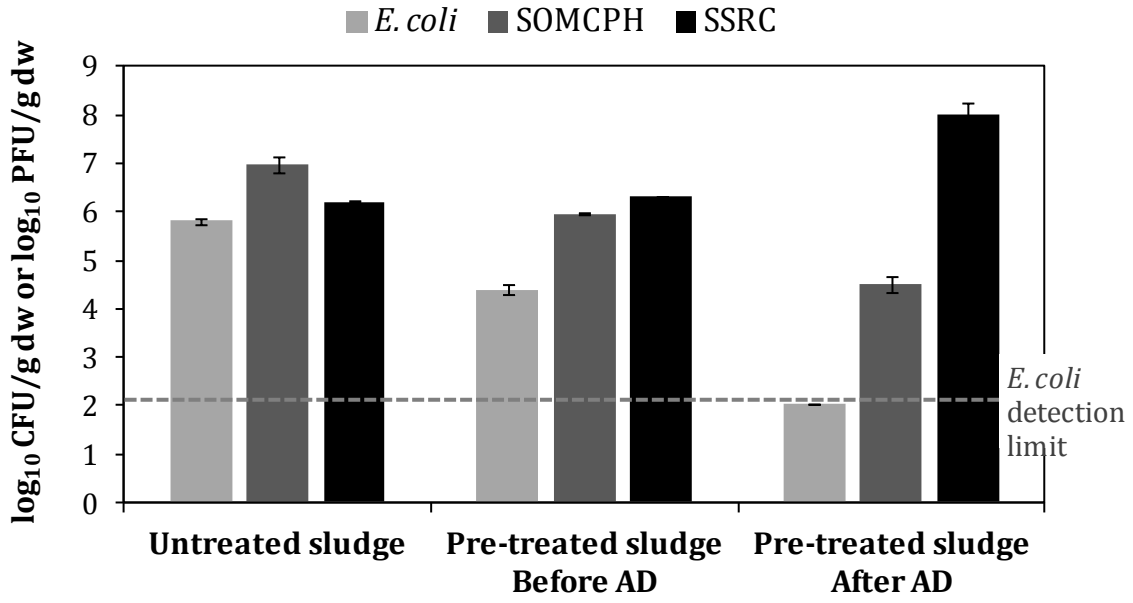

Figure 8.12. Effect of the alkali pre-treatment (157 g NaOH/kg TS) and the AD on the microbial populations present in sludge. Error bars represent standard deviations.

The effectiveness of post-treatments in the sanitation of digested sludge has been thoroughly studied in the literature (Allievi et al., 1994; Bujoczek et al., 2002; Astals et al., 2012b). The microbiological results for the three post-treatments applied after mesophilic AD are displayed in Figure 8.13.

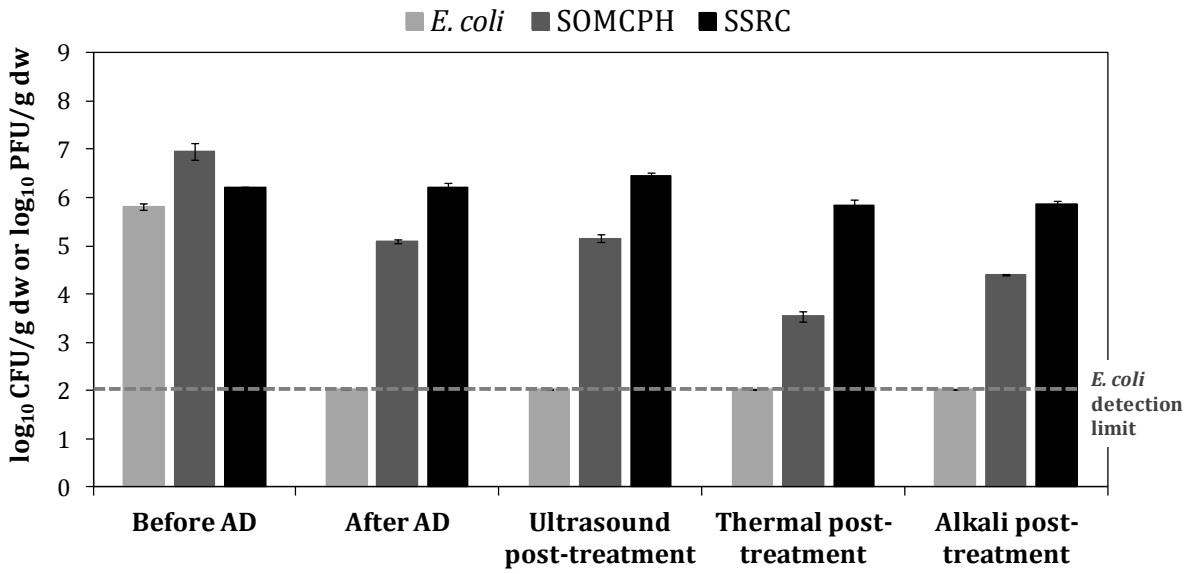

Figure 8.13. Effect of the anaerobic digestion and different post-treatments on the microbial populations present in sludge. Error bars represent standard deviations. Ultrasound post-treatment: 27,000 kJ/kg TS; thermal post-treatment: 80 ºC, 15 min; alkali post-treatment: 157 g NaOH/kg TS. Error bars represent standard deviations.

The digestion was sufficient to meet the *E. coli* requirements established by the normative, reaching reductions of more than 3.78 $\log_{10}$. These results were below the detection limit of the technique, making impossible to evaluate the *E. coli* reductions achieved by the assayed post-treatments. In contrast, the SSRC levels were not changed due to the mesophilic AD or post-treatments. A single mesophilic AD reduced SOMCPH levels by 1.88 $\log_{10}$, and the combination of AD followed by the low-temperature thermal and alkali post-treatments resulted in reductions of 3.42 $\log_{10}$ and 2.56 $\log_{10}$, respectively. However, no additional effect was observed with ultrasound post-treatment with respect to a single AD. Taking into account that *E. coli* levels decayed

below detection limits and that SSRC levels remained unchanged, the level of SOMCPH was the parameter that allowed the evaluation of the efficacy of post-treatments. As was the case for pre-treatments, the low-temperature thermal post-treatment seems to be the best option for hygienisation.

8.3.4. Assessment of the feasibility of the treatments in a WWTP

By considering an energy balance with the assessment of the different treatment scenarios an estimate can be made to determine whether the energy (i.e., electricity and heat) required by the pre-treatment can be recovered through the improved methane production. However, these estimates rely exclusively on laboratory data; therefore, the results would not be entirely conclusive for an operational WWTP. Moreover, it should be considered that the heat balance is highly influenced by the solid concentration; therefore, a concentrated WAS will lead to a better balance, while a diluted sludge will lead to a worse balance (Carrère et al., 2012). The assessment is based on a novel WWTP approach, where the primary sludge and WAS are digested separately to increase the opportunities to use digested WAS in agriculture.

Ultrasound treatment (27,000 kJ/kg TS) was able to solubilise organic matter and improve WAS specific methane production, but was not able to disinfect the WAS. Therefore, the most reasonable configuration for ultrasonication would be to use it as a pre-treatment prior to AD and composting or thermal post-treatment (if the digestate is intended for use as fertiliser). The electricity balance of the ultrasound pre-treatment shows that an increase in methane production (15 mL CH_4/g COD) results in an increased electrical production of 240 kJ/kg TS, which is very low when compared to the supplied energy (27,000 kJ/kg TS). Nevertheless, on an industrial scale, this difference would be lower due to the higher efficiency of commercial ultrasonic devices.

Low-temperature pre-treatments (< 100 ºC) are characterised by a low energy demand, which may be supplied by a combined heat and power (CHP) unit fueled with biogas (Passos et al., 2013). On the one hand, the heat required to increase the temperature of the WAS from 15 to 80 ºC were estimated to be 4600 kJ/kg TS, assuming a WAS specific heat of 4.18 kJ/kg/ºC, a density of 1000 kg/m^3, and 8% of the process

heat losses (Astals et al., 2012b). On the other hand, the heat produced by the CHP unit after burning the biogas was 3600 kJ/kg TS, which represents the energy required to increase the WAS temperature from 15 to approximately 65 ºC. The value was obtained assuming a 35,800 kJ/kg TS methane caloric value and a 0.55 CHP unit yield for heat generation (Astals et al., 2012b; Passos et al., 2013). However, if a 80 ºC pre-treatment is required, it would be necessary to install a sludge-to-sludge heat exchanger, where the pre-treatment effluent would be used to pre-heat WAS. The energy recovered in the sludge exchanger should be at least the 23% of the heat contained by the pre-treated WAS, which is below than the 80-85% efficiency reported for this type of unit (Astals et al., 2012b; Carrère et al., 2012). As shown in the BMP tests, the low-temperature thermal pre-treatment (80 ºC, 15 min) scarcely increased the biodegradability of the WAS, possibly due to the shorter contact time. It is likely that a longer exposure time would result in an increase of the methane production and induce an improvement of the energy balance (Li and Noike, 1992). Nonetheless, a higher capital cost would be required due to the larger digester volume. Additionally, both the thermal pre-treatment and the post-treatment were successful in reducing the microbiological parameters. However, the pre-treatment does not guarantee hygienisation after the AD. Therefore, the configuration for this treatment seems to depend on the final destination of the sludge: if the sludge is intended for agriculture, it should undergo post-treatment to satisfactorily meet the current microbiological levels for land application. If the sludge is not intended for agriculture, it may be appropriate to perform a pre-treatment (the effect of the exposure time should be further investigated) to enhance the AD.

Alkali conditioning (157 g NaOH/kg TS) has been successful in improving methane production, and has reduced the levels of *E. coli* below the limits established by the EPA and EU. However, as a pre-treatment, it unexpectedly increased the levels of SSRC after AD and required neutralisation prior to AD. In addition, it resulted in a negative economic balance. The selling price of industrial NaOH and HCl are highly variable, but average at 300 and 200 €/ton, respectively (Solvay, 2013). Consequently, dosing 157 g NaOH/kg TS and 218 g $HCl_{35\%}$/kg TS for their subsequent neutralisation requires 0.094 €/kg TS and 0.044 €/kg TS, respectively. The sum of the reagents cost (0.138 €/kg TS) was much larger that the incomes generated through the extra methane

production. Specifically, 43 mL CH_4/g COD will represent an extra electricity production of 680 kJ/kg TS that, at a tariff of 0.10 €/kWh, will lead to a revenue of 0.019 €/kg TS. Another drawback linked to alkali pre-treatment is the rising sodium concentration in the digester, which can drive the AD process to inhibition (Mouneimne et al., 2003; Carrère et al., 2012); therefore, the use of NaOH as a pre-treatment is rather limited.

In accordance with what has been discussed, the different scenarios for WAS treatment are outlined in Figure 8.14.

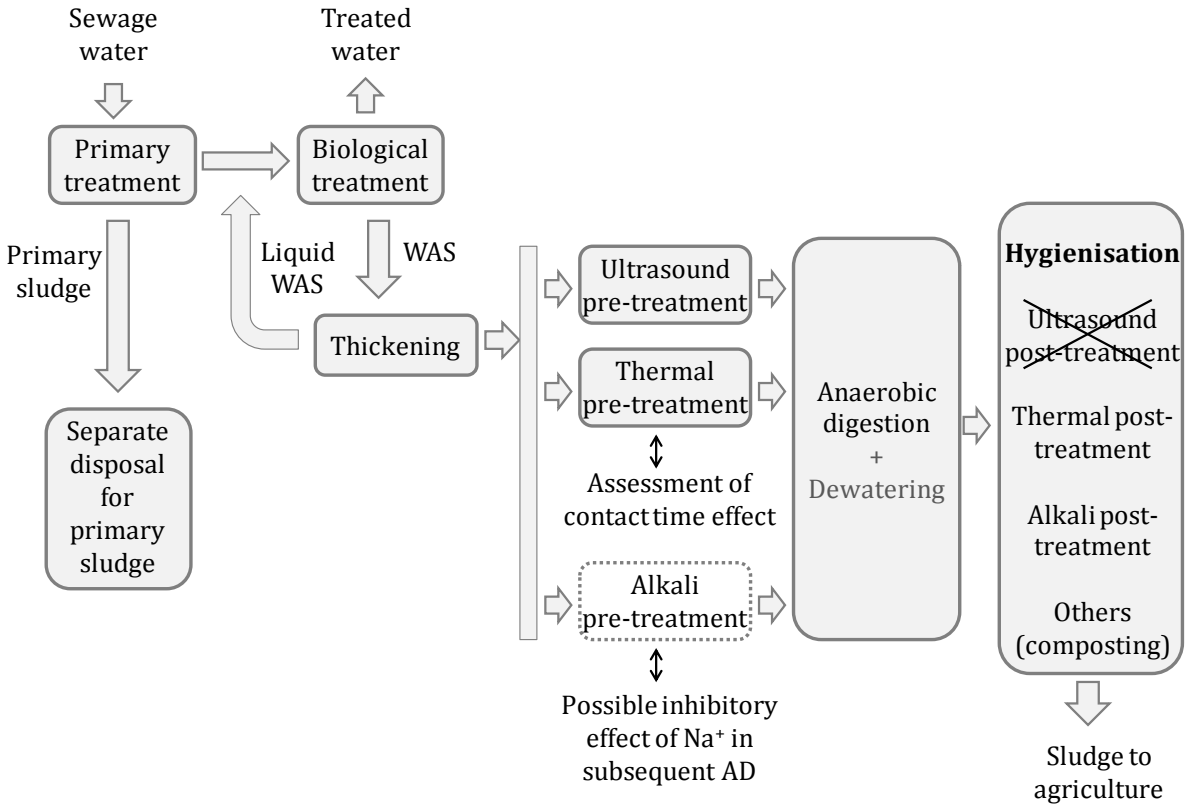

Figure 8.14. Possible scenarios for WAS management according to the treatments studied and with primary sludge and WAS digested separately. The alkali pre-treatment is shown with dashed line because the use of NaOH as a pre-treatment is rather limited.

Chapter 9 Conclusions and recommendations

9.1. Conclusions

The main conclusions obtained from this work are detailed below:

Conclusions regarding the rheological characterisation:

- Within the linear viscoelastic region, the rheological creep tests showed that the elasticity and zero shear rate viscosity were decreased with the three treatments, indicating a higher degree of disruption of the sludge structure.
- Under flow conditions, the untreated and treated sludge samples showed pseudoplastic and thixotropic behaviour, which were evidenced by the good fit of the experimental data to the Ostwald–de Waele model and the presence of the hysteresis area, respectively.
- The three treatments reduced the steady state viscosity and the hysteresis area of the sludge. This reduction was higher when increasing the intensity of the ultrasound and alkali treatments, whereas the reduction of both parameters after the thermal treatment was very similar between the different tested temperatures.

- The model used to evaluate the thixotropic behaviour of the WAS was based on the definition of the time dependence of a structural parameter and the instantaneous variations in the alignment and deformation of flocs. The kinetic coefficients for the breakdown and build-up processes showed dependence with the shear rate. Specifically, the kinetic coefficients for the breakdown process decreased when increasing both the treatment intensity and shear rate probably because the smaller flocs take longer to reach the equilibrium. Similarly, the *m* parameter, which represents the instantaneous alignment and deformation of structures when changing the shear rate, was decreased due to the reduction in size of structures.

Conclusions regarding the dewatering and EPSs solubilisation:

- The treatments changed the water distribution in sludge by releasing part of the interstitial water and slightly increasing the vicinal water.
- In spite of the increase of vicinal water content, the three conditions of the thermal treatment (60, 80 and 90 ºC; 1 h of treatment, including the heating time to reach the temperature) and the higher intensities of ultrasound (27,000 kJ/kg TS) and alkali (157 g NaOH/kg TS) treatments caused very significant dewatering by centrifugation. It is conceivable that part of the vicinal water was removed because it passed to the supernatant fraction together with colloidal and hydrophilic organic material.
- The treatments improved sludge dewatering by different mechanisms. The thermal treatment gradually increased the water removed by centrifugation, denatured the high-molecular-weight proteins acting as flocculants and reduced the CST at temperatures above 80 ºC. Conversely, the ultrasound and alkali treatments highly increased the CST. Moreover, although all the conditions tested for the ultrasound and alkali treatments were able to reduce the viscosity of the sludge, only the stronger conditions resulted in an improvement of the sludge dewatering.

- The untreated sludge contained a very low amount of EPSs in the form of LB-EPSs and a high amount of EPSs in the form of TB-EPSs. Proteins were the major constituent on EPSs, followed by humic acids and polysaccharides.
- The three treatments highly solubilised the EPSs, which was decisive for WAS dewatering. Specifically, the alkali treatment (157 g NaOH/kg TS) solubilised more EPSs than the ultrasound (27,000 kJ/kg TS) and thermal (80 ºC, 1 h) treatments and consequently was more efficient when removing water from the sludge. At the same time, this treatment produced the maximum increase in the zeta potential of the LB-EPS fraction.

Conclusions regarding the hygienisation and methane potential:

- SOMCPH was an appropriate microbial indicator for evaluating the different sludge treatments and would be a suitable candidate to complement *E. coli* measurements. The thermal treatment at 80 ºC and the alkali treatment at 157 g NaOH/kg TS allowed the hygienisation of the sludge, thus satisfying normal levels accepted by the EPA and the 3rd official draft from the EU. Conversely, the conditions tested for the ultrasound treatment barely reduced the levels of microbial indicators.
- The ultrasound treatment (27,000 kJ/kg TS) increased the sludge biodegradability and the specific methane production (13%), but did not succeed in hygienisation, suggesting that the most appropriate configuration for ultrasonication is as a pre-treatment before anaerobic digestion.
- The low-temperature thermal treatment (80 ºC; 15 min of treatment, including the heating ramp) barely increased the sludge biodegradability, but allowed hygienisation, which suggests that it would be more suitable as a post-treatment. However, the use of longer contact times would increase the chances for use as a pre-treatment.
- The alkali treatment (157 g NaOH/kg TS) increased the methane production (34%) and was successful in hygienisation. However, when used as a pre-treatment, it resulted in a high amount of sodium because of the high concentrations of NaOH required, which may inhibit anaerobic digestion.

- The energy balance revealed that under the tested conditions, the ultrasound and alkali treatments required higher operating costs.

9.2. Recommendations

For further investigation, the following recommendations are proposed:

- It would be interesting to further analyse the effect of the thermal treatment on protein denaturation. For this purpose, it would be worthwhile to continuously monitor the sludge viscosity when increasing the temperature in order to analyse the changes in the sludge internal structure.
- It would be interesting to conduct entire rheological oscillatory assays in order to offer a more complete rheological characterisation of the sludge.
- It would be interesting to evaluate the impact of the exposure time in the low-temperature thermal pre-treatment for anaerobic digestion in order to provide a more complete insight into the feasibility of the treatment.
- It would be interesting to complement the study on a pilot scale in order to provide a more realistic scenario for the treatments.
- It would be interesting to evaluate the effect of the treatments on sludge mixtures of primary sludge and WAS.

Annexes

Annex I: Limit values for concentrations of heavy metals in sludge for use on land. Values set by the Directive 86/278/EEC (CEC, 1986) and the 3rd official draft from the EU (Environment DG, EU, 2000).

Elements	**Limit values (mg/kg dry matter)**		**Limit values (mg/kg P)**
	Directive 86/278/EEC	3rd official draft	3rd official draft
Cd	20-40	10	250
Cr	-	1000	25,000
Cu	1000-1750	1000	25,000
Hg	16-25	10	250
Ni	300-400	300	7500
Pb	750-1200	750	18,750
Zn	2500-4000	2500	62,500

Annex II: Calculation of the specific energy supplied to the sludge after the low-temperature thermal treatment.

Heat required for heating the sludge (J):

$$Q_{heating} = m \cdot C_p \cdot (T - T_i) + S \cdot h \cdot (T - T_i) \cdot t_1$$

where m is the sludge sample mass, C_p is the specific heat of sludge at constant pressure (1 cal/g·K), T is the final temperature, T_i is the initial temperature, S is the surface of the tank containing the sample, h is the thermal transmittance (10 W/m²·K) and t_i is time of heating until the desired temperature.

Heat required for temperature maintenance (J):

$$Q_{maintenance} = S \cdot h \cdot (T - T_i) \cdot t_2$$

where t_2 is the time of temperature maintenance.

Total specific energy supplied (kJ/kg TS):

$$Q = \frac{Q_{heating} + Q_{maintenance}}{m \cdot \%_{TS}}$$

where $\%_{TS}$ is the percentage of the total solid content of the sludge sample.

Annex III: Molecular weight distributions of the (A) LB-EPS and (B) TB-EPS fractions for the untreated and treated sludges. The proteins are measured at 280 nm, without correcting the interference of nucleic acids.

Untreated sludge

A

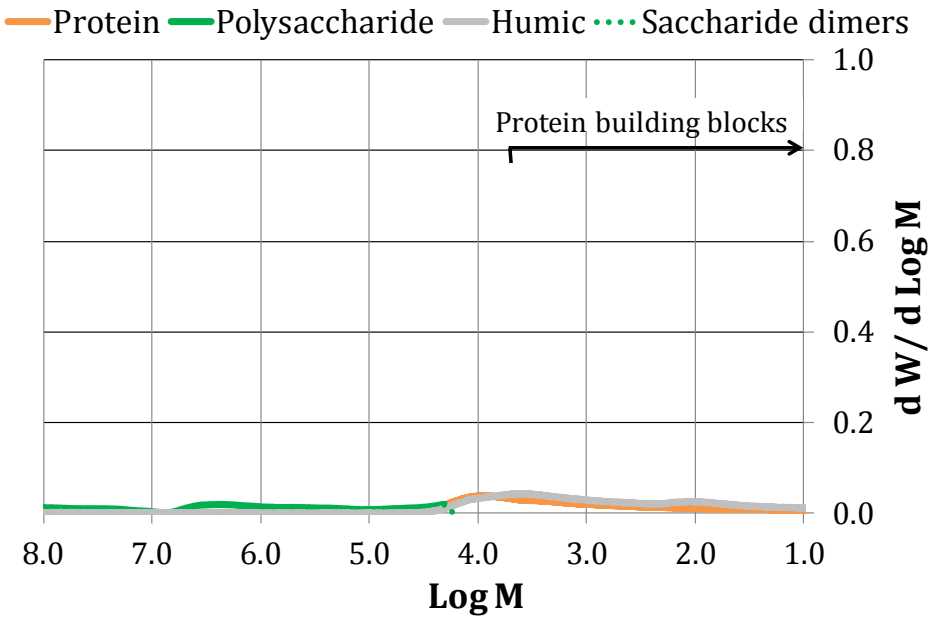

B

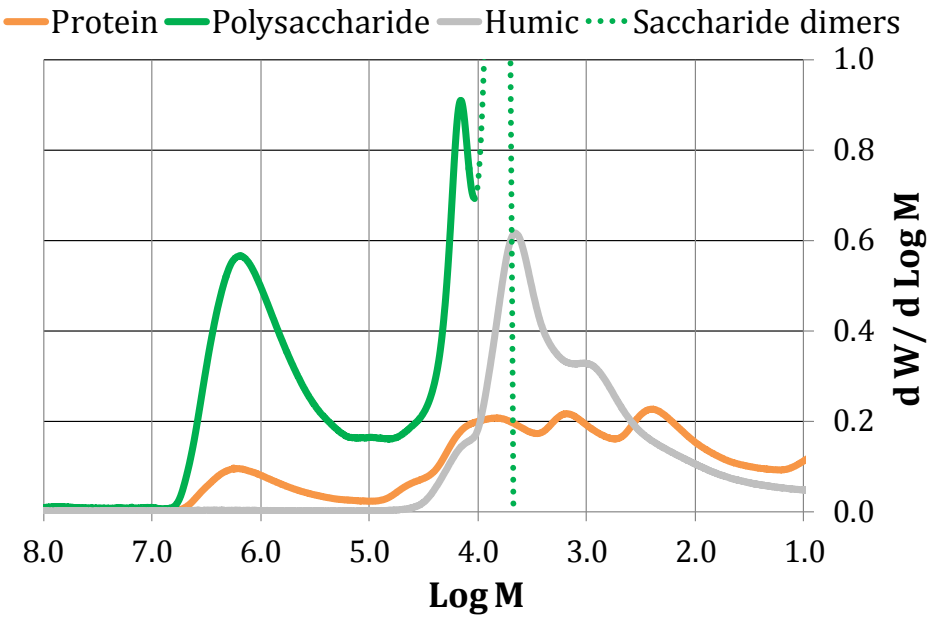

Ultrasonicated sludge (27,000 kJ/kg TS)

A

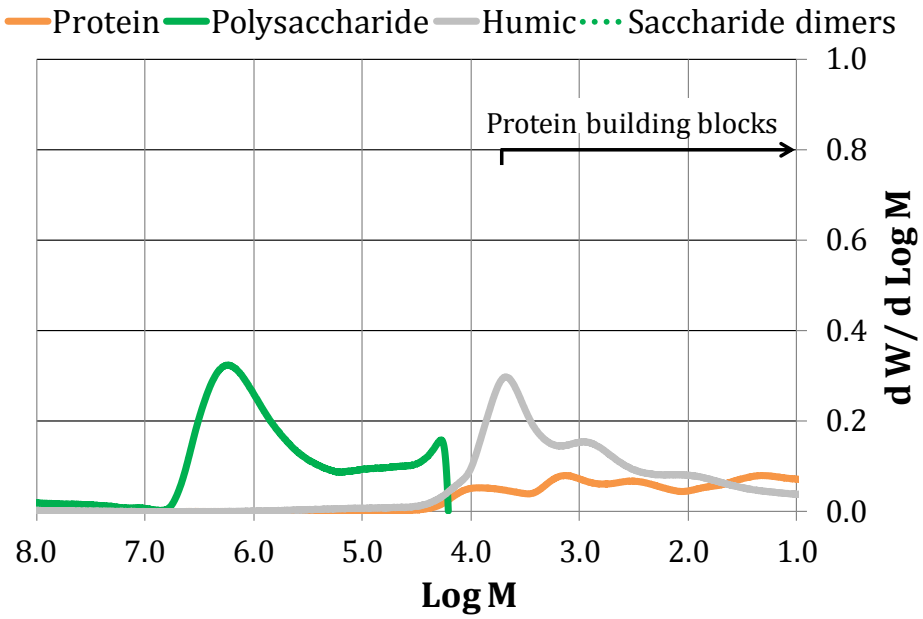

B

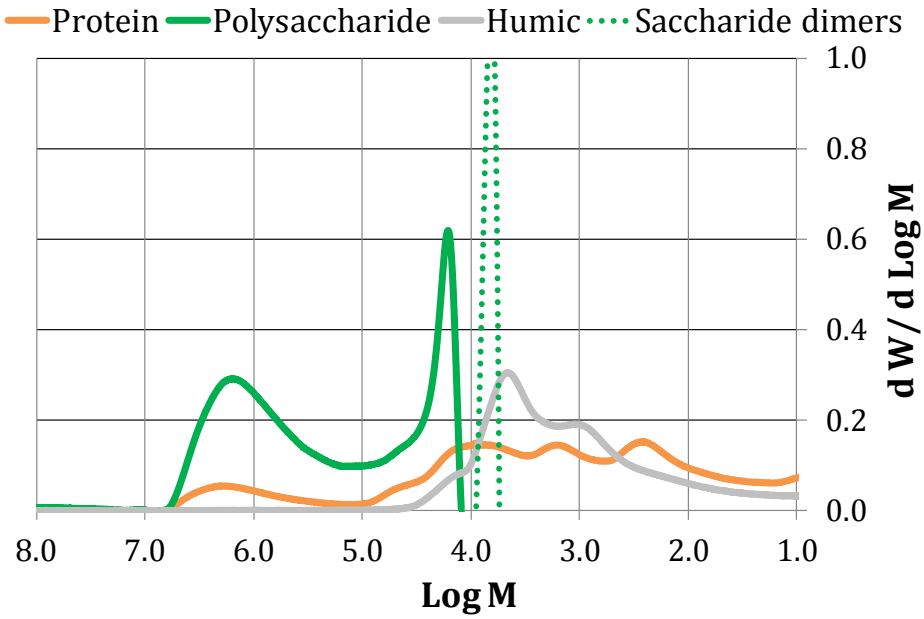

Thermally treated sludge (80 ºC; 15,000 kJ/kg TS)

A

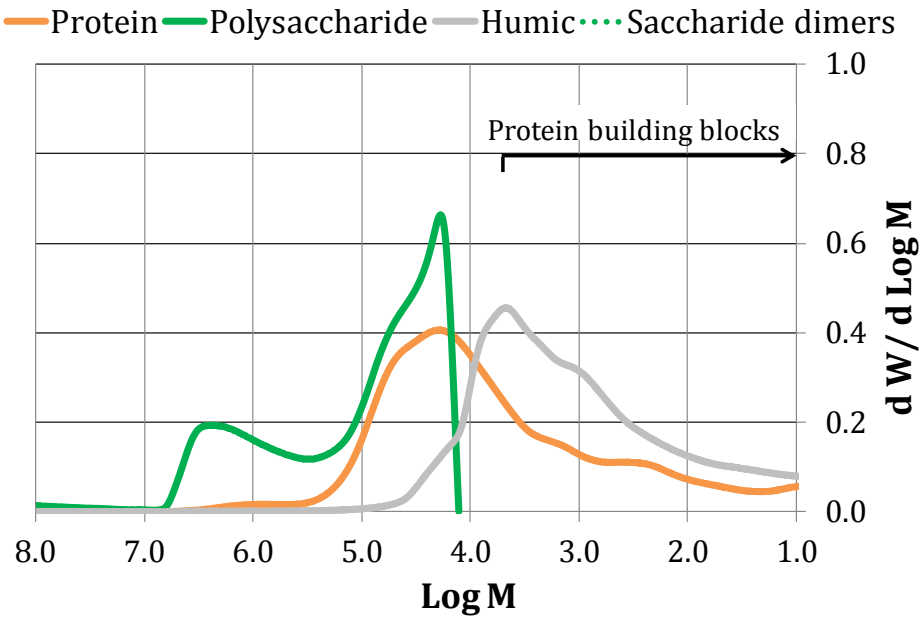

B

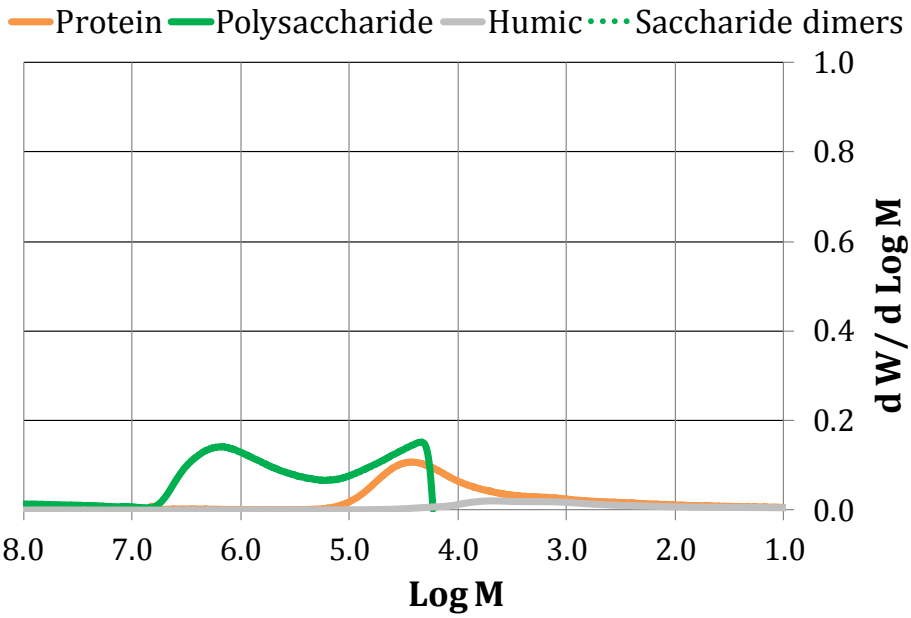

Alkali-treated sludge (157 g NaOH/kg TS)

A

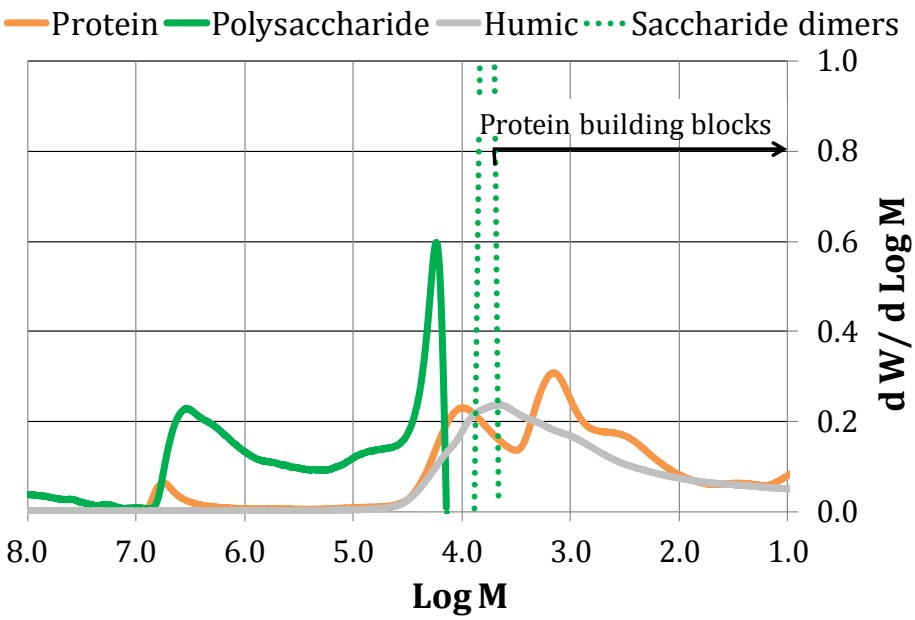

B

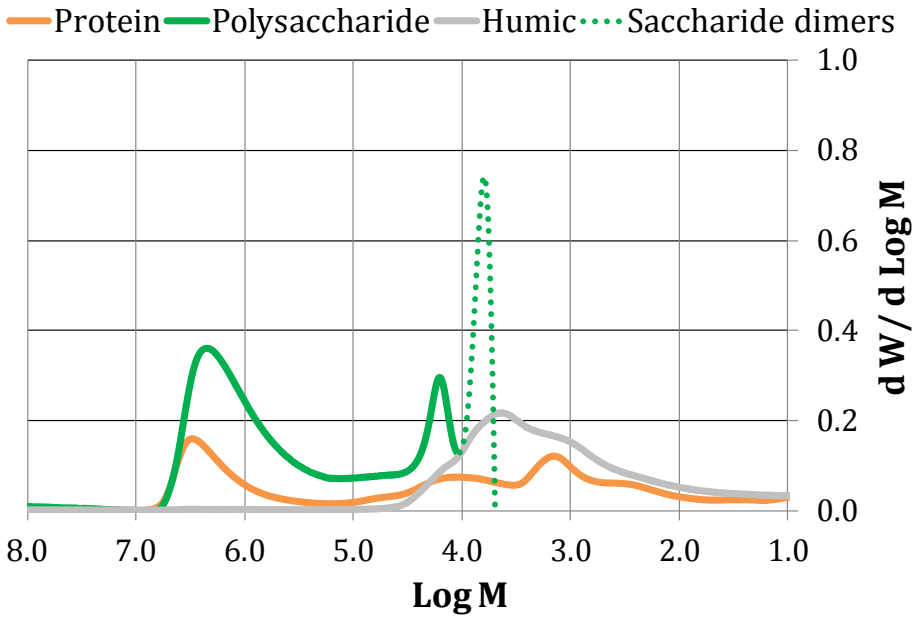

Nomenclature

G	Shear modulus [Pa]
G_0	Initial elasticity [Pa]
γ	Shear strain [-]
λ	Relaxation time [s]
$\dot{\gamma}$	Shear rate (s^{-1})
η	Viscosity [Pa·s]
η_0	Zero shear rate viscosity [Pa·s]
η_∞	High shear rate viscosity or limit viscosity [Pa·s]
η_e	Steady state viscosity [Pa·s]
η_i	Initial viscosity when a shear rate is applied (viscosity at t=0) [Pa·s]
τ	Shear stress [Pa]
τ_0	Yield stress [Pa]
τ_a	Applied stress in creep assays [Pa]
a	Consistency index [$Pa \cdot s^n$] (Chapter 6)
Ha	Hysteresis area [$Pa\ s^{-1}$]

J	Compliance [Pa^{-1}]
J_0	Instantaneous elastic compliance [Pa^{-1}]
J_i	Retarded compliance [Pa^{-1}]
K	Consistency index [$Pa \cdot s^n$] (Chapter 5)
K	Thixotropic kinetic coefficient [s^{-1}]
k_D	Kinetic coefficient for destruction process [s^{-1}]
K_{down}	Thixotropic kinetic coefficient for breakdown process [s^{-1}]
k_R	Kinetic coefficient for restructuration process [s^{-1}]
K_{up}	Thixotropic kinetic coefficient for build-up process [s^{-1}]
m	Parameter that quantifies the instantaneous alignment and deformation of sludge flocs [-]
n	Power law index [-]
S	Structural parameter [$Pa \cdot s^{1-m}$]
S'	Structural parameter at time t' (t'=t-Δt) [$Pa \cdot s^{1-m}$]
S_0	Limiting value of the structural parameter at zero shear rate [$Pa \cdot s^{1-m}$]
S_∞	Limiting value of the structural parameter at infinite shear rate [$Pa \cdot s^{1-m}$]
S_e	Steady state structural parameter [$Pa \cdot s^{1-m}$]
S_i	Initial structural parameter when a shear rate is applied, at t=0 [$Pa \cdot s^{1-m}$]
t	Shear time [s]
α_{down}	Kinetic parameter for breakdown process [$s^{\beta_{down}-1}$]
α_{up}	Kinetic parameter for build-up process [$s^{\beta_{up}-1}$]
β_{down}	Kinetic parameter for breakdown process [-]
β_{up}	Kinetic parameter for build-up process [-]
ζ	Zeta potential [mV]
f_{WAS}	Substrate biodegradability [-]
$k_{hyd,WAS}$	First order hydrolysis rate constant of the sludge [day^{-1}]
r_{WAS}	Hydrolysis process rate [mL CH_4/L·day]

Acronyms and abbreviations

AD	Anaerobic digestion
BMP	Biomethane potential
BSA	Bovine serum albumin
CCiTUB	Scientific and technological centers of the University of Barcelona
CFU	Colony-forming unit
CHP	Combined heat and power
COD	Chemical oxygen demand
CST	Capillary suction time
CV	Coefficient of variation
DG Environment	Directorate-General for the Environment (European Commission)
DS	Dry solids
dw	Dry weight
E. coli	*Escherichia coli*
EPA	United States Environmental Protection Agency
EPS	Extracellular polymeric substance

E_S	Specific energy
EU-13	New member states of the European Union
EU-15	Old Member States of the European Union
EU-28	All member mtates of the European Union
GPC	Gel permeation chromatography
LB-EPS	Loosely bound extracellular polymeric substance
MPN	Most probable number
MW	Molecular weight
MWD	Molecular weight distribution
NaOH-WAS	Alkali pre-treatment for anaerobic digestion (157 g NaOH/kg TS)
O/N	Overnight
PBS	Phosphate buffered saline
PDA	Photodiode array
PE	Population equivalent
PFU	Plaque-forming unit
RI	Refractive index
sCOD	Soluble chemical oxygen demand
SD	Solubilisation degree (Chapter 8)
SD	Standard deviation
SOMCPH	Somatic coliphages
spp.	Species
SRT	Solid retention time
SSRC	Spores of sulfite-reducing clostridia
sTOC	Soluble total organic carbon
TB-EPS	Tightly bound extracellular polymeric substance
tCOD	Total chemical oxygen demand
TOC	Total organic carbon
TS	Total solids

TSS	Total suspended solids
T-WAS	Thermal pre-treatment for anaerobic digestion (80 ºC, 15 min)
US-WAS	Ultrasound pre-treatment for anaerobic digestion (27,000 kJ/kg TS)
VFA	Volatile fatty acids
VS	Volatile solids
VSS	Volatile suspended solids
WAS	Waste activated sludge
ww	Wet weight
WWTP	Wastewater treatment plant

References

Abu-Jdayil, B., 2003. Modelling the time dependent rheological behaviour of semisolid foodstuffs. J Food Eng 57, 97–102.

Aigües de Barcelona: http://www.aiguesdebarcelona.cat/ca/estaciones-depuradoras (last access 24/02/2015).

Allievi, L., Colombi, A., Calcaterra, E., Ferrari, A., 1994. Inactivation of fecal bacteria in sewage sludge by alkaline treatment. Bioresource technology 49, 25-30.

Angelidaki, I., Alves, M., Bolzonella, D., Borzacconi, L., Campos, J.L., Guwy, A.J., Kalyuzhnyi, S., Jenicek, P., Van Lier, J.B., 2009. Defining the biomethane potential (BMP) of solid organic wastes and energy crops: a proposed protocol for batch assays. Water Sci. Technol. 59, 927-934.

Anonymous, 2000. ISO 10705-2: Water Quality - Detection and Enumeration of Bacteriophages - Part 2: Enumeration of Somatic Coliphages. International Organisation for Standardisation, Geneva, Switzeland.

APHA. Standard Methods for the Examination of Water and Wastewater. 2005. Ed. American Public Health Association, Washingthon. ISBN 978-0-87553-047-5.

Appels, L., Baeyens, J., Degrève, J., Dewil, R., 2008. Principles and potential of the anaerobic digestion of waste-activated sludge. Prog. Energy Combust. Sci. 34, 755–781.

Appels, L., Degrève, J., Van der Bruggen, B., Van Impe, J., Dewil, R., 2010. Influence of low temperature thermal pre-treatment on sludge solubilisation, heavy metal release and anaerobic digestion. Bioresour. Technol. 101, 5743–5748.

Astals, S., Nolla-Ardèvol, V., Mata-Alvarez, J., 2012a. Anaerobic co-digestion of pig manure and crude glycerol at mesophilic conditions: biogas and digestate. Bioresour. Technol. 110, 63-70.

Astals, S., Venegas, C., Peces, M., Jofre, J., Lucena, F., Mata-Alvarez, J., 2012b. Balancing hygienisation and anaerobic digestion of raw sewage sludge. Water Res. 46, 6218-6227.

Astals, S., 2013. Optimització i modelització de processos avançats de digestió anaeròbia. PhD thesis (Barcelona).

Audrey, P., Julien, L., Christophe, D., Patrick, L., 2011. Sludge disintegration during heat treatment at low temperature: A better understanding of involved mechanisms with a multiparametric approach. Biochem. Eng. J. 54, 178–184.

Ayol, A. Filibeli, A., Dentel, S.K., 2006. Evaluation of conditioning responses of thermophilic-mesophilic anaerobically and mesophilic aerobically digested biosolids using rheological properties. Water Sci. Technol. 54, 23-31.

Baccay, R.A., Hashimoto, A.G., 1984. Acidogenic and methanogenic fermentation of causticized straw. Biotechnol. Bioeng. 26, 885–891.

Barjenbruch, M., Kopplow, O., 2003. Enzymatic, mechanical and thermal pretreatment of surplus sludge. Adv. Environ. Res. 7, 715–720.

Batstone, D.J., Keller, J., Angelidaki, I., Kalyuzhnyi, S.V., Pavlostathis, S.G., Rozzi, A., Sanders, W.T., Siegrist, H., Vavilin, V.A., 2002. The IWA Anaerobic Digestion Model No 1 (ADM1). Water Sci. Technol. 45, 65–73.

Batstone, D.J., Pind, P.F., Angelidaki, I., 2003. Kinetics of thermophilic, anaerobic oxidation of straight and branched chain butyrate and valerate. Biotechnol. Bioeng. 84, 195-204.

Batstone, D.J., Tait, S., Starrenburg, D., 2009. Estimation of hydrolysis parameters in full-scale anerobic digesters. Biotechnol. Bioeng. 102, 1513-1520.

Battistoni, P., Fava, G., Stanzini, C., Cecchi, F., Bassetti, A., 1993. Feed characteristics and digester operative conditions as parameters affecting the rheology of digested municipal solids wastes. Water Sci. Technol. 27, 37-45.

Baudez, J.C., 2006. About peak and loop in sludge rheograms. J. Environ. Manage. 78, 232–239.

Baudez, J.C., Slatter, P.T., Eshtiaghi, N., 2013. The impact of temperature on the rheological behaviour of anaerobic digested sludge. Chem. Eng. J. 215-216, 182-187.

Bitton, G., 2005. Wastewater microbiology. John Wiley & Sons Inc. Publication, 3rd Edition, Hoboken, New Jersey.

Bougrier, C., Carrère, H., Delgenès, J.P., 2005. Solubilisation of waste-activated sludge by ultrasonic treatment. Chem. Eng. J. 106, 163–169.

Bougrier, C. Albasi, C., Delgenès, J.P., Carrère, H., 2006. Effect of ultrasonic, thermal and ozone pre-treatments on waste activated sludge solubilisation and anaerobic biodegradability. Chem. Eng. Process. 45, 711–718.

Bougrier, C., Delgenès, J.P., Carrère, H., 2008. Effects of thermal treatments on five different waste activated sludge samples solubilisation, physical properties and anaerobic digestion. Chem. Eng. J. 139, 236–244.

Braguglia, C.M., Mininni, G., Gianico, A. 2008. Is sonication effective to improve biogas production and solids reduction in excess sludge digestion?. Water Sci. Technol. 57, 479-483.

Braguglia, C.M., Gagliano, M.C., Rossetti, S., 2012. High frequency ultrasound pretreatment for sludge anaerobic digestion: Effect on floc structure and microbial population. Bioresour. Technol. 110, 43–49.

Büchi, F.N., Inaba, M., Schmidt, T.J., 2009. Polymer Electrolyte Fuel Cell Durability. Springer, Feb. 2009, ISBN: 0387855343.

Bujoczek, G., Oleszkiewicz, J.A., Danesh, S., Sparling, R.R., 2002. Co-processing of organic fraction of municipal solid waste and primary sludge – Stabilization and disinfection. Environ. Technol. 23, 227-241.

Cadoret, A. Conrad, A., Block, J.C., 2002. Availability of low and high molecular weight substrates to extracellular enzymes in whole and dispersed activated sludges. Enzyme Microb. Technol. 31, 179–186.

Carrère, H., Bougrier, C., Castets, D., Delgenes, J.P., 2008. Impact of initial biodegradability on sludge anaerobic digestion enhancement by thermal pretreatment. J. Environ. Sci. Health Part A-Toxic/Hazard. Subst. Environ. Eng. 43, 1551–1555.

Carrère, H., Dumas, C., Battimelli, A., Batstone, D.J., Delgenès, J.P., Steyer, J.P., Ferrer, I., 2010. Pretreatment methods to improve sludge anaerobic degradability: A review. J. Hazard. Mater. 183, 1–15.

Carrère, H., Rafrafi, Y., Battimelli, A., Torrijos, M., Delgenes, J.P., Motte, C. 2012. Improving methane production during the codigestion of waste-activated sludge and fatty wastewater: Impact of thermo-alkaline pretreatment on batch and semi-continuous processes. Chem. Eng. J. 210, 404-409.

Carrington, E.G., Davis, R.D., Hall, J.E., Pike, E.B., Smith, S.R. and Unwin, R.J., 1998. Review of the scientific evidence relating to the controls on the agricultural use of sewage sludge. Report DETR 4415/3 [part1] and Report DETR 4454/4 [part 2] WRc plc, Medmenham.

CEC (Council of the European Communities), 1986. Council Directive of 12 June 1986 on the protection of the environment, and in particular of the soil, when sewage sludge is used in agriculture (86/278/EEC). Official Journal of the European Communities No. L 181/6-12.

CEC (Council of the European Communities), 1991. Council Directive of 21 May 1991 concerning urban waste water treatment (91/271/EEC). Official Journal of the European Communities No. L 135/40-52.

Chang, G.R., Liu, J.C., Lee, D.J., 2001. Co-conditioning and dewatering of chemical sludge and waste activated sludge. Water Res. 35, 786-794.

Chen, Y., Yang, H., Gu, G., 2001. Effect of acid and surfactant treatment on activated sludge dewatering and settling. Water Res. 35, 2615–2620.

Chen, Y., Cheng, J.J., Creamer, K.S., 2008. Inhibition of anaerobic digestion process: A review. Bioresour. Technol. 99, 4044–4064.

Chen, J.L., Ortiz, R., Steele, T.W., Stuckey, D.C., 2014. Toxicants inhibiting anaerobic digestion: A review. Biotech. Adv. 32, 1523–1534.

Cheng, D.C. H., 2003. Characterisation of thixotropy revisited. Rheol. Acta 42, 372–382.

Chu, C.P., Chang, B.V., Liao, G.S., Jean, D.S., Lee, D.J., 2001. Observations on changes in ultrasonically treated waste-activated sludge. Water Res. 35, 1038–1046.

Chu, C.P., Lee, D.J., Chang, B.V., You, C.S., Tay, J.H., 2002. "Weak" ultrasonic pretreatment on anaerobic digestion of flocculated activated biosolids. Water Res. 36, 2681–2688.

Chu, L., Yan, S., Xing, X.H., Sun, X., Jurcik, B., 2009. Progress and perspectives of sludge ozonation as a powerful pretreatment method for minimization of excess sludge Production. Water Res. 43, 1811 – 1822.

Climent, M., Ferrer, I., Baeza, M.M., Artola, A., Vazquez, F., Font, X., 2007. Effects of thermal and mechanical pretreatments of secondary sludge on biogas production under thermophilic conditions. Chem. Eng. J. 133, 335–342.

Cobbledick, J., Nguyen, A., Latulippe, D.R., 2014. Demonstration of FBRM as process analytical technology tool for dewatering processes via CST correlation. Water Res. 58, 132-140.

Colin, F., Gazbar, S., 1995. Distribution of water in sludges in relation to their mechanical dewatering. Water Res. 29, 2000-2005.

Coussot, P., 2005. Rheometry of Pastes, Suspensions, and Granular Materials: Applications in Industry and Environment, John Wiley & Sons Inc., Hoboken, NJ, USA.

Cui, X., Talley, J.W., Liu, G., Larson, S.L., 2011. Effects of primary sludge particulate (PSP) entrapment on ultrasonic (20 kHz) disinfection of *Escherichia coli*. Water Res. 45, 3300 – 3308.

Deng, W., Li, X., Yan, J., Wang, F., Chi, Y., Cen, K., 2011. Moisture distribution in sludges based on different testing methods. J. Environ. Sci. 23, 875–880.

Dwyer, J., Starrenburg, D., Tait, S., Barr, K., Batstone, D.J., Lant, P., 2008. Decreasing activated sludge thermal hydrolysis temperature reduces product colour, without decreasing degradability. Water Res. 42, 4699–4709.

EC (European Commission), 2001. Evaluation of sludge treatments for pathogen reduction – Final report. Study Contract No B4-3040/2001/322179/MAR/A2.

EC (European Commission), 2009. Fifth Commission summary on the implementation of the Urban Waste Water Treatment Directive, Commission Staff Working Document, SEC (2009) 1114 final, Brussels, 3.8.2009.

EC (European Commission)-EUROSTAT web: http://epp.eurostat.ec.europa.eu/ (last access 19/09/2014).

Edelhoch, H., Osborne, J.C., 1976. The thermodynamic basis of the stability of proteins, nucleic acids and membranes. Advances in Protein Chemistry 30,183–250.

Environment DG, EU, 2000. Working Document on Sludge, 3rd Official Draft. Brussels. URL: http://ec.europa.eu/environment/waste/sludge/pdf/sludge_en.pdf.

Erden, G., Filibeli, A., 2009. Ultrasonic pre-treatment of biological sludge: consequences for disintegration, anaerobic biodegradability, and filterability. J. Chem. Technol. Biotechnol. 85, 145–150.

Erdincler, A., Vesilind, P.A., 2003. Effect of Sludge Water Distribution on the Liquid–Solid Separation of a Biological Sludge. J Environ. Sci. Health. A Tox. Hazard. Subst. Environ. Eng. 38, 2391–2400.

Eshtiaghi, N., Markis, F., Yap, S.D., Baudez, J.C., Slatter, P., 2013. Rheological characterisation of municipal sludge: a review. Water Res. 47, 5493-5510.

Farno, E., Baudez, J.C., Parthasarathy, R., Eshtiaghi, N., 2014. Rheological characterisation of thermally-treated anaerobic digested sludge: Impact of temperature and thermal history, Water Res. 56, 156–161.

Feng, X., Deng, J., Lei, H., Bai, T., Fan, Q., Li, Z., 2009a. Dewaterability of waste activated sludge with ultrasound conditioning. Bioresour. Technol. 100, 1074–1081.

Feng, X., Lei, H.Y., Deng, J.C., Yu, Q., Li, H.L., 2009b. Physical and chemical characteristics of WAS treated ultrasonically. Chem. Eng. Process. 48, 187-194.

Feng, G., Liu, L., Tan, W., 2014. Effect of Thermal Hydrolysis on Rheological Behavior of Municipal Sludge. Ind. Eng. Chem. Res. 53, 11185−11192.

Ferreira, G., 2013. Alternative Energies: Updates on Progress. Springer Heidelberg New York Dordrecht London.

Foladori, P., Laura, B., Gianni, A., Giuliano, Z., 2007. Effects of sonication on bacteria viability in wastewater treatment plants evaluated by flow cytometry - Fecal indicators, wastewater and activated sludge. Water Res. 41, 235 – 243.

Foladori, P., Andreottola, G., Ziglio, G., 2010. Sludge Reduction Technologies in Wastewater Treatment Plants. IWA Publishing.

Frølund, B., Griebe, T., Nielsen, P.H., 1995. Enzymatic activity in the activated-sludge floc matrix. Appl. Microbiol. Biotechnol. 43, 755–761.

Frølund, B., Palmgren, R., Keiding, K., Nielsen, P.H., 1996. Extraction of extracellular polymers from activated sludge using a cation exchange resin. Water Res. 30, 1749–1758.

Fytili, D., Zabaniotou, A., 2008. Utilization of sewage sludge in EU application of old and new methods—A review. Renew. Sust. Eereg. Rev. 12, 116–140.

Gallipoli, A., Braguglia, C.M., 2012. High-frequency ultrasound treatment of sludge: Combined effect of surfactants removal and floc disintegration. Ultrason. Sonochem. 19, 864–871.

Garnier, C., Görner, T., Guinot-Thomas, P., Chappe, P., De Donato, P., 2006. Exopolymeric production by bacterial strains isolated from activated sludge of paper industry. Water Res. 40, 3115–3122.

Gavala, H.N., Yenal, U., Skiadas, I.V., Westermann, P., Ahring, B.K., 2003. Mesophilic and thermophilic anaerobic digestion of primary and secondary sludge. Effect of pre-treatment at elevate temperature. Water Res. 37, 4561–4572.

Giachino, N., 2011. Anaerobic digestion degradability of waste sludge after ultrasound and enzymic hydrolysis pretreatment. Master Thesis. Politecnico di Milano and Universidad de Oviedo.

Gianfreda, L., Rao, M.A., 2004. Potential of extracellular enzymes in remediation of polluted soils: a review. Enzyme Microb. Technol.35, 339–354.

Gogate, P.R., Pandit, A.B., 2004. A review of imperative technologies for wastewater treatment I: oxidation technologies at ambient conditions. Adv. Environ. Res. 8, 501–551.

Graczyk, T.K, Kacprzak, M., Neczaj, E., Tamang, L., Graczyk, H., Lucy, F.E, Girouard, A.S., 2008. Occurrence of Cryptosporidium and Giardia in sewage sludge and solid waste landfill leachate and quantitative comparative analysis of sanitization treatments on pathogen inactivation. Environ. Res. 106, 27–33.

Green, H., Weltmann, R.N., 1946. Equations of thixotropic breakdown for rotational viscometer, Ind. Eng. Chem. Anal. Ed. 18, 167–172.

Guan, B.H., Yu, J., Fu, H.L., Guo, M.H., Xu, X.H., 2012. Improvement of activated sludge dewaterability by mild thermal treatment in $CaCl_2$ solution. Water Res 46, 425–432.

Guibaud, G., Tixier, N., Baudu, M., 2005. Hysteresis area, a rheological parameter used as a tool to assess the ability of filamentous sludges to settle. Process Biochem. 40, 2671–2676.

Guzmán, C., Jofre, J., Blanch, A.R., Lucena, F., 2007. Development of a feasible method to extract somatic coliphages from sludge, soil and treated biowaste. J Virol Methods, 144, 41–48.

Hammadi, L., Ponton, A., Belhadri, M., 2013. Temperature effect on shear flow and thixotropic behavior of residual sludge from wastewater treatment plant. Mech. Time-Depend. Mat. 17, 401-412.

Herwijn, A.J.M., 1996. Fundamental aspects of sludge characterization. PhD dissertation, Eindhoven University of Technology, The Netherlands.

Heukelekian, H., Weisberg, E., 1956. Bound water and activated sludge bulking, Sewage Ind. Wastes 28, 558-574.

Hii, K., Baroutian, S., Parthasarathy, R., Gapes, D.J., Eshtiaghi, N., 2014. A review of wet air oxidation and Thermal Hydrolysis technologies in sludge treatment. Bioresour. Technol. 155, 289-299.

Hiraoka, M., Takeda, N., Sakai, S., Yasuda, A., 1984. Highly efficient anaerobic digestion with thermal pretreatment. Water Sci. Technol. 17, 529-539.

Huisman, M., van Kesteren, W.G.M., 1998. Consolidaton theory applied to the Capillary Suction Time (CST) apparatus. Water Sci.Technol. 37 , 117–124.

IAWPRC, 1991. Study group on health related water microbiology. Bacteriophages as model viruses in water quality control. Water Res. 25, 529-545.

Jensen, P.D., Ge, H., Batstone, D.J., 2011. Assessing the role of biochemical methane potential tests in determining anaerobic degradability rate and extent. Water Sci. Technol. 64, 880-886.

Jiang, J.Q., Zhao, Q.L., Wang, K., Wei, L.L., Zhang, G.D., Zhang, J.N. 2010. Effect of ultrasonic and alkaline pretreatment on sludge degradation and electricity generation by microbial fuel cell. Water Sci. Technol. 61, 2915-2921.

Jin, B., Wilen, B.M., Lant, P., 2004. Impacts of morphological, physical and chemical properties of sludge flocs on dewaterability of activated sludge. Chem. Eng. J. 98, 115–126.

Kato, S., Reimers, R.S., Fogarty, E.A., Bowman, D.D., 2001. Effect of Aerobic Digestion, Anaerobic Digestion, and Ammonia on the Viability of Oocysts of Cryptosporidium parvum and the Eggs of Ascaris suum in Sewage Sludges, San Diego, CA.

Katsiris, N., Kouzeli-Katsiri, A., 1987. Bound water content of biological sludges in relation to filtration and dewatering. Water Res. 21, 1319-1327.

Kelessidis, A., Stasinakis, A.S., 2012. Comparative study of the methods used for treatment and final disposal of sewage sludge in European countries. Waste Manage. 32, 1186–1195.

Khanal, S.K., 2008. Anaerobic Biotechnology for Bioenergy Production: Principles and Applications. John Wiley & Sons, Inc., Iowa.

Kim, Y.U., Kim, B.I., 2003. Effect of ultrasound on dewaterability of sewage sludge. Japan J. Appl. Phys. Part 1 42 (9A), 5898–5899.

Kim, J., Park, C., Kim, T.H., Lee, M., Kim, S., Kim, S.W., Lee, J., 2003. Effects of various pretreatments for enhanced anaerobic digestion with waste activated sludge, J. Biosci. Bioeng. 95, 271–275.

Kim, J., Yu, Y., Lee, C. 2013a. Thermo-alkaline pretreatment of waste activated sludge at low-temperatures: Effects on sludge disintegration, methane production, and methanogen community structure. Bioresour. Technol. 144, 194-201.

Kim, D.H., Cho, S.K., Lee, M.K., Kim, M.S., 2013b. Increased solubilisation of excess sludge does not always result in enhanced anaerobic digestion efficiency. Bioresour. Technol. 143, 660–664.

Kopp, J., Dichtl, N., 2001. Influence of the free water content on the dewaterability of sewage sludges. Water Sci. Technol. 44, 177-183.

La Heij, E.J., 1994. An analysis of sludge filtration and expression. PhD dissertation, Eindhoven University of Technology, The Netherlands.

Labanda, J., 2003. Desarrollo de modelos estructurales para la cuantificación del comportamiento tixotrópico de sistemas coloidales. PhD thesis (Barcelona).

Labanda, J. Llorens, J., 2005. Improvement of the deflocculating power of polyacrylates in ceramic slips by small additions of quaternary ammonium salts, Powder Technol. 155, 181 – 186.

Labanda, J., Llorens, J., 2006. A structural model for thixotropy of colloidal dispersions. Rheol. Acta 45, 305-314.

Labanda, J. Sabaté, J. Llorens, J., 2007. Rheology changes of Laponite aqueous dispersions due to the addition of sodium polyacrylates of different molecular weights. Colloids Surf., A: Physicochem. Eng. Aspects 301, 8–15.

Laera, G., Giordano, C., Pollice, A., Saturno, D., Mininni, G., 2007. Membrane bioreactor sludge rheology at different solid retention times. Water Research 41, 4197-4203.

Layne, E. (1957). Spectrophotometric and turbidimetric methods for measuring proteins. Methods Enzymol. 3, 447–454.

Lee, D.J., 1994. Measurement of bound water in waste activated sludge: use of the centrifugal settling method. J. Chem. Technol. Biotechnol. 61, 139–144.

Lee, D.J., Hsu, Y.H., 1995. Measurement of bound water in sludges: a comparative study. Water Environ. Res. 67, 310–317.

Lee, D.J., Lee, S.F., 1995. Measurement of bound water content in sludge: The use of differential scanning calorimetry (DSC). J. Chem. Technol. Biotechnol. 62, 359- 365.

Lepeuple, A.S., Gaval, G., Jovic M., de Roubin, M.R. 2004. Literature review on levels of pathogens and their abatement in sludges, soil and treated biowaste. The Energy Research Centers of the Netherlands, WP3 Hygienic Parameters, Horizontal Project. Retrieved from www.ecn.nl/docs/society/horizontal/hor6_pathogens.pdf

Li, Y-.Y., Noike, T. 1992. Upgrading of anaerobic digestion of waste activated sludge by thermal pretreatment. Water Sci. Technol. 26, 857-866.

Li, X.Y., Yang, S.F., 2007. Influence of loosely bound extracellular polymeric substances (EPS) on the flocculation, sedimentation and dewaterability of activated sludge. Water Research 41, 1022–1030.

Li, H., Jin, Y., Mahar, R., Wang, Z., Nie, Y., 2008. Effects and model of alkaline waste activated sludge treatment. Biores. Technol. 99, 5140–5144.

Li, H., Jin, Y., Nie, Y., 2009. Application of alkaline treatment for sludge decrement and humic acid recovery. Bioresour. Technol. 100, 6278–6283.

Li, H., Li, C., Liu, W., Zou, S., 2012. Optimized alkaline pretreatment of sludge before anaerobic digestion. Bioresour. Technol. 123, 189–194.

Lin, J.G., Chang, C.N., Chang, S.C., 1997. Enhancement of anaerobic digestion of waste activated sludge by alkaline solubilization. Bioresour. Technol. 62, 85–90.

Lin, Y., Wang, D., Wu, S., Wang, C., 2009. Alkali pretreatment enhances biogas production in the anaerobic digestion of pulp and paper sludge. J. Hazard. Mater. 170, 366–373.

Liu, Y., Fang, H.H.P., 2003. Influence of extracellular polymeric substances (EPS) on flocculation, settling, and dewatering of activated sludge. Crit. Rev. Env. Sci. Technol. 33, 237–273.

Llorens, J., Rude, E., Marcos, R.M., 2003. Polydispersity index from linear viscoelastic data: unimodal and bimodal linear polymer melts. Polymer 44, 1741–1750.

Lowry, O.H., Rosebrough, N.J., Farr, A.L., Randall, R.J., 1951. Protein measurement with the folin phenol reagent. J. Biol. Chem. 193, 265–275.

Lu, J., Gavana, H.N., Skiadas, I.V., Mladenovska, Z., Ahring, B.K., 2008. Improving anaerobic sewage sludge digestion by implementation of a hyper-thermophilic prehydrolysis step. J. Environ. Manage. 88, 881-889.

Lucena, F., Bosch, A., Ripoll, J. and Jofre, J., 1988. Faecal pollution in Llobregat river: interrelationship of viral, bacterial and physico-chemical parameters. Water, Air, and Soil Poll. 39, 15-25.

Lundin, M., Olofsson, M., Pettersson, G.J., Zetterlund, H., 2004. Environmental and economic assessment of sewage sludge handling options. Resour. Conserv. Recy. 41, 255–278.

Malerius, O., Werther, J., 2003. Modelling the adsorption of mercury in the flue gas of sewage sludge incineration. Chem. Eng. J. 96, 197–205.

Mewis, J., Wagner, N.J., 2009. Thixotropy. Adv. Colloid Interface Sci. 147–148, 214–227.

Milieu Ltd., WRc and Risk & Policy Analysts Ltd (RPA), 2010. Environmental, economic and social impacts of the use of sewage sludge on land. Final Report, Part III: Project Interim Reports, DG ENV.G.4/ETU/2008/0076r, 10.2.2010.

Mocé-Llivina, L., Muniesa, M., Pimenta-Vale, H., Lucena, F., Jofre, J., 2003. Survival of bacterial indicator species and bacteriophages after thermal treatment of sludge and sewage. Appl. Environ. Microb. 69, 1452–1456.

Moeller,G., Torres, K.G., 1997. Rheological characterization of primary and secondary sludges treated by both aerobic and anaerobic digestión. Bioresour. Technol. 61, 207-211.

Moore, F., 1959. The rheology of ceramic slips and bodies, Trans Br Ceramics Soc 58, 470–475.

Moreau, A.A., Ratkovich, N., Nopens, I., Van der Graff, J.H.J.M., 2009. The (in)significance of apparent viscosity in full-scale bioreactor treating municipal sewage. J. Membr. Sci. 317, 65-70.

Mori, M., Seyssiecq, I., Roche, N., 2006. Rheological measurements of sewage sludge for various solids concentrations and geometry. Process Biochem. 41, 1656–1662.

Mottet, A., Steyer, J.P., Déléris, S., Vedrenne, F., Chauzy, J., Carrère, H., 2009. Kinetics of thermophilic batch anaerobic digestion of thermal hydrolysed waste activated sludge. Biochem. Eng. J. 46, 169–175.

Mouneimne, A.H., Carrère, H., Bernet, N., Delgenès, J.P., 2003. Effect of saponification on the anaerobic digestion of solid fatty residues. Bioresour. Technol. 90, 89–94.

Mowla, D., Tran, H.N., Grant Allen, D., 2013. A review of the properties of biosludge and its relevance to enhanced dewatering processes. Biomass Bioenergy 58, 365-378.

Nabarlatz, D., Vondrysova, J, Jenicek, P., Stüber, F., Font, J., Fortuny, A., Fabregat, A., Bengoa, C., 2010. Hydrolytic enzymes in activated sludge: Extraction of protease and lipase by stirring and ultrasonication. Ultrason. Sonochem. 17, 923–931.

Nah, I.W., Kang, Y.W., Hwang, K.Y., Song, W.K., 2000. Mechanical pretreatment of waste activated sludge for anaerobic sludge digestion process. Water Res. 34, 2362–2368.

Navia, R., Soto, M., Vidal, G., Bornhardt, C., Diez, M.C., 2002. Alkaline pretreatment of kraft mill sludge to improve its anaerobic digestion. Bull. Environ. Contam. Toxicol. 69, 869–876.

Nelson, T.C., Huang, J.Y.C., Ramaswami, D., 1998. Decomposition of exopolysaccharide slim by a bacterio phage enzyme. Water Res. 22, 1185-1188.

Neptune Project-Deliverable 1.3: Strategies for a sustainable and safe sludge management. 2009.

Neyens, E., Baeyens, J., 2003. A review of thermal sludge pre-treatment processes to improve dewaterability. J. Hazard. Mater. B98, 51–67.

Neyens, E., Baeyens, J., Dewil, R., De heyder, B., 2004. Advanced sludge treatment affects extracellular polymeric substances to improve activated sludge dewatering. J. Hazard. Mater. 106B, 83–92.

Ni, B.J., Fang, F., Xie, W.M., Sun, M., Sheng, G.P., Li, W.H., Yu, H.Q., 2009. Characterization of extracellular polymeric substances produced by mixed microorganisms in activated sludge with gel-permeating chromatography, excitation–emission matrix fluorescence spectroscopy measurement and kinetic modeling. Water Res. 43, 1350-1358.

Nielsen, P.H., Jahn, A., 1999. Extraction of EPS. In: Wingender, J., Neu, T.R., Flemming, H.C., editors. Microbial extracellular polymeric substances: characterization, structure and function. Berlin Heidelberg: Springer-Verlag.

Nielsen, P.H., 2002. Activated sludge – The floc, In: Encyclopedia of Environmental Microbiology, G. Bitton, editor-in-chief, Wiley-Interscience, Hoboken, N.J.

Nielsen, P.H., Saunders, A.M., Hansen, A.A., Larsen, P., Nielsen, J.L., 2012. Microbial communities involved in enhanced biological phosphorus removal from wastewater - a model system in environmental biotechnology. Curr. Opin. Biotechnol. 23, 452-459.

Onyeche, T.I., 2007. Economic benefits of low pressure sludge homogenization for wastewater treatment plants, in: IWA specialist conferences. Moving forward wastewater biosolids sustainability, Moncton, New Brunswick, Canada.

Parawira, W., 2012. Enzyme research and applications in biotechnological intensification of biogas production. Crit. Rev. Biotechnol. 32, 172–186.

Passos, F., García, J., Ferrer, I. 2013. Impact of low temperature pretreatment on the anaerobic digestion of microalgal biomass. Bioresour. Technol. 138, 79-86.

Paul, E., Liu, Y., 2012. Biological Sludge Minimization and Biomaterials/Bioenergy Recovery Technologies. John Wiley & Sons, Inc.

Paulsen, P., Hagen, U., Bauer, F., 2006. Changes in biogenic amine contents, non-protein nitrogen and crude protein during curing and thermal processing of M. longissimus, pars lumborum of pork. European Food Research and Technology 223, 603–608.

Payment, P. and Franco, E., 1993. Clostridium perfringens and somatic coliphages as indicators of the efficiency of drinking water treatment for viruses and protozoan cysts. Appl. Environ. Microbiol. 59, 2418-2424.

Pecson, B.M., Barrios, J.A., Jiménez, B.E., Nelson, K.L., 2007. The effects of temperature, pH, and ammonia concentration on the inactivation of Ascaris eggs in sewage sludge. Water Res. 41, 2893– 2902.

Penaud, V., Delgenès, J.P., Moletta, R. 1999. Thermo-chemical pretreatment of a microbial biomass: Influence of sodium hydroxide addition on solubilization and anaerobic biodegradability. Enzym. Microb. Technol. 25, 258-263.

Pérez-Elvira, S.I., Ferreira, L. C., Donoso-Bravo, A., Fdz-Polanco, M., Fdz-Polanco, F., 2010. Full-stream and part-stream ultrasound treatment effect on sludge anaerobic digestion. Water Sci. Technol. 61, 1363-1372.

Perret, D., Locat, J., Martignoni, P., 1996. Thixotropic behavior during shear of a fine-grained mud from Eastern Canada, Eng. Geol. 43, 31–44.

Pham, T.T.H., Brar, S.K., Tyagi, R.D., Surampalli, R.Y., 2010. Influence of ultrasonication and Fenton oxidation pre-treatment on rheological characteristics of wastewater sludge. Ultrason. Sonochem. 17, 38–45.

Pilli, S., Bhunia, P., Yan, S., LeBlanc, R.J., Tyagi, R.D., Surampalli, R.Y., 2011. Ultrasonic pretreatment of sludge: A review. Ultrason. Sonochem. 18, 1–18.

Pollice, A., Giordano, C., Laera, G., Saturno, D., Mininni, G., 2006. Rheology of sludge in a complete retention membrane bioreactor. Environmental Technology 27, 723–732.

Quarmby, J., Scott, J.R., Mason, A.K., Davies, G., Parsons, S.A., 1999. The application of ultrasound as a pre-treatment for anaerobic digestion. Environ. Technol. 20, 1155–1161.

Ratkovich, N., Horn, W., Helmus, F.P., Rosenberger, S., Naessens, W., Nopens, I., Bentzen, T.R., 2013. Activated sludge rheology: A critical review on data collection and modelling. Water Res. 47, 463-482.

Ruiz-Hernando, M., Labanda, J., Llorens, J., 2010. Effect of ultrasonic waves on the rheological features of secondary sludge. Biochem. Eng. J. 52, 131-136.

Ruiz-Hernando, M., Martinez-Elorza, G., Labanda, J., Llorens, J., 2013. Dewaterability of sewage sludge by ultrasonic, thermal and chemical treatments. Chem. Eng. J. 230, 102-110.

Ruiz-Hernando, M., Martín-Díaz, J., Labanda, J., Mata-Alvarez, J., Llorens, J., Lucena, F., Astals, S., 2014a. Effect of ultrasound, low-temperature thermal and alkali pre-treatments on waste activated sludge rheology, hygienization and methane potential. Water Res. 61, 119-129.

Ruiz-Hernando, M., Simón, F.X., Labanda, J., Llorens, J., 2014b. Effect of ultrasound, thermal and alkali treatments on the rheological profile and water distribution of waste activated sludge. Chem. Eng. J. 255, 14-22.

Ruiz-Hernando, M., Labanda, J., Llorens, J., 2015a. Structural model to study the influence of thermal treatment on the thixotropic behaviour of waste activated sludge. Chem. Eng. J. 262, 242–249.

Ruiz-Hernando, M., Cabanillas, E., Labanda, J., Llorens, J., 2015b. Ultrasound, thermal and alkali treatments affect extracellular polymeric substances (EPSs) and improve waste activated sludge dewatering. Process Biochem. 50, 438-446.

Salsabil, M.R., Prorot, A., Casellas, M., Dagot, C., 2009. Pre-treatment of activated sludge: Effect of sonication on aerobic and anaerobic digestibility. Chem. Eng. J. 148, 327–335.

Sanin, F.D, Clarkson, W.W., Vesilind, P.A., 2011. Sludge Engineering: The Treatment and Disposal of Wastewater Sludges. DEStech Publications, Inc.

Schramm, G., 2004. A Practical Approach to Rheology and Rheometry. Second Edition. (Thermo Electron (Karlsruhe) GmbH), Germany.

Seyssiecq, I., Ferrasse, J.H., Roche, N., 2003. State-of-the-art: rheological characterisation of wastewater treatment sludge. Biochem. Eng. J. 16, 41–56

Seyssiecq, I., Marrot, B., Djerroud, D., Roche, N., 2008. In situ triphasic rheological characterisation of activated sludge, in an aerated bioreactor. Chem. Eng. J. 142, 40–47.

Sheng, G.P., Yu, H.Q., Li, X.Y., 2010. Extracellular polymeric substances (EPS) of microbial aggregates in biological wastewater treatment systems: A review. Biotechnol. Adv. 28, 882–894.

Simon, S., Païro, B., Villain, M., D'Abzac, P., Van Hullebusch, E., Lens, P., Guibaud, G., 2009. Evaluation of size exclusion chromatography (SEC) for the characterization of extracellular polymeric substances (EPS) in anaerobic granular sludges. Bioresour. Technol. 100, 6258–6268.

Solvay, 2013. URL: http://www.solvaychemicals.com/EN/Home.aspx.

Stephenson, F.H., 2010. Calculations for Molecular Biology and Biotechnology. Second Edition. Chapter 11 – Protein, 369-412.

Storm, D.R., Kelly, B., Gannon, G., Meyer, E., 1981. Pathogen survival in lime-stabilized sludge. BioCycle 22, 48-51.

Strauch, D., 1991. Microbiological treatment of municipal sewage waste and refuse as a means of disinfection prior to recycling in agriculture. Studies in Environmental Science, 42, 121-136.

Stuckey, D.C., McCarty, P.L., 1984. The effect of thermal pretreatment on the anaerobic biodegradability and toxicity of waste activated sludge. Water Res. 18, 1343–1353.

Sutherland, I.W., 2001. Biofilm exopolysaccharides: a strong and sticky framework. Microbiology-SGM 147, 3–9.

Tang, Y., Yang, Y.L., Li, X.M., Yang, Q., Wang, D.B., Zeng, G.M., 2012. The isolation, identification of sludge-lysing thermophilic bacteria and its utilization in solubilization for excess sludge. Environ. Technol. 33, 961–966.

Tixier, N., Guibaud, G., Baudu, M., 2003a. Towards a rheological parameter for activated sludge bulking characterisation, Enzyme Microb. Tech. 33, 292–298.

Tixier, N., Guibaud, G., Baudu, M., 2003b. Determination of some rheological parameters for the characterization of activated sludge. Bioresour. Technol. 90, 215–220.

Tornberg, E., 2005. Effects of heat on meat proteins – Implications on structure and quality of meat products. Meat Science 70, 493–508.

Urbain, V., Block, J.C., Manem, J., 1993. Bioflocculation in activated sludge: an analytic approach. Water Res. 27, 829-838.

US Environmental Protection Agency, 2000. Alkaline Stabilization of Biosolids. Biosolids Technology Fact Sheet. http://1.usa.gov/1hcSQP3.

US Environmental Protection Agency, 2003. Control of Pathogens and Vector Attraction in Sewage Sludge. Under 40 CFR Part 503. EPA 625/R-92/013. Cincinnati.

Valo, A., Carrère, H., Delgenès, J.P. 2004. Thermal, chemical and thermo-chemical pre-treatment of waste activated sludge for anaerobic digestion. J. Chem. Technol. Biotechnol. 79, 1197-1203.

Vaxelaire, J., Cézac, P., 2004. Moisture distribution in activated sludges: a review. Water Res. 38, 2215–2230.

Vesilind, P.A., 1994. The role of water in sludge dewatering. Water Environ. Res. 66, 4–11.

Vliet, T.V., Lyklema, H., 2005. Rheology. In: LYKLEMA, J. (Editor). Fundamentals of Interface and Colloid Science 4, 6.1–6.88.

Wang, Q., Noguchi, C., Hara, Y., Sharon, C., Kakimoto, K., Kato, Y., 1997. Studies on anaerobic digestion mechanism: influence of pretreatment temperature on biodegradation of waste activated sludge. Environ. Technol 18, 999–1008.

Wang, F., Wang, Y., Ji, M., 2005. Mechanisms and kinetics models for ultrasonic waste activated sludge disintegration. J. Hazard. Mater. 123, 145–150.

Wang, R., Liu, J., Hu, Y., Zhou, J., Cen, K., 2014. Ultrasonic sludge disintegration for improving the co-slurrying properties of municipal waste sludge and coal. Fuel Process Technol. 125, 94–105.

Weemaes, M., Verstraete, W., 2001. Other treatment techniques. In: L Spinosa, PA Vesilind (Eds.), Sludge into biosolids, IWA Publishing, London, pp. 364-383.

Wett. B., Phothilangka, P., Eladawy, A., 2010. Systematic comparison of mechanical and thermal sludge disintegration technologies. Waste Manage. 30, 1057–1062.

Wetzel, R.G., 1991. Extracellular enzymatic interactions: storage, redistribution and interspecific communication. In: Chróst, R.J. (Ed.), Microbial Enzymes in Aquatic Environments. Springer, New York, USA.

Whiteley, C.G., Heron, P., Pletschke, B., Rose, P.D., Tshivhunge, S., Van Jaarsveld, F.P., Whittington-Jones, K., 2002. The enzymology of sludge solubilisation utilising sulphate reducing systems Properties of proteases and phosphatases. Enzyme Microb. Technol. 31, 419–424.

Whiteley, C.G., Burgess, J.E., Melamane, X., Pletschke, B., Rose, P.D., 2003. The enzymology of sludge solubilisation utilising sulphate-reducing systems: the properties of lipases. Water Res. 37, 289–296.

Wilson, C.A., Novak, J.T., 2009. Hydrolysis of macromolecular components of primary and secondary wastewater sludge by thermal hydrolytic pretreatment. Water Res. 43, 4489–4498.

Wingender, J., Neu, T.R., Flemming, H.C., 1999. What are bacterial extracellular polymeric substances? In: Wingender J, Neu TR, Flemming HC, editors. Microbial extracellular polymeric substances: characterization, structures and function. Berlin Heidelberg: Springer-Verlag.

Xu, J., Yuan, H., Lin, J., Yuan, W., 2014. Evaluation of thermal, thermal-alkaline, alkaline and electrochemical pretreatments on sludge to enhance anaerobic biogas production. J. Taiwan Inst. Chem. E. 45, 2531-2536.

Yang, Q. et al., 2010. Enhanced efficiency of biological excess sludge hydrolysis under anaerobic digestion by additional enzymes. Bioresour. Technol. 101, 2924–2930.

Yin, X., Han, P., Lu, X., Wang, Y., 2004. A review on the dewaterability of bio-sludge and ultrasound pretreatment. Ultrason. Sonochem. 11, 337–348.

Yu, G.H., He, P.J., Shao, L.M., 2009. Characteristics of extracellular polymeric substances (EPS) fractions from excess sludges and their effects on bioflocculability. Bioresour. Technol. 100, 3193–3198.

Yu, S., Zhang, G., Li, J., Zhao, Z., Kang, X., 2013. Effect of endogenous hydrolytic enzymes pretreatment on the anaerobic digestion of sludge. Bioresour. Technol. 146, 758–761.

Ziemba, C., Peccia, J., 2011. Net energy production associated with pathogen inactivation during mesophilic and thermophilic anaerobic digestion of sewage sludge. Water Res. 45, 4758-4768.

Publications derived from this work

Ruiz-Hernando, M., Labanda, J., Llorens, J., 2010. Effect of ultrasonic waves on the rheological features of secondary sludge. Biochemical Engineering Journal 52, 131-136.

Biochemical Engineering Journal 52 (2010) 131–136

Contents lists available at ScienceDirect

Biochemical Engineering Journal

journal homepage: www.elsevier.com/locate/bej

Effect of ultrasonic waves on the rheological features of secondary sludge

Maria Ruiz-Hernando, Jordi Labanda*, Joan Llorens

Department of Chemical Engineering, University of Barcelona, Martí i Franquès 1, 08028 Barcelona, Spain

Ruiz-Hernando, M., Martinez-Elorza, G., Labanda, J., Llorens, J., 2013. Dewaterability of sewage sludge by ultrasonic, thermal and chemical treatments. Chemical Engineering Journal 230, 102-110.

Chemical Engineering Journal 230 (2013) 102–110

Contents lists available at SciVerse ScienceDirect

Chemical Engineering Journal

journal homepage: www.elsevier.com/locate/cej

Dewaterability of sewage sludge by ultrasonic, thermal and chemical treatments

Maria Ruiz-Hernando, Guillermo Martinez-Elorza, Jordi Labanda*, Joan Llorens

Department of Chemical Engineering, University of Barcelona, Martí i Franquès 1, 08028 Barcelona, Spain

Ruiz-Hernando, M., Martín-Díaz, J., Labanda, J., Mata-Alvarez, J., Llorens, J., Lucena, F., Astals, S., 2014. Effect of ultrasound, low-temperature thermal and alkali pre-treatments on waste activated sludge rheology, hygienization and methane potential. Water Research 61, 119-129.

WATER RESEARCH 61 (2014) 119–129

Available online at www.sciencedirect.com

ScienceDirect

journal homepage: www.elsevier.com/locate/watres

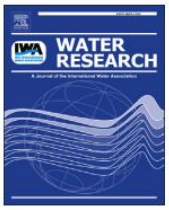

Effect of ultrasound, low-temperature thermal and alkali pre-treatments on waste activated sludge rheology, hygienization and methane potential

M. Ruiz-Hernando [a], J. Martín-Díaz [b,c], J. Labanda [a,c,], J. Mata-Alvarez [a,c], J. Llorens [a,c], F. Lucena [b,c], S. Astals [a,d]*

[a] *Department of Chemical Engineering, University of Barcelona, C/Martí i Franquès 1, 6th Floor, 08028 Barcelona, Spain*
[b] *Department of Microbiology, University of Barcelona, Av. Diagonal 645, 08028 Barcelona, Spain*
[c] *The Water Research Institute, University of Barcelona, Av. Diagonal 684, 08034 Barcelona, Spain*
[d] *Advanced Water Management Centre, The University of Queensland, St Lucia, QLD 4072, Australia*

Ruiz-Hernando, M., Simón, F.X., Labanda, J., Llorens, J., 2014. Effect of ultrasound, thermal and alkali treatments on the rheological profile and water distribution of waste activated sludge. Chemical Engineering Journal 255, 14-22.

Chemical Engineering Journal 255 (2014) 14–22

Contents lists available at ScienceDirect

Chemical Engineering Journal

journal homepage: www.elsevier.com/locate/cej

Effect of ultrasound, thermal and alkali treatments on the rheological profile and water distribution of waste activated sludge

Maria Ruiz-Hernando, Francesc-Xavier Simón, Jordi Labanda *, Joan Llorens

Department of Chemical Engineering, University of Barcelona, C/Martí i Franquès 1, 6th Floor, 08028 Barcelona, Spain

Ruiz-Hernando, M., Labanda, J., Llorens, J., 2015. Structural model to study the influence of thermal treatment on the thixotropic behaviour of waste activated sludge. Chemical Engineering Journal 262, 242–249.

Chemical Engineering Journal 262 (2015) 242–249

Contents lists available at ScienceDirect

Chemical Engineering Journal

journal homepage: www.elsevier.com/locate/cej

Structural model to study the influence of thermal treatment on the thixotropic behaviour of waste activated sludge

Maria Ruiz-Hernando, Jordi Labanda *, Joan Llorens

Department of Chemical Engineering, University of Barcelona, Martí i Franquès 1, 6th floor, 08028 Barcelona, Spain

Ruiz-Hernando, M., Cabanillas, E., Labanda, J., Llorens, J., 2015. Ultrasound, thermal and alkali treatments affect extracellular polymeric substances (EPSs) and improve waste activated sludge dewatering. Process Biochemistry 50, 438-446.

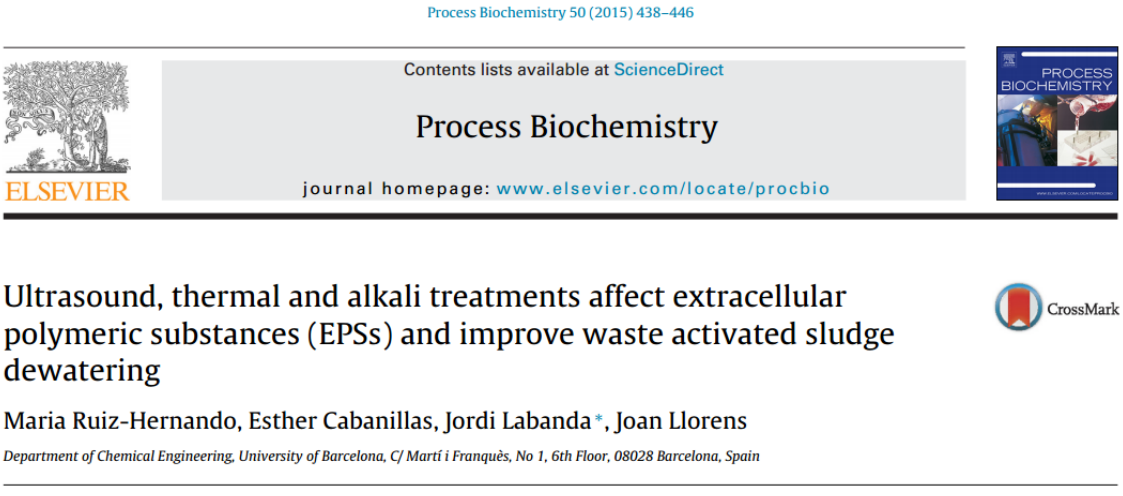

Process Biochemistry 50 (2015) 438–446

Contents lists available at ScienceDirect

Process Biochemistry

journal homepage: www.elsevier.com/locate/procbio

Ultrasound, thermal and alkali treatments affect extracellular polymeric substances (EPSs) and improve waste activated sludge dewatering

Maria Ruiz-Hernando, Esther Cabanillas, Jordi Labanda *, Joan Llorens

Department of Chemical Engineering, University of Barcelona, C/ Martí i Franquès, No 1, 6th Floor, 08028 Barcelona, Spain

Martín-Díaz, J., **Ruiz-Hernando, M.**, Astals, S., Lucena, F. Monitoring of clostridia in the assessment of biosolids treatments (**in preparation)**.

Resumen

Abreviaciones

DQOt	Demanda química de oxígeno total
DQOs	Demanda química de oxígeno soluble
EPSs	Sustancias poliméricas extracelulares
LB-EPSs	EPSs débilmente unidas a la superficie de la célula
TB-EPSs	EPSs fuertemente unidas a la superficie de la célula
E_S	Energía específica
HE	Habitantes equivalentes
GPC	Cromatografía de permeación en gel
SD	Grado de solubilización
SSRC	Esporas de clostridios sulfito-reductores
SOMCPH	Colifagos somáticos
ST	Sólido total
SV	Sólido volátil

1. INTRODUCCIÓN

La generación de lodos es una causa inherente del proceso de depuración de las aguas residuales. Durante dicho proceso, la contaminación del agua residual pasa al lodo, el cual deberá ser posteriormente tratado y evacuado. A raíz de la implantación de la Directiva 91/271/CEE (CEC, 1991), la cual establece el nivel de tratamiento que requiere el agua antes de ser descargada al medio ambiente, la producción de lodos aumentó notablemente. Dicha directiva establece que el tratamiento biológico es obligatorio para aglomeraciones de más de 2000 habitantes equivalentes (HE) que descargan en aguas dulces o estuarios, y también para aglomeraciones de más de 10000 HE que descargan en aguas costeras. Las estimaciones apuntan que la producción anual de lodos en el conjunto de la unión europea superará los 13 millones de toneladas (lodo seco) en el año 2020, lo cual representa un incremento del 30% respecto a la producción anual de 2005 (Milieu Ltd., WRc and RPA, 2010). En consecuencia, el desarrollo de procesos para la reducción y/o reutilización de los lodos resulta determinante para una apropiada gestión medioambiental.

Los dos tipos de lodos generados durante el proceso de depuración de las aguas residuales son el lodo primario y el lodo activado (también denominado lodo secundario o biológico). Ambos lodos se caracterizan por tener un elevado contenido en agua, el cual representa más del 95% del volumen del lodo (Colin and Gazbar, 1995). Por lo tanto, la deshidratación de lodos es fundamental para reducir su volumen. Por su parte, el lodo activado contiene el doble de nutrientes y menor carga contaminante que el lodo primario. Por lo tanto, si se trata por separado el lodo activado del primario (y no la mezcla como suele hacerse) se favorece el uso del lodo activado en agricultura tras su digestión. No obstante, las características de ambos lodos son muy distintas, de manera que el tratamiento exclusivo de lodo activado requiere ciertas atenciones. Por ejemplo, el lodo activado cuesta más de deshidratar que el primario debido principalmente a la presencia de las sustancias poliméricas extracelulares (EPSs, por sus siglas en inglés), las cuales atrapan fuertemente el agua. Este comportamiento atribuye al lodo una elevada viscosidad (Neyens and Baeyens, 2003). Las EPSs se componen mayoritariamente de proteínas, polisacáridos y sustancias húmicas (Frølund et al., 1996) y son el principal componente de la matriz de los flóculos del lodo. Dicha matriz

suele representarse mediante una estructura dinámica de EPSs dispuesta en doble capa: la capa interna está constituida por las EPSs fuertemente unidas a la superficie de la célula (TB-EPSs) y la capa externa por las EPSs débilmente unidas (LB-EPSs) (Li and Yang, 2007). Por otro lado, el lodo activado es también más difícil de digerir anaeróbicamente debido a las cadenas de glicanos presentes en las paredes celulares de las bacterias. De este modo, para poder deshidratar y digerir un lodo activado será necesario acondicionarlo previamente con el fin de (1) solubilizar las EPSs, favoreciendo así la liberación del agua retenida en la matriz de los flóculos del lodo, y (2) liberar la materia orgánica confinada en el interior de los flóculos y microorganismos, aumentando así su biodegradabilidad.

Existen diversos métodos para hidrolizar el lodo, como por ejemplo el tratamiento ultrasonido, térmico o alcalino (Ruiz-Hernando et al., 2013). El tratamiento ultrasonido hidroliza el lodo mediante la generación de burbujas de cavitación, las cuales crecen hasta un tamaño crítico y luego colapsan violentamente. El colapso cavitacional produce poderosas fuerzas hidromecánicas de cizalla en la masa del líquido (en este caso el lodo) que rodea las burbujas y unos focos locales de intenso calor y de altas presiones (Bougrier et al., 2006) que dan lugar a la generación de radicales hidroxilos muy reactivos. De este modo, la desintegración del lodo por ultrasonido es debido principalmente a las fuerzas hidromecánicas de cizalla y, en menor medida, al efecto oxidante de los radicales hidroxilos. Por otro lado, el tratamiento térmico se realiza generalmente a temperaturas comprendidas entre 60 y 180 ºC, ya que por encima de los 180 ºC la biodegradabilidad del lodo disminuye debido a la formación de compuestos refractarios (Wilson and Novak, 2009). Los tratamientos térmicos realizados a temperaturas inferiores o igual a 100 ºC se consideran tratamientos térmicos a baja temperatura. Estos tratamientos suponen un menor coste energético, pero requieren de un mayor tiempo de contacto que los realizados a temperaturas más elevadas. Además de solubilizar y mejorar la biodegradabilidad del lodo, el tratamiento térmico tiene la ventaja de higienizarlo. Finalmente, el tratamiento alcalino se basa en añadir un agente alcalino (por ejemplo, NaOH) al lodo durante un tiempo determinado. Durante ese tiempo, el reactivo en cuestión reacciona con las paredes celulares, lo cual

provoca la ruptura de las células microbianas. Así, este tratamiento también puede higienizar el lodo.

Si el lodo quiere destinarse a agricultura deberá estar higienizado. La higienización de lodos se mide mediante microorganismos indicadores. No obstante, los indicadores convencionales (como por ejemplo las bacterias fecales) tienen el inconveniente de ser poco resistentes y poco duraderos, por lo que no son representativos de los patógenos reales del lodo. Por poner un ejemplo; podría darse el caso que un lodo no mostrase presencia de *E*. *coli* (por lo que aparentemente estaría higienizado) y sin embargo tuviese una gran cantidad de formas resistentes de protozoos. Por este motivo, es interesante utilizar microorganismos indicadores que representen a aquellos patógenos más resistentes. Las esporas de clostridios sulfito-reductores (SSRC, por sus siglas en inglés) se han propuesto como indicadores de ooquistes de protozoarios (Payment and Franco, 1993), mientras que los bacteriófagos de bacterias entéricas (como los colifagos somáticos; SOMCPH) se han propuesto como indicadores de los virus transmitidos por el agua (IAWPRC, 1991).

Por último, cabe señalar que entender el comportamiento reológico de los lodos es esencial para poder controlar los procesos de tratamiento. Como ya se ha comentado, los lodos presentan una elevada viscosidad, lo cual dificulta su manejo y representa elevados costes de bombeo. Debido a que los tratamientos antes mencionados modifican ciertas características de los lodos, tales como la estructura, el tamaño de los flóculos y su composición, es evidente que inciden directamente sobre el perfil reológico de los lodos. Los lodos se consideran fluidos no-newtonianos pseudoplásticos, lo cual indica que su viscosidad se reduce al incrementar el gradiente de velocidad, y tixotrópicos, lo cual indica que su viscosidad disminuye con el tiempo. El modelo de Ostwald–de Waele es uno de los más utilizados para representar el comportamiento pseudoplástico de los lodos (Ratkovich et al., 2013). También existen otros modelos, como por ejemplo el modelo de Herschel-Bulkley o el de Bingham. A diferencia del modelo de Ostwald, estos modelos se caracterizan por la presencia del límite de fluencia (*yield stress*, en inglés), por debajo del cual la muestra que se está analizando no fluye. No obstante, encontrar el valor del límite de fluencia real es realmente complicado, ya que su determinación no es unívoca y puede variar según el modelo utilizado (Labanda et al., 2007). El

comportamiento tixotrópico de los lodos suele detectarse mediante la medición del área de histéresis, que es el área delimitada entre la curva ascendente y descendente en un ensayo de aumento y disminución del gradiente de velocidad. No obstante, el área de histéresis es sólo un método para observar tixotropía y no diferencia ni revela los comportamientos cinéticos individuales de los procesos de destrucción y construcción. En este sentido, es mejor utilizar modelos estructurales. El modelo reológico estructural planteado en este trabajo permitió obtener los coeficientes cinéticos tixotrópicos para el proceso de destrucción (K_{down}) y los coeficientes cinéticos tixotrópicos para el proceso de construcción (K_{up}), así como el parámetro que cuantifica la alineación instantánea y la deformación de los flóculos de lodo (m).

2. OBJETIVO

El objetivo general de esta tesis ha sido estudiar la influencia de los tratamientos ultrasonido, térmico a baja temperatura y alcalino sobre las propiedades fisicoquímicas y biológicas de lodos activados. Concretamente, se ha estudiado el efecto de estos tres tratamientos sobre la reología, la deshidratabilidad, el potencial de biometanización y la higienización de los lodos.

3. MATERIALES Y MÉTODOS

3.1. Muestras de lodo

Las muestras de lodo activado e inóculo (lodo digerido) utilizadas en el presente estudio proceden de depuradoras municipales de la provincia de Barcelona. En la depuradora, el lodo activado se espesó mediante centrifugación. Una vez en el laboratorio, las muestras de lodo se guardaron en la nevera a 4 ºC para minimizar el efecto de la actividad bacteriana.

3.2. Tratamientos realizados

Los tratamientos realizados fueron el ultrasonido, el térmico a baja temperatura y el alcalino con NaOH. El dispositivo de ultrasonido utilizado fue el HD2070 ultrasonic homogenizer (Sonopuls Bandelin), el cual opera a una frecuencia de 20 kHz y tiene una potencia máxima de 70 W. Para realizar el tratamiento se fijó una potencia determinada y se ultrasonicó siempre el mismo volumen de lodo a diferentes tiempos de tratamiento. El nivel de tratamiento se midió en términos de energía específica (E_S):

$$E_S = \frac{P \cdot t}{V \cdot ST}$$

donde *P* es la potencia, *t* es el tiempo de ultrasonicación, *V* es el volumen de lodo a tratar y ST el contenido de sólidos totales de la muestra de lodo. Las E_S estudiadas fueron de 3000 a 33000 kJ/kg ST. Durante la ultrasonicación, la muestra se refrigeró con hielo para evitar el incremento de temperatura debido al tratamiento.

Para el tratamiento térmico se realizaron dos ensayos diferentes. El tratamiento térmico para el estudio de la reología y deshidratabilidad del fango se realizó en un reactor (Autoclave Engineers) muy bien cerrado para evitar pérdidas de agua por evaporación. Las temperaturas estudiadas fueron de 60 a 100 ºC. El tratamiento consistió en calentar el lodo hasta la temperatura deseada (aproximadamente 30 min de calentamiento) más 30 min de mantenimiento de dicha temperatura. Durante este tiempo, el lodo fue sometido a agitación para garantizar la homogeneidad del tratamiento. El tratamiento térmico para el estudio de la higienización y el potencial de biometanización se llevó a cabo en un baño termostático (Huber Polystat CC2) a 70 y 80 ºC. Los tiempos de exposición para la temperatura de 80 ºC fueron 10, 15 y 30 min. Estos tiempos incluyen la rampa de subida de la temperatura hasta alcanzar los 80 ºC, la cual fue de 10 min; es decir, el tiempo de exposición de 15 min corresponde a 10 min de calentamiento más 5 min de mantenimiento a 80 ºC.

El tratamiento alcalino consistió en añadir NaOH al lodo y pasadas 24 horas neutralizar con HCl en un rango de pH de 6,5-7,5. Las concentraciones de NaOH fueron de 0,784 a 235 g NaOH/kg ST.

3.3. Estudio reológico en la región viscoelástica no lineal

El comportamiento reológico en la región viscoelástica no lineal se analizó mediante los ensayos *loop* y *step*. El reómetro utilizado fue un reómetro de control de esfuerzo (Haake RS300). La geometría utilizada fue un cono de 4º y una placa estacionaria de 35 mm.

Para el ensayo *step*, la muestra de lodo se sometió a un gradiente de velocidad fijo de 5 s^{-1} durante 10 min. Posteriormente el gradiente de velocidad se cambió repentinamente a 30, 125 o 300 s^{-1} durante 10 min para alcanzar estados estables. La evolución de la viscosidad con el tiempo se ajustó siguiendo una ecuación de primer orden (Ruiz-Hernando et al., 2010), lo que permitió determinar la K_{down} y la viscosidad en estado estacionario. Finalmente, las viscosidades en estado estacionario se ajustaron mediante el modelo de Ostwald-de Waele:

$$\eta_e = K \cdot \dot{\gamma}^{n-1}$$

donde η_e es la viscosidad en estado estacionario, $\dot{\gamma}$ es el gradiente de velocidad (s^{-1}), K es el índice de consistencia ($Pa \cdot s^n$) y n es el índice de comportamiento al flujo (-).

El ensayo *loop* consistió en aumentar linealmente el gradiente de velocidad hasta alcanzar un gradiente máximo (30, 125 o 300 s^{-1}) en 5 min, posteriormente mantener el máximo gradiente de velocidad 10 min más y finalmente reducir linealmente el gradiente de velocidad hasta 0 s^{-1} en 5 min. Antes de iniciar el test, el lodo se sometió a un gradiente de 5 s^{-1} durante 10 min para eliminar el historial de deformaciones previas sobre el material. El área de histéresis (Ha) se midió mediante la siguiente ecuación:

$$Ha = \int_0^t \tau \cdot d\dot{\gamma}(t)$$

Donde τ es el esfuerzo de cizalla (Pa).

3.4. Valoración de la deshidratación

Para la cuantificación del agua ligada (*bound water*, en inglés) primero fue necesario medir el agua libre y el agua total del lodo. El agua libre se midió mediante calorimetría diferencial de barrido (DSC, por sus siglas en inglés). El agua total se midió secando la muestra de lodo a 105 ºC. La diferencia entre el agua total y el agua libre fue el agua ligada, la cual se expresó como kg agua ligada/kg sólido seco.

Para el test de centrifugación, los tubos de la centrífuga se llenaron con aproximadamente 12 g de lodo (se anotó el peso exacto) y posteriormente se centrifugaron a 2500 x g durante 15, 30 o 45 min. Tras la centrifugación se extrajo el sobrenadante generado y se volvieron a pesar los tubos de la centrífuga. La diferencia entre el peso inicial y el peso obtenido tras extraer el sobrenadante corresponde al agua extraída del lodo mediante centrifugación. El agua extraída se expresó como porcentaje:

$$\%_{Agua\ extraída} = \frac{W_{inicial} - W_{después\ de\ extraer\ el\ sobrenadante}}{W_{inicial}} \cdot 100$$

3.5. Extracción y caracterización de las EPSs

3.5.1. Protocolo de extracción de las EPSs

La muestra de lodo se centrifugó a 2000 x g durante 10 min. El sobrenadante se descartó, mientras que el lodo sedimento restante se enrasó hasta alcanzar el volumen inicial utilizando una solución tampón (pH 7) compuesta de Na_3PO_4, NaH_2PO_4, NaCl, y KCl en proporciones molares de 2:4:9:1 (Frølund et al., 1995). La conductividad de la

solución tampón se ajustó a la conductividad de las muestras de lodo activado. La suspensión (lodo + solución tampón) se centrifugó a 5000 x *g* durante 15 min y seguidamente se recogió el sobrenadante, la materia orgánica soluble del cual fue la fracción LB-EPS. Este paso se repitió una vez más para conseguir un mayor lavado de LB-EPSs del lodo. A continuación, el lodo sedimento se enrasó de nuevo hasta alcanzar el volumen inicial utilizando la ya mencionada solución tampón y se sometió a ultrasonicación (HD2070 ultrasonic homogeniser, Sonopuls Bandelin) durante 10 min. Finalmente, la suspensión se centrifugó a 20000 x *g* durante 20 min y seguidamente se recogió el sobrenadante, la materia orgánica soluble del cual fue la fracción TB-EPS. Ambas fracciones de EPSs se filtraron mediante un filtro de 0,45 mm de baja retención de proteína (PVDF). El protocolo de extracción se realizó por triplicado.

3.5.2. Caracterización de las EPSs

Las EPSs se caracterizaron en base al contenido de carbono orgánico total, proteína, ácido húmico y polisacárido. Las proteínas y polisacáridos se midieron mediante espectrofotometría (Perkin Elmer UV/VIS Lambda 20 spectrophotometer). El protocolo utilizado para cuantificar los polisacáridos fue el de la antrona, utilizando glucosa como estándar (Frølund et al., 1996). Las proteínas se midieron mediante el protocolo de Lowry, utilizando albúmina de suero bovino (BSA) como estándar (Lowry et al., 1951). Estos análisis se realizaron por triplicado para cada extracción.

3.5.3. Distribución de los pesos moleculares de las proteínas

La distribución de pesos moleculares de las proteínas en las EPSs se llevó a cabo mediante cromatografía de permeación en gel (GPC, por sus siglas en inglés). Se utilizó un cromatógrafo (Waters Alliance 2695) equipado con dos columnas en serie (Ultrahydrogel 500; 10 µm; 7,8 x 300 mm y Ultrahydrogel 250; 6 µm; 7,8 x 300 mm). La fase móvil consistió en una solución tampón de fosfato 50 mM que contenía 0,9% de NaCl. Las proteínas se midieron a 280 nm (detector Waters 2996 photo diode array), corrigiendo la interferencia de los ácidos nucleicos (260 nm). La calibración de los pesos

moleculares se realizó utilizando 5 estándares de proteínas: beta-amilasa: 200000 Da; albúmina de suero bovino: 66000 Da; anhidrasa carbónica: 29000 Da; citocromo c: 12400 Da; y el aminoácido 3,4-dihydroxy-DL-fenilalanina: 197 Da.

3.6. Valoración de la higienización

3.6.1. Recuento de *E. coli* y SSRC

Se mezclaron 5-10 g de lodo con PBS (pH 7,2) en proporciones 1:10 (m/v). La solución se homogeneizó mediante agitación (900 osc/min durante 30 min) y finalmente se centrifugó (300 x *g* durante 3 min, 4 ºC). El sobrenadante obtenido tras la centrifugación se utilizó para hacer el recuento de *E. coli* y SSRC. Los análisis se realizaron por duplicado y se hicieron varias diluciones.

El recuento de *E. coli* se realizó mediante la siembra en placa en agar Chromocult (Merck, Germany) complementado con un suplemento selectivo para *E. coli*/coliformes. Las placas se incubaron toda la noche a 44 ºC y pasado este tiempo se contaron la colonias de color azul oscuro y violeta, las cuales corresponden a la *E. coli*.

Para el recuento de las SSRC fue necesario someter las muestras a un choque térmico de 80 ºC durante 10 min. Posteriormente las muestras se sembraron anaeróbicamente por inoculación en masa en un medio de agar selectivo (*Clostridium perfringens*) y se incubaron toda la noche a 44 ºC. Pasado este tiempo se contaron las esferas de color negro, las cuales corresponden a las SSRC.

3.6.2. Recuento de SOMCPH

Se mezclaron 5-10 g de lodo con una solución (pH 7,2) que contenía un 10% de extracto de carne (Becton Dickinson, France) en proporciones 1:10 (m/v). La solución se homogeneizó mediante agitación (900 osc/min durante 30 min) y finalmente se centrifugó (4000 x *g* durante 30 min, 4 ºC). El sobrenadante se filtró por 0,22 µm y se utilizó para analizar los SOMCPH siguiendo la norma ISO 10705-2 (Anonymous, 2000).

3.7. Potencial de biometanización

El potencial de biometanización se midió en condiciones mesófilas siguiendo el procedimiento descrito por Angelidaki et al. (2009). Los ensayos de biometanización se realizaron por triplicado en botellas de 115 mL cerradas con un septum de PTFE/butilo. Las botellas se llenaron con inóculo (lodo digerido) y lodo activado en proporción de ratio 2 en base al contenido de sólidos volátiles (SV) de las muestras. Antes de sellar las botellas se rociaron con nitrógeno gas durante un minuto (3 L/min). Finalmente, las botellas se colocaron en un baño a 37 ± 1 ºC. Las botellas se mezclaron manualmente dos veces al día. La producción de biogás se midió mediante un vacuómetro modelo Ebro - VAM 320 (previamente se había descargado la sobrepresión). El contenido de metano del biogás generado se analizó utilizando un cromatógrafo (Shimadzu GC-2010+ gas chromatograph) equipado con una columna capilar (Carboxen®-1010 PLOT) y un detector de conductividad térmica.

4. RESULTADOS Y DISCUSIÓN

4.1. Efecto de los tratamientos sobre la reología en la región viscoelástica no lineal

Los datos reológicos mostrados a continuación corresponden a una muestra de lodo con un contenido de ST de 45,9±0,9 g/L. Tanto el lodo no tratado como los lodos tratados mostraron comportamiento pseudoplástico; es decir, su viscosidad disminuyó potencialmente al aumentar el gradiente de velocidad. La Figura 1 muestra este comportamiento para el lodo no tratado y para una condición de cada tratamiento en formato de doble eje logarítmico. Como puede observarse, los resultados experimentales se ajustan muy bien al modelo de Ostwald-de Waele.

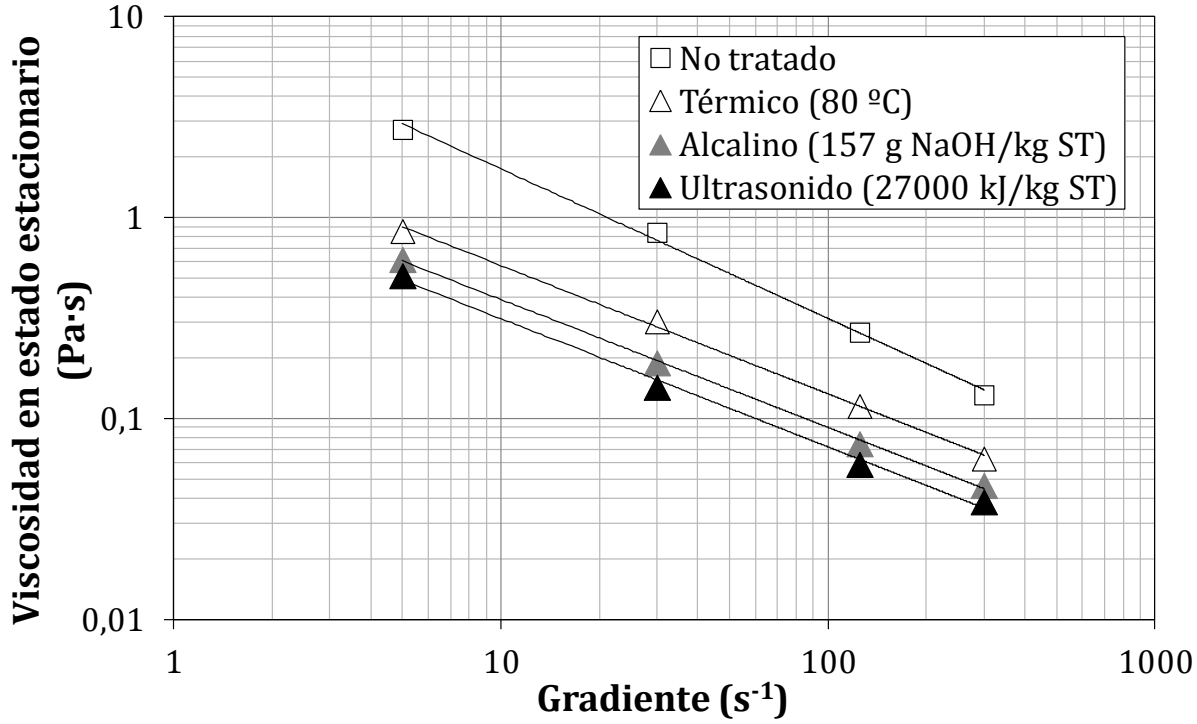

Figura 1. Viscosidad en estado estacionario en función del gradiente de velocidad. Las líneas continuas corresponden al ajuste del modelo de Ostwald-de Waele.

La Tabla 1 muestra los parámetros obtenidos del ajuste del modelo de Ostwald-de Waele; el índice de consistencia, *K*, y el índice de comportamiento al flujo, *n*. El índice de consistencia es una medida de la firmeza media de la muestra; así, cuanto mayor es el valor de *K*, mayor es la viscosidad. El índice de comportamiento al flujo está ligado a la dependencia de la viscosidad con el gradiente; así, $n<1$ en fluidos pseudoplásticos, $n=1$ en fluídos newtonianos y $n>1$ en fluidos dilatantes. Al aumentar la intensidad de los tratamientos el índice de consistencia disminuyó mientras que el índice de comportamiento aumentó (aunque siempre quedó por debajo de la unidad), lo cual indica que los lodos perdieron parte de su pseudoplasticidad y se volvieron menos viscosos con los tratamientos.

Tabla 1. Parámetros reológicos.

	K (Pa·s^n)	***n (-)***	**Área de histéresis (Pa·s^{-1})[1]**
Sin tratar	9,67	0,256	1569
Ultrasonido (kJ/kg ST)			
5000	4,56	0,261	198
11000	2,67	0,311	120
27000	1,36	0,392	44,3
Térmico (kJ/kg ST; ºC)			
11000 (60 ºC)	2,83	0,337	420
15000 (80 ºC)	2,50	0,362	335
18000 (90 ºC)	2,15	0,371	89,1
Alcalino(g NaOH/kg ST)			
35,3	7,38	0,222	1161
70,6	4,84	0,257	558
157	1,70	0,363	306

[1] El valor del área de histéresis corresponde a un gradiente de 300 s^{-1}.

La Figura 2 muestra la viscosidad en estado estacionario correspondiente a un gradiente de 5 s^{-1} para el lodo sin tratar y los lodos tratados. La viscosidad se redujo tras los tratamientos, especialmente después del ultrasonido; la viscosidad se redujo alrededor de un 80% con respecto al lodo sin tratar al aplicar una E_S de 27000 kJ/kg ST. Por el contrario, las concentraciones más bajas del tratamiento alcalino fueron las que menos redujeron la viscosidad. En cuanto al tratamiento térmico, la reducción fue similar para las tres temperaturas analizadas.

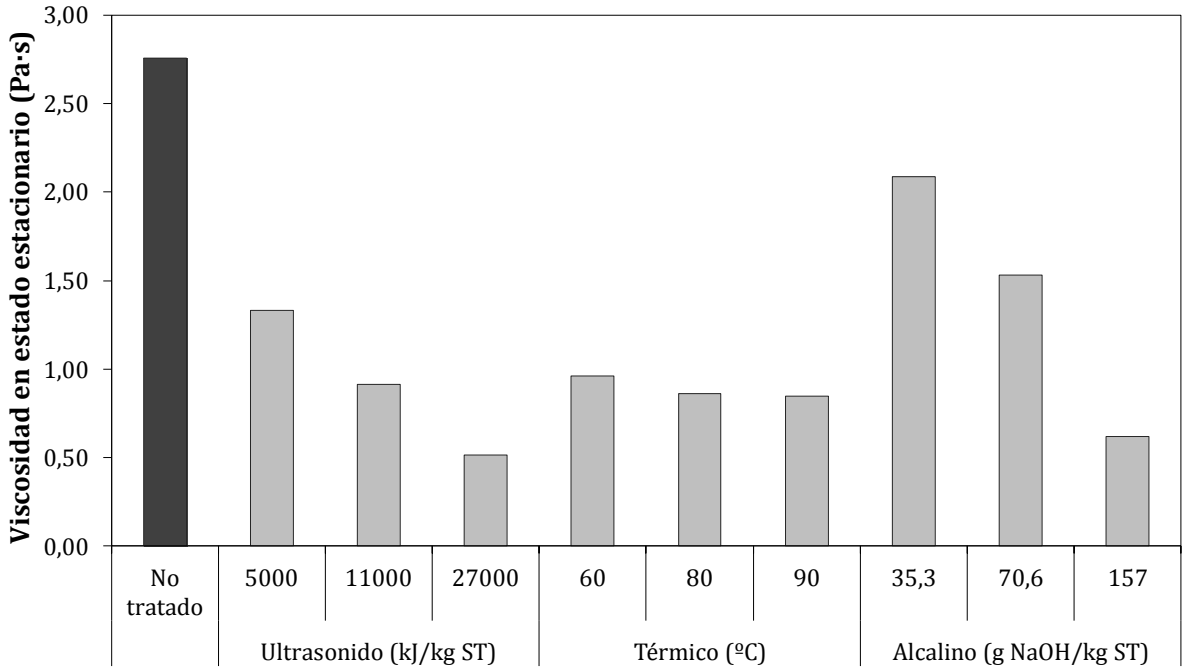

Figura 2. Viscosidad en estado estacionario a un gradiente de 5 s^{-1}.

En condiciones no estacionarias, todos los lodos mostraron comportamiento tixotrópico, tal y como se observa por la presencia del área de histéresis (Figura 3).

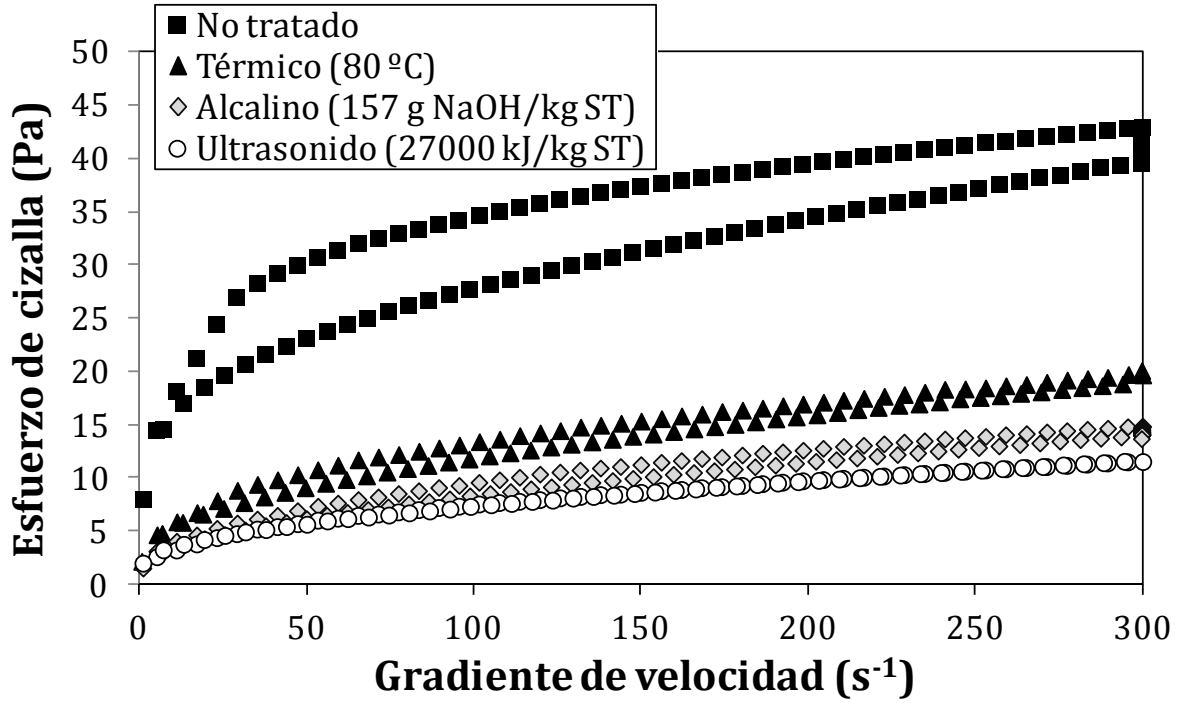

Figura 3. *Loops* para el lodo sin tratar y tres lodos tratados.

La Tabla 1 muestra los valores de las áreas de histéresis para el lodo sin tratar y los tratados. Como puede apreciarse, los tratamientos redujeron notablemente el área de histéresis.

El modelo estructural utilizado en este trabajo para examinar el comportamiento tixotrópico de los lodos se basa en la definición del parámetro estructural, *S*, el cual cuantifica el nivel estructural de la estructura interna para cualquier tiempo y velocidad de cizallamiento (Ruiz-Hernando et al., 2015a). Los resultados del modelo mostrados a continuación (Tabla 2) corresponden a una muestra de lodo con un contenido de ST de 56,7 ± 0,7 g/L.

Tabla 2. Parámetros obtenidos del modelo estructural.

	K_{down} (s^{-1}) [1]	**K_{up} (s^{-1}) [1]**	**m (-)**
Sin tratar	0,688	0,361	0,622
Ultrasonido (kJ/kg ST)			
3000	0,453	0,281	0,604
7000	0,419	0,196	0,593
17000	0,390	0,156	0,590
27000	0,354	0,120	0,580
33000	0,329	0,101	0,573
Térmico (kJ/kg ST; ºC)			
12000 (60 ºC)	0,435	0,274	0,612
15000 (70 ºC)	0,351	0,208	0,577
17000 (80 ºC)	0,249	0,175	0,534
20000 (90 ºC)	0,151	0,106	0,517
22000 (100 ºC)	0,089	0,079	0,474
Alcalino (g NaOH/kg ST)			
0,784	0,638	0,274	0,594
7,84	0,543	0,257	0,520
78,4	0,470	0,217	0,542
157	0,475	0,180	0,483
235	0,414	0,169	0,452

[1] Valores de K_{down} y K_{up} proporcionados para un gradiente de 5 s^{-1}.

Como puede apreciarse, los tratamientos redujeron los coeficientes cinéticos para el proceso de destrucción (K_{down}) y construcción (K_{up}), así como el parámetro que cuantifica la alineación instantánea y la deformación de los flóculos de lodo (m). Concretamente, K_{down} se redujo tanto al aumentar el gradiente de velocidad como la intensidad de los tratamientos. Esto puede deberse a que cuando los flóculos son pequeños (ya sea por el efecto del tratamiento o por el gradiente) les cuesta más alcanzar el equilibrio. Los valores de K_{up} fueron siempre más bajos que sus correspondientes valores de K_{down}, lo cual indica que el proceso de construcción fue más lento que el de destrucción. El hecho de que m no haya alcanzado un valor próximo a cero en ningún caso significa que las estructuras de los lodos siempre experimentaron alineación.

4.2. Efecto de los tratamientos sobre la deshidratación

4.2.1. Agua ligada y agua extraída mediante centrifugación

Como puede verse en la Tabla 3, los tratamientos aumentaron ligeramente el agua ligada. Esto podría hacer pensar que los tratamientos empeoraron la deshidratación. Sin embargo, esto no fue así, tal y como se muestra a continuación. Este hecho puede explicarse si se entiende que el agua libre medida mediante el ensayo DSC comprende tanto el agua libre como el agua intersticial. Por lo tanto, lo que incrementó con los tratamientos fue principalmente el agua superficial (Ruiz-Hernando et al., 2014b).

Tabla 3. Contenido de agua ligada en los lodos.

	Agua ligada (agua superficial + agua de hidratación) (kg/kg lodo seco)
Sin tratar	3,06
Ultrasonido (kJ/kg ST)	
5000	3,05
11000	3,23
27000	3,83
Térmico (kJ/kg ST; ºC)	
11000 (60 ºC)	4,00
15000 (80 ºC)	3,55
18000 (90 ºC)	4,37
Alcalino (g NaOH/kg ST)	
35,3	4,23
70,6	4,28
157	4,29

La Figura 4 muestra la cantidad de agua que fue posible extraer del lodo sin tratar y de los lodos tratados tras centrifugarlos a 2500 x *g* durante 15 min. Al comparar la cantidad de agua extraída de los lodos tratados con respecto al lodo sin tratar pueden identificarse aquellas condiciones de tratamiento que mejorar o empeoran la deshidratación. Así, las tres condiciones del tratamiento térmico mejoraron la deshidratación, especialmente las temperaturas más altas (80 y 90 ºC). En cambio, sólo las condiciones más intensas del tratamiento por ultrasonidos (27000 kJ/kg ST) y alcalino (157 g NaOH/kg ST) permitieron mejorar la deshidratación.

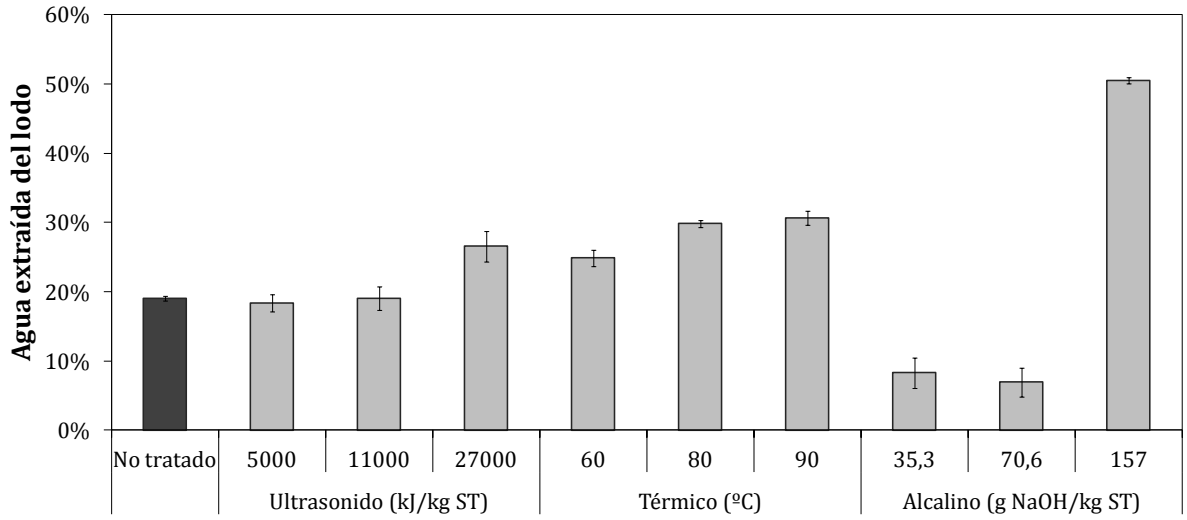

Figura 4. Agua extraída mediante centrifugación a 2500 x *g* durante 15 min.

Con el fin de evaluar con más detalle el efecto de los tratamientos sobre la deshidratación, se llevó a cabo la extracción y posterior caracterización de la EPSs. Las EPSs son componentes integrales de la matriz de los flóculos del lodo y se caracterizan por retener fuertemente el agua. Por este motivo, la presencia de las EPSs constituye una de las principales razones de la mala deshidratación de los lodos activados. Los análisis de las EPSs se realizaron sobre el lodo sin tratar y sobre una única condición de cada tratamiento. La condición óptima de cada tratamiento se seleccionó en base a criterios reológicos y de deshidratación. Así, la E_S seleccionada para el tratamiento por ultrasonidos fue 27000 kJ/kg ST, ya que fue la que más redujo la viscosidad y la única que permitió extraer agua del lodo. Para el tratamiento térmico se seleccionó la temperatura de 80 ºC, ya que tanto la reducción de la viscosidad como la cantidad de agua extraída por centrifugación fue muy similar a la temperatura de 90 ºC. Para el tratamiento alcalino se seleccionó la concentración de 157 g NaOH/kg ST, ya que fue la única que permitió extraer agua del lodo.

4.2.2. Caracterización de las EPSs

La Figura 5 muestra el contenido en proteína y polisacárido de las fracciones LB-EPS y TB-EPS.

A

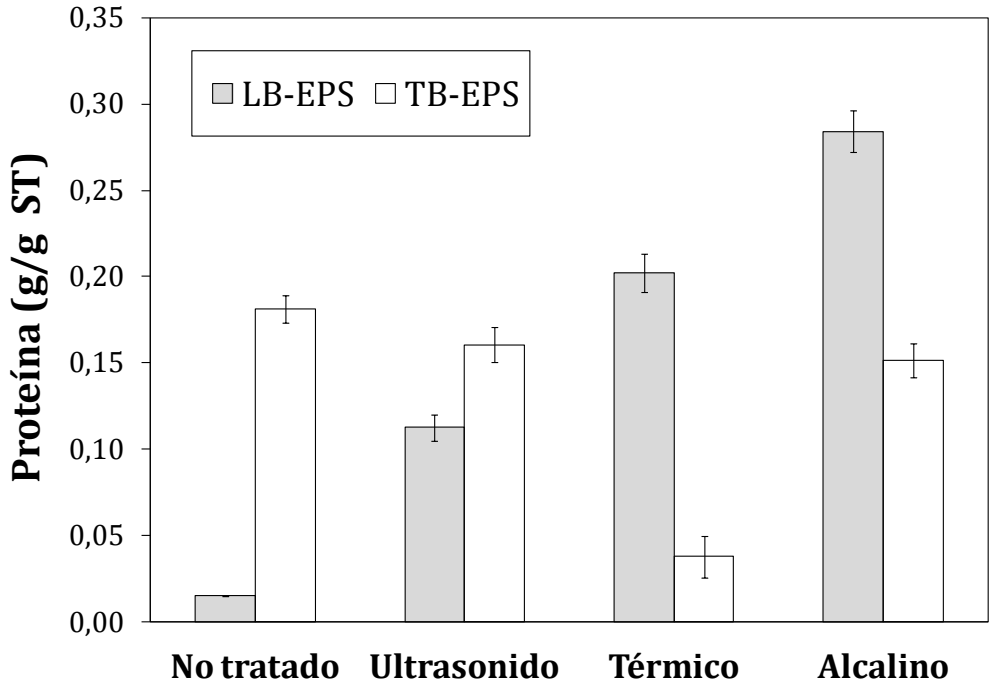

B

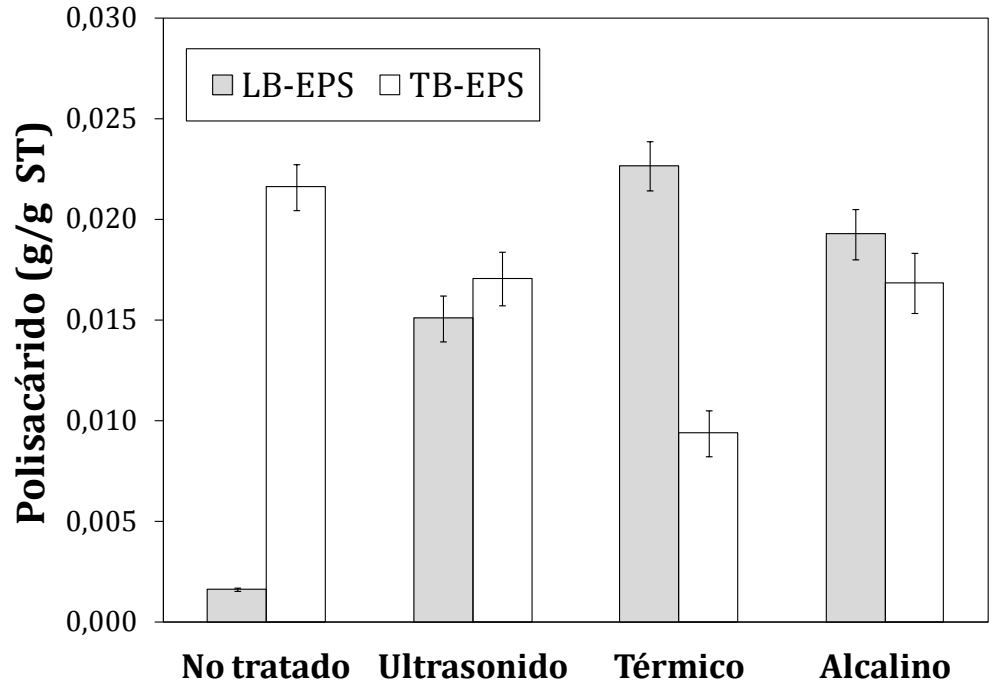

Figura 5. Caracterización bioquímica de las EPSs: (A) Concentración de proteína y (B) Concentración de polisacárido. Tratamiento por ultrasonidos: 27000 kJ/kg ST; Tratamiento térmico: 80 ºC (1h); Tratamiento alcalino: 157 g NaOH/kg ST.

El análisis del lodo sin tratar reveló que las proteínas son el principal constituyente de las EPSs. Estas proteínas se encontraron principalmente en la fracción TB-EPS (92% en peso) y apenas en la fracción LB-EPS (8%) para el lodo no tratado, lo cual es consistente con los resultados encontrados en la bibliografía. El predominio de las proteínas en las EPSs podría atribuirse a la presencia de una gran cantidad de exoenzimas. Los polisacáridos representaron una pequeña porción de las EPSs debido a que son muy biodegradables. En comparación con el lodo sin tratar, los lodos tratados mostraron un aumento importante de proteínas y polisacáridos en la fracción LB-EPSs. Por lo tanto, los tratamientos solubilizaron las EPSs. El tratamiento alcalino fue el tratamiento que más EPSs solubilizó (muestra el mayor contenido de proteínas en la fracción en LB-EPS), seguido del térmico y finalmente del ultrasonido (Figura 5a). Como ya se ha comentado, las EPSs atrapan fuertemente el agua del lodo, así que es concebible que tras su solubilización se libere parte del agua intersticial retenida. De hecho, se observó una relación directa entre el agua extraída mediante centrifugación y la solubilización de las EPSs (Ruiz-Hernando et al., 2015b). Así, el tratamiento alcalino fue el tratamiento que más agua permitió extraer (Figura 4) debido a que fue el que más EPSs solubilizó (Figura 5a). Por el contrario, la fracción TB-EPS se redujo ligeramente con los tratamientos ultrasonido y alcalino, y notablemente con el tratamiento térmico. Concretamente, el tratamiento térmico redujo el contenido de proteínas de la fracción TB-EPS aproximadamente un 80% en comparación con el lodo sin tratar.

4.2.3. Distribución de pesos moleculares de las proteínas

Las Figuras 6a y 6b muestran la distribución de pesos moleculares de las proteínas en las fracciones LB-EPS y TB-EPS, respectivamente. La distribución de los pesos moleculares se ha representado como dW/dLogM vs. LogM, donde W es la masa de material proteico de peso molecular M (M está expresado en Daltons).

A

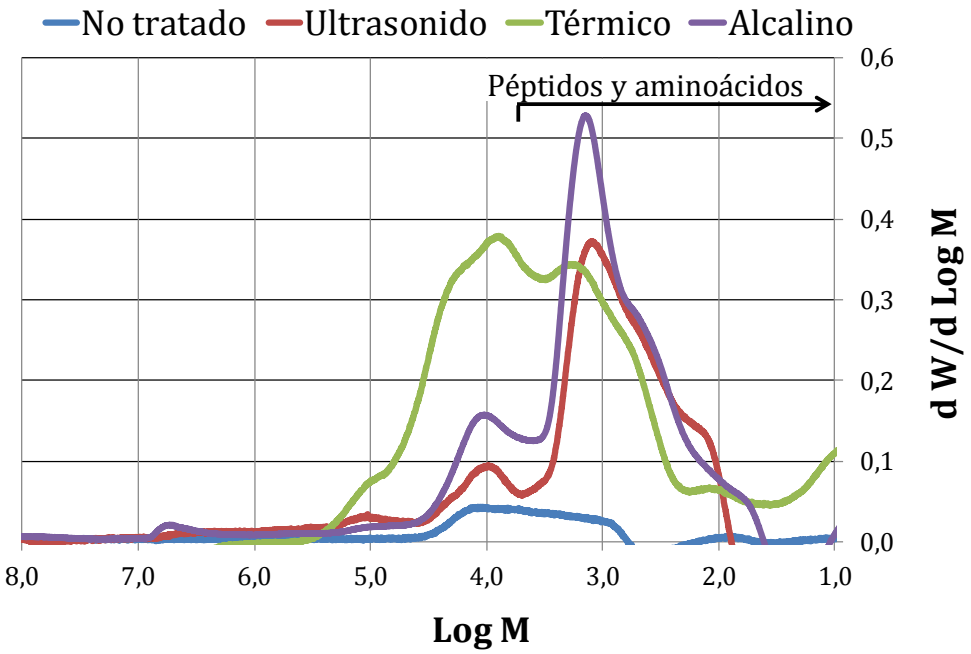

B

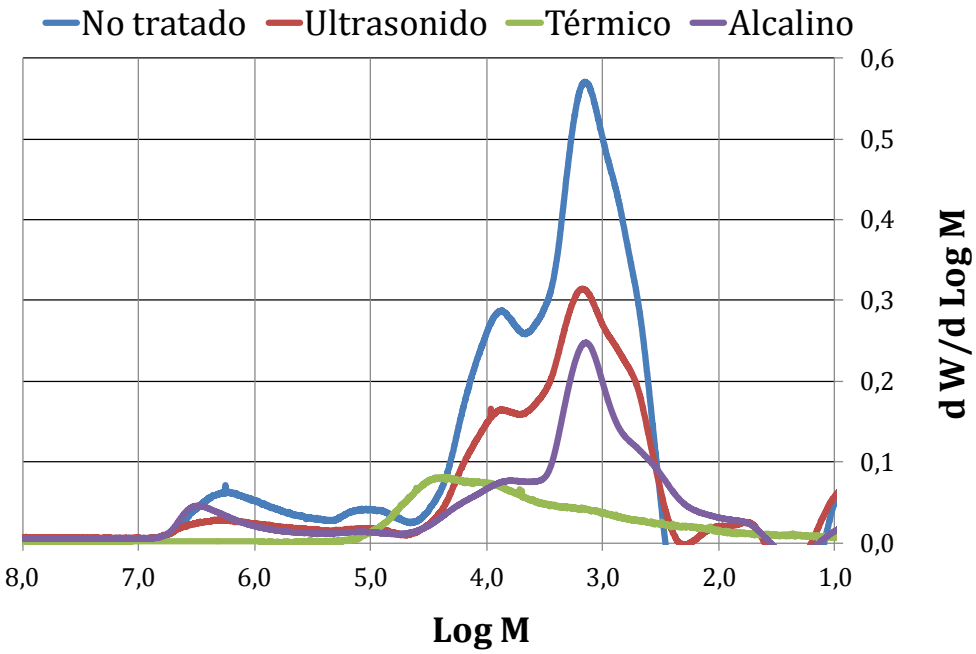

Figura 6. Distribución de pesos moleculares de las proteínas en las fracciones (A) LB-EPS y (B) TB-EPS. Tratamiento por ultrasonidos: 27000 kJ/kg ST; Tratamiento térmico: 80 ºC (1h); Tratamiento alcalino: 157 g NaOH/kg ST.

Para el lodo sin tratar, la mayoría de las proteínas se encontraron en la fracción TB-EPS (Figura 6b) y muy pocas en la fracción LB-EPS (Figura 6a). Por el contrario, los lodos tratados mostraron grandes cantidades de proteína en la fracción LB-EPS, como ya se ha mostrado en la Figura 5a. Los cromatogramas muestran la existencia de tres grupos de sustancias proteicas: péptidos, proteínas de bajo peso molecular (de aproximadamente 10 kDa) y proteínas de elevado peso molecular (de aproximadamente 1500 kDa).

El tratamiento ultrasonido solubilizó una porción de los péptidos y proteínas de bajo peso molecular. El tratamiento alcalino solubilizó la mayoría de los péptidos y proteínas pequeñas, más una pequeña porción de las proteínas grandes. El tratamiento térmico solubilizó la mayoría de las sustancias proteicas. Sin embargo, se observa la ausencia de proteínas de elevado peso molecular en ambos cromatogramas después del tratamiento térmico. Este hecho puede deberse a la modificación de la estructura terciaria de estas proteínas (desnaturalización) debido a la elevada temperatura. Así, el tratamiento térmico habría destruido la capacidad de floculación de las proteínas grandes, reduciendo la capacidad de éstas para retener el agua y liberando, finalmente, el agua retenida en la matriz de los flóculos del lodo. No obstante, a pesar de la desnaturalización de las proteínas grandes, el tratamiento térmico no permitió extraer tanta agua mediante centrifugación como el alcalino (Figura 4), lo cual sugiere que la solubilización de las EPSs es decisiva para una deshidratación óptima.

4.3. Efecto de los tratamientos sobre la higienización y la digestión anaerobia

4.3.1. Estudio de la higienización del lodo

La Figura 7 muestra las concentraciones de los microorganismos indicadores para el lodo sin tratar y para una condición de cada tratamiento (ultrasonido: 27000 kJ/kg ST; térmico: 80 ºC (15 min); alcalino: 157 g NaOH/kg ST).

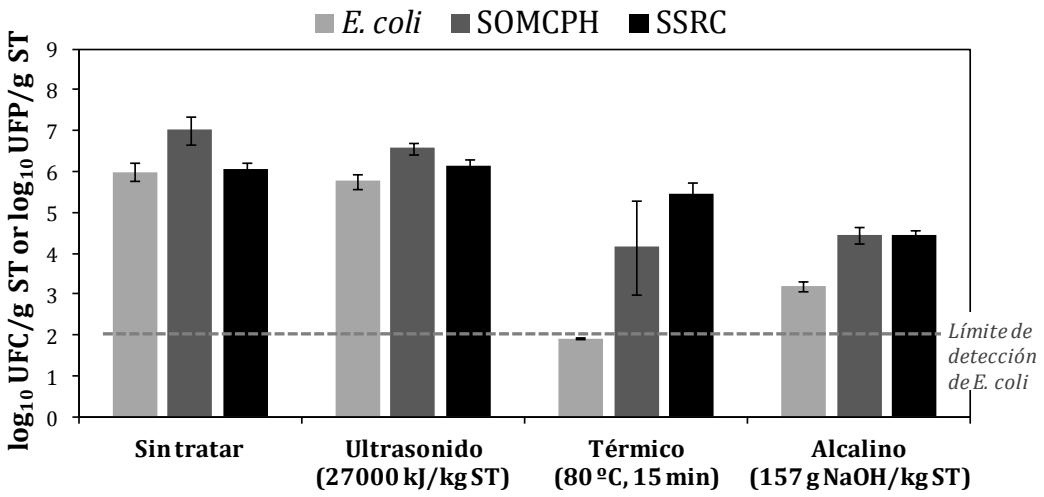

Figura 7. Efecto de los tratamientos ultrasonido, térmico y alcalino sobre las poblaciones de microorganismos indicadores en un lodo activado (*E. coli*, SOMCPH y SSRC).

En el caso del ultrasonido apenas se observaron cambios en los niveles de microorganismos indicadores. Como se ha comentado en la metodología, durante la ultrasonicación, la muestra de lodo se refrigeró para evitar la subida de la temperatura debido al tratamiento. Por lo tanto, el mecanismo de desinfección del ultrasonido se basó exclusivamente en la cavitación, fenómeno que está influenciado por varios factores. De este modo, es concebible que la E_S analizada fuera suficientemente efectiva para disgregar los flóculos del lodo, pero no para matar bacterias y esporas o inactivar bacteriófagos (Ruiz-Hernando et al., 2014a).

En cuanto al tratamiento térmico, los microorganismos indicadores respondieron de distinta manera; se observó una ligera reducción de los niveles de SSRC (0,54 $\log_{10}$ de reducción), 3,25 $\log_{10}$ de reducción para los SOMCPH y un grado muy elevado de higienización para la *E. coli* (> 4,07 $\log_{10}$ de reducción). En concreto, las poblaciones de *E. coli* cayeron por debajo del límite de detección de la técnica (2,02 $\log_{10}$ UFC/g ST o 4,00 UFC/g peso húmedo), satisfaciendo los niveles normales aceptados por la EPA (US Environmental Protection Agency, 2003) y el tercer borrador oficial de la Unión Europea (Environment DG, EU, 2000) para la aplicación de biosólidos en el suelo (UFC es la abreviación de "unidades formadoras de colonias").

El tratamiento alcalino dio lugar a un patrón de inactivación similar entre los tres microorganismos indicadores. La concentración más elevada de NaOH (157 g/kg ST) mostró un pH extremo (~12) durante las 24 horas que duró el tratamiento, lo que resultó letal para los microorganismos. Así, el nivel de higienización requerido para *E. coli* se cumplió, obteniendo un valor de 3,20 log_{10} UFC/g ST (95,6 UFC/g peso húmedo) y 2,57 log_{10} de reducción. Del mismo modo, los niveles de SOMCPH y SSRC se redujeron 2,79 y 1,72 log_{10}, respectivamente.

Es importante señalar que las bacterias pueden experimentar múltiples estados fisiológicos, lo cual dificulta la medición de las concentraciones reales. En cambio, los virus sólo pueden ser infecciosos o no infecciosos, simplificando su uso como indicadores. Teniendo en cuenta esto, los SOMCPH son un buen indicador para evaluar los distintos tratamientos en lodos y podrían ser el candidato adecuado para complementar las mediciones de *E. coli* en las directivas.

4.3.2. Resultados de los ensayos de biometanización

La Tabla 4 muestra la eficiencia de solubilización y el potencial final de metano para el lodo sin tratar y para una condición de cada tratamiento (ultrasonido: 27000 kJ/kg ST; térmico: 80 ºC (15 min); alcalino: 157 g NaOH/kg ST). Los tres tratamientos fueron capaces de solubilizar la materia orgánica particulada del lodo, tal y como se muestra por la relación DQOs/DQOt y por el grado de solubilización (SD, por sus siglas en inglés) (Tabla 4). El grado de solubilización se calculó de la siguiente manera:

$$SD\ (\%) = \frac{DQOs_f - DQOs_0}{DQOt_0 - DQOs_0} \cdot 100$$

donde la $DQOs_f$ es la DQO soluble después del tratamiento, la $DQOs_0$ es la DQO soluble antes del tratamiento y la $DOQt_0$ es DQO total antes del tratamiento.

En concreto, el tratamiento ultrasonido y el térmico presentaron eficiencias de solubilización similares (de aproximadamente 11%), las cuales fueron menores que la del tratamiento alcalino (de aproximadamente 15%). Sin embargo, el tratamiento alcalino mostró una pérdida de 5 g DQO/L debido a la mineralización de la materia orgánica, fenómeno que no se detectó en los otros dos tratamientos.

Aunque en un principio es de esperar que las condiciones óptimas de tratamiento (en términos de producción de metano) sean aquellas que presenten una elevada solubilización de la DQO y una baja mineralización de la materia orgánica, el aumento de la solubilización no siempre se traduce en un aumento de la biodegradabilidad. Por lo tanto, para hacer una valoración completa de los tratamientos sobre la digestión anaerobia es necesario llevar a cabo los ensayos de biometanización. El potencial final de metano para el tratamiento térmico fue muy similar al del lodo sin tratar, mientras que el tratamiento ultrasonido y el alcalino mostraron incrementos de alrededor del 13% y 34%, respectivamente, con respecto al lodo no tratado (Tabla 4).

Tabla 4. Eficiencia de la solubilización y ensayos de biometanización. Los errores representan la desviación estándar.

	Sin tratar	**Ultrasonido**	**Térmico**	**Alcalino**
sDQO/tDQO (%)	1,1 ± 0,1	12,8 ± 0,2	11,7 ± 0,2	16,0 ± 0,2
SD (%)	-	11,8 ± 0,4	10,8 ± 0,6	14,0 ± 0,6
B_0 (mL CH_4/g DQO)	141,3 ± 3,1	155,9 ± 5,3	145,2 ± 6,9	183,8 ± 6,3

Tratamiento ultrasonido: 27000 kJ/kg ST; Tratamiento térmico: 80 ºC (15 min); Tratamiento alcalino: 157 g NaOH/kg ST.

Estos incrementos son bajos en comparación con los resultados encontrados en la bibliografía, lo cual puede estar relacionado con la selección de las condiciones de tratamiento (dicha selección se realizó en base a los resultados de higienización y deshidratación, y no en base al aumento del rendimiento de metano). En cualquier caso, el tratamiento que más incrementó la biodegradabilidad del lodo fue el alcalino. No obstante, este tratamiento tiene el inconveniente de concentrar sodio en el digestor, lo

cual puede acabar inhibiendo el proceso de digestión. De hecho, una posible inhibición debido a la alta concentración de sodio (3,6 g Na+/L) podría haber sido enmascarada por el efecto de dilución (aproximadamente 1/4) del inóculo. Por lo tanto, el uso de NaOH como tratamiento previo a la digestión es bastante limitado.

5. CONCLUSIONES

Las principales conclusiones derivadas del trabajo son las siguientes:

- Todos los lodos (tratados y sin tratar) mostraron comportamiento pseudoplástico y tixotrópico. Los resultados experimentales se ajustaron muy bien al modelo de Ostwald-de Waele.
- Los tres tratamientos redujeron la viscosidad y el área de histéresis del lodo; a medida que se incrementó la intensidad del tratamiento esta disminución fue más importante, especialmente en el caso de los tratamientos ultrasonido y alcalino.
- Los tratamientos redujeron los coeficientes cinéticos para el proceso de destrucción (K_{down}) y construcción (K_{up}), así como el parámetro que cuantifica la alineación instantánea y la deformación de los flóculos de lodo (m).
- El tratamiento alcalino (157 g NaOH/kg ST) fue el que más EPSs solubilizó y, en consecuencia, fue el que permitió extraer más agua del lodo. Aunque el tratamiento térmico (80 ºC; 1 h) fue capaz de desnaturalizar las proteínas de elevado peso molecular, no solubilizó tantas EPSs, por lo que la mejora de la deshidratación fue menor. El tratamiento ultrasonido (27000 kJ/kg ST) fue el que menos EPSs solubilizó, de manera que fue el que permitió extraer menos agua del lodo.
- El tratamiento térmico (80 ºC, 15 min) y el alcalino a elevada dosis (157 g NaOH/kg ST) permitieron higienizar el lodo, cumpliendo con las normativas europea y americana. En cambio, el tratamiento ultrasonido apenas redujo los niveles de los microorganismos indicadores.
- El tratamiento que más aumentó la biodegradabilidad del lodo fue el alcalino (157 g NaOH/kg ST), seguido del ultrasonido (27000 kJ/kg ST) y, finalmente,

el térmico (80 ºC, 15 min). No obstante, el tratamiento alcalino tiene el inconveniente de concentrar sodio en el digestor, lo cual puede acabar inhibiendo el proceso de digestión.

REFERENCIAS

Angelidaki, I., Alves, M., Bolzonella, D., Borzacconi, L., Campos, J.L., Guwy, A.J., Kalyuzhnyi, S., Jenicek, P., Van Lier, J.B., 2009. Defining the biomethane potential (BMP) of solid organic wastes and energy crops: a proposed protocol for batch assays. Water Sci. Technol. 59, 927-934.

Anonymous, 2000. ISO 10705-2: Water Quality - Detection and Enumeration of Bacteriophages - Part 2: Enumeration of Somatic Coliphages. International Organisation for Standardisation, Geneva, Switzeland.

Bougrier, C. Albasi, C., Delgenès, J.P., Carrère, H., 2006. Effect of ultrasonic, thermal and ozone pre-treatments on waste activated sludge solubilisation and anaerobic biodegradability. Chem. Eng. Process. 45, 711–718.

CEC (Council of the European Communities), 1991. Council Directive of 21 May 1991 concerning urban waste water treatment (91/271/EEC). Official Journal of the European Communities No. L 135/40-52.

Colin, F., Gazbar, S., 1995. Distribution of water in sludges in relation to their mechanical dewatering. Water Res. 29, 2000-2005.

Environment DG, EU, 2000. Working Document on Sludge, 3rd Official Draft. Brussels. URL: http://ec.europa.eu/environment/waste/sludge/pdf/sludge_en.pdf.

Frølund, B., Griebe, T., Nielsen, P.H., 1995. Enzymatic activity in the activated-sludge floc matrix. Appl. Microbiol. Biotechnol. 43, 755–761.

Frølund, B., Palmgren, R., Keiding, K., Nielsen, P.H., 1996. Extraction of extracellular polymers from activated sludge using a cation exchange resin. Water Res. 30, 1749–1758.

IAWPRC, 1991. Study group on health related water microbiology. Bacteriophages as model viruses in water quality control. Water Res. 25, 529-545.

Labanda, J. Sabaté, J. Llorens, J., 2007. Rheology changes of Laponite aqueous dispersions due to the addition of sodium polyacrylates of different molecular weights. Colloids Surf., A: Physicochem. Eng. Aspects 301, 8–15.

Li, X.Y., Yang, S.F., 2007. Influence of loosely bound extracellular polymeric substances (EPS) on the flocculation, sedimentation and dewaterability of activated sludge. Water Research 41, 1022–1030.

Lowry, O.H., Rosebrough, N.J., Farr, A.L., Randall, R.J., 1951. Protein measurement with the folin phenol reagent. J. Biol. Chem. 193, 265–275.

Milieu Ltd., WRc and Risk & Policy Analysts Ltd (RPA), 2010. Environmental, economic and social impacts of the use of sewage sludge on land. Final Report, Part III: Project Interim Reports, DG ENV.G.4/ETU/2008/0076r, 10.2.2010.

Neyens, E., Baeyens, J., 2003. A review of thermal sludge pre-treatment processes to improve dewaterability. J. Hazard. Mater. B98, 51–67.

Payment, P. and Franco, E., 1993. Clostridium perfringens and somatic coliphages as indicators of the efficiency of drinking water treatment for viruses and protozoan cysts. Appl. Environ. Microbiol. 59, 2418-2424.

Ratkovich, N., Horn, W., Helmus, F.P., Rosenberger, S., Naessens, W., Nopens, I., Bentzen, T.R., 2013. Activated sludge rheology: A critical review on data collection and modelling. Water Res. 47, 463-482.

Ruiz-Hernando, M., Labanda, J., Llorens, J., 2010. Effect of ultrasonic waves on the rheological features of secondary sludge. Biochemical Engineering Journal 52, 131-136.

Ruiz-Hernando, M., Martinez-Elorza, G., Labanda, J., Llorens, J., 2013. Dewaterability of sewage sludge by ultrasonic, thermal and chemical treatments. Chemical Engineering Journal 230, 102-110.

Ruiz-Hernando, M., Martín-Díaz, J., Labanda, J., Mata-Alvarez, J., Llorens, J., Lucena, F., Astals, S., 2014a. Effect of ultrasound, low-temperature thermal and alkali pre-treatments on waste activated sludge rheology, hygienization and methane potential. Water Research 61, 119-129.

Ruiz-Hernando, M., Simón, F.X., Labanda, J., Llorens, J., 2014b. Effect of ultrasound, thermal and alkali treatments on the rheological profile and water distribution of waste activated sludge. Chemical Engineering Journal 255, 14-22.

Ruiz-Hernando, M., Labanda, J., Llorens, J., 2015a. Structural model to study the influence of thermal treatment on the thixotropic behaviour of waste activated sludge. Chemical Engineering Journal 262, 242–249.

Ruiz-Hernando, M., Cabanillas, E., Labanda, J., Llorens, J., 2015b. Ultrasound, thermal and alkali treatments affect extracellular polymeric substances (EPSs) and improve waste activated sludge dewatering. Process Biochemistry 50, 438-446.

US Environmental Protection Agency, 2003. Control of Pathogens and Vector Attraction in Sewage Sludge. Under 40 CFR Part 503. EPA 625/R-92/013. Cincinnati.

Wilson, C.A., Novak, J.T., 2009. Hydrolysis of macromolecular components of primary and secondary wastewater sludge by thermal hydrolytic pretreatment. Water Res. 43, 4489–4498.